Examining the Effects of Aviation NO_x Emissions as a Short-Lived Climate-Forcer

Sarah J Freeman

A thesis submitted in partial fulfilment of the requirements of the Manchester Metropolitan University for the degree of Doctor of Philosophy

Manchester Metropolitan University

Faculty of Science and Engineering
School of Science and the Environment

2017

Abstract

Examining the effects of aviation NO_x emissions as a short-lived climate-forcer

As the earth's climate continues to change, it is becoming increasingly clear that the mitigation of anthropogenically released greenhouse gases, such as those emitted by the growing aviation industry, is a high priority. Through the emission of short–lived and long–lived climate–forcing chemical species, there are several ways in which the aviation industry affects the climate. The long–lived greenhouse gas CO_2 has been well–studied, but the effects of the short–lived climate forcer NO_x , which perturbs ambient O_3 and CH_4 in the atmosphere, is less well understood. Through changes in aircraft engine design and behaviour, the relative emissions of these two climate forcers can be tuned to address specific mitigation targets. However, a trade-off exists between aviation NO_x and CO_2 emissions as reducing one results in an increase in the other, and vice versa.

Here, the trade–off between CO_2 and NO_x is investigated using the MOZART–3 chemistry transport model (CTM) and a simple climate model (SCM), LinClim. LinClim, which is much less computationally intensive, assumes a linear relationship between aviation NO_x emissions and associated O_3 burden and CH_4 lifetime change. By using the more sophisticated MOZART–3, it was found that both these NO_x – O_3 and NO_x – CH_4 relationships are linear while aviation emissions are below 3 Tg N Yr^{-1} but thereafter, become non–linear.

A new non-linear net NO_x RF parameterisation is developed from the results of the CTM runs and used to investigate this trade-off. Experiments showed that a small CO_2 increase (+2 percent) raised the overall forcing from aviation, despite a larger reduction in NO_x emissions (-20 percent). When background NO_x levels were high the experiments showed that a 43 percent reduction in NO_x emissions was required to counteract the radiative forcing of the additional CO_2 emissions, and when NO_x was reduced by 20 percent, only a 0.5 percent CO_2 penalty could be allowed before an additional forcing was incurred. When background NO_x emissions were low, the results were more complex as net NO_x forcing became negative. Therefore, any reduction in aviation NO_x emissions actually increased the net forcing. In this case additional NO_x emissions were necessary to reduce overall forcing from aviation emissions.

These results indicate that the most important emission to mitigate in the aviation industry is CO_2 , its long–lived cumulative nature causes it to contribute substantially more to global climate change than aviation NO_x emissions, which, depending on the state of the background atmosphere, contribute either a small positive or small negative, net forcing.

Acknowledgements

I would like to thank my Supervisors Professor David S. Lee and Dr Ling Lim for all of their advice, time and patience over the last four years, particularly David's wealth of knowledge in all things aviation and thesis writing and Ling's incredible patience when assisting me in all things technical! I would also like to thank my colleagues Dr Agnieszka Skowron and Dr Ruben Rodriguez De Leon, Agnieszka for teaching me how to run MOZART and providing helpful PhD advice and Ruben for running the Edwards–Slingo RTM. I would also like to thank Manchester Metropolitan University and the UK Department for Transport for providing the funding for this work.

This PhD has been quite a journey and I've met some fantastic people along the way. I would like to thank all the other PhD students whom I met on the ERCA course in Grenoble 2013, who have provided an irreplaceable network of friendship and support over the last 4 years. Watching many of you graduate has inspired me to keep going!

Personally I'd like to thank my parents for all their support, for putting up with me and listening to me lecture them about climate change. I'd also like to thank my best friend Clare Taylor for the endless coffees you have endured listening to me complain, and still always managing to cheer me up!

Finally I'd like to thank Neil, for your incredible patience, love and support, for helping me fix my LaTeX and my maths problems, but mostly, for taking me to see the ducks and sitting in a bird hide with me for hours on end when it was all too much - thank you.

Acronyms

ACARE - Advisory Council for Aeronautics Research in Europe
AIC - aviation induced cloudiness
AR5 - Assessment Report 5 of the IPCC
ATM - air traffic management
BAU - business as usual
CAEP - ICAOs Committee on Aviation Environmental Protection
CATE - Centre for Aviation, Transport and the Environment, located at MMU
CCM - chemistry climate model
CCS - carbon capture and storage
CH4 - methane
CMIP5 - coupled model inter comparison project
CO_2 - carbon dioxide
CORSIA - ICAOs Carbon Offsetting and Reduction Scheme for International Aviation
CTM - chemistry transport model
EBM - energy balance model
ECMWF - European Centre for Medium-range Weather Forecasts
$EINO_x$ - NO_x emission index
EU ETS - European Union Emissions Trading Scheme
FAST - The Future civil Aviation Scenario software Tool
GCAM - global change assessment model
GCM - global or general circulation model
GHG - greenhouse gas
GTP - global temperature change potential
GWP - global warming potential
HIRDLS - High Resolution Dynamics Limb Sounder
IAM - integrated assessment model
ICAO - International Civil Aviation Organisation
IPCC - Intergovernmental Panel on Climate Change
IPCC SRES - IPCC Special Report Emissions Scenarios
ISCCP - International Satellite Cloud Climatology Project
LinClim - a simple climate model
LLCF - long–lived climate–forcer
LTTG - ICAOs long-term technology goals
MAGICC - The Model for the Assessment of Greenhouse Gas Induced Climate Change
MATCH - Model of Atmospheric Transport and Chemistry
MMU - Manchester Metropolitan University
MOZART - The Model for Ozone and Related Chemical Tracers
MTTG - ICAOs medium term technology goal
NASA – National Aeronautics and Space Administration
N_2 - molecular nitrogen
NO - nitrogen oxide

NO_2 - nitrogen dioxide
NO_x - NO and NO_2
O_3 - molecular oxygen
OAG - Official Aviation Guide
OAGCM - ocean atmosphere general circulation model
OPE - ozone production efficiency
PAN - peroxyacyl nitrates
PIANO - aircraft performance model
RCP - Representative Concentration Pathways
REACT4C - Reducing Emissions from Aviation by Changing Trajectories for the benefit of Climate, emissions scenario
RF - radiative forcing
SCM - simple climate model
SHADOZ - Southern Hemisphere ADditional OZonesondes
SLCF - short–lived climate–forcers
SO_x - sulphur oxides
SWV - stratospheric water vapour
UNFCCC - United Nations Framework - Convention on Climate Change
UTLS - upper-troposphere lower-stratosphere
VOC - volatile organic compounds
WDCGG - World Data Centre for Greenhouse Gases
WMGHG - well-mixed greenhouse gas
WOUDC - World Ozone and Ultraviolet Radiation Data Centre

Contents

List of Figures

List of Tables

Chapter 1

Introduction

1.1 Science of Climate Change

The earth's climate is changing. It is changing at an unprecedented rate as a consequence of the anthropocence – the time in which human activities have begun to influence the earth's natural processes. A major factor of climate change relates to the carbon cycle, the cycling of carbon between reservoirs. Humanity is perturbing the earth's natural carbon cycle by taking carbon from within the earth's crust and releasing it into the atmosphere as carbon dioxide – a greenhouse gas – on a faster scale than would happen naturally, forcing the climate out of equilibrium. In order to study these changes in the earth's climate we have developed computer models to attempt to increase the level of understanding of the atmosphere, its constituents and the interactions with the biosphere and oceans.

In their fifth assessment report, the Intergovernmental Panel on Climate Change state that global warming is now unequivocal and is a result of increasing greenhouse gas concentrations. Much of the warming experienced since 1950 is "unprecedented over decades to millennia" (Stocker et al., 2013). Effects of a warming climate include increased atmospheric and ocean temperatures, diminished amounts of snow and ice and sea level rise. Atmospheric climate variables such as precipitation changes, heat waves, cloudiness and water vapour are likely to respond quickly to rising temperatures, whereas thermal expansion of oceans and ice sheet melt will take place over a longer time scale, and continue even if CO_2 emission should cease.

The concentration of CO_2 (and other greenhouse gases such as CH_4) are higher at present than at any time over the last 650 000 years, CO_2 has risen to no more than $\sim$300 ppmv in interglacial periods during this time (Forster et al., 2007) but currently atmospheric concentration is over 400 ppmv. Policy makers require current, reliable, scientific predictions of how industries such as aviation are affecting the climate in order to implement suitable mitigation policies aimed at reducing climate change.

1.2 The Effects of Short–Term and Long–Term Climate–Forcers on Global Climate Change

The mitigation of climate change ultimately relies on the reduction and eventually cessation of anthropogenic greenhouse gas release. Although there are several greenhouse gases of interest in this campaign, the climate will not stop warming until CO_2 is successfully mitigated, with peak warming not occurring until many decades after CO_2 emissions have stopped rising (Allen et al., 2016). Although CO_2 does not have the greatest warming effect per molecule, its cumulative nature and sheer volume of release make it by far the most dangerous greenhouse gas in term of climate change. As climate change advances it is becoming necessary to include short–term forcers in climate policies (Deuber et al., 2014). A short–term climate forcer is generally described as any species which substantially affects global mean radiative forcing while only having an atmospheric residence time of less than one year, this includes both precursor and direct emissions. (Although methane has a lifetime of around a decade, it is considered a short–lived climate–forcer in the study of aviation).

The short–lived versus long–lived pollutants debate stems from the fact that, although long lived gasses such as CO_2 cause more warming of the climate, shorter lived greenhouse gases such as CH_4 are cheaper and simpler to mitigate, as well as their mitigation having additional benefits associated with human health and agriculture. The immediate mitigation of these shorter lived gases will incur a reduction in global temperature in the short term – the next few decades, however future peak warming will not be affected unless CO_2 emissions are also mitigated now.

In terms of policy making, there is a danger that short–term climate–forcer mitigation is seen as far more cost effective and shown to give more immediate results than CO_2

mitigation and therefore is favoured over CO_2 mitigation. As stated above this will reduce warming in the short term, but will not mitigate the long–term trend. It has also given rise to the view that mitigating short–term forcers 'buys more time' in which to tackle climate warming, when in fact, CO_2 is still accumulating in the background, increasing warming, the only thing that is delayed is peak warming.

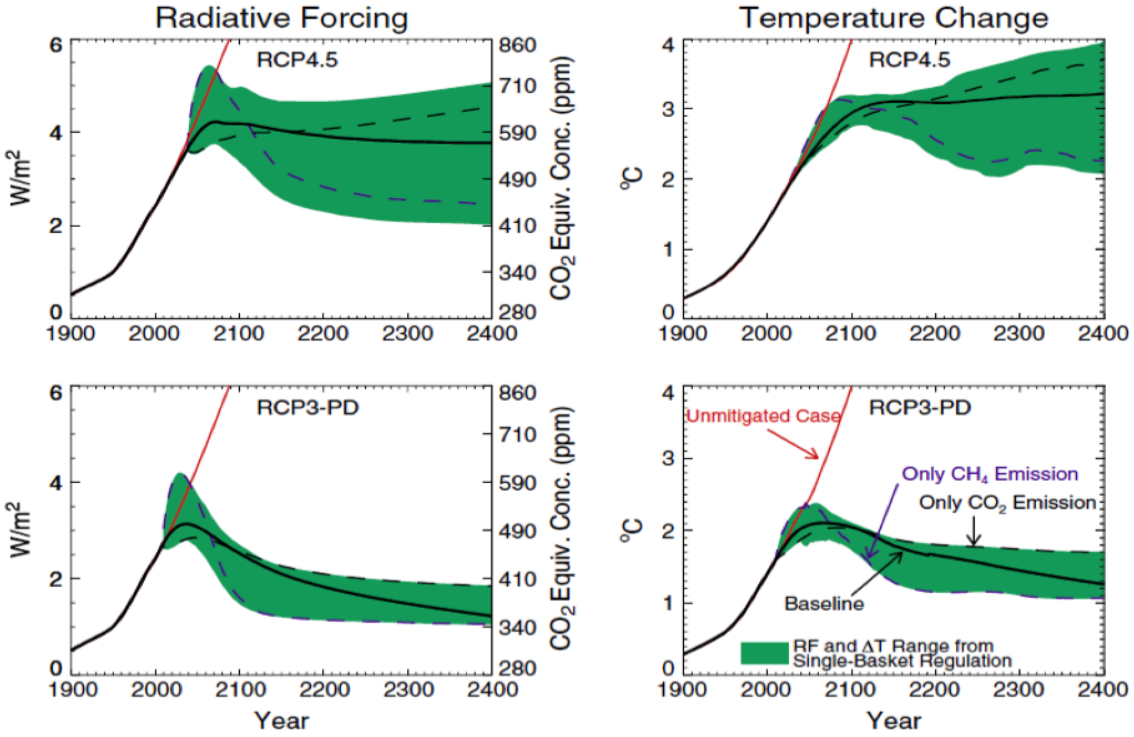

Figure 1.1: An example of the trade-off between the effects of mitigating two different greenhouse gases, a long-lived climate-forcer in the case of CO_2 and a relatively short-lived climate-forcer in term of CH_4. When the individual emissions are shown, it is clear that, while methane emissions are contributing to warming over the short–term, over the longer term the CO_2 emissions have a much greater impact. Taken from (Daniel et al., 2012).

Figure 1.1 shows the importance of implementing appropriate policies in the present day as decisions made now can have repercussions lasting centuries. The figure shows that while methane is a greenhouse gas and in the short–term its emission looks to have greater impacts than CO_2 emissions, in the long–term the impacts from CO_2 are shown to outweigh those of methane, raising temperatures by $\sim$1°C more than methane would alone over the next few hundred years. Also, a fraction of anthropogenic CO_2 is thought to persist in the atmosphere for up to hundreds of thousands of years (Archer, 2005) emphasising the importance of managing its release.

Targets have been set by the European Union in order to keep global temperature change limited to 2°C , this involves reducing greenhouse gas emissions 80–95 percent by 2050 compared to 1990 levels, which implies that the transport sector alone will have to reduce greenhouse gas emissions by at least 60 percent by 2050. The UNFCCC objectives (Article 3) on the matter of climate change focus on the 'threats of serious or irreversible damage' which, it has been suggested, negate the importance of greenhouse gas emission (e.g. CO_2) in the longer term (Solomon et al., 2007).

1.3 Impacts of Aviation

Aviation is the key to international travel, allowing people to travel around the world in a matter of hours, but as an ever growing industry, it is contributing anthropogenic emissions in a physically and chemically complex region of the atmosphere (8 – 10 km altitude), and is the only anthropogenic source perturbing the chemistry in this region. Growth of the industry is continuing, despite economic depression and acts of terrorism, meaning emissions are continuing to increase.

Aviation affects the atmosphere in many different ways. Additionally to long–lived greenhouse gases, emissions consist of many short–lived climate–forcers, which contribute additional positive and negative radiative forcings to the atmosphere. Aviation emissions consist primarily of carbon dioxide (CO_2) – a long–lived climate–forcer, nitrogen oxides (NO, NO_2 collectively: NO_x), which perturb atmospheric ozone and methane all of which are short–lived climate–forcers. Of additional concern are the perturbations to cirrus clouds and associated water vapour, the generation of contrails and additional aerosol loading and sulphur oxides (SO_x), which also result from aviation (Stevenson et al., 2004); (Lee et al., 2010).

This thesis will focus mainly on the NO_x component of aviation emissions and examine its role as a short–lived climate–forcer. Aviation NO_x emissions have the potential to both warm and cool the climate. However, the radiative forcing (RF) metric expresses a global mean and many forcings, such as those from NO_x , are spatially heterogeneous and therefore cannot simply cancel each other out (Skowron et al., 2015). As of 2005, the total radiative forcing resulting from aviation was calculated to be $\sim$55 mW m^{-2}, which contributes 3.5 percent of total anthropogenic radiative forcing. This calculation excluded the effects of aviation induced cloudiness (AIC) due to the uncertainty associated with

the phenomenon, if estimates of AIC are included the figures rise to 78 mW m^{-2} and 4.9 per cent respectively. While this estimate may be considered modest compared to other sources, unless fleet emissions are reduced as the industry grows, this figure will likely increase and is predicted to be $\sim$84 mW m^{-2} by 2020 (Lee et al., 2009).

Aviation emissions can be reduced, whether this is through new aircraft design, economic or operational changes or a change in fuel (e.g. biofuel). In Europe it is thought that improving air traffic management (ATM) and airport operations could reduce emissions by 7–12 percent for the average flight, which saves 16 million tonnes of CO_2 annually. Although the optimum routes for aircraft are mapped out prior to flight, high traffic volume and weather events often mean that the optimum routes are not available (European-Commission, 2008). Currently aviation is not covered in the Kyoto Protocol although reductions in greenhouse gases are encouraged from all sectors; instead ICAO (the International Civil Aviation Organisation) is charged with regulating aviation emissions. Decreasing aviation NO_x and subsequent O_3 production however, is more complicated. The production of ozone depends heavily on local chemical and transport conditions, thus the reduction of NO_x will only be effective in some areas in decreasing overall O_3 (Gilmore et al., 2013). Decreasing NO_x emissions through engine modification is also possible, however, this method presents a new set of challenges.

1.4 The Trade-off Between Aviation NO_x and CO_2 Emissions

As with every other polluting industry, aviation is being encouraged to reduce its emissions, particularly those of CO_2 – to reduce the anthropogenic greenhouse effect and therefore warming of the planet – and NO_x emissions, which contribute to air pollution. To reduce fuel use and therefore CO_2 emissions, a higher engine efficiency is desirable. However, an increase in engine temperature and pressure, which would promote fuel burn efficiency, results in an increase in NO_x emissions. Conversely, fitting engine technology to reduce NO_x emissions in an aircraft increases weight and therefore, fuel burn, resulting in a CO_2 penalty. The main aim of this thesis will be to investigate this trade–off to determine the effects on the climate of reducing one species at the expense of another.

1.5 Research Questions

Archer et al. (2009) emphasises that policy makers and the public want, and need, to know how long the effects of CO_2 will impact the climate and if a trade–off between CO_2 emissions and emissions of other gases is viable. The IPCC place a low or 'fair' level of scientific understanding on aviation NO_x emissions and the comparison between NO_x and CO_2 , short–lived and long–lived forcers with regards to aviation emissions is somewhat under-studied, hence the rationale behind this study. Policy makers require scientific understanding of the trade–offs associated with reducing SLCF such as NO_x at the expense of CO_2 . The best options regarding which emissions will either benefit or further degrade the atmosphere in the long term needs to be assessed as do the trade–offs between substances which provide a negative radiative forcing but act primarily as air pollutants. In terms of the aviation, or other multi-GHG and pollution emitting industries, this research aims to determine the direction of climate change mitigation. For the aviation industry the fundamental question is whether the next technology improvements should aim to primarily reduce NO_x or CO_2 emissions, taking into account the fact that a reduction in one will likely lead to an increase in the other.

The aim of this PhD is to examine the role of aviation NO_x emissions as a short-lived climate-forcer (SLCF).

The objectives are as follows;

- To examine the perturbations to the atmosphere caused by aircraft using the MOZART Chemistry Transport Model (CTM).
- To assess the MOZART models' ability to reproduce trace gas species in the upper troposphere by comparison to observations and measurements.
- To determine the potential mitigation response of aircraft NO_x emissions on climate using detailed 3D aircraft emission inventories.
- To determine whether reduction of SLCFs such as aircraft NO_x, at the expense of CO_2 emissions is a potentially worse outcome or better outcome for global climate in the longer ($\sim$100 years) term, and therefore examine whether controlling aviation NO_x emissions would reduce or limit global warming

1.6 Thesis Structure

Chapter 2 will provide a literature review, including the current state of the science regarding both climate modelling and aviation emissions. Chapters 3 and 4 discuss the data and models used in this study and the legitimacy of their use. Chapter 5 outlines the work done on the MOZART chemistry transport model, where the effects of aviation NO_x emissions are assessed in different background atmospheric states using several aviation emissions scenarios. This work results in the formation of a new parameterisation for use in a simple climate model, which is tested in Chapter 6 and is then used to look at the long–term effects of short– and long–term climate–forcers resulting from aviation emissions in Chapters 7. Conclusions and Further Work are presented in Chapter 8.

"Despite the uncertainties and limitations associated with climate modelling, they are not enough to justify political and public inaction at this point, the research clearly provides more than enough scientific evidence to support the fact that the climate is changing rapidly and that it is due to human action" - (Maslin and Austin, 2012).

Chapter 2

The Effects of Aviation Emissions on the Atmosphere and Global Climate

This chapter outlines the effects of aviation emissions and the metrics used to compare and assess them. It will address the chemical impacts of aviation on the atmosphere and thus their effects on the climate. It will summarise the potential trade–off between aviation NO_x and CO_2 emissions and outline current mitigation policies.

2.1 Introduction: The Impacts of Aviation on Atmospheric Chemistry

Aviation impacts the atmosphere on a global scale, releasing emissions into a physically and chemically complex region of the atmosphere. Aviation accounts for approximately 3.5 percent of global anthropogenic radiative forcing (RF) mainly through emissions of carbon dioxide (CO_2), nitrogen oxides (NO, NO_2 collectively: NO_x) and sulphur oxides (SO_x). The emissions perturb radiaitvely active species in the upper troposphere resulting in changes to the radiative forcing (RF) of the atmosphere, both positively and negatively, therefore influencing global climate (Lee et al., 2009), (Dessens et al., 2014). Of additional concern are the perturbations to cirrus clouds and associated water vapour, the generation of contrails, additional aerosol loading, hydrocarbons, CO, volatile organic compounds (VOCs) and non-VOCs which also result from aviation (Stevenson et al.,

AIR	+	FUEL	=	EMISSIONS
N_2, O_2		CmHn		CO_2 , H_2O, N_2, O_3 , NO_x , CO, SO_x, soot, unburnt hydrocarbons

2004); (Lee et al., 2010).

Put simply, the chemistry of an aircraft engine is shown in this basic equation (Antoine and Kroo, 2004)

The Intergovernmental Panel on Climate Change (IPCC) predicts the continued growth of the industry and estimate aviation fuel consumption to increase by a factor of 2.7 – 3.9 by 2050. While the impact of CO_2 emissions is assigned a high level of understanding by the IPCC, the chemistry of NO_x is assigned a low level of scientific understanding (Solomon et al., 2007). The concentration of NO_x present in the upper–troposphere lower–stratosphere (UTLS) region is expected to increase as fuel consumption does – hence the need to fully understand the impacts this will have on the atmosphere and, in turn, the climate (Gauss et al., 2006). Recent quantification has assessed current and future aviation NO_x impact in terms of radiative forcing (RF) from the short–term tropospheric ozone response (a positive, warming response) and the consequential destruction of ambient methane through the enhancement of OH radicals (a negative, cooling response) (equations 2.1 – 2.12; (Lee et al., 2009).

This study is set to address the comparison between short– and long–lived climate forcers emitted from aviation. A climate forcer defines any chemical species that reflects or absorbs radiation, thereby altering the earth's radiation balance. Short–lived climate–forcers (SLCFs) define species that affect the climate on a short time scale due to their highly reactive nature and therefore short lifetime in the atmosphere. In their fifth assessment report, the IPCC refer to short–term forcers as 'near–term climate–forcers' (NTCF) and define them as radiatively active compounds whose main impact on the earth's climate happens within a decade of its initial release. Thus a 'short–term climate–forcer' is synonymous with 'near–term climate–forcer' throughout the literature and within this study. The term 'long–lived climate–forcer' (LLCF) has been replaced in the latest IPCC report (AR5) with the term 'well mixed greenhouse gas' (WMGHG) as it was felt that this term better reflects the homogeneous distribution of certain species throughout the troposphere which is a result of their long lifetime in it, but again the two terms are synonymous.

With the main effect of methane occurring within 10 – 12 years of its release, the IPCC classify it as both a near–term forcer and a well–mixed greenhouse gas (Myhre et al.,

2013). While SLCFs affect the atmosphere over a short time scale and regional spatial scale, the effects of LLCFs or WMGHGs span the entire globe over centuries. Although SLCFs were excluded from the Kyoto Protocol, they are believed to have contributed significantly to anthropogenic climate change (Shine et al., 2005). In the case of aviation, NO_x is classed as a SLCF as are the initial effects of associated ozone, whereas CO_2 emissions are considerably longer lived and thus, CO_2 is defined as a long-lived climate forcer (LLCF). The effects of NO_x on methane lifetime, has a mid-range effect of approx. $\sim$12 years, but compared to CO_2 , it is short lived and hence, is considered a short–lived climate–forcer in this study.

2.2 Metrics

To consider the potential trade–offs between SLCFs and CO_2 , metrics are required to place the emissions to be studied onto a comparable scale. Metrics are tools that allow the comparison and quantification of each emission species in terms of its impact on climate change, therefore, they enable the implementation of multi-emission policies. (Shine et al., 2005) note that NO_x emissions are notoriously difficult to place on a similar scale as the effects include both positive and negative RF over different time horizons.

2.2.1 Radiative Forcing

The 'radiative forcing' (RF) metric has been commonly used by the IPCC in their assessment reports and is used to examine and compare natural and anthropogenic forcers which contribute to climate change. It denotes the change in the Earth's energy balance at the tropopause, due to a perturbation within the atmosphere or a change in solar output. When something perturbs the Earth's energy balance, the climate system changes in order to counteract the perturbation and restore temperature equilibrium, hence the use of RF in climate change studies (Mhyre et al., 2013). Radiatively active chemicals can perturb the earth's radiation balance by either absorbing or scattering incoming and outgoing radiation, eventually leading to a new equilibrium state of the climate. A species RF value denotes by how much it changes the radiation balance compared to a point in the past (usually pre–industrial), a positive value implies a warming effect (absorption) while a negative implies cooling (scattering).

The RF from aviation however, is complex. While the RF from CO_2 builds over time in accordance with its emissions, the RF from the short–term forcers; O_3 , CH_4 and contrails, are described by Lee et al. (2010) as being in a 'quasi-steady state' as they reflect only recent emissions. For example, Gilmore et al. (2013) show that the direct RF from aviation O_3 in 2005 is approximately equal to that of aviation CO_2 (within $\sim$6 percent), however they note that while the CO_2 RF represents the history of its emissions, the O_3 RF described the forcing of only the past 2 months. However, RF does not account for the time scale of climate response, it gives one value for each calculation, accurate only to the time of calculation, it cannot suggest future outcomes. This creates issues when using it as a metric for aviation; the cessation of a short–term forcing agent will remove its RF but in reality the climate response (change in temperature) requires a much longer time scale to decay (see Chapter 6 and 7). The long lifetime and cumulative nature of CO_2 in the atmosphere means it is coupled to the climate response, hence even if emissions were to cease the previous emissions would continue to affect the temperature response causing temperature to continue to increase before slowly decaying (Lee et al., 2010).

2.2.2 Global Warming Potential

The Global Warming Potential (GWP) metric is defined as the time-integrated RF value due to a pulse of emissions of a certain species relative to that of a pulse emission of an equal mass of CO_2 . The integration is implemented from the time of emission release to a specified time horizon, determined by the user (Olivie and Peters, 2013). In most studies, including the IPCC Assessment reports, GWP is integrated over 20, 100 and 500 years and uses global mean inputs (Shine et al., 2005). The integration here ensures that the memory of a short-lived emission pulse is retained even after the initial pulse has decayed (Shine, 2009). There have been concerns with the use of GWP. Mainly that the GWP value assigned to a gas does not give details as to exactly how that gas affects the atmosphere, two gases with the same GWP value could have very different effects. Secondly, the uncertainties associated with short–lived forcers in chemistry transport models (CTM) calculations, such as those within the $NO_x - O_3$ cycle, result in uncertainties in the corresponding GWP values (Shine et al., 2007). The nature of the 100 year GWP metric is also in danger of neglecting the long term effects of CO_2 , as a fraction of anthropogenic CO_2 will remain in the atmosphere much longer than 100 years (Solomon et al., 2009).

Gas	GWP 20	GWP 100	GTP 20	GTP 40	GTP 100
Carbon dioxide	1	1	1	1	1
Nitrous oxide	264	265	277	285	234
Methane	84	28	67	26	4
HFC- 134a	3710	1300	3050	1173	201
HFC – 152a	506	138	174	36	19
Black carbon	3200	910	925	n.a.	130

Table 2.1: The equivalent values of a tonne of each greenhouse gas displayed compared to that of CO_2 for each climate metric (taken from Allen, 2015)

2.2.3 Global Temperature Change Potential

(Shine et al., 2005) proposed an alternative to the GWP, the Global Temperature Change Potential (GTP) which is thought to be more relevant and better captures the nature of short lived emissions. While GWP quantifies the energy gained by system, GTP quantifies the energy lost (Olivie and Peters, 2013). The GTP metric denotes the change in surface temperature at a particular point in the future, rather than integration over time, due to either a pulse or sustained emissions and is known as an 'end-point' metric. For long time horizons it will give a much lower value for short-lived forcers than GWP would, due to its 'end-point' nature (Shine, 2009). It denotes the ratio of change in global mean surface temperature from the emission in question, relative to CO_2 at a point in the future (Mhyre et al., 2013). An integrated GTP (iGTP) is another option; it compares the temperature change integrated over the time from the emission release until the specified time horizon (Olivie and Peters, 2013). The GTP metric is useful as it assesses the response in global mean surface temperature using the same inputs as GWP, and therefore provides an indicator of how different species will affect the surface temperature at a particular point in the future (Fuglestvedt et al., 2010). It also allows for assessment of short-lived species (Shine et al., 2007). Fuglestvedt et al. (2010) notes that GWP has been questioned as suitable tool for assessing aviation impact as it does not adequately represent the global mean impact of NO_x for example, due to the locations of emissions and the contrasting RFs of ozone (positive) and methane (negative) associated with aviation NO_x release. This however, is the case with many climate change metrics and the GTP is considered most useful to policy makers as it directly addresses 'a more tangible impact of emissions on climate' (Shine et al., 2007). Table 2.1 shows a comparison of the GWP and GTP of several different forcers compared to CO_2 .

An alternative metric, Global mean surface temperature change is suggested as more fitting metric in the study of aviation, as it incorporates the time scales over which the climate system responds and takes into account the history of RF. (Fuglestvedt et al., 2010) also suggest that it reflects the real impacts and potential damage of the emissions involved One must also remember that climate metrics such as GWP and GTP do not take other, non-climate effects into account, such as air pollution, effects on human health and ocean acidification which are substantial effects of GHG release.

2.3 Chemistry of Aviation Emissions

2.3.1 Carbon Dioxide (CO_2)

Carbon dioxide (CO_2) is the main emission resulting from aviation (50 percent) as a product of the combustion of kerosene, currently the primary fuel used in the industry. The amount of CO_2 emitted is fixed to the amount of fuel used, with 3.16 kg of CO_2 being produced for each kilogram of kerosene burned (Fichter, 2009) therefore, the longer the flight, the more CO_2 emitted. As CO_2 has a long lifetime it accumulates in the atmosphere and once released, the effects of aviation emitted CO_2 are no different than those emitted from any other anthropogenic source.

The carbon cycle – consequences of CO_2 emissions

CO_2 has a long lifetime in the atmosphere and so perturbations become well mixed over time and therefore affect the entire atmosphere. Unlike many other forcing agents, CO_2 does not break down in the atmosphere or deposit on the surface, instead it is relatively unreactive and therefore cumulative in the atmosphere, thus, it gradually cycles through the earth's carbon reservoirs (Figure 2.1; (Archer et al., 2009)). The exact lifetime of atmospheric CO_2 is uncertain and varies depending on location and the intensity of sources and sinks. As a greenhouse gas, CO_2 absorbs outgoing thermal infrared radiation of wavelength 15 μm causing a positive radiative forcing or warming of the lower atmosphere. Atmospheric concentrations reached 400 ppm in 2013, measured at Mauna Loa, Hawaii, compared to 278 ppm in 1750, and a maximum of $\sim$300 ppm during the last interglacial. As of March 2016 atmospheric CO_2 levels are 404 ppm. Cumulatively, approximately

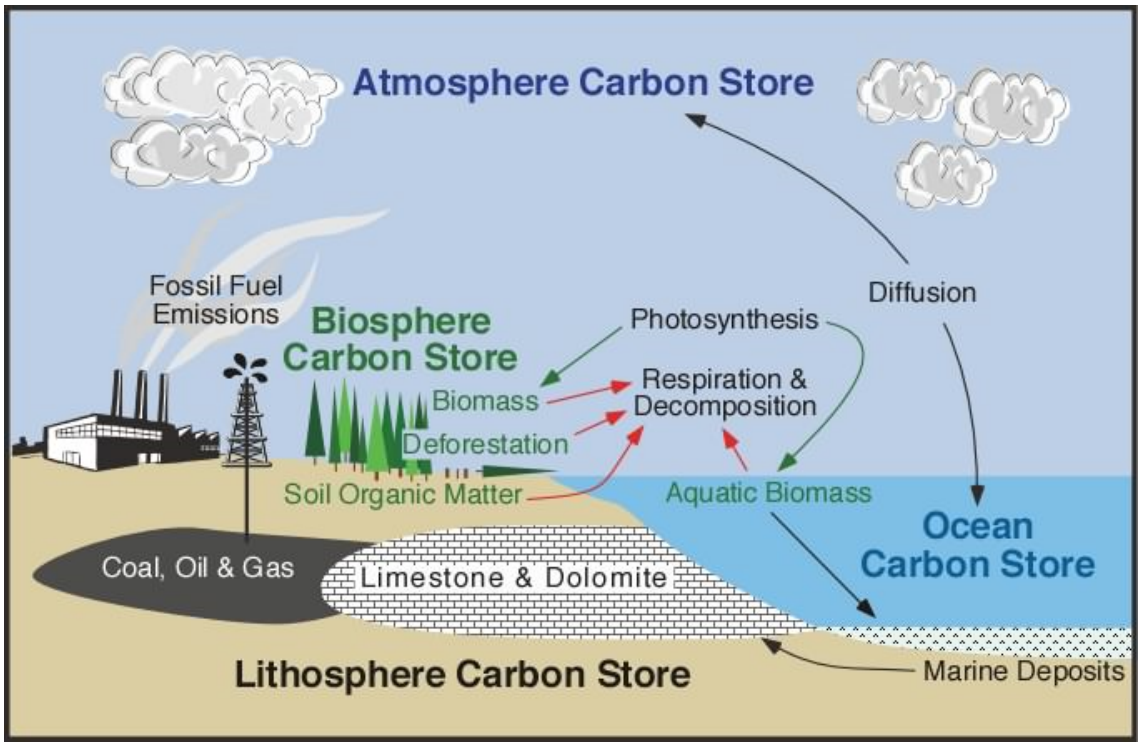

Figure 2.1: The Earths Carbon Cycle - anthropogenically released CO_2 gradually circulates through the earths carbon reservoirs (Pidwirny, 2006).

2000 billion tonnes of CO_2 emissions have been released since 1750 (Forster et al., 2007), (Allen et al., 2016). The long lifetime and cumulative nature of CO_2 means that even if concentrations cease, stop rising or start to decrease, the anthropogenic induced build–up of CO_2 already in the atmosphere will be impacting on global temperatures, and therefore the earth's climate, for centuries due to the slow response times of the atmosphere and oceans. Thus, peak temperature rise will only occur once excess CO_2 emissions are nearly zero. Joos et al. (2013) modelled the effects of a 100 Gt–C emission pulse and found that approx. 25 percent of the pulse was still present in the atmosphere after 1000 years; the land had absorbed $\sim$16 percent and the ocean $\sim$59 percent. The global mean surface air temperature was found to rise $\sim$0.2°C in the first 20 years and after 1000 years ocean heat content and sea level were still rising. As fossil fuels are a finite resource, CO_2 emissions will eventually peak and then decline, however the time–scale is uncertain, and depends mainly on anthropogenic activities. Most of the CO_2 emitted since pre-industrial times will dissolve in sea water, lowering pH and disrupting the development of marine organisms, its presence in the atmosphere will keep temperatures sufficiently high that the sea ice and continental ice sheets will continue to melt, and sea levels continue to rise. Schmittner et al. (2008) modelled the IPCC SRES A2 CO_2 emission scenario up to the

year 4000 AD, which forecasts business as usual (BAU) CO_2 emissions until 2100 followed by a linear decrease and zero emissions by 2300 totalling 5100 GtC release. They found that atmospheric CO_2 peaked around year 2300 at more than 2000 ppmv and had declined gradually to 1700 ppmv by year 4000. The model predicted a surface warming of $\sim$10°C , ocean circulation collapse and the melting of sea ice to 10 percent of its former area by year 4000. The delay between peak emissions, peak atmospheric CO_2 and peak temperatures reported in Schmittner et al. (2008), along with many other studies which contributed to the IPCCs assessment reports, shows that temperature will continue to rise and the climate continue to be affected long after CO_2 emissions cease or start to decline, whenever that may be.

The lifetime of carbon dioxide in the atmosphere

Atmospheric CO_2 lifetime is a topic of debate as estimates range from 200 years (Prentice et al., 2001) to 35 000 years (Archer, 2005), prompting the need for study focussed on the longer term, in order to gauge the effects of CO_2 centuries after its emission. The perturbation lifetime of CO_2 is difficult to calculate as many different processes influence its existence in the atmosphere, over different time–scales. Terrestrial sinks such as soil respiration and vegetation act over decades to centuries whereas ocean uptake and $CaCO_3$ compensation dominate over periods of 10 000 years. The shorter-term processes are thought to contribute to the removal of up to 80 percent of anthropogenic CO_2 from the atmosphere over 300 – 400 years leaving the remaining percentage in the atmosphere for thousands of years, explaining some of the variation between lifetime calculations (Montenegro et al., 2007). Montenegro et al. (2007) modelled the effects of a pulse of carbon (5000 Pg) on the atmosphere over the long term. They found that the average perturbation lifetime of 75 percent of the CO_2 emissions was 1800 years and the remaining 25 percent, +5000 years.

Zickfeld and Herrington (2015) also suggest that it indeed takes decades to centuries for the full warming effect of a CO_2 emission to felt, and depends heavily on the size of the emission. Although, they stress that the majority of the warming is felt within the first decade or so. This research emphasises both the importance of mitigating CO_2 in the short term as well as considering its long-term nature, once in the atmosphere.

Carbon dioxide release in the context of the aviation industry

When calculating the RF of aviation CO_2 it is necessary to include historical data; as CO_2 emissions are cumulative in the atmosphere, a calculation where historical activity was not included would give an underestimation of the impact of aviation. Between 1940 (used as the starting point for major aviation activity) and 2005 the integrated CO_2 emissions from aviation were 21.3 Pg CO_2 , which corresponds to 2.1 percent of fossil fuel CO_2 emissions over the same period. Aviation emissions are estimated to contribute 34.6 Pg in 2020 (Lee et al., 2009). Integrating the radiative forcing of aviation CO_2 since 1940 gives values of 23.4 mW m^{-2} (Fichter, 2009), 24.3 mW m^{-2} (Sausen et al., 2005) and 21.7 mW m^{-2} (Stordal et al., 2006). Gillett et al. (2013) note that due to the cumulative nature of CO_2 , no matter what the scenario, location or magnitude of CO_2 release, surface temperatures will rise proportionally in response to an increase in atmospheric CO_2 concentration.

At present, policies regarding aviation CO_2 emissions have had limited success, likely because many emissions are international and fuel tax remains very unpopular. For airlines, the prospect of more fuel-efficient aircraft is attractive as fuel is a major fraction of an airlines operating cost.

Modelling of the carbon cycle and inherent non-linearity

Predicting the future climate is challenging, uncertainties stem from both the unknowns in future greenhouse emissions and in knowing the sensitivity of the climate to the changes in these emissions (Booth et al., 2012). The carbon cycle is inherently non-linear. The non-linearities in the system result from variations in the uptake of CO_2 by the biosphere and oceans, the rate of which varies depending mainly on partial pressure of atmospheric CO_2 and land use change (Jones et al., 2013; Khodayari et al., 2013). The IPCC place 'high confidence' in the fact that as atmospheric CO_2 rises, this will lead to an increased uptake by the biosphere and oceans, but there is a question as to, by how much? In their latest report (AR5, IPCC 2015) however, they note that as climate continues to change, the fraction of uptake of CO_2 by the land and oceans will decrease over time, compared to a scenario where climate remains constant (Ciais et al., 2013). Jones et al. (2013) report that all the models in the CMIP5 (Coupled Model Intercomparison Project) campaign show an increase in ocean uptake of CO_2 under all four RCP scenarios as atmospheric CO_2 concentrations rose, while the uptake by the biosphere was shown to either increase

or decrease depending on the future scenario, although overall, it too showed an increase. The CMIP5 models showed a much higher agreement on ocean carbon changes than those in the biosphere, and it was concluded that the major uncertainties in the projected forcing stemmed from the concentration scenarios rather than the models climate- carbon cycle processes (Jones et al., 2013). The IPCC place 'low' confidence in the understanding of high latitude land carbon sinks, due to additional factors such as permafrost, and conclude that models are correctly predicting the sign of land carbon sinks (increasing) but remain uncertain on the magnitude (Booth et al., 2012; Ciais et al., 2013). Booth et al. (2012) propose that the biosphere process that yields the highest uncertainty is the sensitivity of photosynthesis to temperature changes and is thus one of many aspects that require further study. They also note that study of the biosphere and it's predicted role in future climate and CO_2 cycling is not aided by the lack of global CO_2 observations and measurements (Booth et al., 2012).

When calculating the impact of anthropogenically released CO_2 , one must be knowledgeable of the background concentrations in order to ascertain the impact of additional CO_2 emissions to the atmosphere. The preferred method when modelling the impacts of aviation is to subtract the background from a perturbation scenario to highlight the impact of aviation, therefore it is important that models representing the carbon cycle take into account the non-linearities associated with increasing CO_2 concentrations in the background atmosphere. When modelling the carbon cycle, uncertainties stem from several factors: the size of the emission pulse being modelled, the state of the background atmosphere into which the pulse is emitted (which includes future scenarios), the model used and its carbon cycle climate feedback routines.

2.3.2 Nitrogen Oxides (NO_x)

Nitrogen oxide emissions result from aviation as molecular nitrogen (N_2) dissociates as high temperature aircraft engines pass through the atmosphere. Only a small proportion of NO_x emitted globally sources from aviation. However, it is the altitude at which aviation NO_x is emitted (8–12 km) that is of greater importance as it presents as a precursor of ozone (O_3) a major greenhouse gas, and impacts on methane (CH_4) chemistry in the upper-troposphere lower-stratosphere (UTLS) region (Azar and Johansson, 2012). It has been well established that NO_x emissions from aviation are a substantial effect of the industry (Hidalgo and Crutzen, 1977; IPCC, 1999) and that the exact chemistry resulting

from NO_x release is still not entirely understood (Sausen et al., 2005; Forster et al., 2007). Aircraft NO_x emissions exist throughout the lower atmosphere with the highest concentrations present at cruising height (8–12 km) (see Chapter 5). This is due to the fact that aircraft burn more fuel, and therefore release most of their emissions whilst cruising. The magnitude of NO_x emissions from aviation depend on the altitude and geographical location of the aircraft (Dessens et al., 2014), along with the combustion features of the engine; temperature, pressure and design. The amount of NO_x (NO_2) emitted per kilogram of fuel, the emission index ($EINO_x$), is currently $\sim$12.9g for the global fleet (Fichter, 2009). Only remaining in the UTLS for a matter of weeks, unlike CO_2 , NO_x emissions are not globally homogeneous; therefore, concentrations of NO_x build up along flight routes (IPCC, 1999). When an aircraft flies through the atmosphere NO_x emissions can form through four different pathways:

- The thermal route – the high temperatures of an exhaust plume allow the thermal dissociation of molecular nitrogen (N_2) and oxygen (O_2) into atomic states N, O. These atoms can then react with molecular nitrogen and oxygen as in equations 2.1 and 2.2.

$$N_2 + O \rightarrow NO + N \tag{2.1}$$

$$N + O_2 \rightarrow NO + O \tag{2.2}$$

- The prompt route – in fuel rich conditions, N_2 reacts with HC radicals forming HCN which then assists in the formation of NO_x .
- The fuel-bound nitrogen route – more complicated but less important than the thermal route, this route involves the reactions of fuel-bound nitrogen with O_2.
- The nitrous oxide route – molecular nitrogen reacts with atomic oxygen and a third body (M) via reaction 2.3 (Lee et al., 2009).

$$N_2 + O \rightarrow M + N_2O + M \tag{2.3}$$

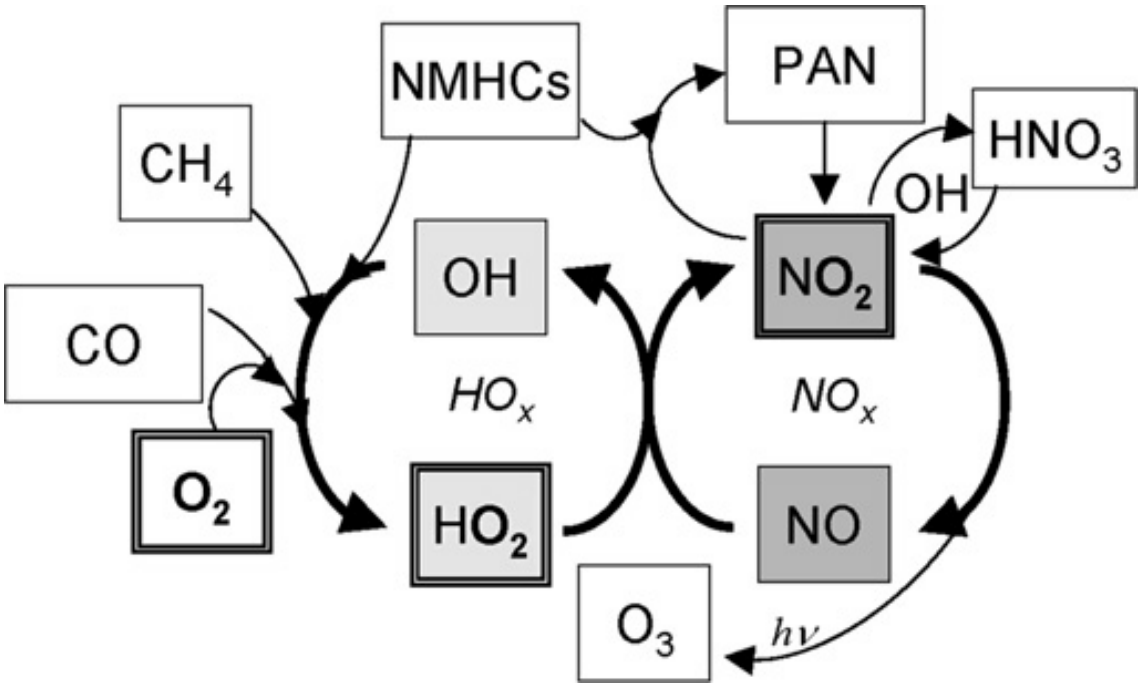

Figure 2.2: Ozone chemistry in the troposphere (taken from Lee et al. (2010).

Ozone (O_3)

Approximately 90 precent of the atmospheric ozone resides in the stratosphere, forming constantly through dissociation of O_2, where it filters the harmful UV rays emanating from the sun. NO_x release from aircraft results in the formation of O_3 in the UTLS through equations 2.4 to 2.15 with the concentrations of O_3 produced depending highly on the altitude of initial NO_x release and available precursors (Gauss et al., 2006). Were aircraft to fly in the stratosphere, as has been suggested historically, the associated NO_x emissions would result in O_3 destruction and therefore deplete the ozone layer (Lee et al., 2010). In the troposphere however, where the majority of aviation takes place, ozone is a strong absorber of thermal radiation – a greenhouse gas – and Figure 2.2 demonstrates how it interacts with the surrounding tropospheric chemistry. Ozone gas is more prominent as an absorber at the altitude of the UTLS (9 – 13km) than at lower altitudes, therefore any O_3 produced at this altitude will increase RF more that if it were emitted at ground level. The radiative forcing of O_3 produced by aircraft emissions was calculated to be 21.9 mW m^{-2} for the year 2000 (Sausen et al., 2005). O_3 concentrations were estimated to be 6 percent higher at cruise altitudes in northern mid-latitudes in comparison with regions not influenced by aviation chemistry, by the IPCC in 1992 and this is predicted to increase by a further 7 percent by 2050 (IPCC, 1999).

Per NO_x molecule, ozone production is most efficient in mid-latitudes at the UTLS. This is due to low HO_x concentrations, low background NO_x levels and high NO/NO_2 ratios (Fichter, 2009). Ozone formation is affected by both the aircraft NO_x emissions and subsequent changes to the OH radical and is shown in equation 2.4 to equation 2.9. The photo-dissociation of NO_2 releases the highly reactive atomic oxygen (O(3P)) which subsequently reacts with molecular oxygen (O_2) (Fichter, 2009). The reaction rates are controlled by background concentrations of NO_x and HO_x (IPCC, 1999).

$$OH + CO \rightarrow H + CO_2 \tag{2.4}$$

$$H + O_2 + M \rightarrow HO_2 + M \tag{2.5}$$

$$HO_2 + NO \rightarrow NO_2 + OH \tag{2.6}$$

$$NO_2 + hv \rightarrow NO + O\ (3P) \tag{2.7}$$

$$O(3P) + O_2 + M \rightarrow O_3 + M \tag{2.8}$$

$$\text{Net: } CO + 2O_2 \rightarrow CO_2 + O_3 \tag{2.9}$$

(Where M is a third body and O(3P) is atomic oxygen in the ground state.) Additional NO_x in the system perturbs the ratio of HO_2:OH in favour of OH, predominantly though reactions in equation 2.10 and through equation 2.11 and equation 2.12 which are then reinforced through the O_3 produced in the reactions of equation 2.4 to equation 2.8. OH promotes the oxidation of CO (and other hydrocarbons) leading to the enhancement of ozone, show by the net reaction in equation 2.9.

$$NO + HO_2 \rightarrow NO_2 + OH \tag{2.10}$$

$$O\ (1D) + H_2O \rightarrow 2OH \tag{2.11}$$

$$O_3 + HO_2 \rightarrow OH + 2O_2 \tag{2.12}$$

Currently, additional NO_x emissions to the background mixing ratio from aviation are resulting in increased O_3 formation in the troposphere and will continue to do so as long as there are sufficient hydrocarbons available for oxidation, such as CO. The IPCC (IPCC, 1999) reported NO_x mixing ratios of 50 – 200 pptv in the upper and mid troposphere and at these levels, and additional NO_x causes an almost linear increase in O_3 production rate at current levels of aviation (see Chapter 5). The IPCC (IPCC, 1999) calculate an O_3 perturbation of up to 12 ppbv due to aviation in flight corridors and northward latitudes. In the lowermost stratosphere at higher latitudes, the background NO_x levels are much

higher and this causes a loss of HO_x through equation 2.13 and equation 2.14 therefore depleting O_3 precursors, in turn leading to a decrease in O_3 production rate.

$$OH + NO_2 \rightarrow M + HNO_3 + M \tag{2.13}$$

$$HO_2 + NO_2 + M \rightarrow HNO_4 + M \tag{2.14}$$

A large increase in background NO_x levels will therefore eventually lead to a decrease in O_3 production in the troposphere. A major focus of this PhD is to model the atmosphere with different background NO_x levels in order to study the effects of O_3 production in different background atmospheres and the results are discussed in Chapter 5. Ozone production varies according to season, the increased sunlight in the summer leads to higher ozone concentrations produced photochemically from NO_x , whereas in winter flights can shift northward without a high O_3 penalty, due to the lack of sunlight.

Methane (CH_4)

NO_x emissions increase the oxidation capacity of the surrounding atmosphere which results in a local decrease in ambient methane (CH_4) concentrations (reaction 15). The aviation induced O_3 and CO increase the levels of OH, particularly in the tropics, thus, causing a decrease in CH_4 lifetime (Holmes et al., 2011). NO_x emissions lead to an increase in OH through equation 2.10 and equation 2.11, reducing methane concentrations through equation 2.15.

$$CH_4 + OH \rightarrow CH_3 + H_2O \tag{2.15}$$

The different lifetime of O_3 and CH_4 mean that the lifetimes of the associated chemical perturbations associated with the decay of a pulse emissions, are also different, approximately 1 month and 10 - 12 years respectively. This shows the time–scales over which tropospheric chemistry would change in response to a change in aircraft emissions (Fichter, 2009) (Lee et al., 2010). Methane is another strong greenhouse gas and therefore any reduction in its concentration leads to a negative radiative forcing, which has been estimated at -12.5 mW m^{-2} for the year 2005 resulting from aircraft emissions (Lee et al., 2009). Methane reduction also has a longer term effect on O_3 . As CH_4 , along with CO, is an ozone precursor, reductions in its concentration decreases ozone formation over the longer term (Stevenson et al., 2004).

2.3.3 Stratospheric Water Vapour

Another secondary effect of the release of aviation NO_x emissions is a decrease in stratospheric water vapour (SWV). The oxidation of methane in the atmosphere leaves water vapour as an end product, therefore a decrease of CH_4 due to aviation NO_x also results in a decrease of water vapour both in the troposphere and stratosphere. The troposphere has a very high water vapour content, therefore a small decrease goes relatively unnoticed, however the relative dryness of the stratosphere means that even a small decrease is significant as $\sim$25 percent of SWV increase is the result of CH_4 oxidation (Khodayari et al., 2014). Until the 21st century, SWV was thought to be increasing, estimates suggests the amount had doubled since the 1950s, however uncertainties surrounding this estimate are high as there are no long term global observations of SWV (Myhre et al., 2007)

2.3.4 Nitrates and the Effects of Aerosols

Aviation emissions also include an aerosol component which derives from the burning of fossil fuel. Some modelling studies suggest that nitrate aerosol formation is increased slightly as a result of aviation NO_x emissions (Barrett et al., 2012; Khodayari et al., 2014). The lifetime of aerosols in the troposphere is on the order of days to weeks, thus, the concentrations respond quickly depending on levels of precursor emissions (IPCC, 1999). Aerosols such as nitrate and ammonium contribute to the scattering of incoming UV radiation, therefore, an increase in aerosol concentration will likely provide a negative RF. Black carbon is the exception as this absorbs solar radiation, thus giving a positive RF (Bauer et al., 2007).

The main precursors of nitrate aerosols in the atmosphere are ammonia and nitric oxide, both of which source from natural and anthropogenic emissions, including aviation. At present, many global chemistry models still exclude ammonium nitrate when calculating aerosol radiative forcing, showing the need for further research in the area (Bauer et al., 2007). However, there is no source of ammonium nitrate in the atmosphere at the altitude of cruise level, the only sources are at ground level, therefore the products have a steep vertical profile and are washed-out of the lower troposphere in about five days, interacting minimally, if at all with the middle troposphere. In their 4th assessment report the IPCC suggest a radiative forcing value of -10 ($\pm$ 10) W m^{-2} for nitrate aerosols but acknowledge that an insufficient number of studies have been undertaken on the topic, leading to the

high uncertainty associated with this value (Solomon et al., 2007).

Additionally, tropospheric aerosols provide cloud condensation nuclei (CCN), affecting the coverage and properties of clouds (McGuffie and Henderson-Sellers, 2005). The majority of uncertainty in assigning aviation RF comes from contrail formation and aviation induced cloudiness (AIC). The longer an aircraft spends in the troposphere, the more likely it is to pass through a supersaturated region and produce persistent linear contrails (Irvine et al., 2013). These persistent linear contrails often spread to form aviation induced cirrus clouds as well as supplying additional CCN for further cirrus cloud development, all contributing a positive RF (Dessens et al., 2014).

2.4 The Trade-off Between CO_2 and NO_x and Mitigation Potential for Aviation

When a carbon based fuel is burnt in a combustion engine, some of the products are unavoidable, for example CO_2 and water vapour. Other products, such as NO_x , CO and VOCs, depend on the combustion characteristics and some on the composition of the fuel i.e. SO_x (Dessens et al., 2014). Measures can be put in place to reduce the amount of CO_2 emitted from an aircraft engine; more complete combustion can be accomplished by increasing the engine pressure ratio, which reduces fuel flow and therefore, CO_2 emissions. However, increasing the engine pressure ratio results in higher combustion temperatures, more dissociation of nitrogen and therefore higher NO_x emissions. Changing the configuration of the combustor to reduce NO_x emissions results in more unburnt hydrocarbons, thus increased CO_2 emissions (Antoine and Kroo, 2004). Reducing the amount of NO_x formed in an aircraft combustor is still a major challenge, mainly due to the number of variables which influence NO_x formation but also due to the rigorous safety requirements of the industry. Another factor is the time taken to implement new technology into the fleet which happens over decades due to the long lifetime of an individual aircraft of over 30 years for passenger aircraft and around 45 years for freight (Owen et al., 2010). Unfortunately, as technology stands in the present day, the trade-off of reducing either CO_2 or NO_x results in an increase in the other.

Changing the cruise altitude of an aircraft also influences the emissions released; in the case of ozone, a higher cruise altitude increases the aviation induced ozone perturbations,

due to a longer lifetime of ozone precursors at higher altitudes, whereas a lower cruise altitude reduces the amount of ozone formed due to a faster removal of ozone precursors at this level (Gauss et al., 2006; Koehler et al., 2008). Lower cruise altitudes also slightly increase the reduction in methane lifetime, due to enhancement of OH. In their multi-model study, Stordal et al. (2006) found that due to the combined CO_2 , O_3 and CH_4 effects, a lower cruise altitude reduced RF by 3.7 – 7.8 percent for the year 2000 whereas higher cruise altitudes increased RF by 1.3 – 2.6 percent. These results were connected to a high degree of uncertainty, however, it demonstrates that cruise altitude is one of many factors that can influence the composition of aircraft emissions.

As for CO_2 , its long lifetime ensures it is well mixed throughout the atmosphere, therefore the altitude of its release does not affect the global RF resulting from aviation. However, being directly linked to the amount of fuel burnt, the extent of emissions release is connected to the route of the aircraft, headwind and drag, thus, lower cruise altitudes would likely lead to more fuel being burnt and therefore more CO_2 being released.

2.4.1 Policy

Recently there has been renewed interest in mitigating SLCF emissions release as CO_2 policies are becoming costly and the effects of such policies will not be apparent in the near term. There is also the necessity for international agreement concerning any CO_2 policy and concern that the 2°C global temperature rise target may now be unachievable. The reduction of SLCF such as methane, NO_x , ozone and BC, as well as being the cheaper option, have several additional benefits such as reduced air pollution and soot emissions. Also, many countries have already pledged to reduce methane under the UNFCCC agreements and are permitted to reduced methane emissions before dealing with CO_2 emissions. There is a danger that with the focus on mitigating SLCFs, CO_2 emissions will be overlooked. Due to the cumulative nature of CO_2 it is imperative that CO_2 emission release is also reduced in order to avoid catastrophic climate change in the future (Allen et al., 2016).

Regarding policies that concern the reduction of short–lived greenhouse gases compared to long–lived, ultimately it depends on time-scale. There is less importance placed on reducing short–lived greenhouse gases now when the targets to be met are far into the future. In terms of GWP it has been suggested that a short term greenhouse gas such as

methane should increase in value, compared to CO_2 , as we approach the mitigation target year (Johansson et al., 2008). Besides the obvious reasons for the long–term reduction of anthropogenically emitted CO_2 , there are arguments which suggest more focus should be put on the reduction of short–lived forcers (Hansen et al., 2000; Jacobson, 2002). For example, Boucher and Reddy (2008) investigate the trade-offs between CO_2 and black carbon (BC) reduction and find that in the short term (20 – 30 years) the temperature change from the reduction of BC is greater than that from CO_2 reduction, however, CO_2 reduction shows more climate benefits over the long term (50 years+).

When considering mitigation options in relation to aviation, policy makers face the pressure of balancing environmental considerations with economic and social consequences that would accompany a reduction or change in the aviation industry. For countries whose economies depend on air travel and tourism, constraining aviation growth for climate reasons could cause losses in economy and disruptions in development (Gossling and Upham, 2009). For transatlantic flights (northern hemisphere) there is high dependency on the position of the jet stream. It influences route choice and therefore affects the amount of fuel burnt and the length of the flight. Eastbound flights can use the winds of the jet to cut the time of a flight and use less fuel whereas westbound flights must use a route which avoids the jet stream in order to avoid headwinds, this means that flights take longer and must use more fuel. In summer, the jet is weaker and often shifted northwards. Westbound flights will always contribute more to emission totals for the reasons explained here (Irvine et al., 2013).

Huntingford et al. (2015) note that changes in lifestyles and technology may make it preferable to abate one greenhouse gas over another, for the purpose of this study and the aviation industry this is where the CO_2 versus NO_x debate becomes important. Huntingford et al. (2015) also suggest that focusing on short–term climate–forcers effectively ignores the long–term CO_2 mitigation issues and that the abatement of short–term forcers is only really effective in mitigating climate change if CO_2 emissions are abated also.

Chapter 3

Modelling of Aviation NO_X Emissions and the Composition of the Background Atmosphere – scenarios and emissions

This chapter outlines the factors involved in modelling aviation NO_x emissions and the importance of the background atmosphere, before discussing the aviation emissions data and scenarios used in the experiments presented in Chapters 5–7.

3.1 Modelling the Composition of the Atmosphere Using Chemistry Transport Models (CTMs)

Computer models are an effective tool used to simulate possible future climatic states and therefore, the impacts of climate change (McGuffie and Henderson-Sellers, 2005). Over the last decade, technological progression has allowed the advancement of computer models that replicate the atmospheric features necessary to study the effects of changes in atmospheric composition, and thus the impact of those changes on climate.

These computer models have been developed in a variety of forms, specific to type of study, ranging in complexity from energy balance models (EBMs) and simple climate models (SCMs) to general circulation models and global climate models (both GCMs). For the study of atmospheric chemistry there are chemistry climate models (CCMs) and

chemistry transport models (CTMs) such as the MOZART model used in this study. Chemistry transport models (CTMs) simulate the chemistry of the atmosphere and have been developed in order to simulate the transport and reactions of most chemical species. Models can be run off–line using a previously run, complete meteorological simulation or on–line where various chemical and physical components can be coupled during the run. Uncertainty is inherent to computer modelling, results and output vary between different models mainly due to the differences in programming and inbuilt chemistry and transport, this is discussed in Section 3.1.2.

Evidence from ice cores, ocean sediments and other climate proxies have shown a clear increase in some of the key greenhouse gases (Schleser et al., 1999; Mann, 2002), modelling can be used to forecast the effects of change in these gases on the atmosphere and therefore on the climate. The simulation of the tropopause and UTLS is critical when modelling atmospheric chemistry and particularly for this study as it is in these regions that most aircraft cruise and consequently release emissions. Radiative processes and vertical concentration gradients are particularly strong in the UTLS making it a region of complex chemistry and emphasising its importance in modelling studies. Chemical exchange across the tropopause is heavily affected by mixing processes and synoptic scale events, presenting a challenge for climate models (Kinnison et al., 2007). An example of the sensitivity of the UTLS is given in Douglass et al., (1999), as they show that different meteorological field inputs to a model can produce a variation in concentrations of particular species in the UTLS relating to aircraft emissions released at the same level.

3.1.1 Modelling aviation NO_x emissions and their effects

For this study, the molecule of most concern for modelling is NO_x emitted from aviation at cruise level, the influence of which depends heavily on the background atmosphere into which it is being emitted (see Chapter 5). Aviation NO_x emissions have a complex effect on chemistry in the UTLS, they create a warming due to associated ozone formation, a longer term cooling due to ambient methane reduction and longer term cooling by reducing tropospheric ozone and stratospheric water vapour (see Chapter 2). Current consensus suggests that despite these cooling effects, aviation NO_x is still thought to have an overall warming radiative effect on the atmosphere, however with increased understanding of methane and aerosols, some recent studies have concluded an overall negative RF from aviation NO_x under certain conditions (Skowron et al., 2015). This emphasises the com-

plexity of modelling aviation NO_x as there are many factors contributing to the overall NO_x effect, all introducing further uncertainty.

Holmes et al. (2011) imply that many uncertainties of modelling NO_x and its effects stem from the reliability of background tropospheric NO_x concentrations. They calculated that modelled results of the induced changes in O_3 due to aviation NO_x varied by up to 100 percent due to differences in modelled background conditions as well as differences in chemical schemes, particularly involving NO:NO_2 and OH:HO_2 chemistry, atmospheric mixing, location and time of emissions and the amount of sunlight. Koehler et al. (2013) also suggest that accurate model results require correct current surface NO_x emissions, as well as reliable convective uplift schemes and lightning parameterisations.

Wild et al. (2001) modelled NO_x emissions sourcing from both anthropogenic and natural sources and found that while overall NO_x emissions contribute a negative RF, and therefore cool the atmosphere, those emissions from the aviation sector alone (predominately in the northern mid-latitudes upper–troposphere), contribute a positive RF as, at these altitudes, the rate of ozone production is greater than that of methane reduction. Stevenson et al. (2004) chose to model the effects of aviation by introducing pulses of aircraft NO_x into simulations run on the HadAM3-STOCHEM chemistry climate model. They found that the emissions pulse created both a positive and negative radiative forcing, the positive sourcing from a short–lived increase in ozone concentration (a few months) and the negative from a longer lived decrease in ambient methane concentrations. The results of Stevenson et al. (2004) also showed the negative anomaly in ozone concentration resulting from the long lifetime of methane but overall, the long–term globally integrated annual mean net forcing was calculated to be approximately zero.

The current consensus is that the overall aviation NO_x effect consists of four main factors, short term ozone burden change, direct methane lifetime change, long lived ozone change due to methane and the change in stratospheric water vapour (SWV). These four factors are used to calculate the effects of aviation NO_x in Chapters 5 and 6, the method of calculation is described in Chapter 4.

Location of aircraft emission also determines the effects of NO_x release. Changes in altitude, latitude and route all affect the chemistry of the emissions released from aircraft and therefore, the associated radiative forcing (Stevenson et al., 2004; Gauss et al., 2006; Koehler et al., 2008). Koehler et al. (2008) have shown that the effects of aircraft NO_x differ with altitude as ozone production efficiency increases with height (Figure 3.1 Lacis

et al. (1990)). Their results show that emissions released at 11 km lead to an ozone increase which is 200 percent larger than if the emissions were released at 5 km. The methane lifetime reduction was also shown to be affected by altitude, as the reduction was 40 percent stronger when emissions were released at 11 km than at 5 km. Gauss et al., (2006) concluded that increased use of polar routes will substantially increase ozone concentrations during summer in the northern hemisphere. They also noted that lowering cruise altitude will cause an increase in ozone concentrations in the troposphere, whilst raising cruise altitudes could lead to build up of ozone in the UTLS.

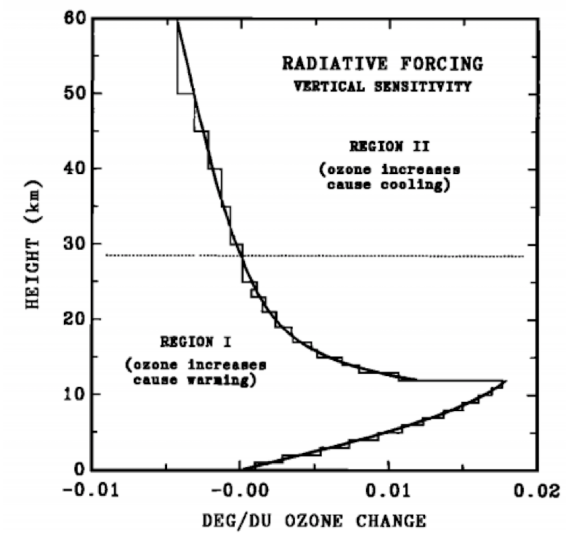

Figure 3.1: Radiative forcing sensitivity of global surface temperature to changes in vertical ozone distribution. The heavy solid line is a least squares fit to one dimensional model radiative convective equilibrium results computed for 10 Dobson unit ozone increments added to each atmospheric layer. Taken from Lacis et al., 1990.

Skowron et al. (2013) note that uncertainties can also arise from the different data sets used. They found that net RF for aviation NO_x emissions could vary by up to 94 percent when six different data sets were run on the same model, resulting in a GWP value ranging from 4 – 60. They concluded that the placement of cruise altitudes and the resulting emissions within a scenario had the greatest impact, thereby emphasising the importance of 'chemically sensitive cruise altitudes'.

3.1.2 Uncertainties and limitations of modelling

"Uncertainty is not a weakness. Understanding uncertainty is a strength, and a key part of using any model, including climate models." Gettelman and Rood (2016)

Climate models are becoming an important tool for policy decisions as well as understanding the earth system. Each model run contributes valuable scientific understanding, however, climate models are limited as they cannot account for every single factor of the earth system, and those factors which are included are not always completely understood (Maslin and Austin, 2012; Gettelman and Rood, 2016).

The internal variability of the climate system is chaotic and contains natural variations that are difficult to capture in climate models. The main criticism of global climate models is their inability to resolve small, sub-grid scale features, crucial to the understanding of weather phenomenon e.g. precipitation and evaporation features, surface wind variability, jet streams, cloud physics and local atmospheric circulation patterns. All of these processes, plus those of which there is insufficient understanding, are represented in models by parameterisations (Lahsen, 2005; Christensen et al., 2007). Modelling studies compare simulation output with that of other models as well as observational data to quantify the accuracy of the results.

Further uncertainty comes from the variation between models, known as 'response uncertainty', as different models will produce slightly different outcomes in climate given the same initial input data. The uncertainty perhaps most relevant to this study is that which accompanies the input scenarios. In order to forecast into the future, models need a scenario which contains expected greenhouse gas and aerosol accumulation and these are generally based on economic factors such as predicted fossil fuel use and the introduction of green technology, both of which are notoriously difficult to predict (Maslin and Austin, 2012). Another source of uncertainty comes from international emissions inventories, whereas measurements from a point source, such as a power station, in northern Europe may provide a reliable dataset, those from developing countries may not be as reliable or even available. This can lead to a large uncertainty when developing data sets of global anthropogenic ground based emissions, that provide the background conditions for many climate modelling studies (Lamarque et al., 2010)

The literature emphasises that there are still many uncertainties associated with the modelling of aviation NO_x emissions. It is suggested that the location and altitude of emission

is important within an aviation scenario in order to obtain accurate results from the models used to simulate them. For long range projections of large spatial scale (global) such as the ones undertaken in this study the main uncertainties will come from scenario uncertainty and model uncertainty, whereas internal variability of the climate will be the greatest source of uncertainty for shorter, decade long, regional scale studies.

3.2 Background Emissions and the Representative Concentration Pathways (RCPs)

The model runs in this study use data from the representative concentration pathways (RCPs) to represent the background atmosphere. These are scenarios of future anthropogenic activities developed by the research community and used to study the interaction between earth's natural systems and human activity. In this study they are used as the background concentrations when investigating CO_2 emissions into the future and provide alternative NO_x background concentrations in MOZART-3. There are four main RCP scenarios created by four Integrated Assessment Models (IAMs) based on multi-gas emission scenarios from the literature and trends in driving forces e.g. technology development, economic growth and population growth. (Moss et al., 2010). They range from a high mitigation scenario which forecasts the smallest impact to climate (RCP 2.6), through business as usual (RCP 4.5) and higher climate impact scenarios where emissions continue to increase (RCP6 and 8.5) (Table 3.1).

The study of future climate requires the use of both emissions scenarios and climate scenarios. Emissions scenarios describe the release of radiatively active species into the atmosphere, and provide an input for climate models. They can also be used to investigate new technology measures, alternative energy sources and RF limits. Emissions scenarios are not predictions but reflect the most current research regarding plausible future emissions release. Climate scenarios are designed to represent possible future conditions of the climate such as average precipitation and temperature (Moss et al., 2010). They are particularly useful for assessing anthropogenic contribution to climate change, and investigating related mitigation measures. The emissions scenarios used in this study are described in Section 3.4.1

Scenario	Radiative Forcing	Concentration (ppm)	Pathway	Model providing RCP
RCP 8.5	>8.5 W m^{-2} in 2100	>1370 CO_2 equivalent in 2100	Rising	MESSAGE
RCP 6.0	~6 W m^{-2} at stabilisation after 2100	~850 CO_2 equiv. (at stabilisation after 2100)	Stabilisation without overshoot	AIM
RCP 4.5	~4.5 W m^{-2} at stabilisation after 2100	~650 CO_2 equiv. (at stabilisation after 2100)	Stabilisation without overshoot	GCAM
RCP 2.6	Peak at ~3 W m^{-2} before 2100 and then declines	Peak at ~490 CO_2 equiv. before 2100 then decline	Peak and decline	IMAGE

Table 3.1: Descriptions of the four RCP scenarios: Model for Energy Supply Strategy Alternative and their General Environmental Impact (MESSAGE), International Institute for Applied Systems Analysis, Austria; Asia-Pacific Integrated Model (AIM), National Institute for Environmental Studies, Japan; Global Change Assessment Model (GCAM), Pacific Northwest National Laboratory, USA; and Integrated Model to Assess the Global Environment (IMAGE), Netherlands Environmental Assessment Agency, The Netherlands. From Moss et al. (2010).

3.2.1 RCP2.6/RCP3 (PD)

RCP 2.6 is a high mitigation scenario where global temperature increase is kept below 2°C on average. The name 'RCP2.6' refers to the predicted additional 2.6 W m^{-2} RF that this scenario would add to climate forcing, however the scenario is also often referred to as RCP3 or RCP3 PD. This scenario is considered technically feasible if all countries participate, particularly large emitters such as the USA and China, and global greenhouse gas emissions are cut by 70 percent between 2010 – 2100. In this scenario, emissions from energy use actually become negative after 2050 due to technology advances in carbon sequestration. While fossil fuels will still be a major energy source, it is predicted that the transport sector will become more reliant on hydrogen (Figure 3.2). Although the RCP2.6 scenario is one of high mitigation, greenhouse gas emissions still rise substantially reaching 27 Gt C equivalent by 2100 compared with 11 Gt C equivalent in 2000. To reach the target of 2.6 W m^{-2} by 2050 emissions need to be reduced by 50 percent from 1990 levels and by 2100, CO_2 emissions need to be reduced by over 100 percent and be –1 Gt C Yr^{-1} by 2100. This translates as an annual 4 percent reduction of year 2000 emissions – well beyond historical rates of reduction, with emissions peaking around the year 2020 (van Vuuren et al., 2011; Jones et al., 2013). Theoretically, this is achieved by substituting fossil fuel burning for renewable energy, nuclear fuel and increased CCS (Figure 3.2). The

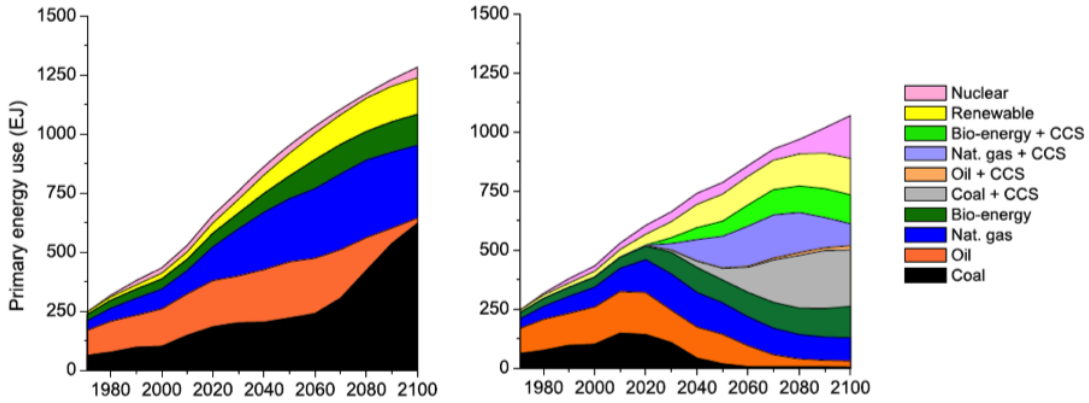

Figure 3.2: Trends in global energy use for the baseline (left) and the mitigation scenario RCP 2.6/3 (right) taken from van Vuuren et al., (2011). The 'baseline' represents scenarios void of climate policy and 'CCS' = carbon capture storage.

reduction of fossil fuel burning, and of coal use in general, has the desirable effect of also reducing emissions of non-CO_2 air pollutants such as sulphur compounds and VOCs. A major assumption in the RCP2.6 scenario is that new technologies are quickly developed and implemented, allowing less reliance on fossil fuels. Another assumption is the political implication of world–wide emissions reductions and policies. Due to the cumulative effect of CO_2 in the atmosphere, much of the temperature and RF rise shown in RCP2.6 is a measure of the damage already done, the unconstrained emissions released up until now.

3.2.2 RCP4.5

The RCP4.5 scenario sees RF stabilise at 4.5 W m^{-2} by 2100, which is equivalent to an atmospheric CO_2 concentration of $\sim$525 ppm and is simulated using the Global Change Assessment Model (GCAM). There are many scenarios that would result in a 4.5 W m^{-2} stabilization at 2100 however, having one defined scenario allows climate model studies to have a standard scenario for comparison projects. RCP4.5 assumes that global emissions mitigation policies are invoked in the early 21st century and are successful in limiting the release of greenhouse gases. As in RCP2.6, it assumes that the world nations unite in reducing climate change, by simultaneously reducing greenhouse gas emissions, also that appropriate technology is developed to allow cost effective mitigation (Thomson et al., 2011).

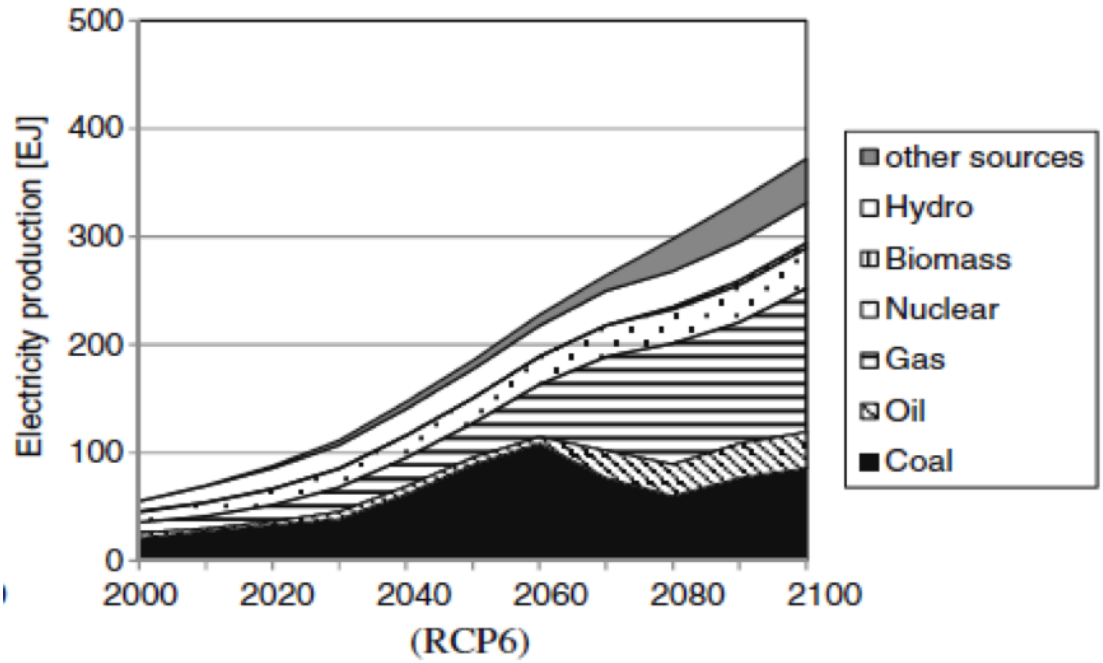

Figure 3.3: Electricity generation by source in the RCP 6 emissions scenario (taken from Masui et al., 2011).

3.2.3 RCP 6

RCP6 is a stabilisation scenario where RF reaches no more than 6 W m^{-2} between 2000 2100, with a peak in major emissions (CO_2 , CH_4 etc.) at 2060 of 17.7 Gt C Yr^{-1}. In RCP6 climate policies prevent RF from exceeding 6 W m^{-2} by mitigating greenhouse gas emissions in the latter half of the 21st century, albeit much less so than RCP2.6 and RCP4.5. The long–term steady–state global mean temperature rise could be expected to be 4.9°C with a CO_2 equivalent concentration of 855 ppm (Table 3.1). Regionally, Asia becomes the biggest emitter releasing 60 percent of the global total CO_2 emissions in 2100, with China and India accounting for 39 percent of the global primary energy supply. Coal production decreases throughout the century in this scenario with energy production shifting towards natural gas, and non-fossil fuel power such as nuclear contributing 30 percent of power by 2100 (Figure 3.3). CCS also becomes prominent, and is implemented in 74 percent of thermal power plants. It is anticipated that a large degree of climate change would result from this scenario (Masui et al., 2011).

3.2.4 RCP 8

RCP 8 does not contain any climate mitigation policies and is therefore classed as a 'baseline scenario' where greenhouse gas emissions are unconstrained and result in a RF increase of 8.5 W m^{-2} by 2100. The scenario is considered a continuation of 'business-as-usual' activity; population continues to increase, reaching 12 billion at 2100. GDP increase is slow as are technology and energy efficiency improvements. The high population creates increasing energy demand, which is focused on coal-intensive production. The technology surrounding fossil fuel extraction does improve and resources that were previously unavailable begin to be exploited. As fossil fuel prices rise, there is some development of hydropower and nuclear energy, however, by 2100 coal use is 10 times year 2000 levels and considerable amounts of oil are still used in the transportation sector.

By 2100 CO_2 equivalent emissions are 120 Gt CO_2 – eq. three times the year 2000 levels. 75 percent of this increase stems from energy sector CO_2 emissions and the rest from increased agriculture and fertilizer needed to meet the growing demands for food, which releases N_2O emissions (Riahi et al., 2011). Studies of the IPCC's A2 scenario, which is similar to RCP8.5, suggest that stabilizing the climate from this type of emissions pathway may not be possible (Rao et al., 2008). In this scenario the options likely to have the most effect regarding stabilizing the climate are switching from coal dependence to natural gas, or better; substituting fossil fuel power for nuclear or renewable and implementing CCS. In order to reduce RF to the levels of the other RCPs, emissions in RCP8.5 would need to be cut by 40 percent, 60 percent and 87 percent to meet with the targets of RCP6, RCP4.5 and RCP2.6 respectively.

3.3 Background Atmospheric NO_x and CO_2 Emissions and Scenarios

3.3.1 Background atmospheric NO_x emissions

The MOZART chemistry transport model (CTM) (see Chapter 4) was run in order to study aviation NO_x emissions. Of interest, is the effect that the background atmosphere has on the ability of NO_x emission to perturb the surrounding atmosphere. For this experiment, two values were chosen from the RCP scenarios for surface NO_x emissions (Figure 3.4),

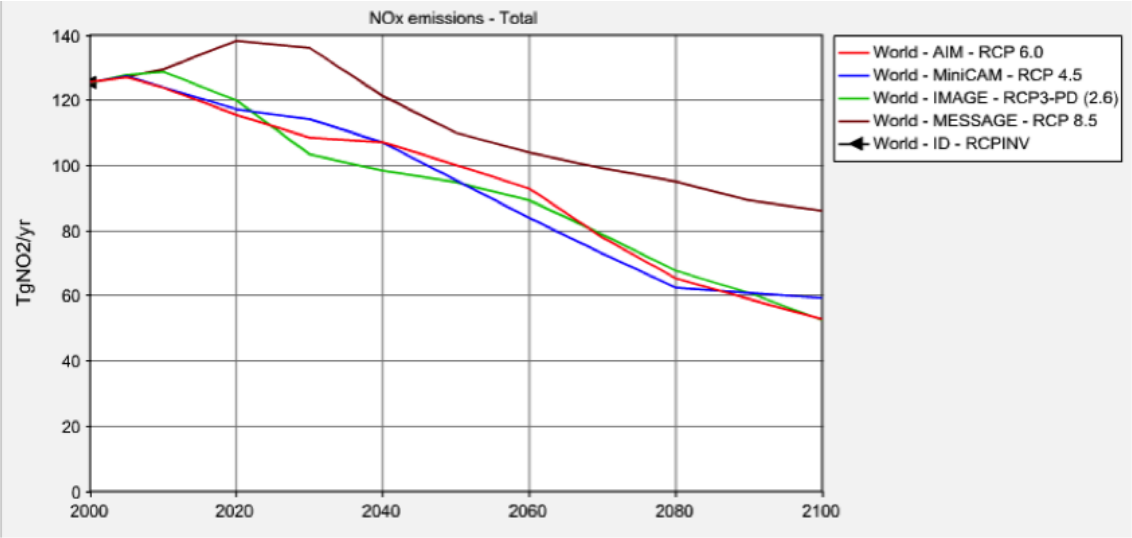

Figure 3.4: Background NO_x emission levels in the four RCP scenarios from the year 2000 - 2100 (http://tntcat.iiasa.ac.at:8787/RcpDb/dsd?Action=htmlpageand page=welcome).

representing a 'low' and 'high' NO_x background (see Chapter 5). The high scenario represents the RCP8 value at 2020 (44 Tg N Yr^{-1}) (note, Figure shows Tg NO_2 Yr^{-1}) and the low scenario represents RCP3 at 2100 (21 Tg N Yr^{-1}). Due to the nature of the MOZART CTM, the background NO_x could not be modelled transiently in this experiment due to constraints on computing time and power, therefore a high and low background NO_x value was modelled in order to create a range, within which actual background emissions are likely to be over the next 100 years.

3.3.2 Background CO_2 concentrations and emissions scenarios

The CO_2 runs were undertaken with the LinClim SCM (see Chapter 4) and experiments will be performed using the transient backgrounds of the RCP scenarios (Figure 3.5) and a constant background of the present day (March 2016) concentration of 404 ppm CO_2 . The constant background value of CO_2 is used to maintain consistency within the experiments, as this is how the NO_x values are modelled, thereby allowing comparison between the two species (see Chapter 6).

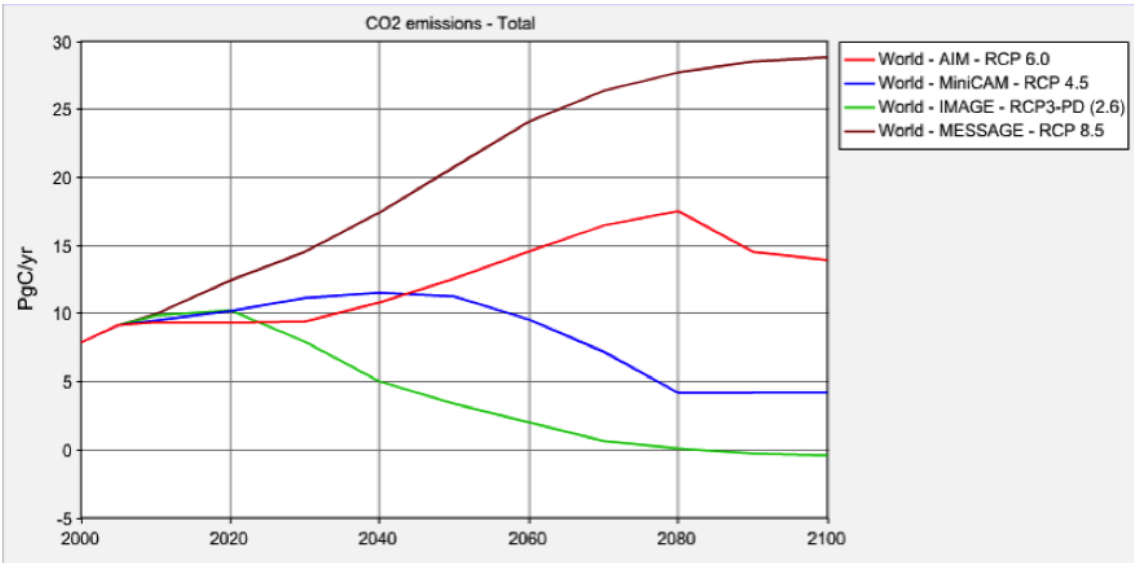

Figure 3.5: Background CO_2 emissions in the four RCP emissions scenarios from the year 2000 - 2100 (http://tntcat.iiasa.ac.at:8787/RcpDb/dsd?Action=htmlpageand page=welcome).

3.4 Current Consensus on Future Aviation Emissions and Aircraft Emissions Data

Most studies anticipate continued growth of the aviation industry, Flemming and Ziegler (2013) show that the growth of the industry is the main driver in the magnitude of effects, and factors such as new technology, new fuel and improved air traffic management (ATM) will determine the range (Figure 3.6). This figure shows the range of anticipated fuel burn for a range of ICAO scenarios, the green dotted line shows the expected fuel burn if ICAOs 2 percent annual fuel efficiency goal was achieved. This is significant in the context of this study, as goals to increase fuel burn efficiency would also result in reducing CO_2 emissions. Aviation is the most convenient way to travel great distances, therefore it is unlikely that demand for aviation will decrease.

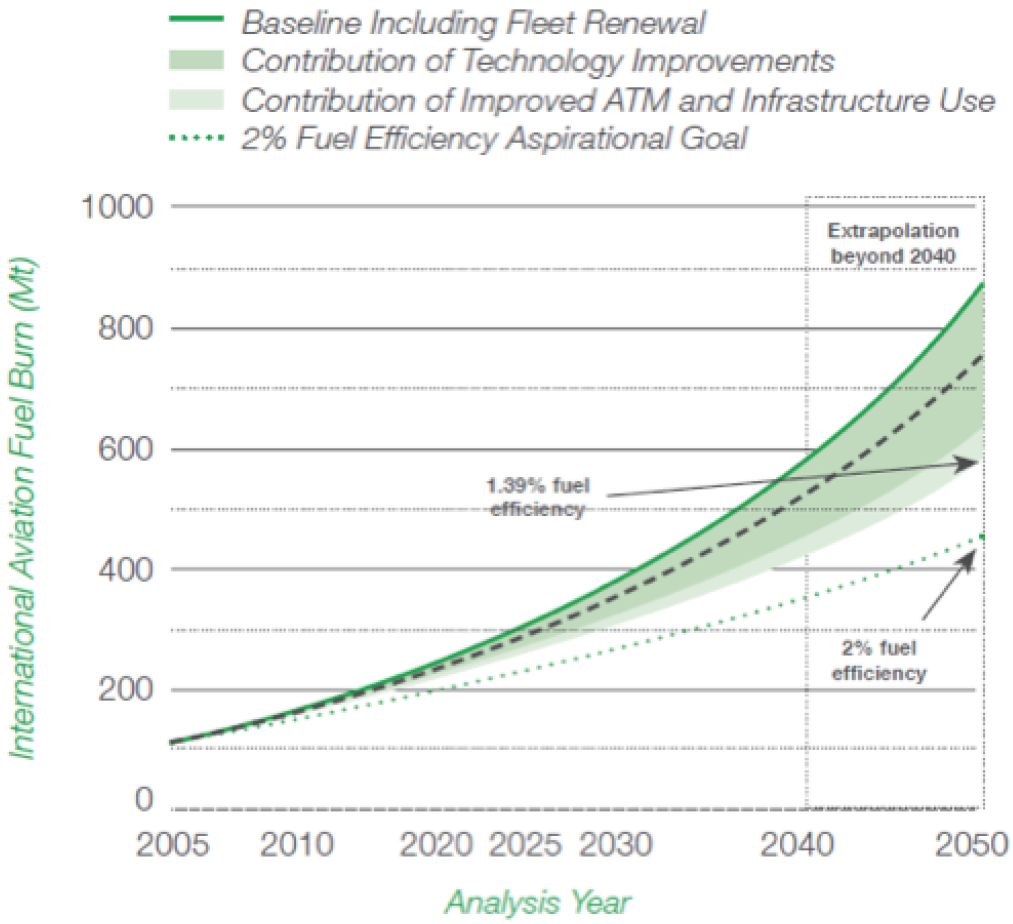

Figure 3.6: ICAO/CAEP fuel trends from international aviation 2005 - 2050, taken from Flemming and Ziegler (2013)

3.4.1 Aviation emissions scenarios

Forecasting into the future is always going to rely on unknown variables but can be sensibly predicted using trends and often, several scenarios are created from a single staring point and can be refined as it becomes clearer as to which route is more representative of real world events. In order to create aviation fuel burn scenarios that extend into the future, a number of variables need to be taken into account. The emissions of concern

in aviation scenarios are CO_2 and NO_x . CO_2 emissions are easy to compute – a simple function of fuel burn, 3.16 kg of CO_2 is released for every 1 kg of fuel burned, conversely NO_x emissions are more complex and depend on temperature, pressure, fuel and ambient air composition (Owen et al., 2010). Essentially, aviation CO_2 emissions are determined by two key variables; the underlying demand and percentage fuel burn improvement, per year, on a fleet wide scale. Within these two variables, uncertainties stem from; demand for fuel, fuel supplies, policy change, perspective technology and efficiency improvements and air traffic management improvements (ICAO, 2009).

The further into the future the scenarios go the more uncertainty occurs, this is mainly due to unknown policies that may come in to force, unknown growth in the industry and changes in the background atmosphere. In the aviation industry there is also the possibility of sudden jumps in technology with the fleet wide implementation of a new fuel or new aircraft yet to be developed along with changes in flight paths and ATM. As aircraft have a long lifetime, new technology may not be introduced gradually but rather as a sudden fleet wide change, or in steps as manufacturers and airlines adopt the technology. Also, annual emissions could drop suddenly due to an unforeseeable event or aviation disaster.

3.4.2 Aviation scenarios for NO_x modelling

In order to assess the effect of aviation NO_x emissions on the atmosphere, aviation scenarios were run with a chemistry transport model (CTM) (see Chapter 4). The aviation scenarios used to run the CTM have come from the European research project REACT4C (www.react4c.eu). The REACT4C data set used here is known as the 'base-case' and comprises of an atmospheric state in which the effect of aviation have been included and a state in which all aviation activities are excluded, representing the 'background' atmosphere. The REACT4C project extrapolated movements data from six representative weeks to one year of data for 2006. The data came from radar information collected from Europe, North America and some parts of South America and this represented about 80 percent of the world's aviation activities. The other 20 percent was obtained from Official Aviation Guide (OAG) data (www.oag.com), which is composed of scheduled flights and timetables (Sovde et al., 2014). Further aviation scenarios were generated using the React4c base case aircraft emissions data set (http://www.react4c.eu/data/) as a starting point, and the value of NO_x emitted in this scenario (0.699 Tg N Yr^{-1}) was multiplied

by different factors to generate several different aviation scenarios each emitting different levels of NO_x (Chapter 5). Table 3.2 shows the current consensus regarding aviation NO_x emissions scenarios up to 2050 and is used to justify the range of NO_x scenarios that are used in Chapter 5.

3.4.3 NO_x emission index ($EINO_x$)

The emission index for NO_x describes the amount of NO_x produced from the fuel used ($EINO_x$ = gNO_x (as NO_2) per kg of fuel burned). Changes in engine technology can reduce $EINO_x$, and therefore NO_x emissions, however, this results in a trade–off between NO_x and CO_2 emissions (see Chapters 2, 6, 7). In order to account for changes in future technology a number of $EINO_x$ scenarios are taken into account in this study, they are described in Table 3.3. The Technology 1 and 2 scenarios are described in (Sausen and Schumann, 2000). Technology 1 assumes conventional technology which results in moderate progress in NO_x production and Technology 2 introduces new technology which in the form of a low NO_x combustor which gradually enters the fleet after 2015.

The ICAO scenarios represent the Medium– and Long–Term Technology Goals (M/LTTG) for NO_x derived during the CAEP 7 process. The original MTTG was to reduced NO_x by 45 percent compared to CAEP 6 values by 2016 and the LTTG was to reduce NO_x by 60 percent compared to CAEP 6 values by 2026, both at OPR 30 (Ralph, 2007). Five NO_x emissions scenarios were derived from these goals, three base cases and two cases based on the technology goals. All are derived from the FESG forecast, scaled to the growth trend used for the IPCC (1999) study, extrapolated to 2050 and then the 2050 value extended to 2100. Base Case 1 (TechBC1LTTG) assumes the current fleet average values, Base Case 2 (TechBC2LTTG) assumes the current best practice and Base Case 3 (TechBC3LTTG) assumes the current best practice with a 0.5 ORP (fuel efficiency) increase per annum. Goals Case 1 (TechGC1LTTG) assumes Base Case 3 from 2020 in line with the Medium Term Technology Goal, and Goals Case 2 (TechGC2LTTG) assumes the same from 2030 in line with the Long Term technology Goal (Newton, 2007). Figure 3.7 shows how NO_x emissions are generated using a single fuel scenario and the effects of different $EINO_x$ values in a simple climate model, in this case, LinClim. This shows the range of NO_x emissions produced from one simple fuel scenario (where fuel use follows observations until 2012 and then increases by 1 percent per year) using different $EINO_x$ scenarios. The following model runs performed in Chapter 6 and 7 will

Year	Scenario/Inventory	NO_x emissions ($Tg\ NO_2\ yr^{-1}$)	EI_{NOx}	Reference
2050	Eab	7.9		Penner *et al.*, 1999
2050	Edh	11.6		Penner *et al.*, 1999
2050	Fa1	7.2	15.2	Penner *et al.*, 1999
2050	Fa2	5.5	11.4	Penner *et al.*, 1999
2050	Fc1	4	15	Penner *et al.*, 1999
2050	Fc2	3.1	11.3	Penner *et al.*, 1999
2050	Fe1	11.4	15.3	Penner *et al.*, 1999
2050	Fe2	8.8	11.4	Penner *et al.*, 1999
2050	IS92a Base (Eab)	7.88		Penner *et al.*, 1999
2050	IS92a High (Eah)	14.39		Penner *et al.*, 1999
2050	IS92c Base (Ecb)	5.77		Penner *et al.*, 1999
2050	IS92d High (Edh)	11.64		Penner *et al.*, 1999
2050	IS92e High (Eeh)	15.84		Fleming *et al.*, 2007
2050	AEDT BASELINE	12.98		Fleming *et al.*, 2007
2050	AEDT SCENARIO1	5.17		Fleming *et al.*, 2007
2050	CONSAVE: Fractured World	3.459		Consave, 2005
2050	CONSAVE: Down to Earth	1.113		Consave, 2005
2050	CONSAVE: Unlimited Skies	7.313		Consave, 2005
2050	CONSAVE: Regulatory Push & Pull (Kerosene)	4.914		Consave, 2005
2050	CONSAVE: Regulatory Push & Pull (H2)	1.382		Consave, 2005
2050	QUANTIFY A1	7.5		Owen *et al.*, 2010
2050	QUANTIFY A2	5.4		Owen *et al.*, 2010
2050	QUANTIFY B1	3.4		Owen *et al.*, 2010
2050	QUANTIFY B2	4.4		Owen *et al.*, 2010
2050	QUANTIFY B1ACARE	2.6		Owen *et al.*, 2010
2100	QUANTIFY A1	15.7		Owen *et al.*, 2010
2100	QUANTIFY A2	11		Owen *et al.*, 2010
2100	QUANTIFY B1	3		Owen *et al.*, 2010
2100	QUANTIFY B2	5.7		Owen *et al.*, 2010
2100	QUANTIFY B1ACARE	1.8		Owen *et al.*, 2010

Table 3.2: NO_x emissions for several different scenarios representing future aviation activities, the red values highlight the scenarios in which aviation NO_x emissions exceed 10 $Tg\ NO_2\ yr^{-1}$.

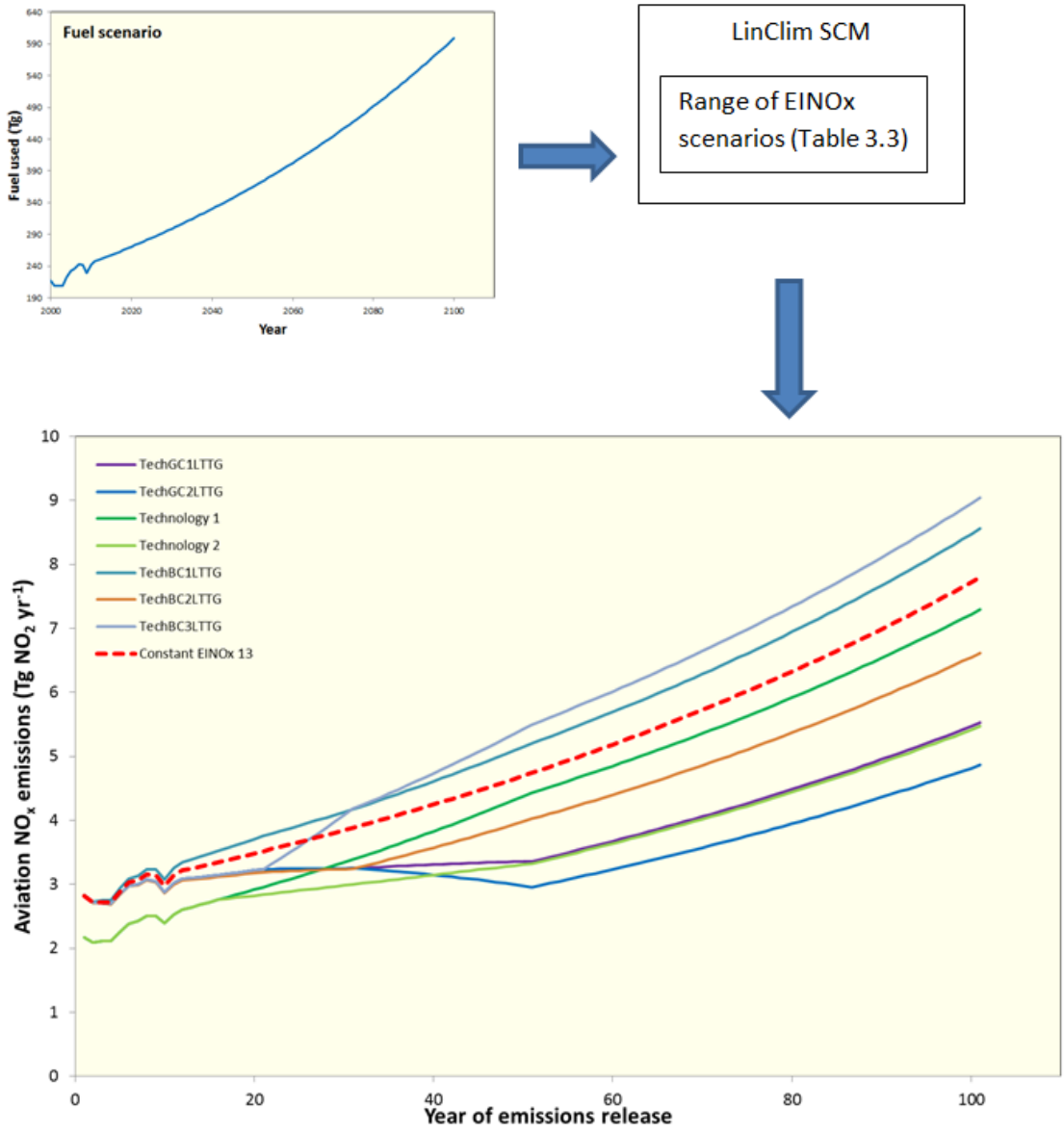

Figure 3.7: The effect of different EINOx values on a single emissions scenario. The emissions scenario used here follows observations of aviation activity until 2012 and then fuel use increases by 1 percent per year until 2100.

Scenario	EINOx										Reference
Year	1976	1984	1992	2000	2015	2020	2030	2040	2050	2100	
Technology 1	9.8	11	12	12.5	13.4	13.6	14.2	14.7	15.2	15.2	Sausen and Schumann 2000
Technology 2	9.8	11	12	12.5	13.4	13.1	12.5	12	11.4	11.4	Sausen and Schumann 2000
TechGC1LTTG	9.8	11	12	13	12.2	12	10.9	10	9.2	9.2	ICAO 2007
TechGC2LTTG	9.8	11	12	13	12.2	12	10.9	9.5	8.1	8.1	ICAO 2007
TechBC1LTTG	9.8	11	12	13	13.7	13.8	14	14.1	14.3	14.3	ICAO 2007
TechBC2LTTG	9.8	11	12	13	12.1	11.8	10.9	10.9	11	11	ICAO 2007
TechBC3LTTG	9.8	11	12	13	12.2	12	14	14.5	15.1	15.1	ICAO 2007

Table 3.3: The main EINOx scenarios taken from the current literature.

use a constant $EINO_x$ of 13 (Figure 3.7) over a 100 year run for a constant emission rate, in order to maintain simplicity and limit the amount of changing variables. Figure 3.7 shows how this constant EINOx scenario fits into the range of scenarios from the current literature, when all were run with a simple aviation fuel scenario where emissions follow observations until 2012 and then increase by 1 percent per year.

Chapter 4

Description of Models and Legitimacy of Use

This chapter summarises the main information and features of the models used in this study. Section 4.1 explains the use of the models employed, Section 4.2 describes the models themselves, Section 4.3 and 4.4 quantifies their legitimacy and Section 4.5 describes the experimental set up.

4.1 Introduction

In order to study the trade–offs between the emissions of short–term and long–term climate forcers from aviation, it is necessary to model them in detail over the long term. For this type of study, computer modelling is desirable to encompass a long timescale and complete global coverage, as opposed to observational measurements which would not provide global coverage and do not allow for any proposed changes in technology, or other theoretical variables than can be incorporated into model simulations. Therefore, this research requires the use of a chemistry transport model (CTM) for short detailed runs and a simple climate model (SCM) for simplified long–term runs. The SCM Lin-Clim, used in this study currently assumes linearity within the NO_x -O_3 -CH_4 system when modelling aviation emissions. Therefore, it is necessary to justify the use of a SCM by using a chemistry transport model to quantify the bounds of non-linearity within the NO_x -O_3 -CH_4 system and thus determine the limits of use for the SCM. To do this the

MOZART chemistry transport model (CTM) is used to model aviation NO_x emissions of different magnitudes, in different background atmospheres – the methodology of which is described in Section 4.5 and undertaken in Chapter 5. The data from the CTM will be used to form a new parameterisation to model the effects of aviation NO_x emissions over the short– and long–term while taking the non–linearity of the NO_x –O_3 –CH_4 system and the background atmosphere into account (Chapters 6 and 7).

4.2 Models Employed in the Study

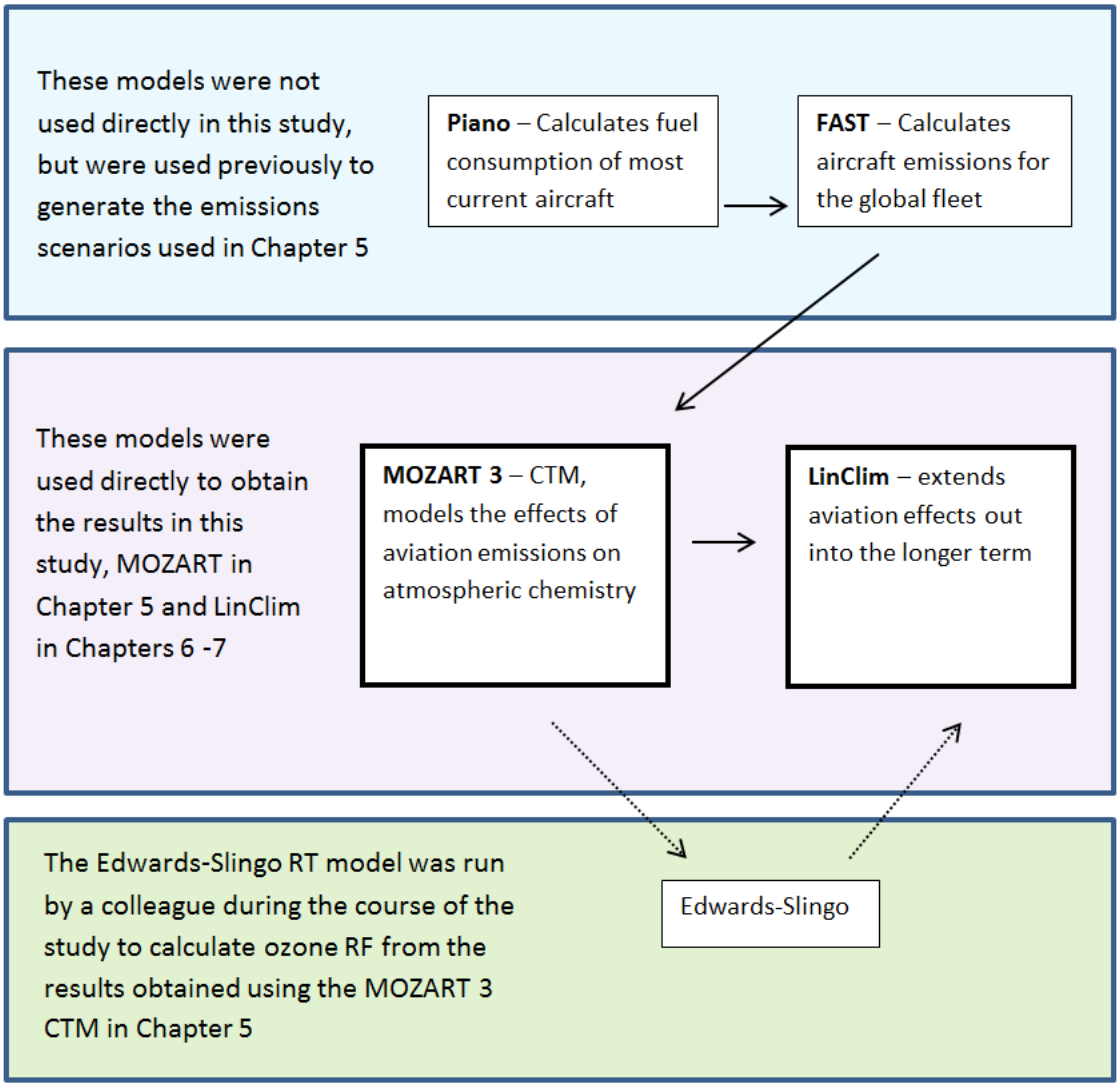

Figure 4.1: A box diagram of the computer models used in this study, the top box shows the models 'Piano' and 'FAST' which are described in Appendix A and were not run during the study but prior to it. The middle box shows the MOZART' and LinClim' models which were key to this study and run throughout and the bottom box shows the Edwards-Slingo' model which was used during the study but run by colleagues.

Figure 4.1 shows the all the models necessary to obtain the data for use in this study. The Piano and FAST models were required to generate aviation emissions scenarios, details of which are shown in Appendix A. The MOZART version 3 CTM, (see section 4.2.1) is used in Chapter 5 where aviation emissions scenarios were run in different background

NO_x levels, the perturbations in ozone burden and methane lifetime were then extrapolated from the MOZART data for further study. The LinClim SCM, (see section 4.2.2), is then used in Chapters 6 and 7 to run long term simulations of aviation NO_x and CO_2 emissions in order to gauge the impact of these emission species on climate.

4.2.1 MOZART 3 (3D chemistry transport model)

The Model for Ozone and Related Chemical Tracers is a global chemistry transport model (CTM) that can simulate the chemical and physical processes throughout the atmosphere from the surface (1000 hPa) up to the lower mesosphere (0.1 hPa) (Figure 4.2). It was developed by The National Center for Atmospheric Research (NCAR), the National Oceanic and Atmospheric Administration (NOAA), the Max–Planck Institute of Meteorology (MPI–Hamburg), the Geophysical Fluid Dynamics Laboratory (GFDL) and Princeton University. The MOZART model builds up on the framework of Rasch et al. (1997)'s Model of Atmospheric Transport and Chemistry (MATCH) accounting for wet and dry deposition, boundary layer exchanges, advection and convection. The model uses hybrid sigma–pressure vertical coordinates allowing the wind components to adhere to orography (Figure 4.2). Vertical velocities are derived using the flux–form semi-Lagrangian scheme of Lin and Rood (1996), and are based on divergence of the horizontal velocity fields. The deep convective routine of Zhang and Mcfarlane (1995) and the shallow and mid–level convection scheme of Hack (1994) are used to derive convection fluxes. Surface dry deposition and wet deposition are taken from Muller (1992) and Brasseur et al. (1998) respectively. Holstag and Boville (1993) provide the formulations necessary for the planetary boundary layer exchanges to be parameterised. The version of MOZART used in this study is MOZART–3, it includes a comprehensive structure of tropospheric physical processes, including boundary layer dynamics and convective transport but requires an input of meteorological fields as described in Table 4.1. MOZART version 4 was also considered, however version 4 extends only as high as the tropopause and therefore chemical perturbations reacted differently to when run in MOZART–3 where the influence of higher atmospheric levels are taken into account. Thus, MOZART–4 was found to be unsuitable for the study of aviation (Personal communication, Jerome Hilaire, Nov 2013).

The chemical mechanism in MOZART–3 includes 218 gas–phase reactions, 17 heterogeneous reactions and 71 photolytic reactions, occurring from 108 species. These species

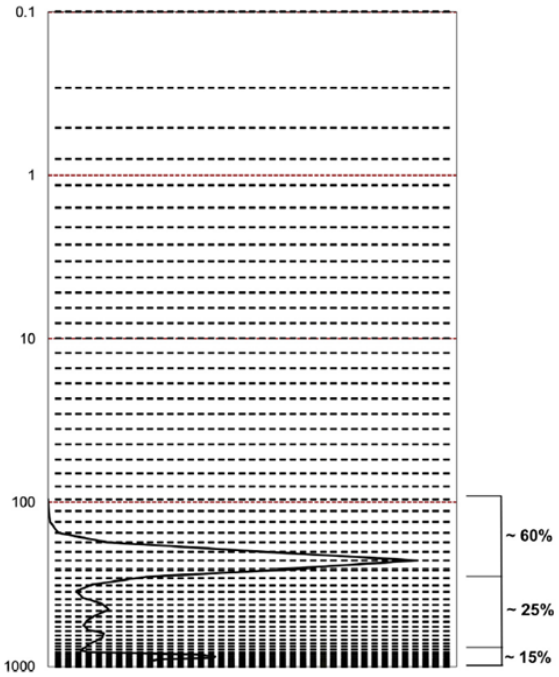

Figure 4.2: The vertical domain of MOZART-3, the dashed lines represent the models 60 hybrid sigma pressure layers and the red lines show the 1000, 100, 1 and 0.1 pressure(hPa) levels. The percentages and solid line show a schematic illustration of the vertical distribution of aircraft NO_x emission in MOZART3, the lower peak shows take off emissions and the higher peak is the main cruising level ,which is represented in MOZART3 at 228 hPa. Figure from Skowron et al., (2013).

Input variable for MOZART 3	**Source**
Temperature, Pressure	ECMWF ERA-Interim reanalysis data*
Solar radiation flux and surface heat	ECMWF ERA-Interim reanalysis data
Wind speed (Zonal, meridional, vertical), Wind surface stress	ECMWF ERA-Interim reanalysis data
Background anthropogenic emissions	Lamarque *et al.*, 2010
Surface emissions, biomass burning	EU project POET (Precursors of Ozone and their effects on Troposphere

*European centre for medium-range weather forecasts (ECMWF) (Dee *et al.*, 2011).

Table 4.1: The meteorological fields required to run the MOZART 3 CTM and the sources of that data.

consist of O_x, NO_x , HO_x, ClO_x, BrO_x, and CH_4 and its degradation products. A 'lumped hydrocarbon species' – (C_4H_{10}) – from previous version of MOZART has been replaced in MOZART–3 by three separate lumped hydrocarbons; TOLUENE – representing aromatic species, BIGALK – representing alkanes with four or more carbons, and BIGENE representing alkenes with four or more carbons. The lightning parameterisation defines the NO_x production from lightning as a function of the location of convective cloud top heights, based on Price et al. (1997) and Pickering et al. (1998).

In this study the MOZART–3 CTM was used to calculate the perturbations in ozone burden and methane lifetime resulting from aircraft NO_x using input parameters described in Table 4.1, and aviation scenarios and background NO_x emissions as described in Chapter 3.

4.2.2 LinClim (Linear climate response model)

In order to investigate the trade–offs in climate response between aviation NO_x and CO_2 emissions, simulations need to be performed over the longer–term. General circulation models (GCM) and CTMs are computationally very expensive and demanding to run, particularly when complex chemistry is involved. Simple climate models provide a way to simulate the future climate temperature responses while running quickly and computationally inexpensively. This type of model can run climate simulations of long duration – up to hundreds of years – using input values of CO_2 and other chemicals generated from full general circulation model (GCM) simulations and impulse response functions.

An impulse response function (IRF) describes the response of a dynamical system to a pulse perturbation and thus describes the systems behaviour (Olivie and Peters, 2013). In simple climate models the response of the climate is simulated in one of two ways, a single impulse response function (IRF) is calibrated to a more sophisticated parent model, creating a parameterization, or a dominant physical process in the system is used to calibrate several IRFs, which are then coupled to form a non–linear convoluted system model. IRFs assume that a perturbation to a systems equilibrium state will result in a linear response. This assumption allows an IRF to reproduce the characteristics of its sophisticated parent model when calculating a systems response. However, once calibrated to a parent model the IRF is fixed, regardless of any further change in background state. Many studies justify the use of IRFs due to their simplicity but acknowledge caution is necessary when

using a single IRF to describe a non–linear system (Khodayari et al., 2013 and references therein). However, several studies have found that carbon cycle models with non–linear couplings better represent the carbon cycle and the response of CO_2 in the atmosphere than those that use a single IRF (Khodayari et al., 2013; Warren et al., 2010).

LinClim is a linear climate response model that has been tailored specifically to aviation, and includes all the effects of aviation as specified by the IPCC (1999). It uses a single impulse response function (IRF) which is calibrated to a more sophisticated model, to depict the carbon cycle and calculate the concentration and resulting RFs of CO_2 , O_3 , CH_4 , water vapour, contrails, sulphate and black carbon aerosols resulting from aviation emissions (Lim et al., 2007).

Aviation fuel data is used to calculate CO_2 emissions in LinClim, CO_2 concentration is then extrapolated using the linear response function (LRF) from Hasselmann et al. (1997):

$$\Delta C(t) = \int_{t_0}^{t} G_c\,(t - t')\,E(t')\,dt' \tag{4.1}$$

Where $\Delta C(t) = \int_{t_0}^{t} G_c(t-t')E(t')\,dt'$ is the e-folding time of mode j and the equilibrium response of mode j to a unit emission of $\alpha_j \tau_j$.

The current carbon cycle in LinClim is based on the Maier-Reimer and Hasselmann (1987) model. The CO_2 RF is calculated by the function used in IPCC AR4 (Solomon et al., 2007)

$$RF_{CO_2}(t) = 5.35 \ln\left(\frac{C(t)}{C(0)}\right) \tag{4.2}$$

Where $C(0)$ is the preindustrial CO_2 concentration.

The experiments performed in Chapter 6 and 7 are part of a parametric study where aviation emissions are run over an arbitrary period of 100 years in background atmospheres of constant CO_2 and NO_x emissions. No historical information was included in the CO_2 runs. The temperature response is then calculated using the method of Hasselmann et al.,

(1997), this assumes that the system responds linearly to the forcing from aviation CO_2 :

$$\Delta T_i(t) = r_i \lambda_{CO_2} \int_{t_0}^{t} \hat{G}_T\,(t - t')\,RF_i(t')\,dt' \tag{4.3}$$
$$\hat{G}_T(t) = \frac{1}{\tau}\text{exp}^{-1/\tau}$$

Where i is a climate forcer, r is the efficacy and rCO_2 =1.

The calculated temperature response is also dependent on the climate sensitivity parameter (λ CO_2) and the lifetime of the temperature perturbation (τ), which are tuned to the LinClims 'parent' GCM, of which the default is the GCM ECHAM4/OPYC3 (Lim et al., 2009). In the experiments performed in Chapters 6 and 7, LinClim was tuned to 19 different parent models and the median temperature response value was taken as described in Chapter 6. LinClim also addresses the heat exchange with the deep ocean in its energy balance model, which is based on an IRF tuned to a coupled ocean-atmosphere GCM (ECHAM5) (Khodayari et al., 2013).

The current parameterisation in LinClim for calculating ozone and methane RF assumes a linear relationship between aviation NO_x emissions and the resulting ozone and methane RF changes:

$$RF_{O_3,CH_4}(t) = RF_{O_3,CH_4}\,(\text{ref. year}) \times \frac{E_a(t)}{E_a\,(\text{ref. year})} \times \frac{EI_{NO_x}(t)}{EI_{NO_x}\,(\text{ref. year})} \tag{4.4}$$

Where E_a is the aircraft fuel burnt per year, and EI_{NO_x} is the nitrogen oxides emission index (Lim et al., 2006).

The LinClim model was designed specifically to model aviation and therefore has a relatively simple representation of the carbon cycle. In general, a single IRF is used to represent the carbon cycle in SCMs used to study aviation as it is assumed that the forcing from aviation CO_2 is weak enough to allow the system to respond linearly. The single IRF in this case calculates changes in atmospheric CO_2 based on specific emissions scenarios. In this study LinClim will be used to calculate the RF and associated temperature response resulting from aviation CO_2 over the long term (+ 100 years) and the temperature response of aviation NO_x emissions.

4.3 Legitimacy of MOZART 3 use

Over the last few decades, progression in technology has allowed the advancement of 3D chemical transport models, which can simulate the chemistry of the atmosphere. These models have been developed in order to simulate the transport and reactions of most chemical species. 3D Chemistry Transport Models (CTMs) such as MOZART are designed to represent the background chemical composition and evolution of chemical pathways in the earth's atmosphere. The simulations run by CTMs are based on in–depth numerical schemes, input data and parameterisation of complex atmospheric processes, all of which introduce uncertainty and errors. Model results therefore require validation by comparison to observational data. For this study global average values of O_3 and CH_4 were used from MOZART–3 runs, therefore the model results will be compared to global averages. Whilst acknowledging MOZART must also perform well regionally, for the purpose of this study, the global average is the number used for comparison.

4.3.1 Literature comparisons

Further tests of the legitimacy of MOZART–3 in representing aircraft emissions are presented by Skowron (2013). Skowron (2013) compared MOZART–3 output with meteorology from 2006 to observational data of NO_x , O_3 , CO, CH_4 and PAN gathered from SHADOZ and WOUDC ozonesonds, WDCGG groundstations and the aircraft TOPSE campaign. Skowron (2013) goes into detail regarding the performance of MOZART-3 on a regional scale, however, for this study the importance lies in MOZART's ability to successfully represent global averages.

Skowron (2013) found that MOZART is in good agreement with observational NO_2 and CO, particularly over Europe. For global average NO_2, differences between MOZART simulations and the observations were below 15 percent for all but two observation stations world–wide. It is possible that the discrepancies stem from the anthropogenic emissions data input. For CO, MOZART–3 again shows comparable results, agreeing with observational data even seasonally, especially at mid and high latitudes of the northern hemisphere. Values in tropical regions are underestimated by MOZART–3 by up to 30 percent, and overestimated by up to 28 percent in southern latitudes. These differences are also apparent in MOZART–4 and thought to be a result of biomass burning activity in the tropics and southern hemisphere (Emmons et al., 2010). For ozone, it is known that

Study	Range ozone (ppbv)
This study, MOZART-3	4 - 12.4
Fichter, (2009)	1.5 – 12
Köhler *et al.*, (2008)	6 – 9
IPCC, (1999)	≤ 12
Gauss et al., (2006) – Zonal	3 – 8
This study, MOZART-3 - Zonal	2.26 – 8.14

Table 4.2: Global annual ozone perturbation (ppbv) resulting from aviation NO_x emissions at flight level for a range of studies and models in the literature.

MOZART–3 shows an overly strong Brewer–Dobson circulation when using ECMWF meteorology, causing excessive downwards transport of O_3 and therefore higher O_3 mixing ratios in the upper troposphere than those seen in observations (van Noije et al., 2006; Kinnison et al., 2007). However, the vertical distribution of ozone is modelled well by MOZART–3 both in the troposphere and stratosphere (Skowron et al., 2014).

Park et al. (2004) compared MOZART–3 output to satellite (HALOE) observations and found that while the model represented methane and water vapour well, it underestimated NO_x near the tropopause, compared to the satellite data. Kinnison et al., (2007) found that although MOZART–3 recreated observations relatively well, it is particularly sensitive to meteorological inputs, a slight difference in temperature and winds led to a large difference in chemical distributions. A comparison of the concentrations of aviation NO_x and O_3 at flight level, modelled by MOZART-3 during this study agreed with other studies on the subject (Table 4.2).

4.3.2 Observational data and Methodology

To validate MOZART against observations, several datasets of O_3 and CH_4 were used. As regional studies comparing MOZART to observations have already been covered (Skowron, 2013), this study chose to do a seasonal study of 2006, as in this study, MOZART uses 2006 climatology.

Observational methane data from the World Data Centre for Greenhouse Gases (WD-

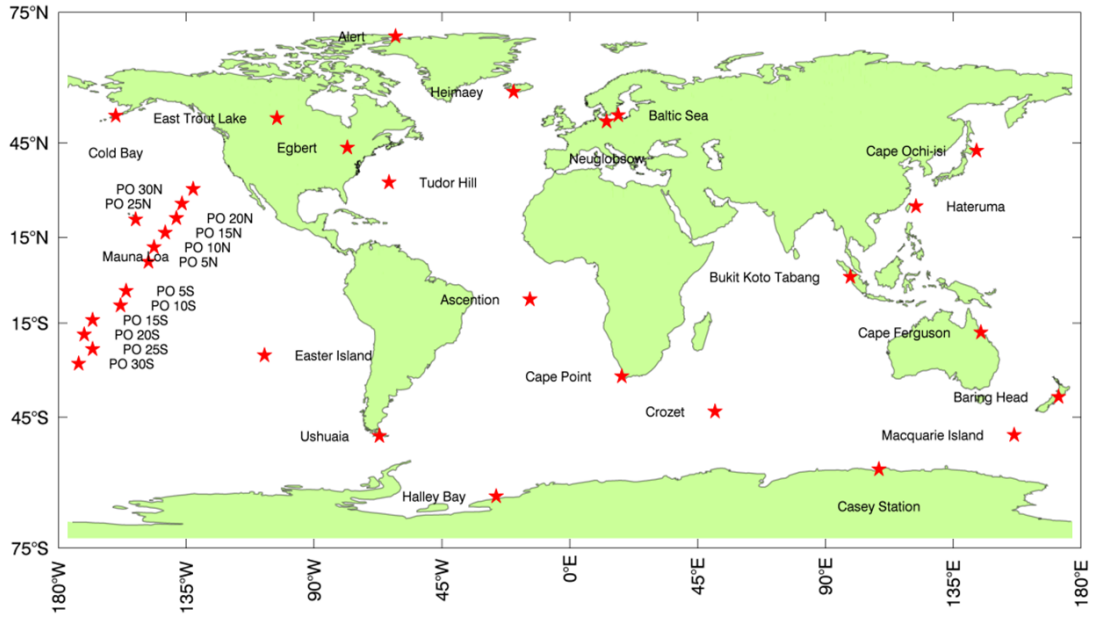

Figure 4.3:
Locations of WDCGG (red star) ground stations from where observational methane data was recorded and collated.

CGG) website (http://ds.data.jma.go.jp/gmd/wdcgg/cgi-bin/wdcgg/catalogue.cgi) (data accessed and downloaded 03.09.2015 and 14.07.2016). The locations of all the ground stations are shown in Figure 4.3. Model set up is described in Section 4.5. Observational ozone data was taken from the HIRDLS instrument on the Aura satellite mission.

WDCGG data

The World Data Centre for Greenhouse Gases (WDCGG) database is part of the World Meteorological Organisation's (WMO) Global Atmospheric Watch (GAW) program, run by the Japanese Meteorological Agency. The network of stations gather observational data from both fixed and mobile stations. In this study, methane data was used from several fixed stations worldwide (Figure 4.3). These stations were chosen as they had complete monthly averages of 2006 methane data and represented a good global spread which included an equal number of both northern and southern hemisphere sites, over both land and ocean.

HIRDLS data

The observational ozone data was taken from the HIRDLS (High Resolution Dynamics Limb Sounder) instrument located on NASA's Aura satellite. The main objectives of the Aura mission are to study complex chemistry and dynamics of the atmosphere from the troposphere to the mesosphere (8 – 80 km altitude). HIRDLS' high vertical resolution aids in the study of the more complex regions such as the UTLS, with one of its main objectives being to study ozone and other radiatively active species in this region (Gille et al., 2008). During launch of the satellite, the optical appature of the HIRDLS instrument became obscured, limiting its latitudinal range to 65 degrees S – 82 degrees N, which has been taken into account in the comparisons shown in the section below.

4.3.3 Comparison of MOZART results to observational data

Figure 4.4 and Figure 4.5 show that MOZART–3 agrees well with the HIRDLS data regarding the vertical ozone profile of the atmosphere. The figure shows monthly average ozone in a vertical profile of atmospheric region 1000 – 1 hPa for each month of the year. HIRDLS is compared to MOZARTs whole atmopsheric profile and then also to MOZARTs atmospheric profile from 65 degrees S - 82 degrees N, to more accurately compare the model to the HIRDLS data which is missing values outside of these latitudes. The zoomed panel on each graph shows the region 400 – 100 hPa in more detail, this region is important in the study of aviation as it is in this region that aircraft cruise. The data shows that cutting the model data to equal latitudes of the HIRDLS data improves the correlation between the two, explaining some of the difference between the original MOZART profile and that of the satellite data. The results also show that while the model generally agrees with the satellite data, there are noticeable discrepancies in the statospheric ozone layer and small differences at the UTLS. Other studies (van Noije et al., 2006; Kinnison et al., 2007) have reported an overly strong Brewer–Dobson circulation is present in ECMWF meteorology, which causes excessive transport of ozone down across the tropopause, which likely explains the differences seen in this region.

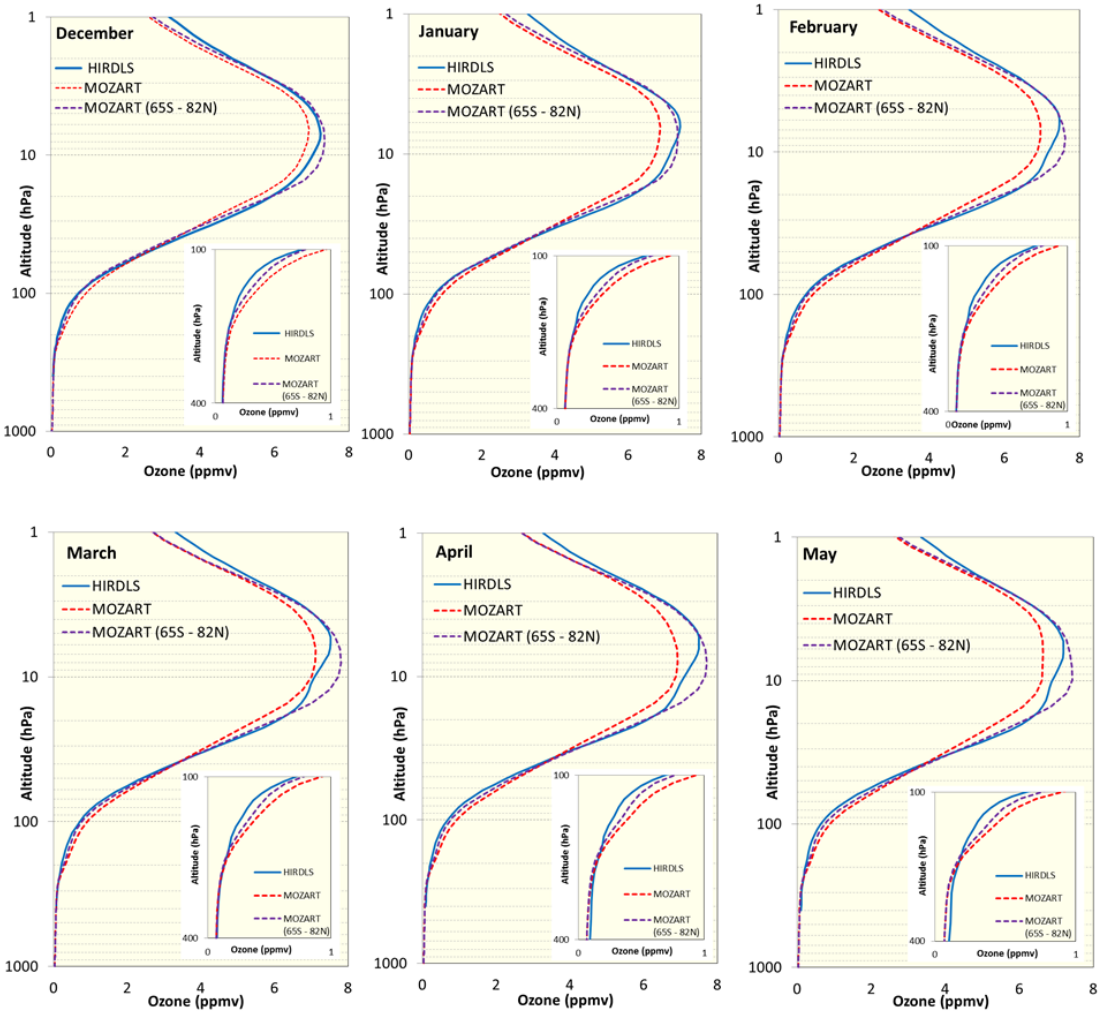

Figure 4.4:

A comparison of the vertical ozone profile from the HIRDLS instrument on board the Aura satellite and the ozone profile generate by MOZART, both for the year 2006, from 1000 – 1 hPa altiude, for winter and spring. An additional profile shows the vertical ozone profile generate by MOZART for the latitudes 65S – 82N, as the HIRDLS instrument suffered an obstruction which limited its viewing range to these latitudes. The zoomed panel shows the region 400 – 100 hPa in greater detail. HIRDLS data was provided by Dr N. Hindley, University of Bath, Personal Communication, July 2016.

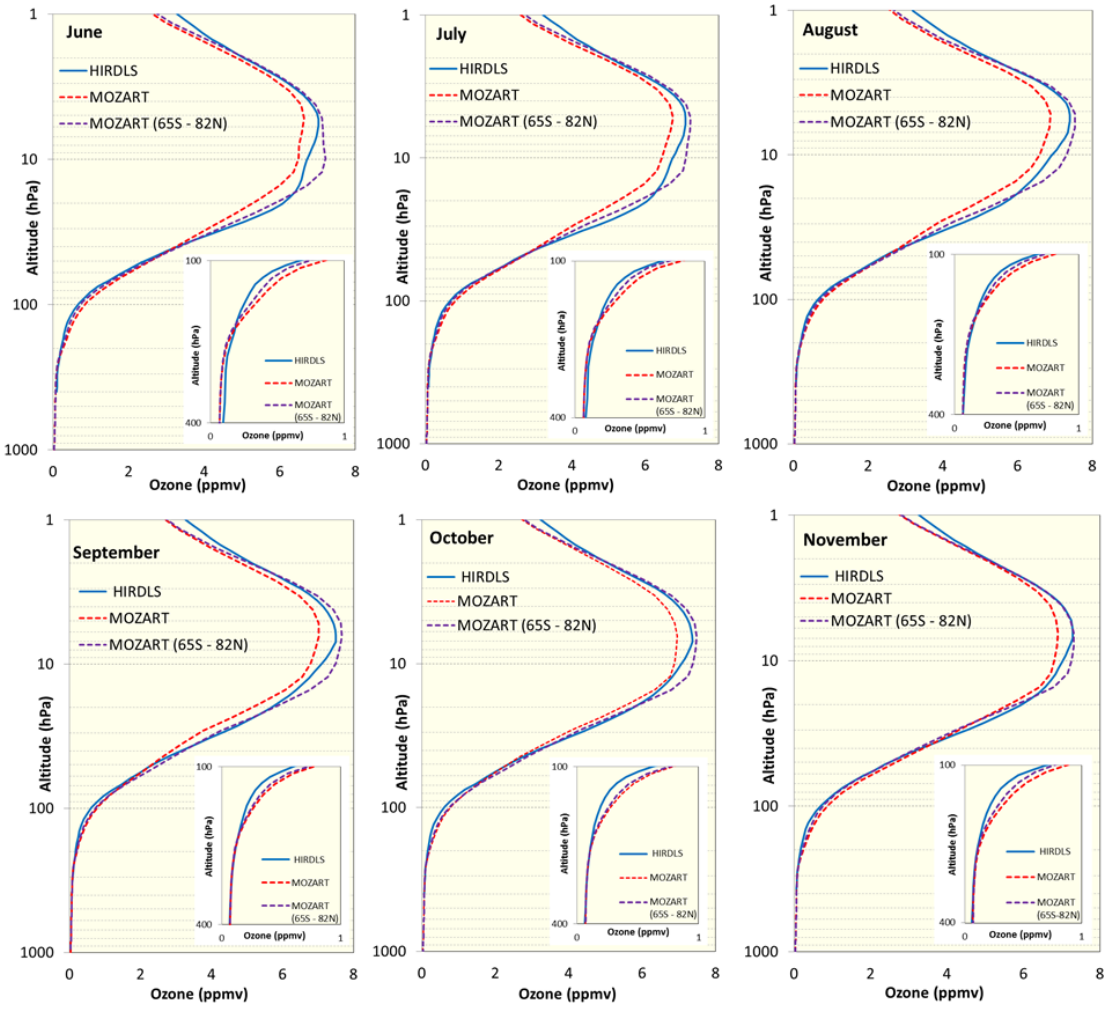

Figure 4.5:

A comparison of the vertical ozone profile from the HIRDLS instrument on board the Aura satellite and the ozone profile generate by MOZART, both for the year 2006, from 1000 – 1 hPa altiude, for summer and autumn. An additional profile shows the vertical ozone profile generate by MOZART for the latitudes 65S – 82N, as the HIRDLS instrument suffered an obstruction which limited its viewing range to these latitudes. The zoomed panel shows the region 400 – 100 hPa in greater detail. HIRDLS data was provided by Dr N. Hindley, University of Bath, Personal Communication, July 2016.

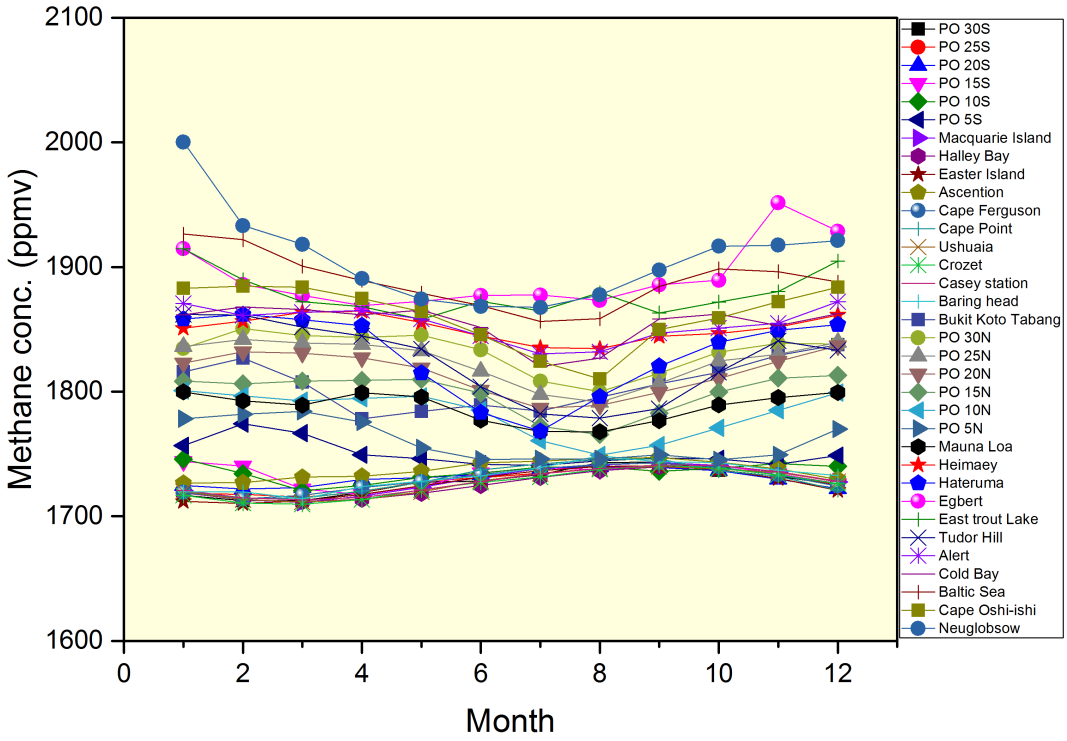

Figure 4.6:

Monthly methane data collected at ground stations worldwide collated at WDCGG (World Data Centre for Greenhouse Gases) (http://ds.data.jma.go.jp/gmd/wdcgg/cgi-bin/wdcgg/catalogue.cgi) (data accessed and downloaded 03.09.2015 and 14.07.2016)

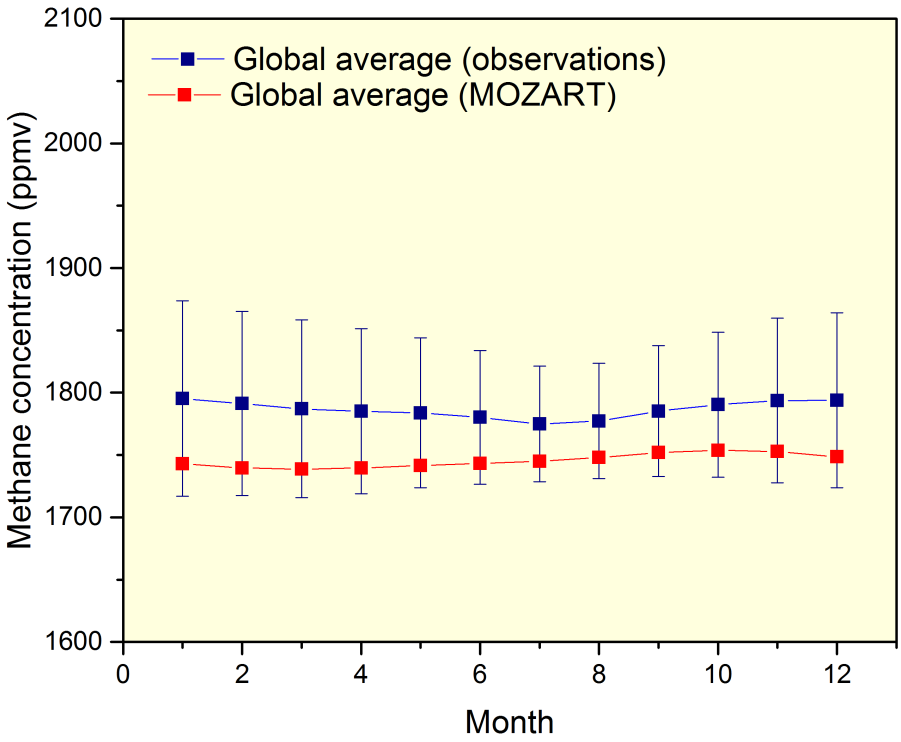

Figure 4.7:

Global average monthly methane data, taken from all the ground stataions shown in figure 4.6 and global average tropospheric monthly methane from MOZART 3 for the year 2006

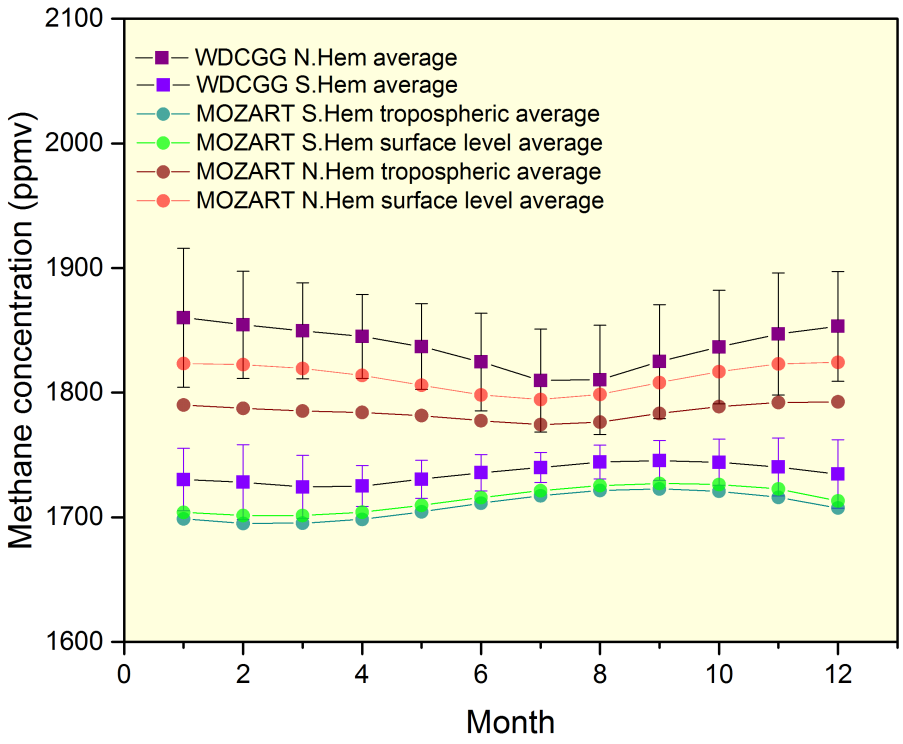

Figure 4.8:

Hemispheric average monthly methane data collated from WDCGG ground stations as shown in figure 4.6 and MOZART tropospheric average methane for the north and southern hemisphere and surface average methane for the southern and northern hemisphere

The methane data was gathered from 34 ground stations worldwide, 17 in each hemisphere. As methane has a lifetime of around a decade, it is relatively well mixed in each hemisphere, therefore the ground stations should be indicative of the tropospheric average values. However, the observational reading are taken at surface level and those near point sources, such as cities or highly populated regions do tend to show higher values. The main sources of methane are wetlands, permafrost, power stations and farming activities, this explains why the northern hemispheric average is higher than the global average – it is significantly more populated and also has greater land mass than the southern hemisphere (Figure 4.7 and Figure 4.8). The surface values of methane from MOZART were also included in the analysis. The average tropospheric methane concentration generated by MOZART–3 is consistently slightly below that of observations, which has been noted

	LinClim CO_2	MAGICC CO_2	TAR CO_2	LinClim O_3	MAGICC O_3	TAR O_3	LinClim CH_4	MAGICC CH_4	TAR CH_4
2000	0.23	0.23	0.28	0.06	0.02	0.06	0.02	0.02	0.02
2025	1.17	1.17	1.19	0.25	0.17	0.25	0.15	0.16	0.15
2050	2.22	2.22	2.24	0.30	0.21	0.30	0.24	0.25	0.24
2075	3.09	3.09	3.15	0.26	0.17	0.28	0.19	0.20	0.19
2100	3.72	3.72	3.84	0.20	0.13	0.20	0.09	0.10	0.10

Table 4.3: Comparison of CO_2 , O_3 , CH_4 and SO4 radiative forcing from LinClim SCM, MAGICC SCM and the IPCC TAR (taken from Lee et al., 2005)

in other studies (Skowron, 2013). The MOZART–3 values are closest to observation in the southern hemisphere (Figure 4.8) with both the surface values and tropospheric average only differing by a maximum of ∼20 ppmv. This is likely due to the explanations stated above, that the southern hemispheric methane is more well mixed throughout the troposphere as there are fewer methane sources. The MOZART data of the northern hemisphere shows a greater difference to observations, with the tropospheric average differing by up to ∼70 ppm methane (Figure 4.8). Plotting the surface methane values from MOZART–3 gives an indication as to why there is a difference, they are much closer to observations, differing only by ∼30 ppm. This may be due to the fact that there are many continuous methane sources at surface level in the northern hemisphere, therefore higher values of methane are present at the surface than throughout the rest of the troposphere.

4.4 Legitimacy of LinClim use

To legitimise the use of LinClim in this study as a SCM, it is necessary to show that the model produces results in line with those from other SCMs. Table 4.3 shows that LinClim generally agrees well with the MAGICC SCM and the data of the IPCC third assessment report (TAR). RFs of CO_2 , O_3 and CH_4 from LinClim are shown to correlate well with TAR and RFs of CO_2 and CH_4 correlate well with those produced in MAGICC. The only differences are apparent in the RFs between LinClim and MAGICC O_3 , however this has been attributed to the fact that O_3 formulation within MAGICC differs from the IPCC TAR (Lee et al., 2005).

Khodayari et al., (2013) made a comprehensive comparison study of six SCMs, assessing their accuracy in simulating aviation CO_2 concentrations. In the study LinClim was compared with data from the Model for the Assessment of Greenhouse–gas Induced Climate

Change version 6 (MAGICC6), the Integrated Science Assessment Model (ISAM) model, two models from the Center for International Climate and Environmental Research–Oslo (CICERO–1 and CICERO–2) and the Aviation Environmental Portfolio Management Tool (APMT) Impacts climate model. The study concluded that LinClim produced CO_2 concentrations comparable to the other SCMs, and fell within 1 standard deviation of the IPCC AR4 projections of CO_2 concentrations, as did five of the six models tested. The temperature change due to aviation over a 50 year time–scale simulated by LinClim was also comparable to five out of the six models. LinClims temperature model performed well, with results lying within 8 percent of the models with ocean up–welling–diffusion sub–models. Khodayari et al., (2013) report that all the models tested produced higher temperature changes than those of IPCC 1999, however, Lim et al. (2007) note that the aviation RF simulated by LinClim compares well to IPCC 1999 present day and future scenarios.

4.5 Experimental Design

4.5.1 MOZART set up

In this study the MOZART–3 CTM was used to calculate the ozone and methane perturbations resulting from aircraft NO_x for a number of aviation emissions scenarios which were emitted into background atmospheres of two different NO_x levels (Chapter 3). MOZART–3 requires dynamical input of temperature, pressure, wind speed (zonal, meridional and vertical), wind surface stress, surface geopotential height, solar radiation flux, surface heat and moisture fluxes, soil moisture fraction and snow height. The ECMWF ERA–Interim reanalysis data for 2000 – 2006 provides the meteorological fields which drive the transport of chemicals within the MOZART; this data set has advantages over the alternative ERA–40 data as several deficiencies have been resolved, such as the stratospheric circulation and hydrological cycle. However, it should be noted that the ERA–Interim reanalysis data still contains errors, inherent to this type of data set and climate modelling in general, as outlined in Chapter 3 (Dee et al., 2011).

The background emissions necessary for MOZART–3 are from Lamarque et al. (2010) which represent the year 2000 and were originally compiled for the IPPC AR5 report. The background data are made up of surface emissions of anthropogenic activity and

Annual Emissions		Year 2000 IPCC AR5
NO_x total (Tg N yr^{-1})		37.1
	Anthropogenic (Tg[NO_2] yr^{-1})	26.5
	Biomass burning (Tg[NO_2] yr^{-1})	4.5
	Lightning (Tg[N] yr^{-1})	4.8
CO total (Tg[CO] yr^{-1})		1245.9
	Anthropogenic (Tg[CO] yr^{-1})	606.2
	Biomass burning (Tg[CO] yr^{-1})	459.2
NMVOC total (Tg[C] yr^{-1})		768.5
	Isoprene (Tg[C] yr^{-1})	473.9

Table 4.4: Annual background atmospheric emissions used in MOZART-3 taken from Lamarque et al., 2010

biomass burning, and the European Union project POET (Precursors of Ozone and their Effects on Troposphere) supply the biogenic surface emissions (Table 4.4). In order to investigate the effects of background NO_x in the formation of aviation emissions, the background NO_x data was sourced from the RCP scenarios (see Chapter 3).

Information pertaining to the data used for aircraft emissions is outlined in Chapter 3. For each experimental simulation run on MOZART–3 the model needs to be run four times, once without aircraft emissions, referred to as the 'reference run' and once with aircraft emissions, referred to as the 'perturbation run'. Each run is preceded by a 'spin up year', which makes up the other two runs, and describes the time take by the model for the atmospheric constituents to reach equilibrium. The reference run is then subtracted from the perturbation run and the difference plotted, thus showing the impact of aviation on the atmosphere. The two year MOZART–3 runs performed here are justified by the work of Skowron (2013). Figure 4.9 shows that the perturbation in tropospheric ozone is accounted for after a model run of two years and shows very little change over a further four years of model run. The perturbation of stratospheric ozone is not completely observed after two years run, as shown in Figure 4.9, however the total ozone change due to aviation is not greatly affected as the majority of aircraft induced ozone change takes place in the UTLS. Skowron (2013) found the change in O_3 RF between a 2 year and 6 year simulation to be –0.6 percent, hence a two year run is thought to be suitable. The perturbation

of aviation emissions to CH_4 is known to happen over a much longer time–scale and is discussed in Section 4.5.2.

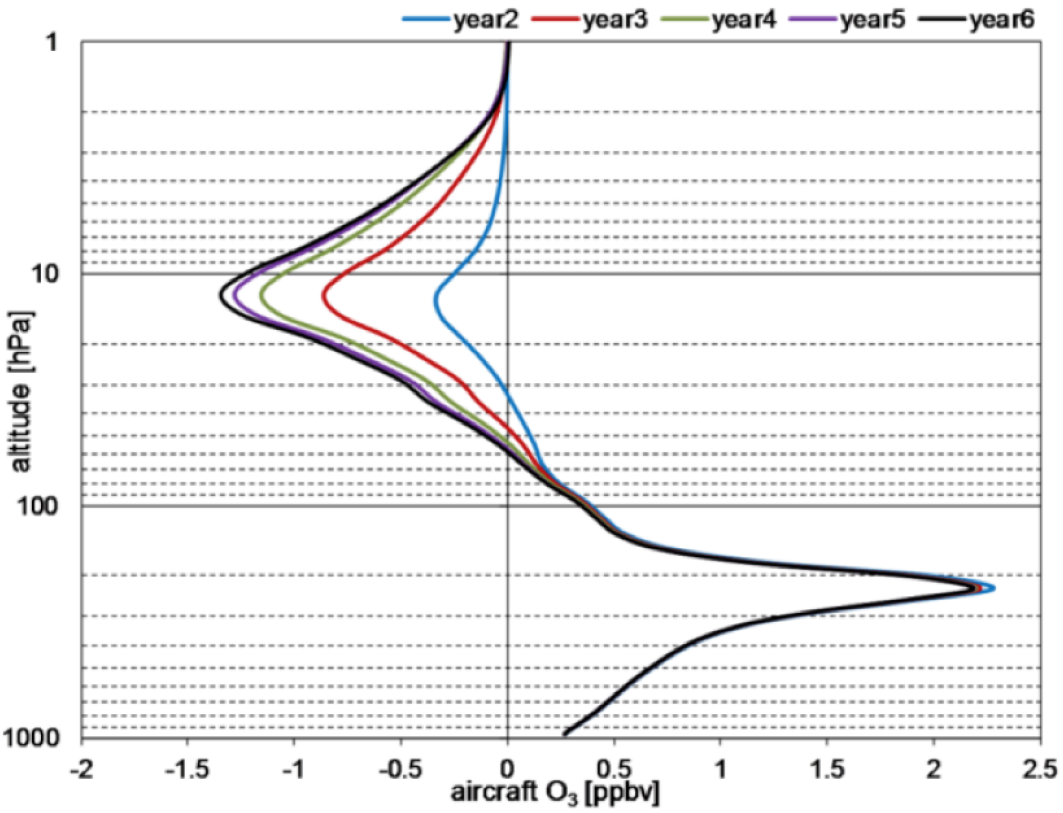

Figure 4.9:
The globally annually averaged vertical distributions of aircraft perturbations of O_3 concentrations for consecutive years of simulations taken from Skowron 2013.

For comparison and validity purposes, Skowron et al., 2013 presents a good case with which to compare the RF values calculated using the method of this study. Both studies use the same aviation scenario – REACT4C base case and the MOZART–3 CTM. The results are compared in Table 4.5 and it is apparent that they closely agree. The slight discrepancy is likely a result of the slight difference in background NO_x emissions, this study included shipping emissions which bought that value up to 41 Tg N Yr^{-1} whereas Skowron et al., used the background of 37.1 Tg N Yr^{-1}.

Study	CH4 lifetime (years)	CH4 lifetime change (years)	RF Short term O3	RF CH4 induced O3	RF Direct CH4	RF SWV	RF Net NOx
Skowron *et al.*, 2013	8.810	-0.073	13.4	-3.1	-7.0	-1.1	2.3
This study	8.806	-0.072	13.5	-3.4	-6.9	-1.04	2.05

Table 4.5: A comparison between the results from this study and the results of Skowron et al., 2013, both of which used the REACT4C data of aviation emissions 0.7 Tg N Yr^{-1} (2.33 Tg NO_2 yr^{-1}) and the MOZART 3 CTM with a background NO_x value of 41 Tg N Yr^{-1} in the case of this study and 37.1 Tg N Yr^{-1} in Skowron et al., 2013 which both represent the year 2000. The CH_4 lifetime represents destruction by OH (between the surface and 1 hPa) and the lifetime reduction shown is due to aircraft NO_x emissions. The radiative forcings are in mW m^{-2} and 'SWV' denotes stratospheric water vapour.

4.5.2 Methane perturbation corrections and additional NO_x effects

The negative RF associated with CH_4 depletion is only evident on the time–scale of 8 – 12 years, which is longer than the model runs of 2 years performed in this study. Therefore, to appropriately represent the new equilibrium steady state of the methane mixing ratio in the perturbation run ([CH_4]ss) a calculation is required as shown in equation 4.5 derived by Fuglestvedt et al. (1999):

$$[CH_4]_{\text{SS}} = [CH_4]_{\text{ref}} \times \left(1 + 1.4\,\frac{\Delta\tau_0}{\tau_{\text{ref}}}\right) \tag{4.5}$$

where $[CH_4]_{\text{ref}}$ is the methane mixing ratio in the reference run, $\Delta\tau_0 = \tau_{\text{per}} - \tau_{\text{ref}}$ is the change in methane lifetime in the perturbation run and 1.4 is the feedback factor to reflect the changes of methane on its own lifetime τ (Prather et al., 2001).

Background methane concentration is fixed in these model runs. This is a common approach used to allow atmospheric steady state to be reached within the time of the model runs as the other species of interest have much shorter atmospheric lifetimes than the decade long lifetime of methane. Future perturbations can then be calculated using the simulated methane lifetime changes (Sovde et al., 2014).

4.5.3 Radiative Forcing Calculations

To ascertain the complete effect of aviation NO_x on the atmosphere, one needs to take into account its effect on other atmospheric components. This is difficult as the various components exhibit different lifetimes and reaction rates in the atmosphere, show heterogeneous dispersal, and take part in non–linear reactions. Current knowledge suggests that there are six components to consider; short term ozone, long term ozone due to methane, methane itself, nitrates, sulphates and SWV – again being influenced by methane changes (Myhre et al., 2013).

For this study, nitrate and sulphate effects are not considered. The short term O_3 radiative forcing is calculated using the Edward–Slingo offline radiative transfer model described in Appendix A. Monthly O_3 reference and perturbation data from MOZART–3 is converted into mass mixing ratios and then interpolated onto the Edward–Slingo RTM vertical and horizontal resolution. Additional O_3 formation in the troposphere leads to cooling in the stratosphere as upwards radiation is reduced, for this reason a more accurate representation of the change in O_3 RF is determined when stratospheric adjustment is taken into account (Stevenson et al., 1998). Stevenson et al., (1998) determine that tropospheric O_3 forcing is overestimated by $\sim$20 percent due to this effect, however more recent studies have shown that 20 percent is too high an adjustment for MOZART results and therefore a more modest -10 percent is applied to the short term O_3 forcing to account for stratospheric adjustment (Dr A. Skowron personal communication, May 2015).

Methane RF is calculated using equations 4.6 and 4.7 – originally from Hansen et al. (1988) and used by the IPCC;

$$\Delta F = 0.036 \left(\sqrt{M} - \sqrt{M_0}\right) - (f(M, N_0) - f(M_0, N_0)) \tag{4.6}$$

$$f(M, N) = 0.47 \ln\left(1 + 2.01 \times 10^{-5}(MN)^{0.75} + 5.31 \times 10^{-15} M(MN)^{1.52}\right) \tag{4.7}$$

Where N is N_2O in ppbv, M is CH_4 (ppbv) and subscript 0 denotes unperturbed concentrations.

The impact of aviation on methane has two other side effects that need to be accounted for when calculating the complete RF of aviation NO_x . These are the impact of CH_4 on stratospheric water vapour (SWV), which is calculated to be 0.15 times the CH_4 RF (Myhre et al., 2007), and also the longer term effect of CH_4 on O_3 , which has a RF of 42

mW m^{-2} DU^{-1} (Ramaswamy et al., 2001) or 0.5 times the CH_4 RF (Kohler et al., 2008).

Chapter 5

The Relationship between Aviation NO_x Emissions and the Background Atmosphere

In this chapter the MOZART–3 CTM is used to run aviation scenarios in two different background atmospheric NO_x states, thereby determining the effect of the background atmosphere on aviation NO_x emissions. The simulations will also assess the non-linearity of the NO_x – O_3 and NO_x – CH_4 relationships. The methodology is described in Section 5.2, Results are presented and discussed in Section 5.3, a regression analysis is described in Section 5.4 and conclusions drawn in Section 5.5.

5.1 Introduction

The background concentrations of chemical species such as NO_x are influenced heavily by changes in surface emissions. This is particularly relevant when modelling aviation as the magnitudes of the chemical perturbations depend strongly on the background atmosphere into which they are emitted. Ozone formation depends on the availability of ozone precursors, mainly CO and OH radicals and the rate of methane destruction is also controlled by the availability of OH (see Chapter 2) (Isaksen et al., 1978; Berntsen and Isaksen, 1999; Stevenson and Derwent, 2009). Emissions from the surface determine the state of the background atmosphere – a change in surface emissions changes the con-

centrations of ozone precursors and therefore, the oxidising capacity of the atmosphere (Fry et al., 2012). Thus, the relationship between aviation NO_x emissions and its related O_3 production is affected by changes in surface emissions of O_3 precursors. These perturbations to the background atmosphere from its natural state occur primarily through anthropogenic activity, soil and lightning. To study the changes caused by anthropogenic activity, scenarios created by the IPCC which represent alternative atmospheric states based on developments in human activity, the RCP scenarios (see Chapter 3), can be used as templates for background concentrations of NO_x . Of particular interest for this study is the response of ozone formation and methane destruction due to aviation NO_x emissions. Previous studies (Fuglestvedt et al., 1999; Wild et al., 2001) have shown that global reductions in surface NO_x emissions decrease ambient OH concentrations and thus decrease the rate of CH_4 destruction. While this also causes a decrease in tropospheric O_3 , overall the positive climate forcing associated with the CH_4 increase is stronger resulting in a positive RF from reductions in surface NO_x . However, it has also been found that surface reductions of other O_3 precursors; NMVOCs, CO and CH_4 , contribute a negative RF by increasing OH and therefore decreasing the greenhouse gases O_3 and CH_4 . Reductions of surface CH_4 directly reduce the overall atmospheric CH_4 concentration due to its long lifetime in the atmosphere, contributing the biggest negative RF of all the changes in O_3 precursors (Prather, 1996; Wild et al., 2001; Fry et al., 2012; Skowron, 2013)

5.1.1 Aviation NO_x emissions

Aviation emissions create a net increase in NO_x concentrations at cruise altitudes. NO_x concentrations are short lived at the UTLS with an average residence time of weeks, therefore concentrations build along high traffic areas (Figures 5.1 and 5.3). The build-up of NO_x is particularly prevalent over Europe and the USA and between these two areas, in the region known as the North Atlantic Flight Corridor. After CO_2 and water vapour, NO_x is the third highest percentage of emitted engine chemicals. Lee et al. (2010) estimates that up to 15 percent of the emissions in a primary aircraft plume are composed of NO_2 when the aircraft is cruising. This leads to an average NO_x increase of approximately 30 – 40 percent in the major flight corridors.

The NO_x perturbation varies according to season with the highest perturbations occurring in late spring, early summer and the lowest generally occurring in winter. This is mainly due to photochemistry, transport and varying NO_x loss rates. Figure 5.3 shows the activity

of atmospheric cells which transport the dispersing emissions pole-wards and downwards through the atmosphere with major fluxes occurring between 40-50 degrees North. Forster et al. (2003) showed that the average residence time of emissions in the North Atlantic flight corridor at the UTLS is ∼23 days, after which they are transported downwards. The meteorology of the region however does affect the residence time, and the longer the residence time of NO_x , the greater the production of O_3 , hence why meteorology is an important model parameter.

The ozone produced as a result of aviation NO_x emissions also becomes concentrated around high traffic areas in the northern mid-latitudes (Figure 5.2). At flight altitudes, O_3 has an atmospheric residence time of weeks, and so persists long enough to be affected by atmospheric transport and circulation. Figure 5.4 shows that O_3 produced from aviation NO_x spreads further pole-wards and downwards in altitude than the NO_x itself before removal, due to its longer lifetime.

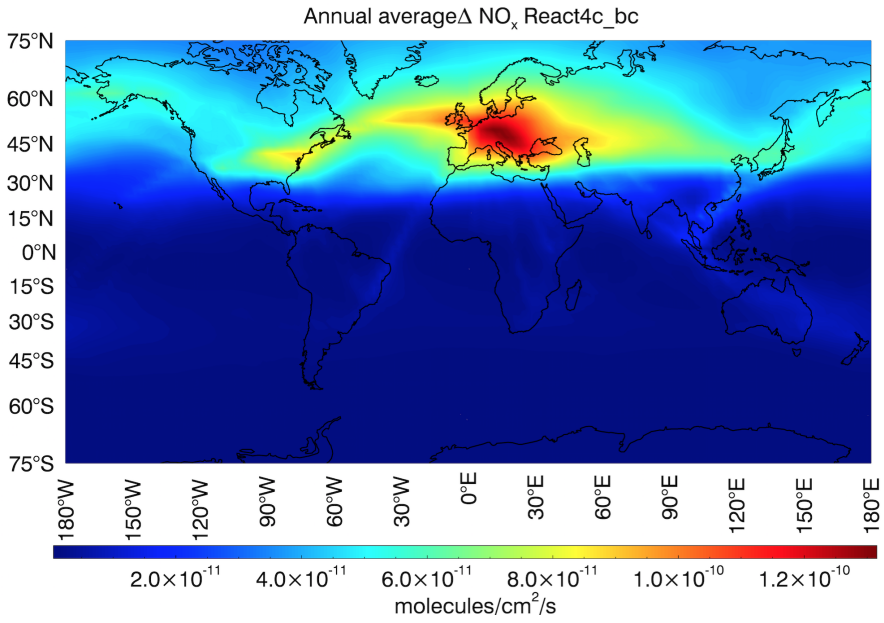

Figure 5.1: An example of the spatial pattern of the NO_x perturbations in the UTLS (228 hPa) as a result of aviation emissions (molecules/cm^2/s). The emissions shown here are an annual average of the React4C base case (described in Chapter 3) run on the MOZART 3 CTM with year 2006 climatology.

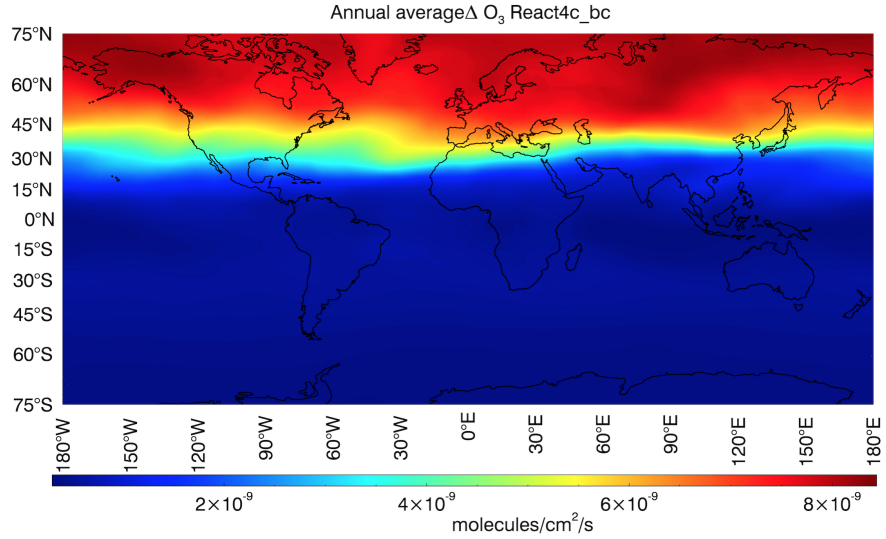

Figure 5.2: An example of the spatial pattern of the ozone perturbations in the UTLS (228 hPa) as a result of aviation emissions (molecules/cm^2/s). The emissions shown here are an annual average of the React4C base case (described in Chapter 3) run on the MOZART 3 CTM with year 2006 climatology. The ozone perturbation spreads further pole-ward than the NO_x due to its relatively longer lifetime in the atmosphere.

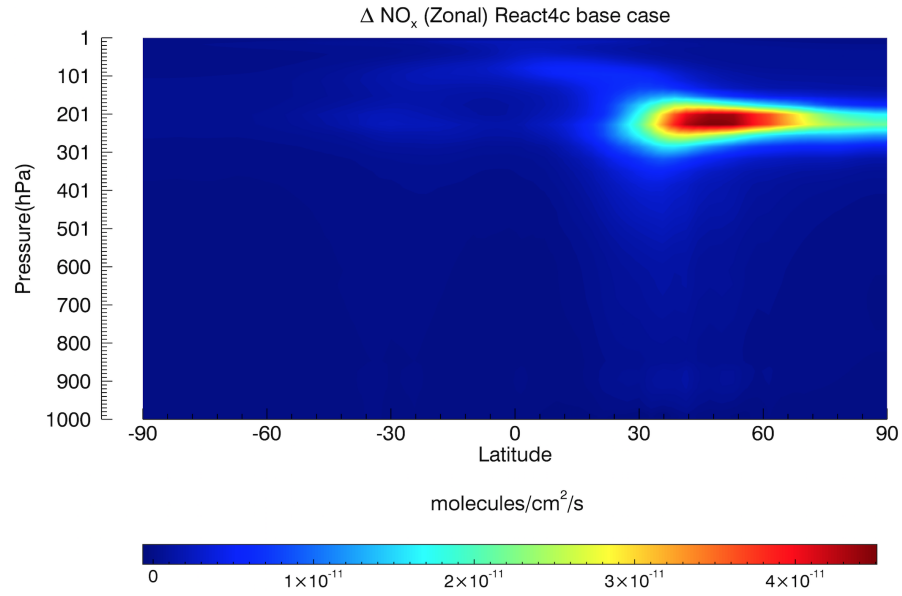

Figure 5.3: An example of the zonal spatial pattern of the NO_x perturbations in the UTLS (228 hPa) as a result of aviation emissions (molecules/cm^2/s). The emissions shown here are an annual average of the React4C base case (described in Chapter 3) run on the MOZART 3 CTM with year 2006 climatology.

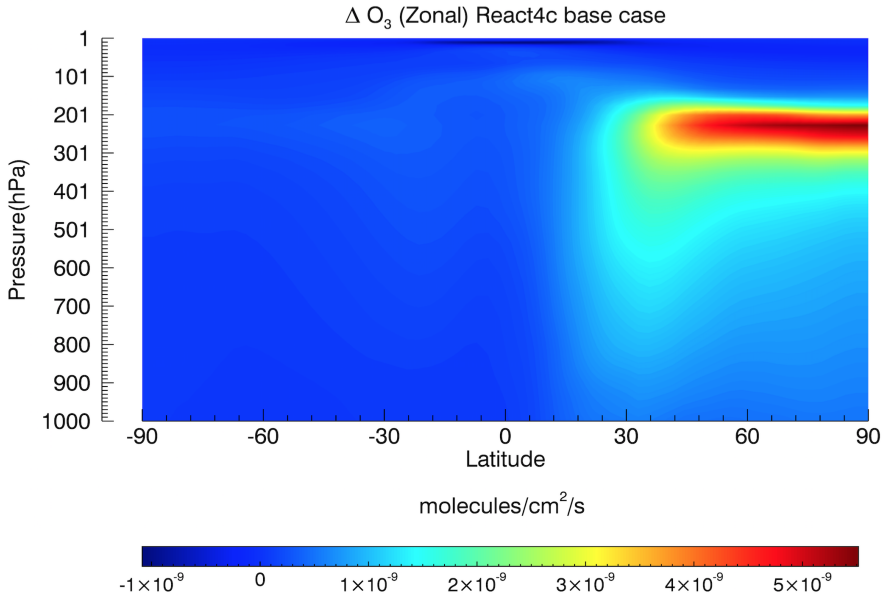

Figure 5.4: An example of the zonal spatial pattern of the ozone perturbations in the UTLS (228 hPa) as a result of aviation emissions (molecules/cm^2/s). The emissions shown here are an annual average of the React4C base case (described in Chapter 3) run on the MOZART 3 CTM with year 2006 climatology. The ozone perturbation spreads further down through the troposphere than the NO_x due to its relatively longer lifetime in the atmosphere.

5.1.2 Experiment outline

The purpose of these experiments is to ultimately improve the way NO_x is modelled using a simple climate model (SCM), which enables the modelling of aviation emission over the longer term. Currently, the LinClim SCM models the effects of aviation NO_x emissions by assuming linear reactions between the NO_x emissions and the associated ozone and methane change. The experiments in this chapter were conducted using the more sophisticated MOZART–3 CTM and will determine the bounds of linearity and then quantify the non–linearity between aviation NO_x emissions and the associated ozone and methane changes. This is accomplished by modelling the ozone and methane perturbations in response to different magnitudes of aviation NO_x emissions using the MOZART–3 CTM. The results of these CTM model runs are then used to create new non–linear parameterisations to more accurately model aviation NO_x over the longer term. The aviation NO_x emissions will also be run against two different background NO_x levels on MOZART–3 to assess the impact of the background atmosphere on ozone and methane change. This

allows the state of the background atmosphere to be considered and included in the new parameterisations.

5.2 Methodology

Ozone and methane are modelled in MOZART–3 using a constant background NO_x level. Therefore, to investigate the impact of a changing background atmosphere, two different background atmospheric NO_x values are used. The values were taken from the RCP scenarios (see Chapter 3) to represent a 'low NO_x ' background (RCP3 in the year 2100; 20.76 Tg N/Yr) and a 'high NO_x ' background (RCP8 in the year 2020; 44.75 Tg N/Yr). The spatial patterns of these backgrounds are different and are shown in Figure 5.5 and Figure 5.6. These figures show the spatial patterns of background NO_x , the NO_x present over the oceans likely sources from shipping emissions as well as chemical distribution of land sources via short-term atmospheric (boundary layer) circulation. Sensitivity studies are carried out in section 5.3.3 to determine the effect of the background spatial pattern of emissions release on aviation NO_x emissions, using a background where the spatial pattern of the low NO_x background is scaled up to the values of the high NO_x background (Table 5.1).

Background atmosphere reference	Surface NO_x emitted (Tg N yr^{-1})
Low NO_x	20.76
High NO_x	44.75
Low NO_x scaled to High NO_x	47.8*

*the slight difference between RCP8 background and the scaled background is due to the scaling process, leading to a difference of approx. 6%, to account for this the resulting ozone burden and methane lifetime have also been scaled by 6%.

Table 5.1: Surface NO_x emissions for each background atmospheric state (Tg N Yr^{-1}), the 'low' NO_x and 'high' NO_x backgrounds were taken from the RCP scenarios as described in the text and a third background was created for comparison, where the spatial pattern of the low NO_x background was scaled up to the magnitude of the high NO_x background and is discussed in Section 5.5.

The aviation scenarios run on MOZART–3 were generated using the React4c base case aircraft emissions data set (see Chapter 3)(http://www.react4c.eu/data/) as a starting point. The value of NO_x emitted in this scenario (0.699 Tg N Yr^{-1}) was multiplied by different

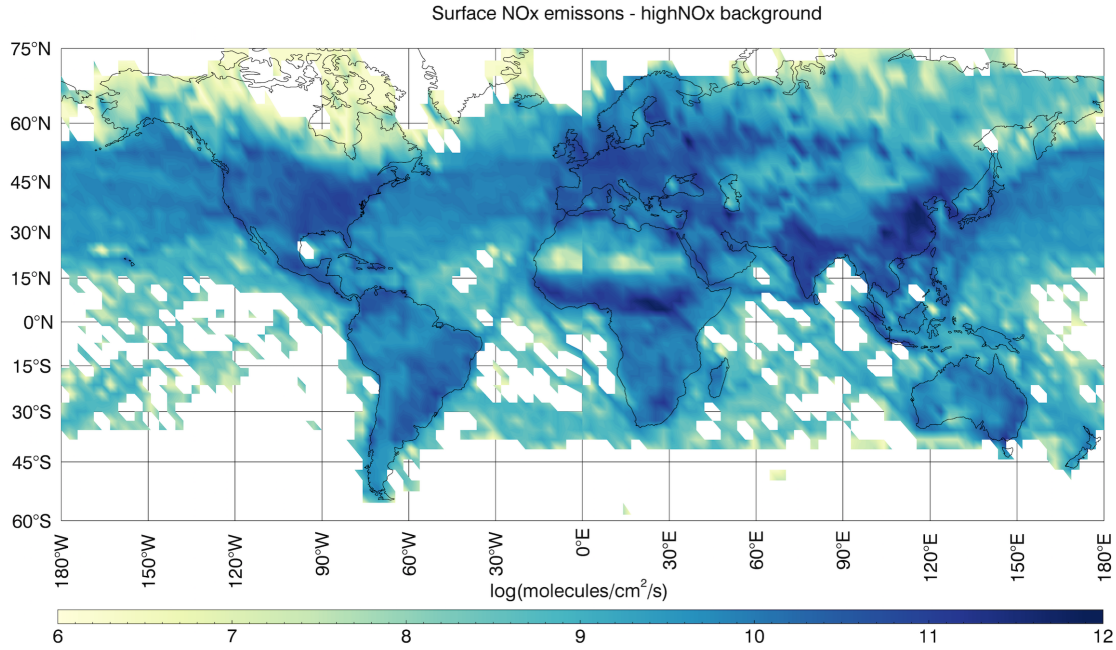

Figure 5.5: The spatial pattern and magnitude of surface NO_x emissions (Log mol cm^{-2} S^{-1}) for the high NO_x background (44.75 Tg N Yr^{-1}). Surface NO_x emissions were taken from the RCP scenarios, the high value representing RCP8 in the year 2100 and the low value representing RCP3 in the year 2020.

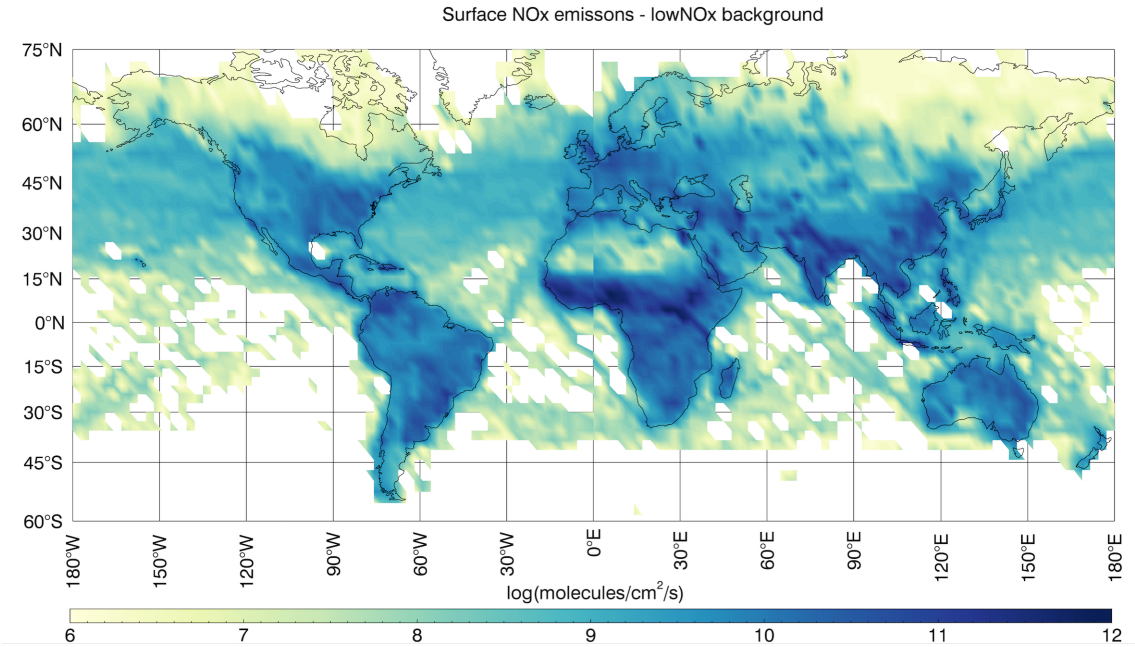

Figure 5.6: The spatial pattern and magnitude of surface NO_x emissions (Log mol cm^{-2} S^{-1}) for the low NO_x background (20.76 Tg N Yr^{-1}). Surface NO_x emissions were taken from the RCP scenarios, the 'high' value representing RCP8 in the year 2100 and the 'low' value representing RCP3 in the year 2020.

factors to generate several different aviation scenarios each emitting different amounts of NO_x , but maintaining the same spatial pattern (Table 5.2). These aviation scenarios were then modelled with MOZART–3 with both the low NO_x and high NO_x background emissions scenarios.

Initially, factors of the React4c base case were used in order to maintain the same spatial structure of aviation emissions throughout the experiment, removing spatial structure as a variable (Table 5.2). Additionally two other aviation scenarios were run which represented aviation at 2050 with optimum and low technology improvements, S6 and S3 respectively, again with a different spatial structure than the React4c emissions scenario (see Chapter 3). This is discussed in section 5.3.3.

Aviation Scenario	NO_x emitted (Tg N Yr^{-1})
React4c base case	0.699
React4c x 1.5	1.048
React4c x 2	1.389
React4c x 2.5	1.748
React4c x 3	2.096
React4c x 3.5	2.446
React4c x4	2.796
React4c x 5.5	3.843
React4c x 7	4.892
React4c x 9	6.289
React4c x 14.9	10.249
React4c x 22	15.374
React4c x 30	20.964
React4c x 45	31.446
React4c x 60	41.928
React4c x 90	62.892
Reacy4c x 120	83.856
S3	2.815
S6	2.865

Table 5.2: Aviation NO_x emissions (Tg N Yr^{-1}) of the React4c base case aviation emissions scenario and the further scenarios used in this study. The 'React4c x' scenarios are the same spatial pattern of the React4c base case but increased in magnitude according to their individual numbers. The 'S3' and 'S6' scenarios have a different spatial pattern of emissions release and are discussed in Section 5.3.3.

5.3 Results

5.3.1 The effects of the background atmospheres on ozone burden change due to aviation NO_x emissions

In the background atmosphere the formation of O_3 from NO_x emissions is a non–linear process, however, it is acknowledged that the chemical reactions involved in the formation of ozone from aviation NO_x take place on a much smaller scale that those of the background atmosphere. This study was thus designed to test the bounds of the non-linearity of the NO_x – O_3 system when applied to aviation. At cruise flight levels, as a result of enhanced ultraviolet radiation, ozone forms more readily from NO_x emissions than it does at ground level (see Chapter 3). Its formation is linked, highly sensitively, to precursor emissions and ambient background concentrations at the time and location of formation. The relationship between background atmospheric NO_x and ozone formation from aviation NO_x is a complex one – in the troposphere NO_x is involved in both the formation and destruction of ozone. The aviation scenarios (Table 5.2) were run on the MOZART–3 CTM as described in Chapter 4 and the results are presented in the following sections (Figure 5.7 Figure 5.21).

The results illustrate that, as aviation NO_x emissions increase, so does ozone burden, this relationship appears linear up to around 3 Tg N Yr^{-1} and then becomes non-linear in both the low NO_x and high NO_x background atmospheric states (Figure 5.7 and Figure 5.8). At values of aviation NO_x emissions release higher than 3 Tg N Yr^{-1} ozone formation per NO_x molecule begins to reduce as aviation emissions increase, reflecting the non–linearity of ozone formation from NO_x in the atmosphere.

Several other modelling studies focused on aviation NO_x emissions have suggested that on the scale at which aviation emits NO_x , its associated interactions with the background atmosphere and subsequent reactions respond linearly, in accordance with the NO_x emission rate. As long as the background atmosphere remains reasonably consistent, this appears true on a global scale (Grewe et al., 1999; IPCC 1999; Sausen and Schumann, 2000; Kohler et al., 2008; Khodayari et al., 2014). Grewe et al. (1999) suggest that, for a given scenario of aviation emissions, the NO_x – O_3 cycle only becomes non–linear at high latitudes during summer when convection enhances background atmospheric NO_x and therefore causes a decrease in ozone productivity, thus, the summer season alone

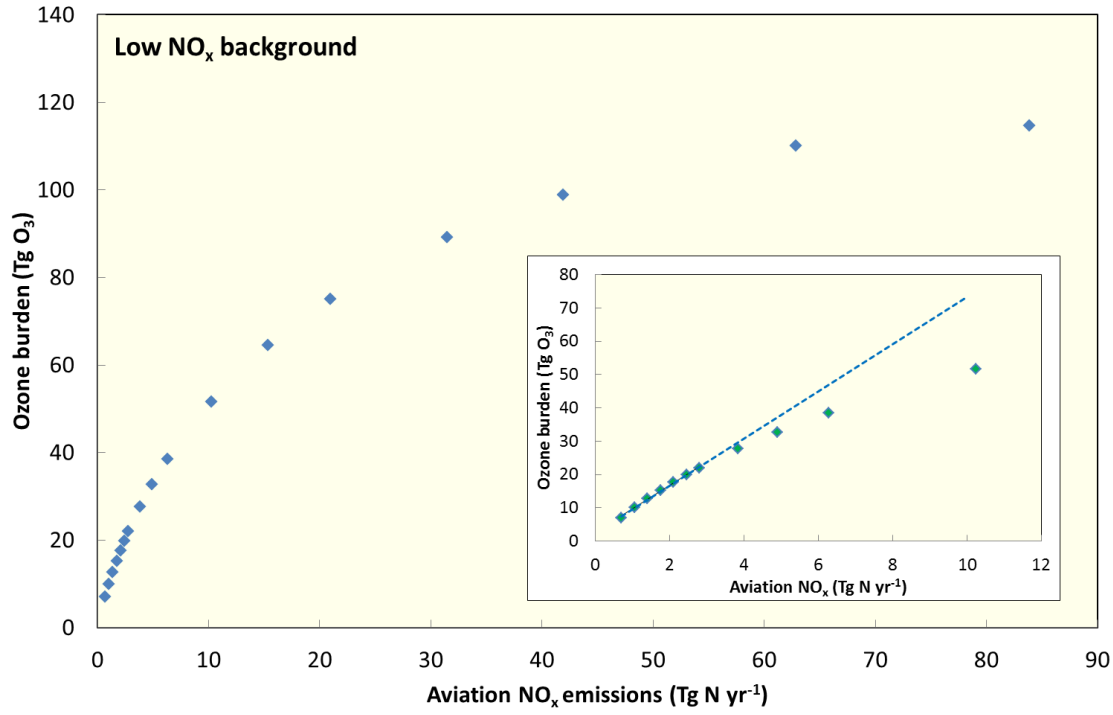

Figure 5.7: The ozone burden (Tg O_3) resulting from the aviation NO_x emissions in the low NO_x atmospheric background state. Each point represents one of the emissions scenarios described in Table5.2 The lowest of which was the React4c base case. The emissions scenarios were modelled on the MOZART CTM with the set up as described in Chapter 4. The bottom right panel shows the emissions scenarios up to 10 Tg N Yr^{-1} with a linear trend line formulated from the values up to 3 Tg N Yr^{-1} to show where the linear relationship between aviation NO_x emissions and the associated ozone burden breaks down.

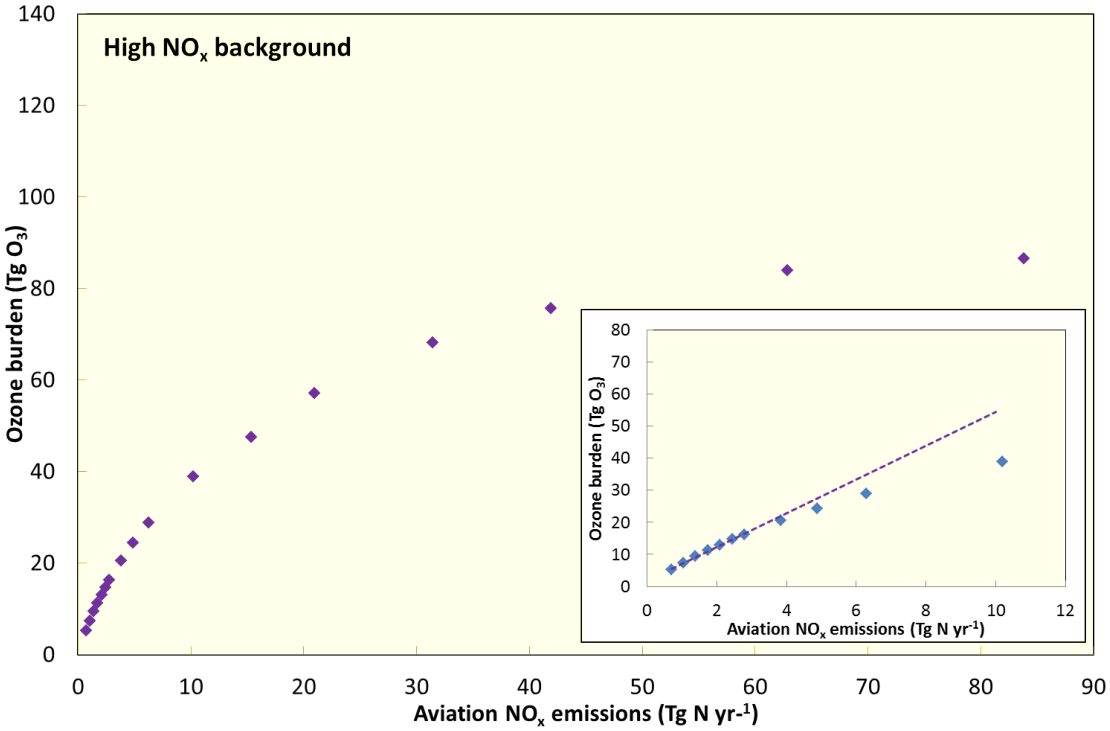

Figure 5.8: The ozone burden (Tg O_3) resulting from the aviation NO_x emissions in the high NO_x atmospheric background state. Each point represents one of the emissions scenarios described in Table5.2 The lowest of which was the React4c base case. The emissions scenarios were modelled on the MOZART CTM with the set up as described in Chapter 4. The bottom right panel shows the emissions scenarios up to 10 Tg N Yr^{-1} with a linear trend line formulated from the values up to 3 Tg N Yr^{-1} to show where the linear relationship between aviation NO_x emissions and the associated ozone burden breaks down.

accounts for most of the non–linearity seen in the aviation NO_x – O_3 cycle.

The non–linearity seen here can be explained through the chemistry involved. The overall production of ozone from NO_x depends on peroxy radicals – HO_2 and RO_2 (R = organinc radical) which oxidise NO to NO_2 which then undergoes photodissociation and results in the formation of ozone through equation 5.1 to equation 5.5 (also discussed in Chapter 2).

$$\text{NMHC} + \text{OH} \rightarrow \text{O}_2 + \text{RO}_2 \tag{5.1}$$

$$\text{RO}_2 + \text{NO} + \text{O}_2 \rightarrow \text{NO}_2 + \text{HO}_2 + \text{CARB} \tag{5.2}$$

$$\text{HO}_2 + \text{NO} \rightarrow \text{NO}_2 + \text{OH} \tag{5.3}$$

$$2\text{NO}_2 + h\nu + 2\text{O}_2 \rightarrow 2\text{NO} + 2\text{O}_3 \tag{5.4}$$

$$\text{Net NMHC} + 4\text{O}_2 + h\nu \rightarrow 2\text{O}_3 + \text{CARB} \tag{5.5}$$

Where NMHC is non-methyl hydrocarbons and CARB is carbonyl compounds

These reactions show that NO_x and NMHC are ozone precursors and form ozone via HO_x and that NO_x and HO_x act as catalysts in the production of O_3 . Therefore, generally ozone production increases as NO_x and HO_x emissions do. However, the destruction of NO_x and HO_x also depend on the background NO_x and NMHC levels, thus the rate of ozone production does not respond linearly to the to the increase in ozone precursors, as the rate of the termination reactions of NO_x and HO_x (ozone precursors) also increase as background NO_x emissions increase (Lin et al., 1988), explaining the non-linear reactions seen in figures 5.7 and 5.8.

The difference in average OPE for the two backgrounds, stems again from changes in the hydroxyl radical. A low NO_x background will promote OH, allowing more production of ozone per NO_x molecule than in a high NO_x background where OH is inhibited. In a low NO_x environment, such as the low background NO_x atmospheric states used here, OH formation is greater than the emission rate of NO_x , excess NO_x is thus removed rapidly through equation 5.6 for example.

$$\text{OH} + \text{NO}_2 \rightarrow \text{HNO}_3 \tag{5.6}$$

This results in an excess of free radicals in the atmosphere, which are available for other reactions such as the sequence of reactions that lead to the formation of ozone (above). In a high NO_x background, NO_x emission rate is greater than the free radical formation rate,

resulting in excess NO_x , peroxide formation is then limited and NO_x removal reactions are slow. In other words, in a low NO_x background the additional input of aviation NO_x emissions are removed by oxidation, leading to the formation of ozone, however, the oxidising capacity of the atmosphere in a high NO_x state is diminished reducing the rate of ozone production in comparison to a low NO_x state (Kleinman, 1994).

5.3.2 The effects of background atmosphere on the changes to methane lifetime due to aviation NO_x emissions

The release of aviation NO_x emissions causes a reduction in methane lifetime in the troposphere due to enhancement in OH concentration (equation 5.7), which therefore leads to a lower steady state methane concentration.

$$CH_4 + OH \rightarrow CH_3 + H_2O \tag{5.7}$$

The change in methane lifetime associated with the release of aviation NO_x thus produces a negative RF. Similarly to the NO_x – O_3 relationship, the relationship between aviation NO_x emissions and methane lifetime reduction appears to show linear correlation until aviation NO_x emissions reach $\sim$3 Tg N Yr^{-1} and it then deviates from linear, more so in the low NO_x than high NO_x background (Figure 5.9 and Figure 5.10).

The effects of aviation NO_x on methane lifetime again differ depending on the background into which the emissions are released. The lifetime of methane is reduced substantially more under the low NO_x background scenario than the high NO_x , by an average of 50 percent (Figure 5.9 and Figure 5.10). The low NO_x background also enables greater formation rates of ozone (Figure 5.7) as described above, which in turn results in an increased concentrations of OH and therefore greater decrease in methane lifetime through the reaction in equation 5.7. As methane is also an ozone precursor, it can be inferred that under the low NO_x background the reduction in ambient methane would eventually contribute to a greater decrease in ozone formation from aviation NO_x than under the high NO_x background.

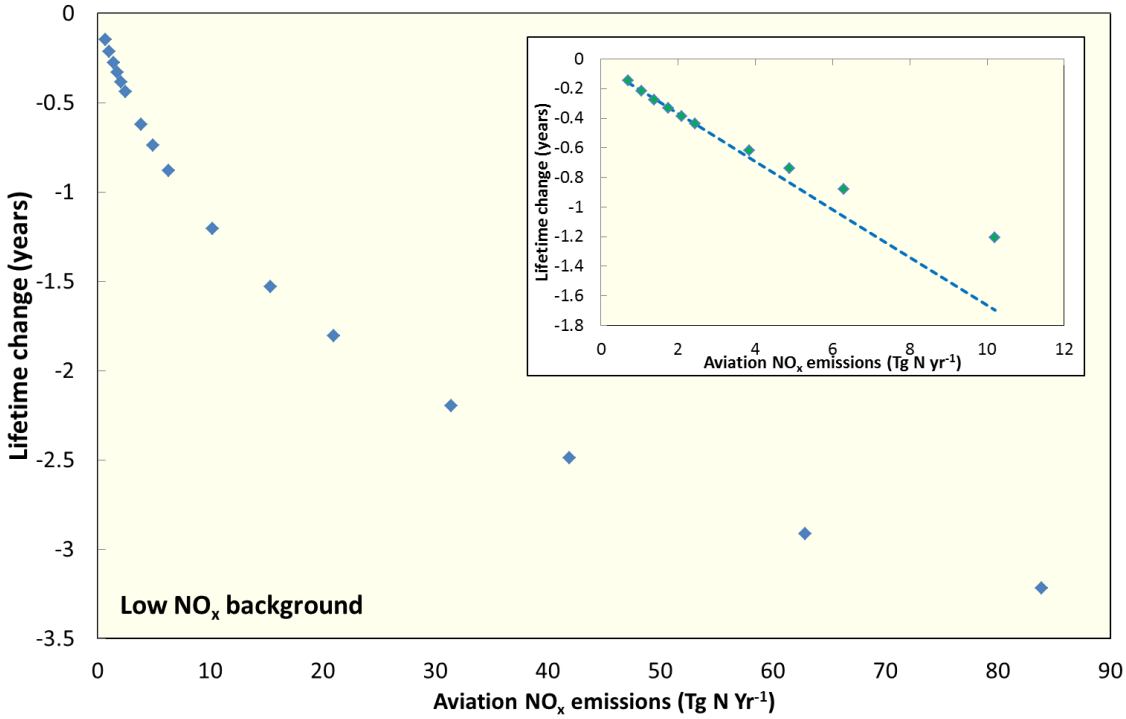

Figure 5.9: The change in methane lifetime, due to destruction by OH, resulting from the aviation NO_x emissions in the low NO_x atmospheric background states. Each point represents one of the emissions scenarios described in Table 5.2 the lowest of which was the React4c base case. The emissions scenarios were modelled on the MOZART CTM with the set up as described in Chapter 4. The smaller panel shows the emissions scenarios up to 10 Tg N Yr^{-1} with a linear trend line formulated from the values up to 3 Tg N Yr^{-1} to show where the linear relationship between aviation NO_x emissions and the associated methane lifetime change breaks down

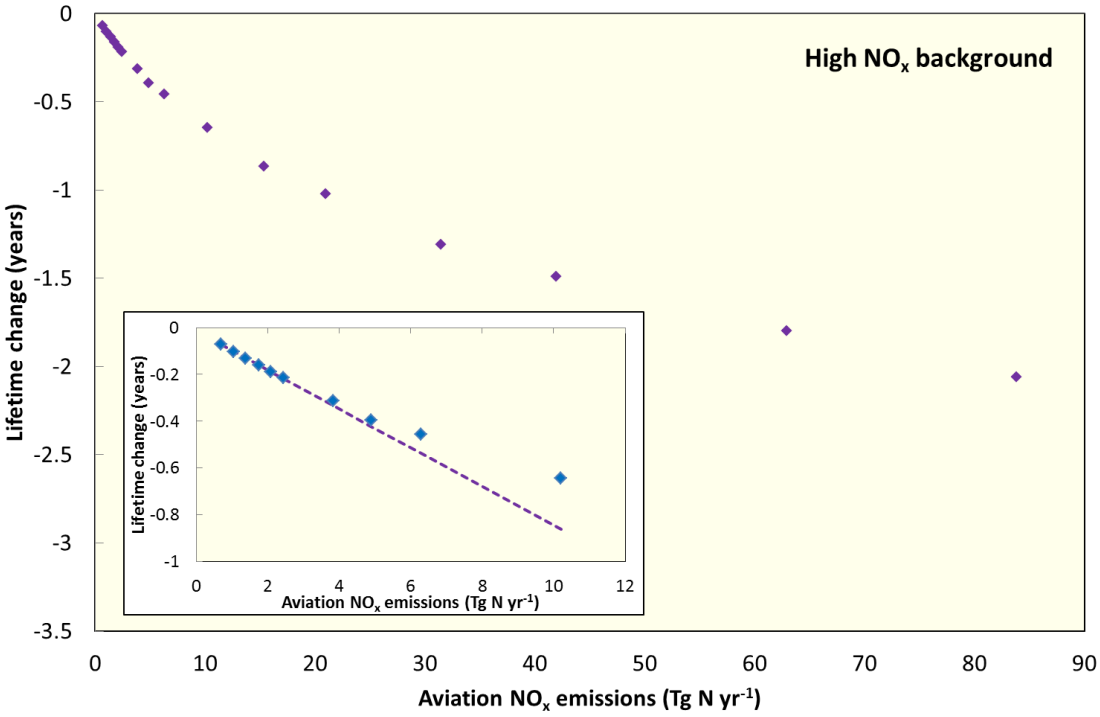

Figure 5.10: The change in methane lifetime, due to destruction by OH, resulting from the aviation NO_x emissions in the high NO_x atmospheric background states. Each point represents one of the emissions scenarios described in Table 5.2 the lowest of which was the React4c base case. The emissions scenarios were modelled on the MOZART CTM with the set up as described in Chapter 4. The smaller panel shows the emissions scenarios up to 10 Tg N Yr^{-1} with a linear trend line formulated from the values up to 3 Tg N Yr^{-1} to show where the linear relationship between aviation NO_x emissions and the associated methane lifetime change breaks down

5.3.3 The effects of spatial structure

Aviation emissions

All the aviation emissions scenarios used until this point had the same spatial structure – that of the React4c base case (Figure 5.11). To determine if the spatial pattern of emissions release had an impact on the resulting ozone and methane perturbations two additional scenarios were run, named S3 and S6 5.12, 5.13 (see Chapter 3). These scenarios have a similar magnitude of emission as React4c x4 scenario but a different spatial pattern of release. These scenarios were designed for ICAO's CAEP project to represent aviation activity in 2050 and therefore have greater NO_x release over SE Asia and China and less over Europe and USA (Lee et al., 2013a).

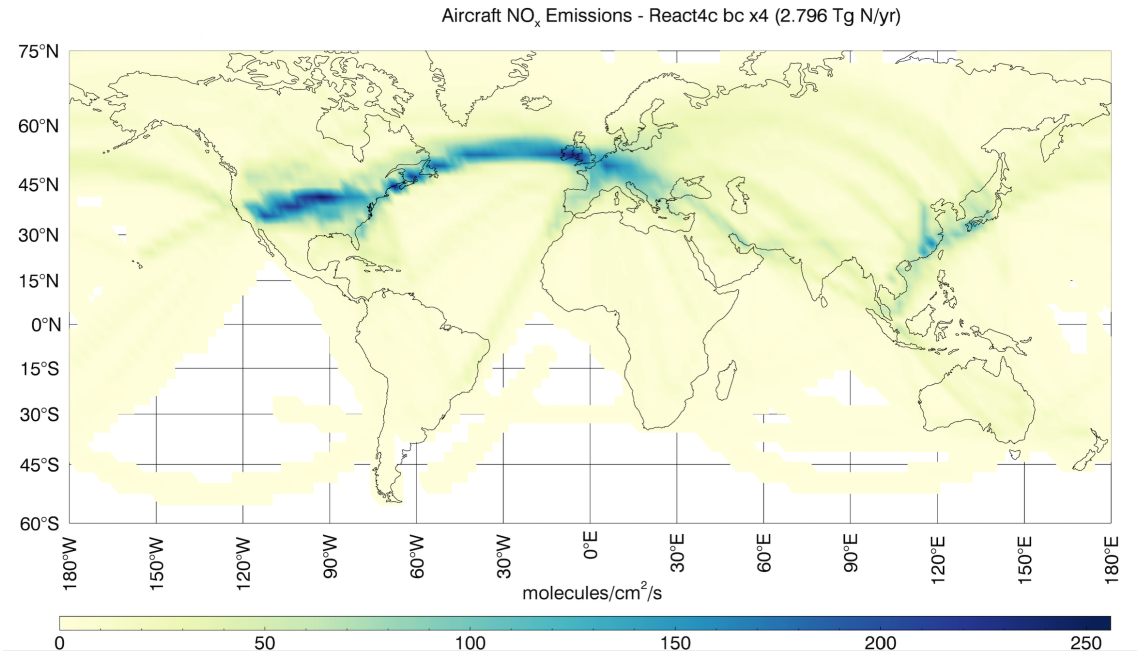

Figure 5.11: The spatial patterns of aviation NO_x emissions release (molecules/cm^2/s) at 228 hPa altitude for the React4c x4 aviation NO_x emissions scenarios, details of each scenario are presented in the text.

The extra emissions scenarios correspond well to the regime of the React4c aviation scenarios, showing that the spatial pattern of emissions release has little impact on the ozone burden and methane lifetime change resulting from aviation NO_x emissions, in either the low or high NO_x background atmospheres, for the scenarios used here (Figure 5.14).The

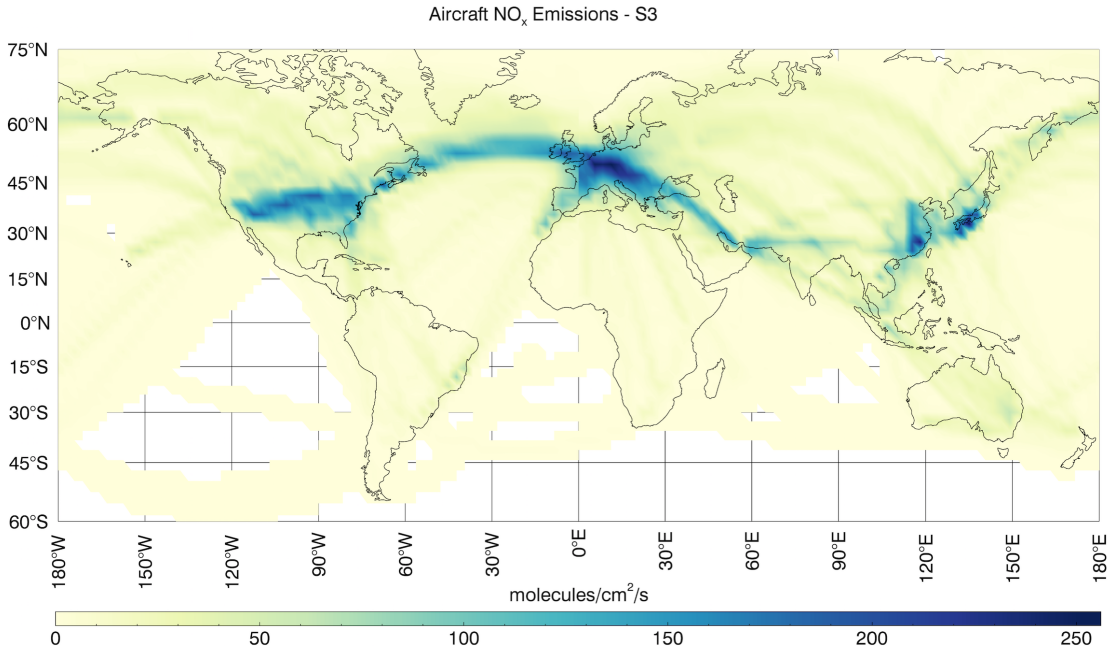

Figure 5.12: The spatial patterns of aviation NO_x emissions release (molecules/cm^2/s) at 228 hPa altitude for the S3 aviation emissions scenario

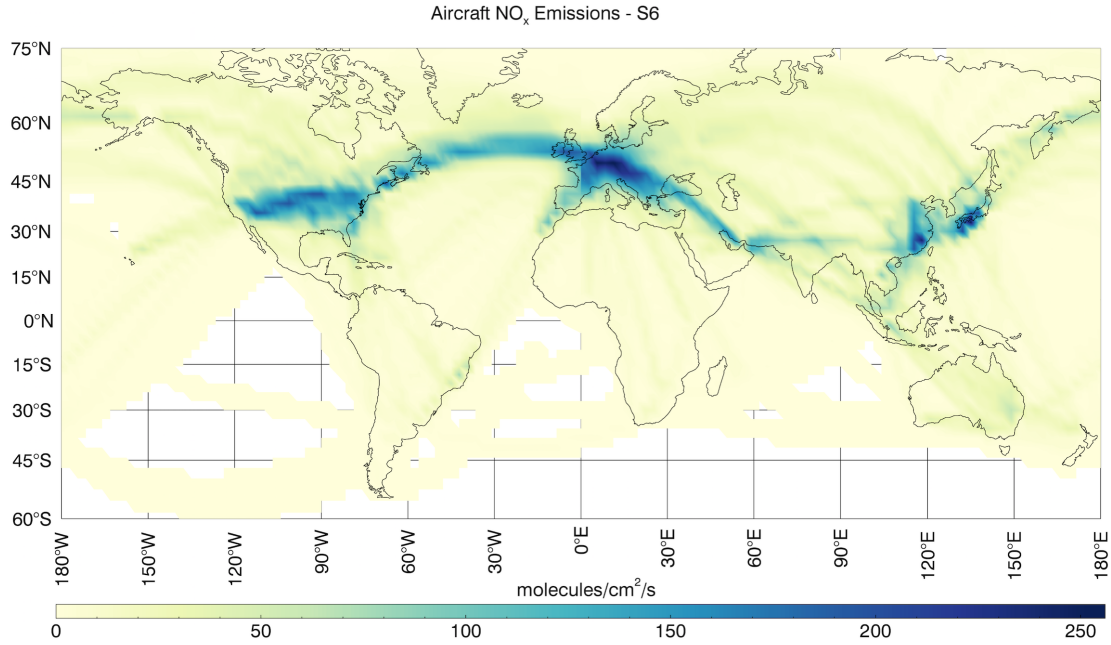

Figure 5.13: The spatial patterns of aviation NO_x emissions release (molecules/cm^2/s) at 228 hPa altitude for the S6 aviation emissions scenario

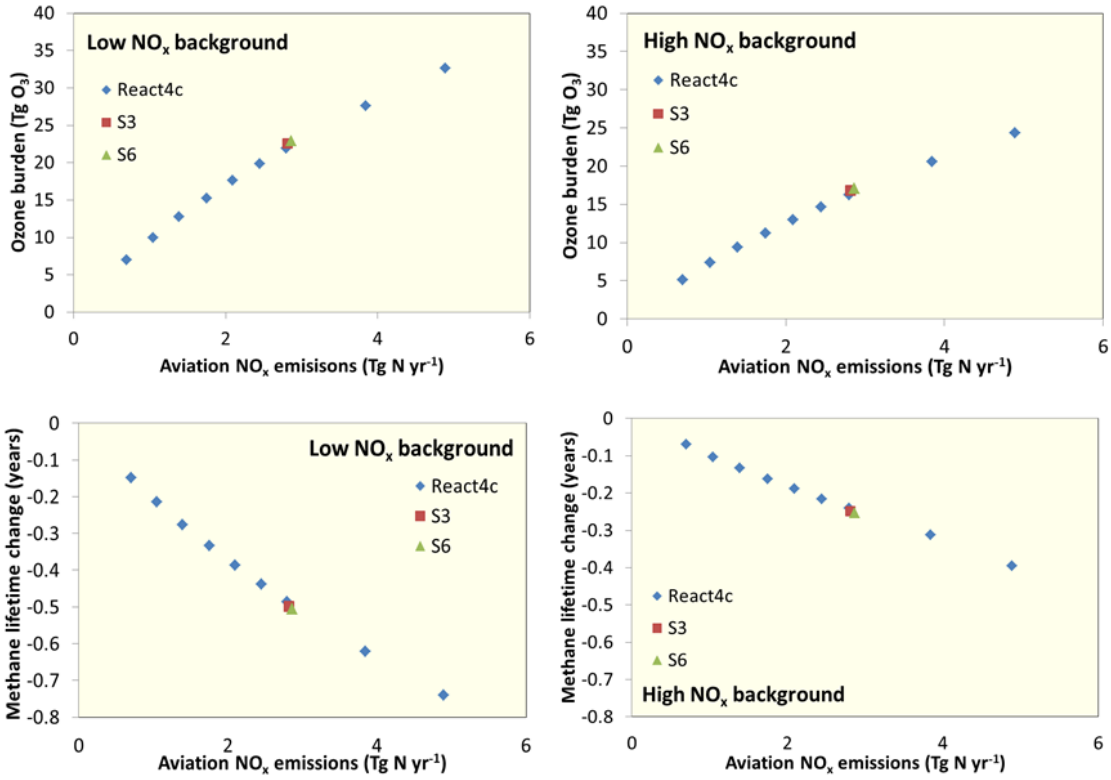

Figure 5.14: A comparison of the S3 and S6 aviation NO_x emissions scenarios to the React4c emissions scenarios. The S3 and S6 scenarios have a different spatial pattern of emissions release to the React4c scenarios. The panels show, ozone burden resulting from aviation NO_x emission in the low NO_x (top left) and high NO_x (top right) background atmospheres and the methane lifetime change due to aviation NO_x emissions in the low NO_x (bottom left) and high NO_x (bottom right) background atmospheres.

S3 and S6 emissions scenarios have aviation NO_x emissions closest to that of four times the React4c base case and so results were scaled to the React4c x4 scenario for comparison (Table 5.3). Table 5.3 and Figure 5.14 show that the difference in spatial pattern between the three aviation scenarios (React4c, S3 and S6) causes results to vary by less than 3 percent, for both ozone burden and methane lifetime change resulting from aviation NO_x emissions in the low NO_x and high NO_x background.

	Scenario	Aviation NO_x emissions (Tg N yr^{-1})	O_3 burden (Tg O_3)	% difference to React4cx4 (when scaled)	CH_4 lifetime reduction (years)	% difference to React4cx4 (when scaled)
Low NO_x background	**S3**	2.815	22.603	*2.27%*	-0.498	*1.54%*
	S6	2.865	22.891	*1.79%*	-0.505	*1.18%*
	Recat4cx4	2.796	21.94		-0.487	
High NO_x background	**S3**	2.815	16.83	*2.85%*	-0.249	*2.56%*
	S6	2.865	17.036	*2.32%*	-0.253	*2.39%*
	Recat4cx4	2.796	16.24		-0.241	

Table 5.3: The differences in ozone burden and methane lifetime change when the spatial pattern of aviation emissions release is changed. The table shows the percentage difference between the S3 and S6 scenarios compared to the React4c x4 emissions scenario. The S3 and S6 emissions scenarios have emissions values closest to that of React4c x4 and have therefore been scaled to allow comparison.

Surface emissions

Further sensitivity studies were performed to ascertain the effect of the differing spatial patterns of the low NO_x and high NO_x background atmospheres (Figure 5.6 and Figure 5.5). The low NO_x background pattern was scaled up to the values of the high NO_x background while retaining its original spatial pattern (Figure 5.15).

Figure 5.16 indicates that the ozone burden changes differ in the 'scaled up' atmosphere from the high NO_x atmosphere by approximately 7 percent. For methane the spatial pattern of the background has more of an impact than it does for ozone burden, as lifetime change differed by approx. 13 percent between the scaled and the high NO_x background atmospheres up to aviation emissions of NO_x of 3 Tg N Yr^{-1} and by approximately 19 percent between 4 -5 Tg N Yr^{-1}.

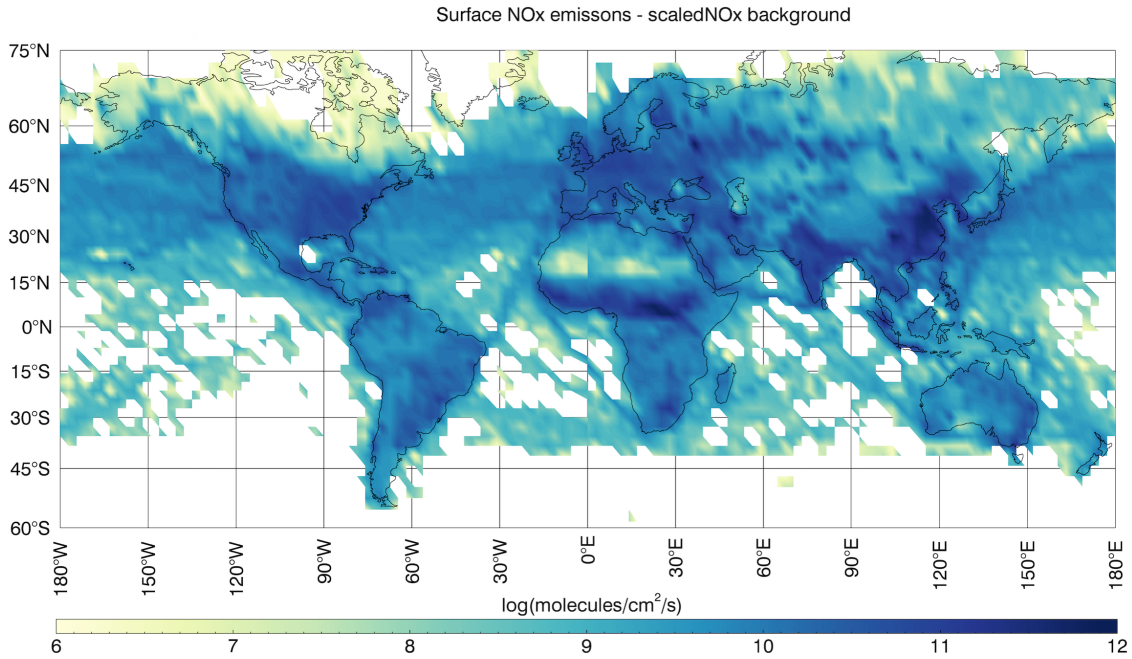

Figure 5.15: The spatial pattern of low NO_x background atmosphere scaled up to the value of the high NO_x background atmosphere, totalling 47.8 Tg N Yr^{-1}. The total NO_x value is higher than the original high NO_x background value of 44.75 Tg N Yr^{-1} due to the method of the scaling process, however results have been scaled to allow comparison.

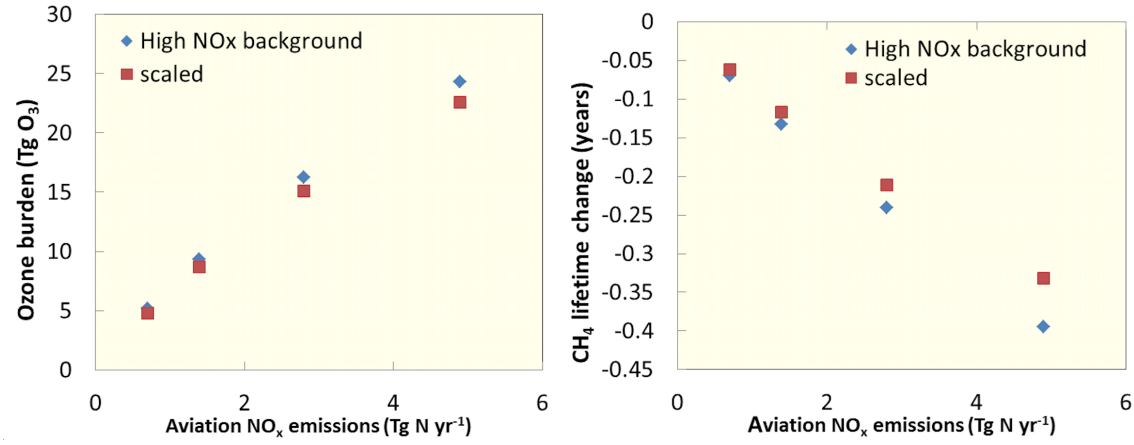

Figure 5.16: The ozone burden from aviation NO_x emissions (left) and methane lifetime reduction (right) for the same aviation scenarios run in the high NO_x background (blue points) and the low NO_x patter–scaled–to–high NO_x values background (red points). This shows the impact of different spatial patterns of background atmospheric NO_x due to surface NO_x emissions release.

5.3.4 Which factors have the biggest impact on the effects of aviation NO_x emissions

The results here suggest that magnitude of emissions is the most important factor in determining the amount of ozone produced from additional NO_x emissions and this agrees with other studies (Fry et al., 2012, Holmes et al., 2011). The difference in surface NO_x emissions between the low and high background NO_x atmospheric states used here causes ozone burden to differ by an average of 25 percent i.e. the same aviation emissions have a greater effect, in this case lead to the production of ∼25 percent more O_3 , in a 'cleaner' low NO_x background emissions scenario. Reducing the background concentrations of NO_x increases the ozone production efficiency per aviation-released NO_x molecule (Berntsen and Isaksen, 1999), and the low background NO_x levels allow reactions involving aircraft emissions to dominate.

OPE was calculated using the method described in Lee et al., (2010):

$$\mathrm{OPE} = \frac{\text{ozone enhancement [kg]}}{\mathrm{NO_x}\text{ emission }\left[\text{kg N yr}^{-1}\right]} \times \frac{\text{N molec. weight}}{\text{ozone molec. weight}} \times \frac{1}{\text{ozone lifetime [yr]}}$$

Where ozone lifetime is assumed to be 28 days.

Average OPE for the whole data series was 23.2 in the low NO_x background and 17.2 in the high NO_x background. The high NO_x background has 55 percent more surface NO_x emissions than the low NO_x background and causes a difference in OPE of 6. The spatial pattern of aviation NO_x emissions release was found to have a negligible effect, causing ozone burden and methane lifetime changes of less than 3 percent. It is noted that there are other factors that affect the RF from aviation NO_x emissions, such as the aircraft cruising altitude, however, the investigation of other factors is beyond the scope of this study.

5.4 The Formation of a New Net NO_x Radiative Forcing Parameterisation

The results presented in Figures 5.7, 5.8, 5.9 and 5.10 quantify the range over which the linear relationship of NO_x emissions to ozone burden and NO_x emissions to methane lifetime change is valid. The radiative forcing from ozone was computed using a linear function on the Edwards–Slingo RTM (See Chapter 4) therefore, the relationship between ozone burden and RF is linear. The new steady state of methane was calculated for each aviation NO_x value according to Fuglestvedt et al., (1999), to enable the radiative forcing of the methane lifetime change to be calculated as described in Chapter 4. Analysis was undertaken to fit an appropriate regime to the data for use in a parametrisation to represent NO_x RF in a simple climate model.

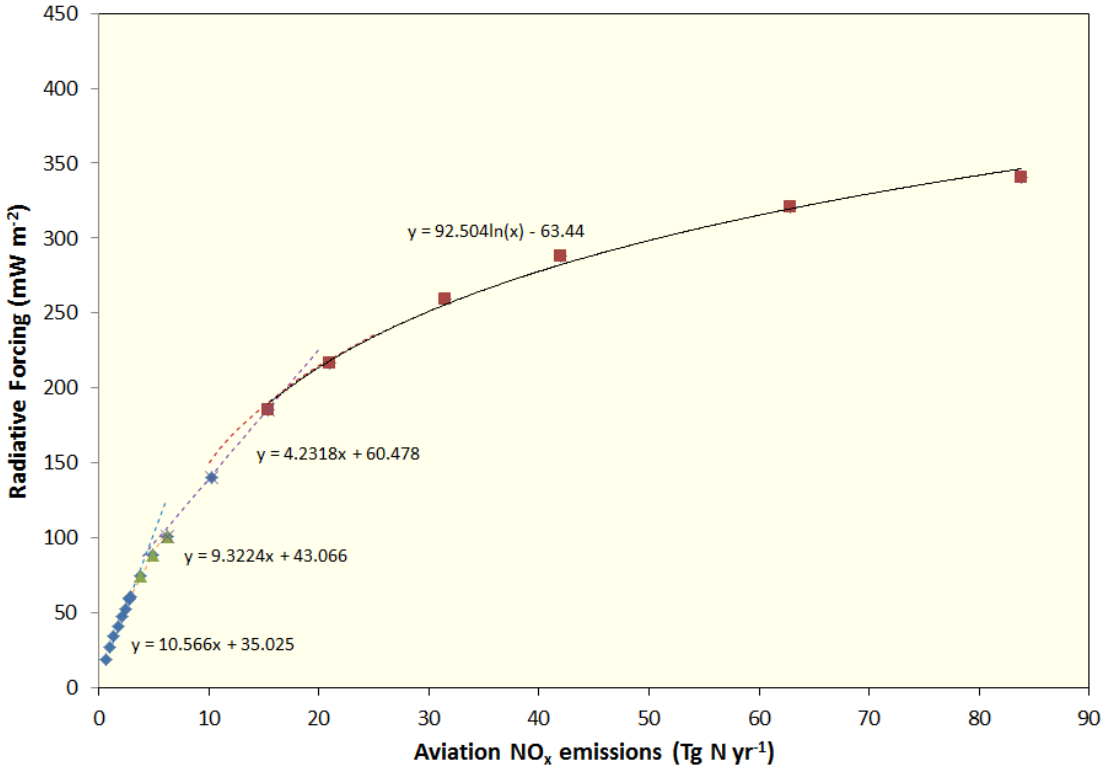

Figure 5.17: In one earlier stage regression attempt, four separate regimes were fitted to the data each representing a separate segment of the curve, this method subsequently gave a somewhat discontinuous response, where the regimes switched form one to the next, when used to calculate the RF from aviation NO_x emissions.

Figures 5.7, 5.8, 5.9 and 5.10 show that both the NO_x – O_3 and NO_x – CH_4 regimes are linear up to ~3 Tg N Yr^{-1} and therefore a linear regression is appropriate, however linearity ceases after 3 Tg N Yr^{-1} and the data is better represented by a natural log regressions. However, the same figures also show that the log regime does not represent the data well over the entire series, especially at the lower values of aviation NO_x emissions. The lower values are the most important for studies of future aviation as the current consensus suggest that NO_x emissions are unlikely to rise much above ~5 Tg N Yr^{-1} in the next few decades (Chapter 3). One attempt involved fitting up to four separate linear fitting for the lower values, to ensure they were represented well, and a natural log regime to encompass the higher values, which fitted the curve well (Figure 5.17). However, when these regimes were used to calculate ozone and methane radiative forcing from NO_x emissions they produced a somewhat discontinuous response, which resulted in the propagation of these errors when temperature response was calculated. Polynomial fits were also tried at this point, but did not fit the curves sufficiently well.

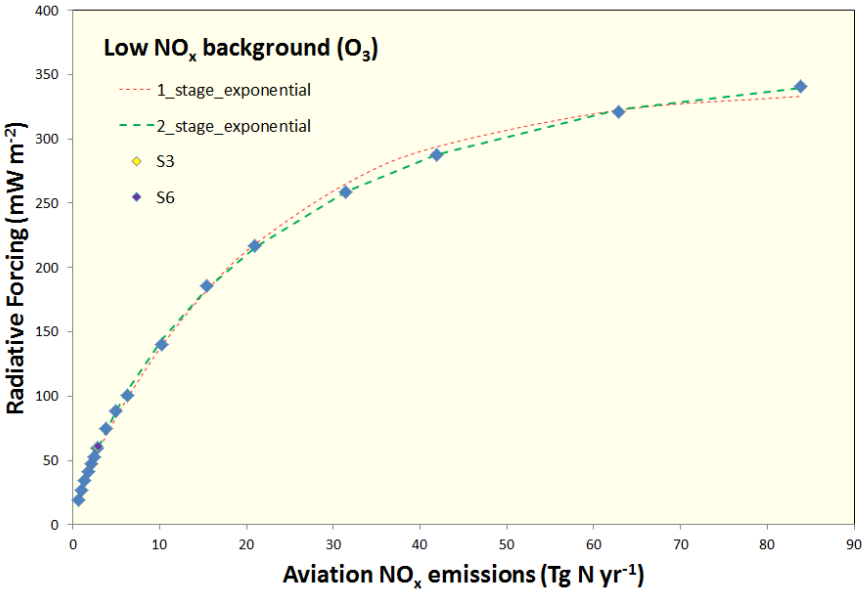

Figure 5.18: Exponential fittings for the ozone radiative forcings resulting from aviation NO_x emissions from the scenarios shown in Table 5.2 in the low NO_x background atmosphere

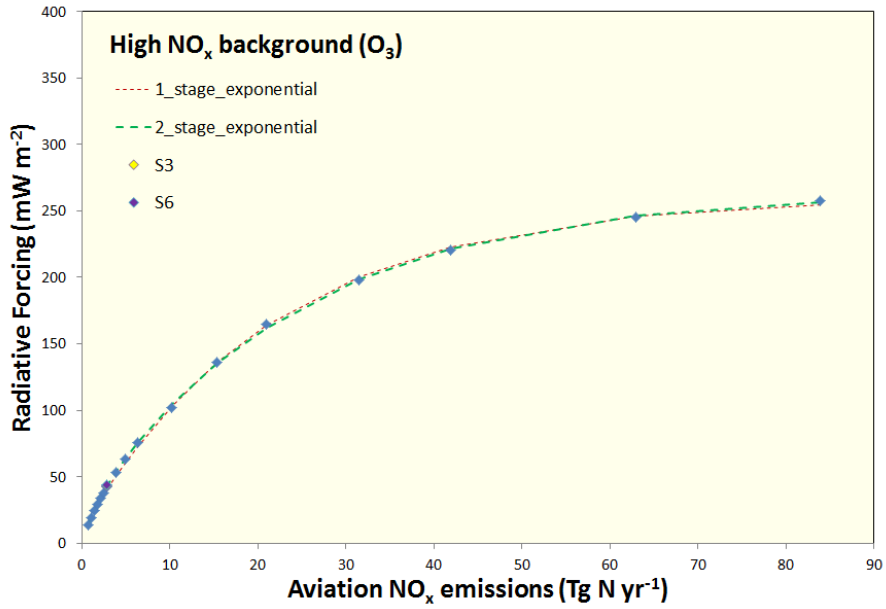

Figure 5.19: Exponential fittings for the ozone radiative forcings resulting from aviation NO_x emissions from the scenarios shown in Table 5.2 in the high NO_x background atmosphere

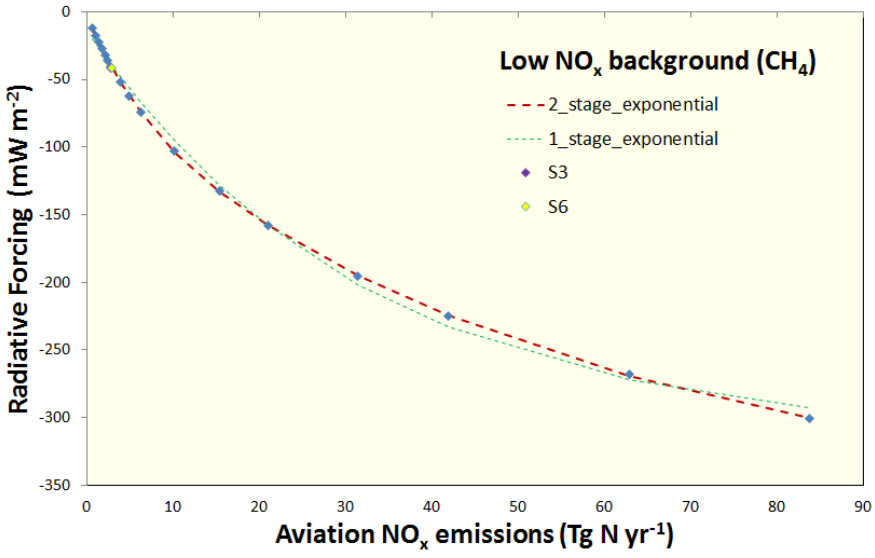

Figure 5.20: Exponential fittings for the methane radiative forcings resulting from aviation NO_x emissions from the scenarios shown in Table 5.2 in the low NO_x background atmosphere

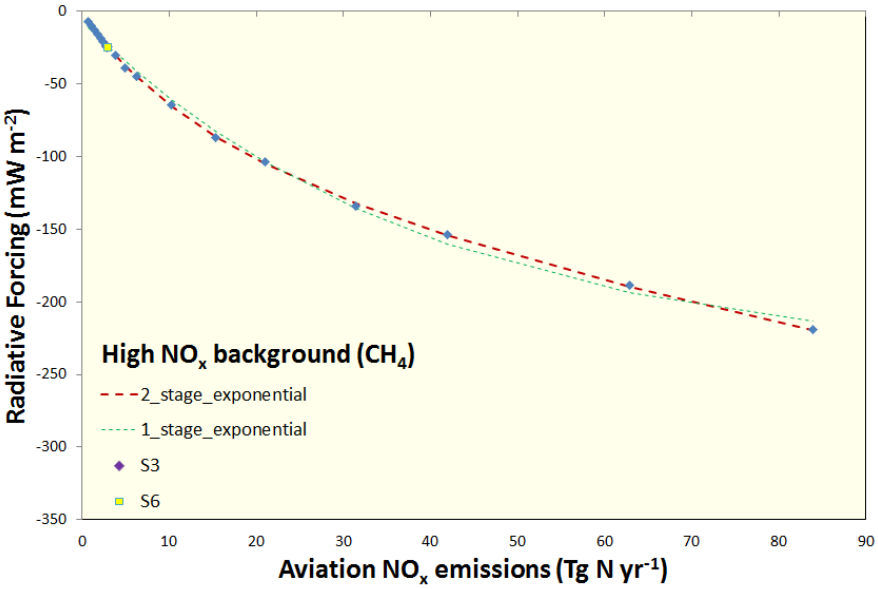

Figure 5.21: Exponential fittings for the ozone radiative forcings resulting from aviation NO_x emissions from the scenarios shown in Table 5.2 in the high NO_x background atmosphere

An exponential fit of the data was applied with more satisfactory results for both ozone and methane, in both the background atmospheric NO_x states (Figures 5.18, 5.19, 5.20 and 5.21). It also became apparent that a 2 stage exponential growth (for ozone) and decay (for methane) were the most accurate. These formula, with the aid of Table 5.4 will be used to calculate the RF of ozone and methane for future aviation scenarios. As noted in Chapter 4, there are errors associated with CTM modelling, and specifically, with MOZARTs ability to accurately model O_3 and CH_4 due to an overestimation of the Brewer–Dobson circulation, Skowron (2013) reported a regional error of up to approx. 50 percent in modelled O_3 compared to observations, whereas the average error associated with regional methane representation is only 1.5 percent. The inherent errors and uncertainty associated with CTM modelling must be acknowledged in any study of the subject.

Low NO_x background		High NO_x background	
CH_4 calcs	y = A1*exp(-x/t1) + A2*exp(-x/t2) + y0	CH_4 calcs	y = A1*exp(-x/t1) + A2*exp(-x/t2) + y0
A1	65.17031	A1	65.12779
t1	6.44003	t1	11.09697
A2	303.6975	A2	315.7442
t2	57.69421	t2	127.5292
y0	-371.57	y0	-382.796
R-square	0.99604	R-square	0.99676
O_3 calcs	y = A1*exp(x/t1) + A2 * exp(x/t2) + y0	O_3 calcs	y = A1*exp(x/t1) + A2 * exp(x/t2) + y0
A1	-63.6653	A1	-18.8407
t1	-6.00316	t1	-1.75771
A2	-283.78	A2	-244.762
t2	-28.9788	t2	-23.7662
y0	355.0657	y0	263.6285
R-square	0.99959	R-square	0.99979

Table 5.4: The constants and statistics resulting from the regressions analysis that are used to form the new net NOx RF paramterisations for use in a SCM.

5.5 Conclusions

The purpose of this study was to determine the bounds of linearity within the perturbed NO_x – O_3 – CH_4 cycle in the atmosphere due to aviation NO_x emissions, in order to create a new NO_x parameterisation for a simple climate model (SCM), LinClim, in the study of long–term aviation activity. The use of this SCM is desirable compared to a CTM as it runs quickly and inexpensively, while retaining the appropriate chemistry from the complex features incorporated in its 'parent' CTM. This allows for the many simulations necessary for the study of trade–offs, between different emissions species.

The ozone burden resulting from aviation NO_x release shows a positive correlation with increasing aircraft NO_x emissions. The results quantify the point at which the NO_x – O_3 relationship becomes non–linear with regards to aviation emissions when the background NO_x levels vary. As aviation NO_x increases, methane lifetime decreases, the new steady state of methane and resulting RF were calculated using Fuglestvedt et al., 1999 (see Chapter 4) in each atmospheric background state for each aviation scenario. Again the results quantify the degree of non–linearity regarding the reduction in methane lifetime due to aviation NO_x release and show that the more NO_x emissions increase, the further from linear the resulting methane lifetime decrease and ozone burden become.

This study shows that it is the magnitude of aviation NO_x emissions and the state of the background atmosphere that are the most important factors which influence the total ozone burden and changes in CH_4 lifetime associated with aviation NO_x emissions on a global scale, rather than the spatial pattern of emissions. The sensitivity studies showed that global mean ozone burden varied by approximately 7 percent and methane lifetime by up to 19 percent, when the spatial pattern of surface NO_x emissions was changed and both varied by less than 3 percent when the spatial pattern of aviation emissions was changed and the magnitude of emission kept the same.

The state of the background atmosphere is important as it affects the concentrations of reaction precursors. The results show that a more polluted background atmosphere with higher ambient levels of NO_x will reduce the rate of ozone formation from aviation NO_x in the upper troposphere as seen in the high NO_x background where average OPE was 17.2 compared to the higher ozone burdens produced in the low NO_x background where the average OPE was 22.2.

The results quantify a range of emissions for which the linear approximation for NO_x – O_3 and NO_x – CH_4 is valid. Beyond this range, new non-linear approximations must be made. Quantifying the point at which the NO_x – O_3 and NO_x – CH_4 relationships become non-linear, creates a more realistic framework that permits the use of the simple climate model for longer term studies. A non–linear exponential function has been derived in order to calculate the additional RF of methane and ozone due to NO_x emissions from aviation; it takes both changes in the background atmosphere and the non–linear nature of the NO_x – O_3 and NO_x – CH_4 systems into account.

Chapter 6

Establishing a Non–Linear Net NO_X Response Model with the use of a New NO_X Parameterisation

In this chapter a new non–linear radiative forcing net NO_x parameterisation is created using the data from a sophisticated CTM, MOZART–3. The new parameterisation is assessed on its ability to model RF from aviation NO_x emissions and is also compared with the current simple linear climate model LinClim.

6.1 Introduction

In order to improve the method of calculating RF resulting from aviation NO_x emissions a new parameterisation was created, which takes the non–linearity of the NO_x system into account. Two parameterisations were created for two different background NO_x conditions, a high and a low, to ensure the effect of the background atmosphere was accounted for (Chapter 5).

The overall aim of this study is to compare the trade–offs between aviation CO_2 and NO_x emissions in terms of their climate response. To do this, it is necessary to calculate the temperature response to a perturbation of aviation NO_x and CO_2 emissions. This is accomplished using a simple climate model, in this case LinCLim, as shown by the mod-

elling sequence in Figure 6.1. It has been established that LinClim is sufficiently accurate in its modelling of CO_2 emissions (see Chapter 4), however it currently assumes that the ozone and methane perturbations resulting from aviation NO_x emissions respond linearly to said emissions, whereas the results from Chapter 5 show that the NO_x – O_3 and NO_x – CH_4 systems are in fact non–linear. Additionally, it does not take the background atmospheric NO_x conditions into account when calculating the radiative forcing of aviation NO_x emissions, which are also shown to affect the resulting perturbations (Chapter 5).

To calculate temperature response from aviation emissions one must begin with the fuel used. From this, a SCM can calculate the resulting emissions of CO_2 and NO_x from aviation, using emission indices for each species. For CO_2 this is simple, for every 1 kg of fuel burned, 3.16 kg of CO_2 is emitted, whereas for NO_x it is not so simple. $EINO_x$ can be calculated for each engine type at ground level, under fixed engine conditions and sea level temperature and pressure. However, as the aircraft burns fuel at higher altitudes, the $EINO_x$ will not be the same as at ground level as the temperature and pressure change. Therefore a scaling factor is used – either a relative correlation, which depends on individual engine parameters, or fuel flow methods which use values of ambient pressure, humidity, temperature and fuel flow (Schulte et al., 1997). As discussed in Chapter 3, $EINO_x$ changes with aircraft type and engine technology, therefore different $EINO_x$ scenarios are employed in simple climate models to account for possible future changes in technology. In the runs performed here, $EINO_x$ was kept constant at a value of 13. Once the emissions have been calculated the SCM can then calculate the radiative forcing of these emissions. In this study, LinClim will calculate the RF of CO_2 and the RF of NO_x will be calculated using the new parameterisation outside of LinClim. Figure 6.1 shows the progression of long–term modelling using a SCM, from fuel use to emissions to the resulting RF.

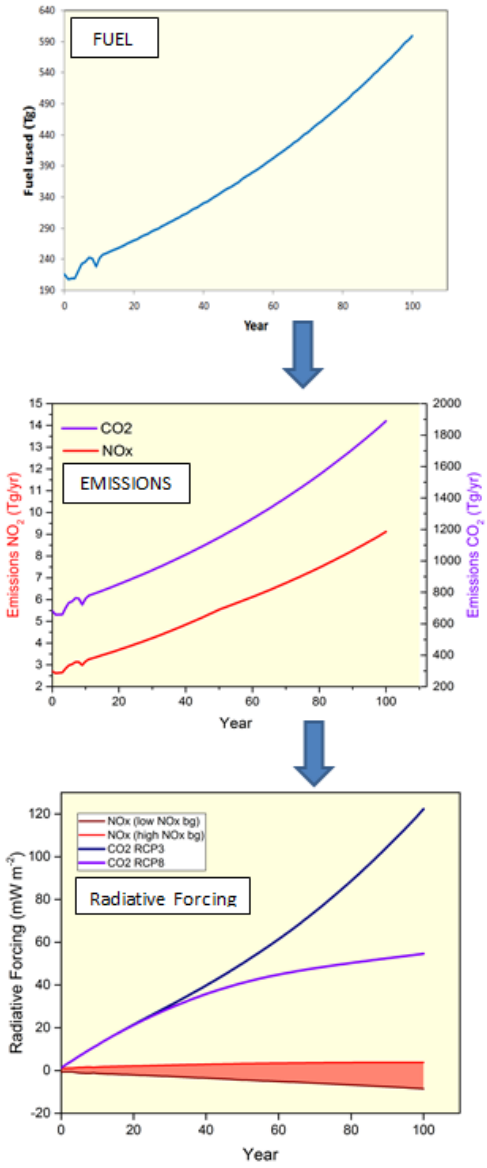

Figure 6.1: The process of modelling the effects of aviation using a simple climate model (SCM). The fuel used (top) generates emission of CO_2 and NO_x (middle), from this, concentrations of CO_2 are calculated and a function is used for NO_x to calculate the radiative forcing (bottom)

Once RF is calculated the SCM can be used to calculate the resulting temperature response. To model temperature response, LinClim tunes to several parent models. To determine which tunings were suitable for this study, several tunings were run as shown in Figure 6.2. The models used had taken part in the CMIP3 CO_2 x2 experiment, which is appropriate, as a doubling of CO_2 is more than enough of a range to accommodate

aviation activities. This tuning was carried out before this study began and is described in Lee et al., 2009.

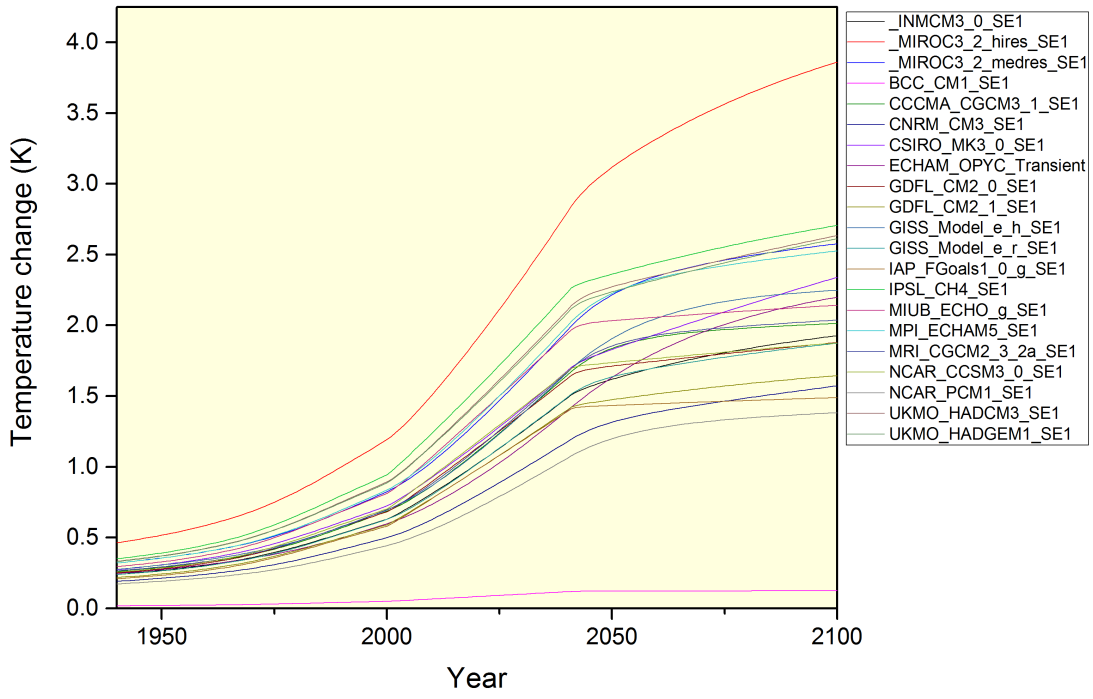

Figure 6.2: Temperature response of the parent GCM models available in LinClim when CO_2 is doubled - SE1 denotes that they have run a AR4(CMIP3) experiment with 1 percent yearly increase in CO_2 increase until doubling after 70 years.

Figure 6.2 shows two models which are obvious outliers (BCC CM1 SE1 and MIROC3 2 hires SE1) which were then omitted from the LinClim model runs performed in this study. The median of the remaining models was taken to represent the temperature response of CO_2 and NO_x in the following LinCim runs. LinClim has the capability to run against other parent OAGCMs which have been tuned to a quadrupling CO_2 experiment, however, for the study of aviation, this level of CO_2 increase is unnecessary, and so those models have not been included. Figure 6.3 shows how the temperature response calculations fit into the modelling sequence.

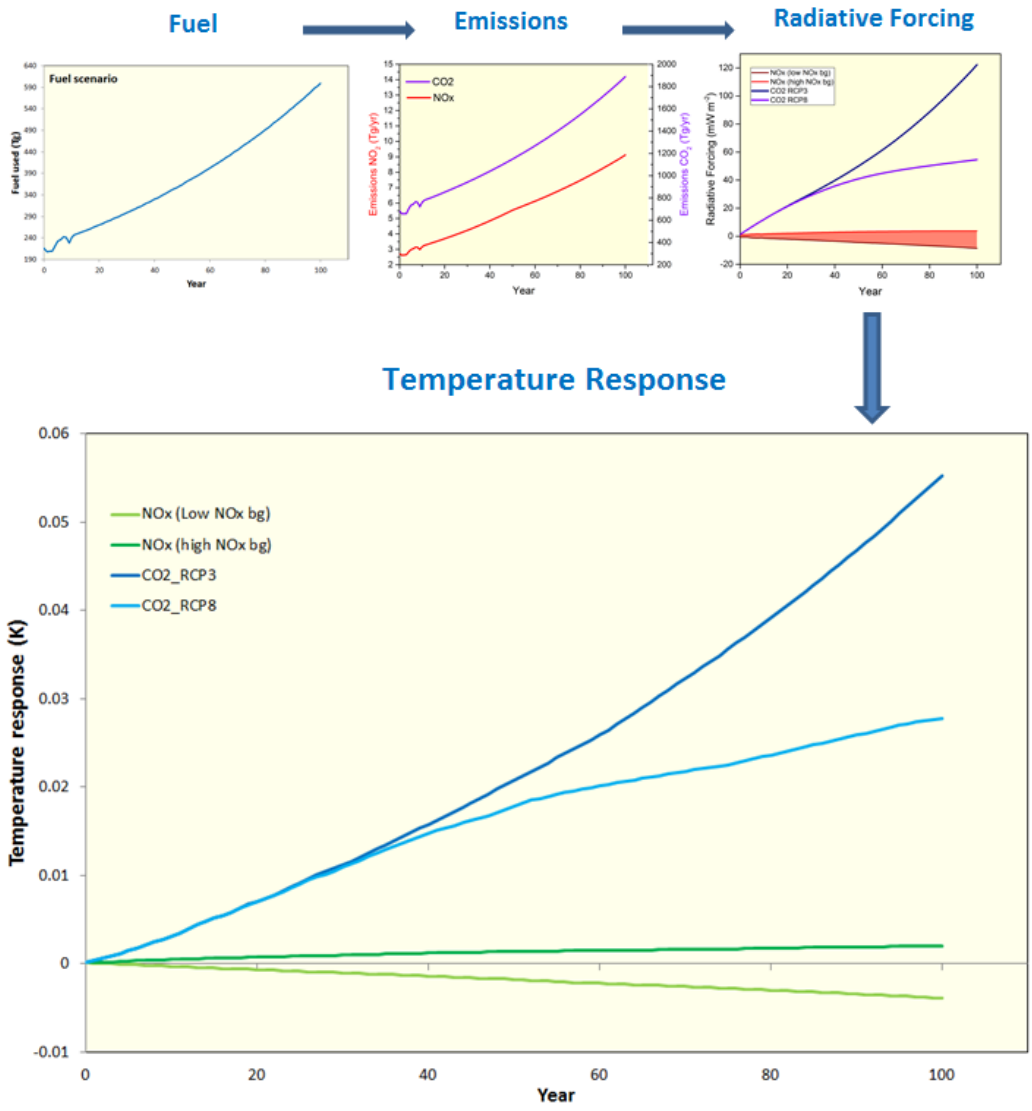

Figure 6.3: The process of modelling the effects of aviation using a simple climate model (SCM continued from Figure 6.1. The fuel used (top left) generates emission of CO_2 and NO_x (top middle), from this, concentrations of CO_2 are calculated and a function is used for NO_x to calculate the radiative forcing (top right). Using the method described in the text, temperature response (K) (bottom) can then be calculated.

6.2 Calculating the Radiative Forcing Response of Aviation NO_x Emissions Using a New NO_x Parameterisation

In order to compare the RF of aviation NO_x emissions calculated using the new parameterisation against the method used in LinClim, two hypothetical scenarios are created. In the first, aviation CO_2 and NO_x emissions are kept constant by using 249.8 Tg fuel per year – the observed value for aviation in 2012, and $EINO_x$ is kept constant at 13. In the second scenario, aviation fuel consumption follows observations until 2012 and then increases by 1 percent per year. This scenario is relevant as current consensus suggests that aviation emissions will continue to increase over the current century. Most scenarios used in the literature show an upward trend for future aviation emissions (IPCC, 1999; Fleming et al., 2013; Owen et al., 2010). Therefore this highly simplified scenario of 'increase by 1 percent per year' captures the main features of what is expected to happen in terms of aviation activity in the near term (∼100 yrs). The difference between the two scenarios will highlight the effect of increasing emissions when all other variables are kept constant.

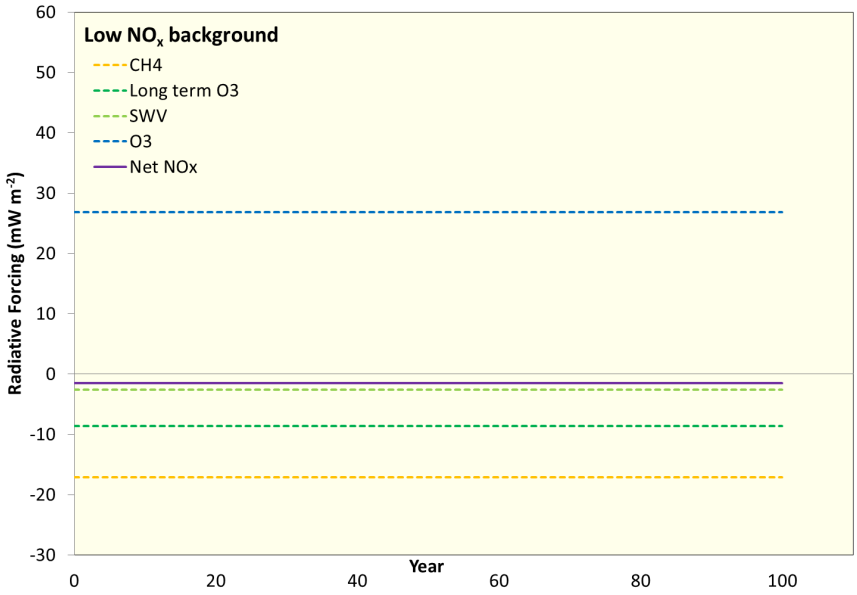

Figure 6.4: The radiative forcing (mW m^{-2}) of aviation NO_x emissions when emissions are kept constant at 249.8 Tg fuel and $EINO_x$ is kept constant at 13 over the 100 year run. The background NO_x is the low NO_x background atmosphere. Forcing is broken down by the four constituents that make up the overall NO_x effect, CH_4 , O_3 , long term O_3 and stratospheric water vapour (SWV) and they are summed to illustrate the overall net NO_x effect.

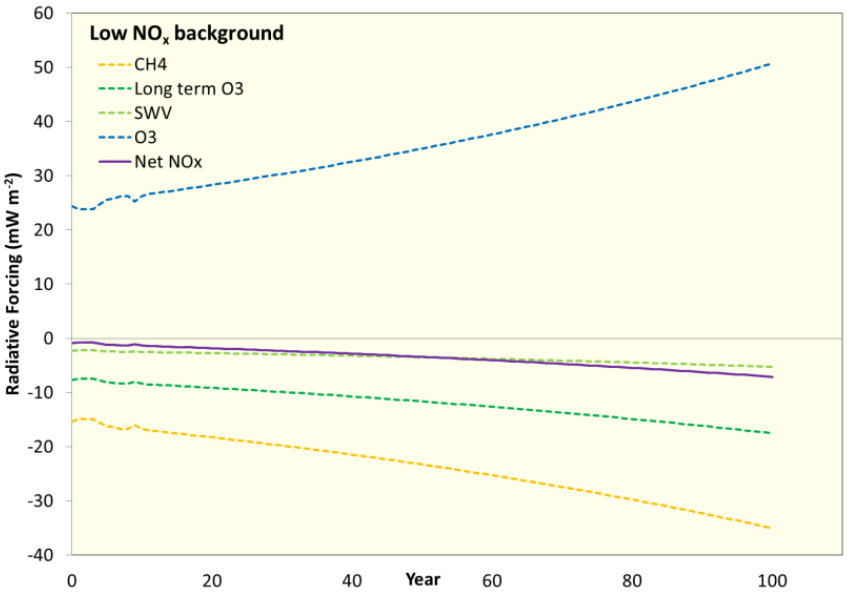

Figure 6.5: The radiative forcing (mW m^{-2}) of aviation NO_x emissions when emissions are increase by 1 percent per year and $EINO_x$ is kept constant at 13 over the 100 year run. The background NO_x is the low NO_x background atmosphere. Forcing is broken down by the four constituents that make up the overall NO_x effect, CH_4 , O_3 , long term O_3 and stratospheric water vapour (SWV) and they are summed to illustrate the overall net NO_x effect.

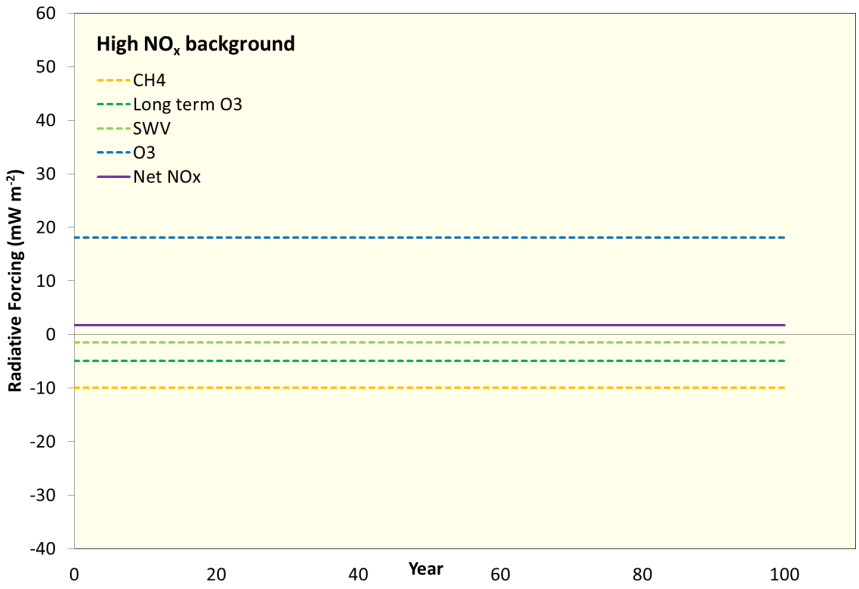

Figure 6.6: The radiative forcing (mW m^{-2}) of aviation NO_x emissions when emissions are kept constant at 249.8 Tg fuel and $EINO_x$ is kept constant at 13 over the 100 year run. The background NO_x is the high NO_x background atmosphere. Forcing is broken down by the four constituents that make up the overall NO_x effect, CH_4 , O_3 , long term O_3 and stratospheric water vapour (SWV) and they are summed to illustrate the overall net NO_x effect.

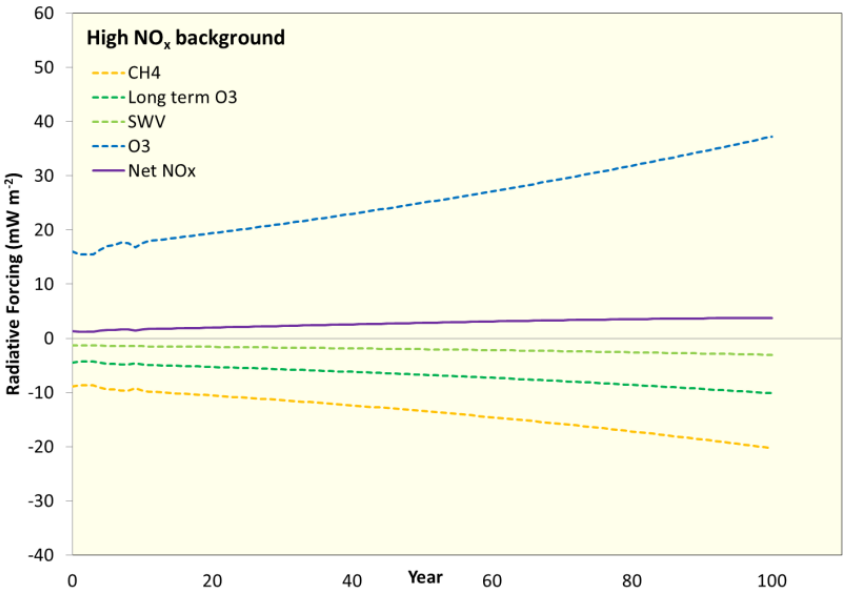

Figure 6.7: The radiative forcing (mW m^{-2}) of aviation NO_x emissions when emissions are increase by 1 percent per year and $EINO_x$ is kept constant at 13 over the 100 year run. The background NO_x is the high NO_x background atmosphere. Forcing is broken down by the four constituents that make up the overall NO_x effect, CH_4 , O_3 , long term O_3 and stratospheric water vapour (SWV) and they are summed to illustrate the overall net NO_x effect.

It becomes clear from Figures 6.4 to 6.7 that the sign of the overall net NO_x RF is determined by the state of the background atmosphere. In the 'cleaner' low NO_x background the net NO_x forcing becomes negative and conversely, the 'dirty' high NO_x background results in an overall positive forcing from net NO_x . A comparison shows that with constant emissions, ozone RF varies by 32 percent between the two background whereas methane varies by 42 percent. The stronger negative forcing of methane in the low NO_x background combined with the two additional negative forcings of SWV and long–term ozone result in the overall net NO_x forcing becoming negative in the low NO_x background.

6.3 Comparison with the LinClim SCM

The current method for calculating the effects of aviation NO_x using LinClim, is to sum the forcings of O_3 and CH_4 to form an overall NO_x effect. The reactions are linear as described in Chapter 3 And the background atmosphere is not taken into account. A comparison between LinClim and the new parameterisation was carried out and presented

in Figure 6.8. LinClim was run for O_3 and CH_4 using the 'increase emissions by 1 percent per year' scenario and compared to the RF from O_3 and CH_4 calculated using the new parameterisation, again using the increase by 1 percent per year scenario, both were run using a constant $EINO_x$ of 13

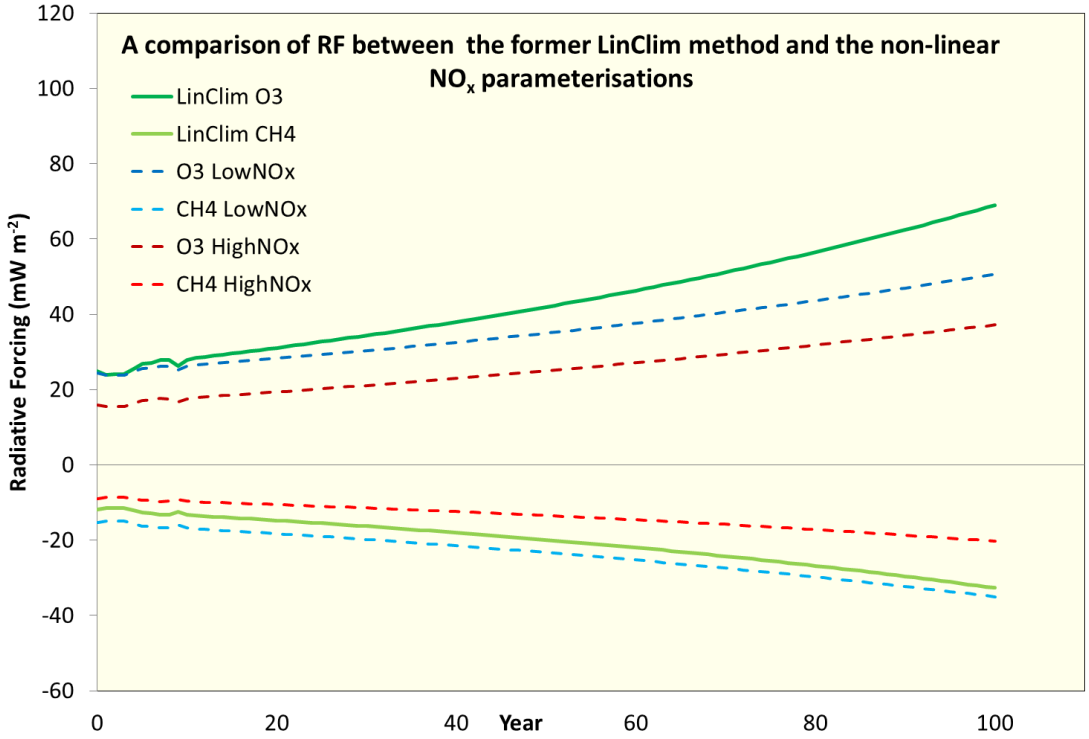

Figure 6.8: A comparison of the radiative forcing (mW m^{-2}) resulting from aviation NO_x emissions when emissions increase by 1 percent per year, between the new non-linear paramterisations and old method using the linear paramterisations with LinClim for ozone and methane. $EINO_x$ was kept constant at 13 over the 100 year run.

Figure 6.8 shows that ozone appears to be overestimated by LinClim compared to the high and low background whereas methane response is in–between the two, although closer to the low NO_x background values. The methane lifetime reduction resulting from NO_x emissions is close to linear at the levels of emission used here, as shown in Chapter 5, hence why the methane results from LinClim are close to those from the new parameterisation. This figure, and those in Chapter 5, show that the relationship between ozone burden and NO_x emissions has become non–linear at these emission levels, hence why the LinClim RF remains higher than the new parameterisation RF, in both backgrounds, over the 100 year run.

Figure 6.8 also shows that the RF calculated by LinClim for O_3 and CH_4 would continue to increase and decrease respectively as aviation emissions increased over time due to the fact that it assumes linear reactions between $NO_x - O_3$ and $NO_x - CH_4$. LinClim does not include the effects of SWV and long term ozone, two additional negative forcings that are neglected unless calculated off–line and included, the omission of which clearly adds to the result of an overall positive forcing. The difference between the results calculated from the new method and those produced in LinClim illustrate the influence of the background atmosphere on the effects of NO_x emissions and reinforce its importance in the calculation of these effects.

To compare the total NO_x effect calculated in LinClim and with the new parameterisation, SWV and long term ozone effects were added and all the forcings summed to provide and overall net NO_x RF as shown in Figure 6.9.

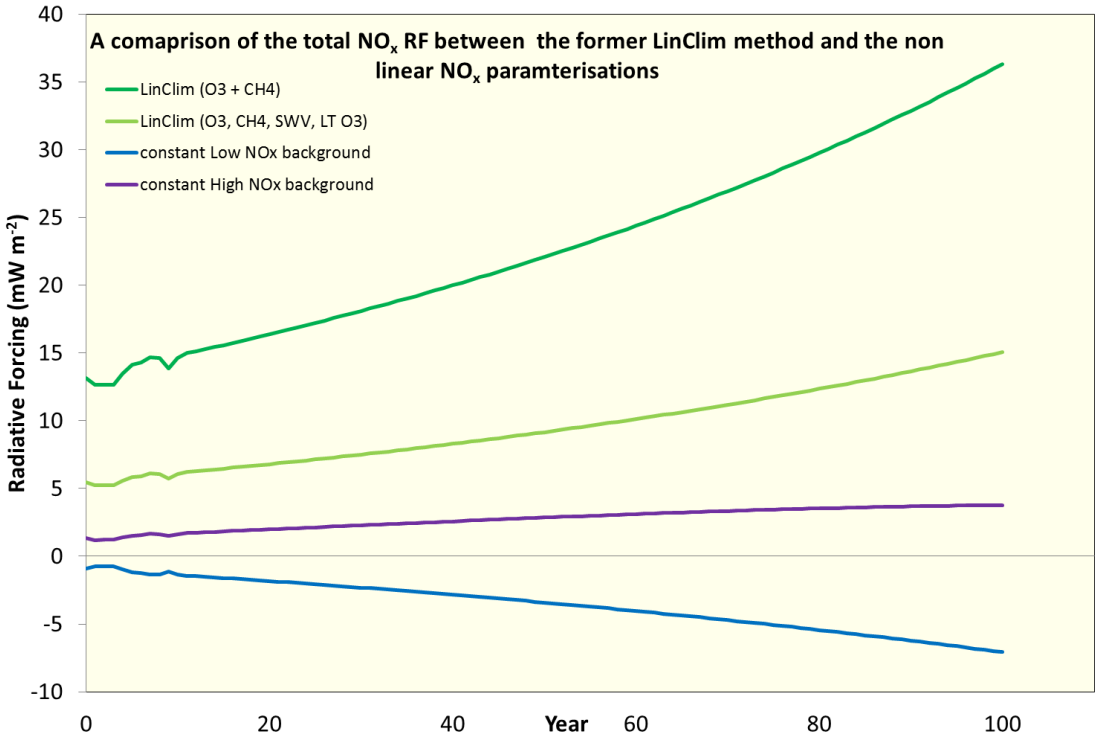

Figure 6.9: A comparison of the radiative forcing (mW m^{-2}) resulting from aviation NO_x emissions when emissions increase by 1 percent per year, between the new non-linear paramterisations and old method using the linear paramterisations with LinClim for ozone and methane. $EINO_x$ was kept constant at 13 over the 100 year run. Stratospheric water vapour (SWV) and the long term ozone (LT O_3) effect were included in the LinClim run to show the effect of the two negative forcings that were not prevously included in the LinClim method of calculating aviation net NO_x radiative forcing.

The results show that LinClim models an overall positive RF for aviation NO_x . The overestimation of the ozone response results in a RF much higher than the high NO_x background result calculated using the new parameterisation. This is a result of the linear reaction between NO_x – O_3 used in LinClim, whereas it was shown in Chapter 5 that ozone does in fact not respond linearly to increasing aviation NO_x emissions.

Temperature response was then calculated for all the RFs using LinClim and its array of sophisticated parent models, using the method described above and results are show in Figure 6.10.

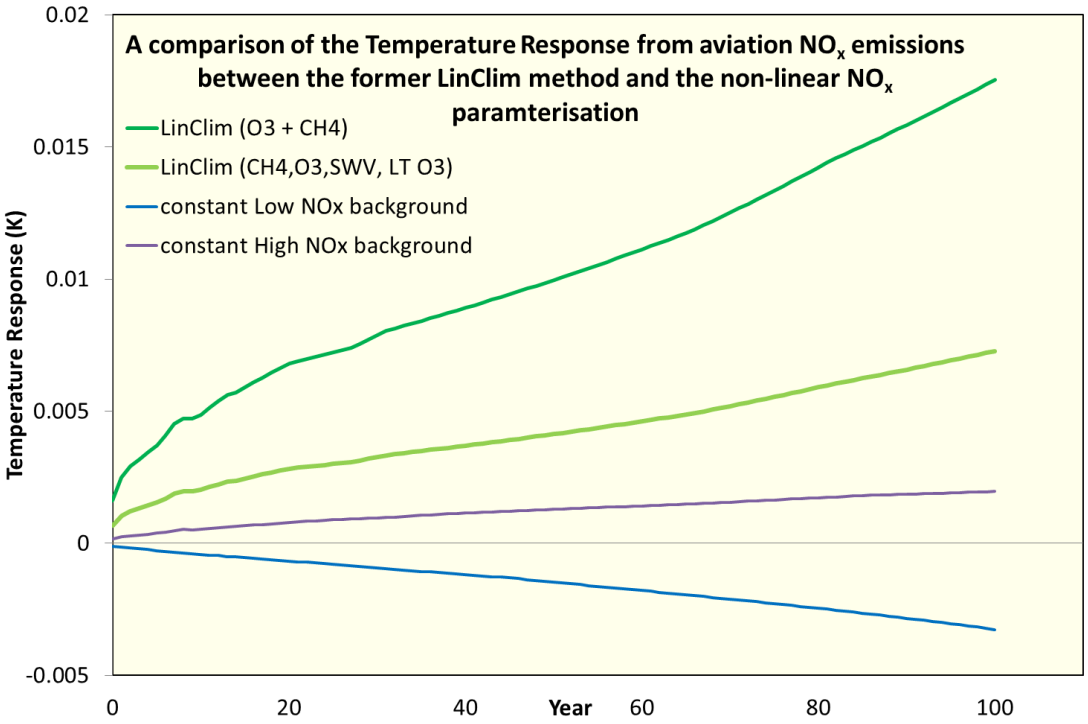

Figure 6.10: A comparison of the temperature response (K) resulting from aviation NO_x emissions when emissions increase by 1 percent per year, between the new non-linear paramterisations and old method using the linear paramterisations with LinClim for ozone and methane. $EINO_x$ was kept constant at 13 over the 100 year run. Stratospheric water vapour (SWV) and the long term ozone (LT O_3) effect were included in the LinClim run to show the effect of the two negative forcings that were not prevously included in the LInClim method of calculating the temperature response resulting from aviation net NO_x emissions.

Again, the temperature response calculated by LinClim is much greater than that given using the new parameterisation, due to the high O_3 RF. When SVW and long term O_3 are factored into the temperature response calculations, LinClim still gives a higher value

than the new parameterisation method, although lower than without SWV and long–term O_3 .

To summarise, the new parameterisation produces NO_x response in a non–linear fashion with input from a sophisticated parent model and a resulting parameterisation, which includes the effects of non–linearity within the NO_x chemical system and the effects of the background atmosphere, which the previous model, LinClim, did not take into account. The results here show that LinClim overestimates the effect of aviation NO_x on O_3 , leading to an overestimated RF and subsequently, temperature response for the overall NO_x effect. The new method will be used for trade–off experiments in Chapter 7, where the effects of the trade–off between aviation NO_x and CO_2 emissions are assessed. The method of modelling CO_2 using the SCM LinClim is outline below.

6.4 Modelling CO_2 using the Simple Climate Model (SCM) LinClim

To compare the effect of short–term climate–forcers such as NO_x , with a long–term climate–forcer, it is necessary to model aviation emissions of CO_2 . CO_2 is cumulative in the atmosphere, generally unreactive and long–lived, the chemistry is well understood and aviation CO_2 emissions responds linearly to the amount of fuel burnt. The simplicity of CO_2 allows the use of a SCM for modelling CO_2 over the long–term while still retaining accuracy. The LinClim SCM can therefore be used to model CO_2 radiative forcing and subsequent temperature response. As the temperature response produces a spread of 19 parent models, it is necessary to take a representative value of the ensemble spread. This is shown in Figure 6.11, a scenario from the literature was run in the 4 RCP backgrounds on LinClim and the darker line shows the median value. It shows that the median or mid-point of the spread can represent the data sufficiently, in this case the mean value could be skewed to the top or bottom end of the spread, as the model ensemble does not show a normal distribution (Lee et al., 2013b).

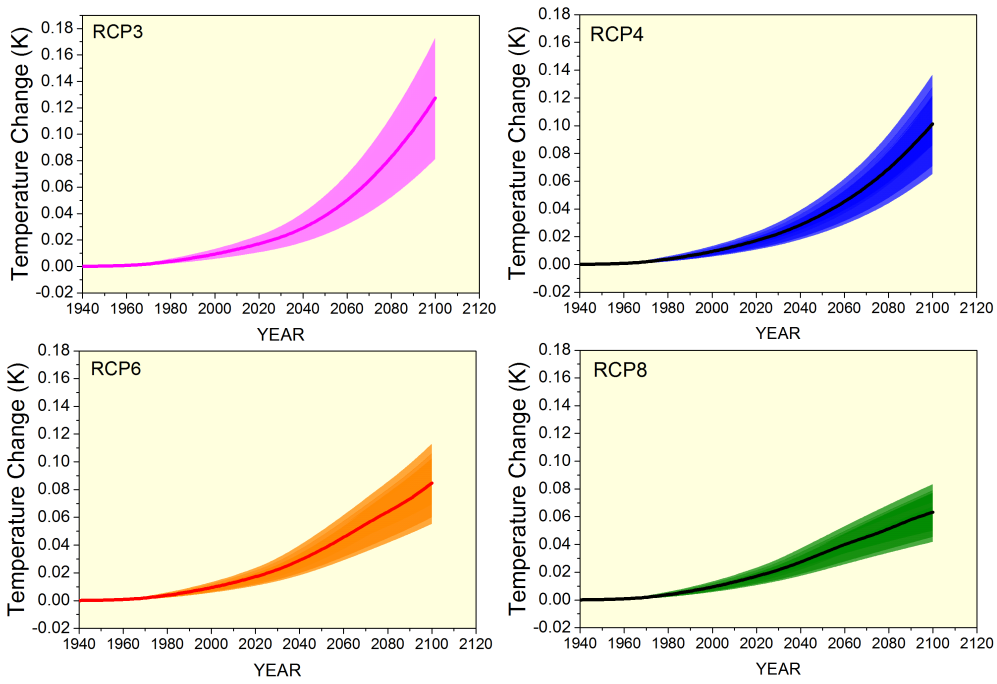

Figure 6.11: An aviation scenario (QUNATIFY A1) was run on LinClim to obtain the temperature response due to aviation CO_2 emissions in four different background atmospheres, the RCP backgrounds. As described above, the temperature response is calculated by running 19 different tunings of LinClim (see Figure 6.2). The median value is shown for each background by the darker line, this shows that the median values of all the tunings used is a sufficient method of representing the range of models used to calculate temperature response.

6.4.1 The effects of transient and constant background when modelling CO_2

Atmospheric concentrations of CO_2 are well mixed and thus, background atmospheric measurements are accurate, enabling the use of a transient background in simple climate models such as LinClim. However, so far in this study, aviation NO_x emissions have been modelled using a constant background NO_x value, with the results representing a higher and lower limit of the effects of background NO_x emissions. To maintain consistency within the experiment, CO_2 was also modelled with a constant rather than transient background CO_2 value using LinClim for the experiments shown in Chapter 7. Figures 6.12 and 6.13 shows the differences in RF and temperature response for aviation CO_2 over a

100 year time period when the same aviation scenario (increase 1 percent scenario, above) is run on LinClim with a transient and then constant CO_2 background. The constant CO_2 backgrounds of choice were derived from the RCP scenarios, where the background CO_2 concentration from 2100 in each RCP scenario was taken and that value was kept constant for a 100 year run (Table 6.1). The transient scenarios used background CO_2 concentrations in the 4 RCP scenarios (see Chapter 3). A fixed CO_2 value of 404.83 ppm is also include here as an additional constant background, it represents the background CO_2 concentration as of March 2016 (http://www.esrl.noaa.gov/gmd/ccgg/trends/). The constant background removes some uncertainty as it creates a higher and lower bound or limit similar to what has been done with the NO_x modelling in this thesis

Constant background scenario name	Low_constant	Middle_constant_1	Middle_constant_2	High_constant
CO_2 concentration (ppmv)	420.89 (end point of RCP 3)	537.87 (end point of RCP 4.5)	669.72 (end point of RCP 6)	935.87 (end point of RCP 8)

Table 6.1: The value of the constant CO_2 backgrounds, each is given a scenario name, 'Low constant' uses the value of background CO_2 at 2100 in RCP3, 'Middle constant 1' uses the value of RCP4.5 at 2100, 'Middle constant 2' uses the value of RCP 6 at 2100 and 'High constant' uses the value of RCP 8 at 2100

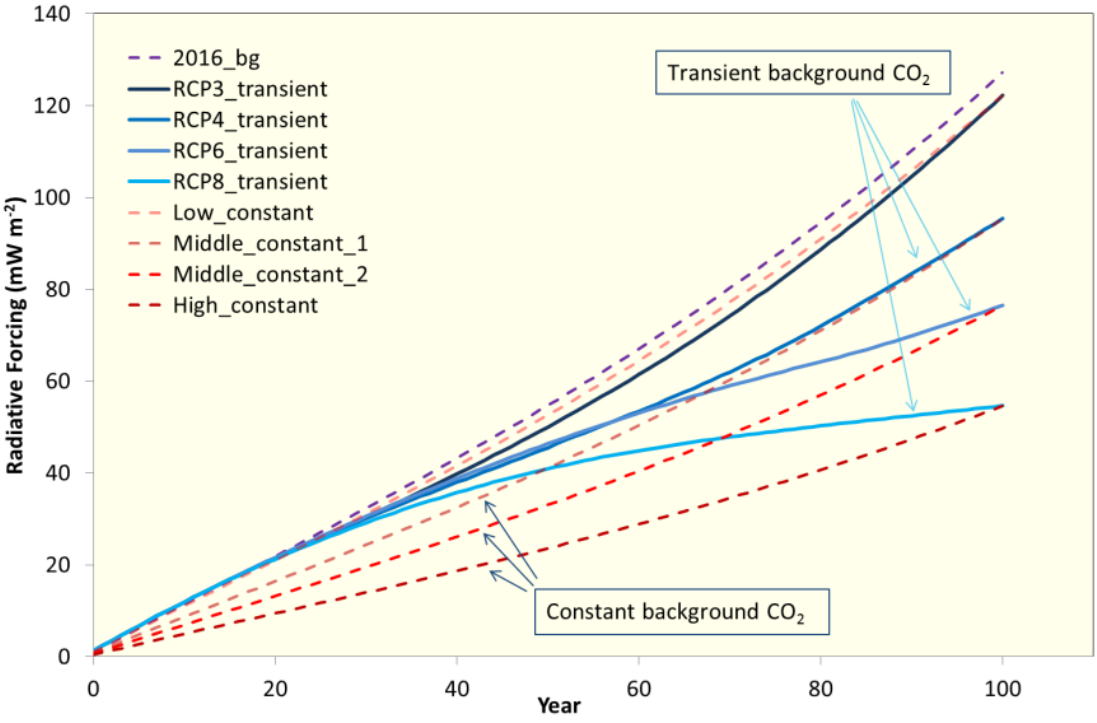

Figure 6.12: The increase by 1 percent scenario was run for aviation CO_2 emissions over a 100 year period. It was run against a background of four different constant CO_2 values and also against four transient CO_2 backgrounds as explained in the text. This figure shows the radiative forcing (mW m^{-2}) resulting from aviation CO_2 over the 100 year run against both the transient and constant CO_2 backgrounds. A constant background of March 2016 CO_2 values was also included (2016 bg).

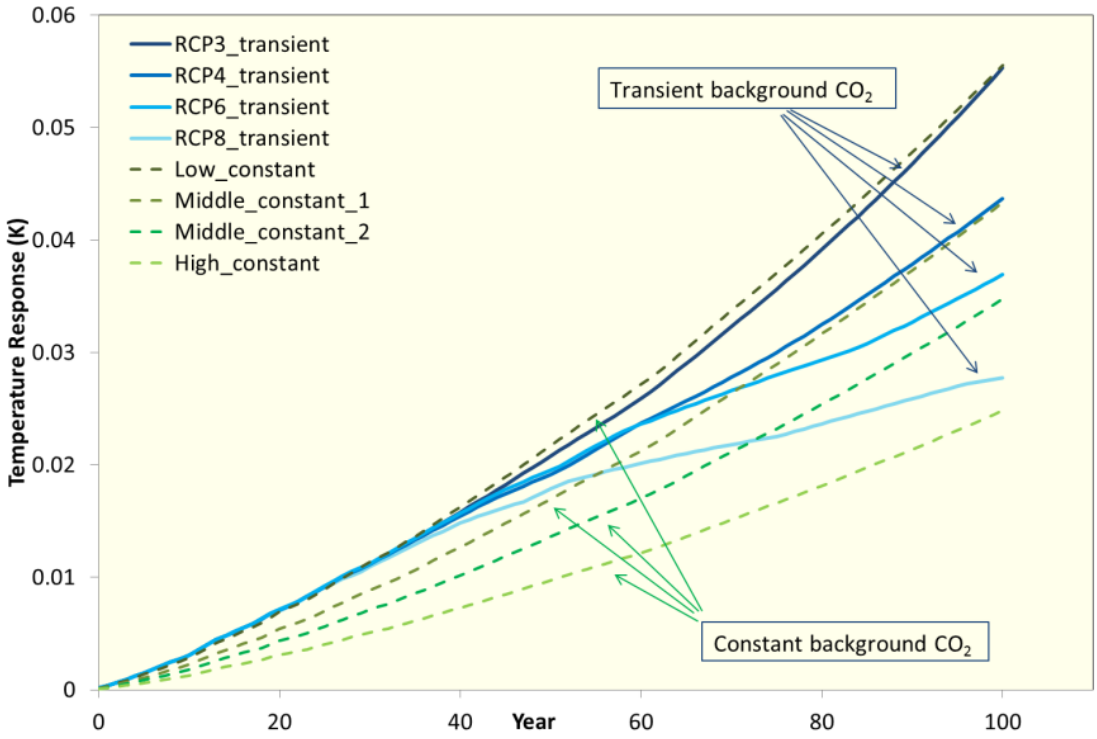

Figure 6.13: The increase by 1 percent scenario was run for aviation CO_2 emissions over a 100 year period. It was run against a background of four different constant CO_2 values and also against four transient CO_2 backgrounds as explained in the text. This figure shows the temperature response (K) resulting from aviation CO_2 over the 100 year run against both the transient and constant CO_2 backgrounds. A constant background of March 2016 CO_2 values was also included (2016 bg).

Figures 6.12 and 6.13 show that, when a scenario of aviation CO_2 emissions are modelled on a SCM with both constant and transient background CO_2 levels, after 100 years the radiative forcing value is the same. This is because RF is an instantaneous metric and so values are calculated for every year of simulation independently of each other. As the constant background values of CO_2 were equal to the last year of the transient background scenarios the last year of simulation has the same value in all cases. The results show that in years 1 – 99 of simulation the RF from aviation CO_2 was different in the constant and transient CO_2 backgrounds.

The temperature response is not an instantaneous forcing as it takes time for the system to respond to the change in RF, as CO_2 is cumulative, the whole 100 year run is taken into account in the last year of simulation. Therefore the background atmosphere CO_2 concentrations have an impact on the final temperature response, and so the end point

temperature response is not the same when comparing the constant and transient background model runs. In the lower CO_2 scenarios (RCP3 transient/low constant, RCP4 transient/middle constant 1) this difference is small (less than 1 percent – 0.47 percent and 0.63 percent respectively) and in the higher CO_2 scenarios the difference is slightly more (6.2 percent between RCP6/middle constant 2 and 11 percent between RCP8/high constant).

Joos et al., (2013) conducted a mulit–model study where CO_2 was modelled with both constant and transient background and found that while the background did have an effect on CO_2 IRF and AGWP (between 4 – 40 percent) they found that the most important factor was the time horizon. It is clear that the constant or transient nature of the background CO_2 concentrations will have an effect on the temperature response of aviation CO_2 when it's modelled on the LinClim SCM. For the purpose of the experiments in Chapter 7, CO_2 background is kept constant as to be consistent with the modelling of aviation NO_x emissions.

6.5 Conclusions

Based on the results in Chapter 5 a new parameterisation was formulated for modelling net NO_x RF resulting from aircraft emissions in a low NO_x and a high NO_x background atmosphere. When used to calculate the RF from aviation NO_x in a low NO_x and high NO_x background, it was shown that the overall net NO_x RF differs in sign between the two backgrounds. In the low NO_x background the net NO_x RF produced an overall negative forcing, whereas in the high NO_x background the net NO_x RF was positive.

This new parameterisation was then compared with net NO_x RF old parameterisation modelled with the LinClim SCM. The comparison showed that the old parameterisation in LinClim overestimates the ozone burden resulting from aviation NO_x emissions as it assumes a linear relationship, independent of background conditions. The results from Chapter 5 show that the relationship between aviation NO_x emissions and the resulting ozone burden, and therefore resulting RF, is in fact non–linear and also depends on the background state into which it is emitted. The methane results from LinClim were closer to that calculated using the new parameterisation, as at the levels of NO_x emission used here, the NO_x – CH_4 system is closer to linear than the NO_x – O_3 system, hence the linear parameterisation of LinClim gave values within the bounds of the new results. Due to this

overestimation of ozone, the resulting net RF and subsequent temperature response of the overall NO_x effect was also overestimated in LinClim. SWV and the long–term ozone effect were also calculated and added to the LinClim results, resulting in a reduction to the overall forcing from LinClim, but the forcing was still higher than that from the new parameterisation (which already included SWV and LT O_3).

It has been shown that LinClim is sufficient to model CO_2 (Chapter 4) and uses the tuning of sophisticated parent models to calculate temperature response. A study to assess the difference in constant and transient modelled CO_2 backgrounds was carried out and results shows that while the RF remained the same after 100 years, albeit through a different pathways, the temperature response differed in the two background after 100 years, negligibly while background values were small, but increasingly so as the background CO_2 levels increased.

The next chapter will go on to assess the impacts of trade–offs between aviation NO_x and CO_2 emissions in terms of climate change mitigation, using the new parameterisations formulated in Chapter 5 and tested here, and the LinClim SCM.

Chapter 7

Analysing the trade–off between short–term (NO_x) and long–term (CO_2) climate–forcers in the aviation industry and the potential for mitigation

This chapter outlines a series of experiments which aim to analyse the effect on the climate due to trade–offs between aviation NO_x and CO_2 emissions when one species is reduced at the expense of the other.

7.1 Introduction

In 1981, ICAO adopted a certification standard to control aircraft NO_x emissions. This was in response to growing concerns over the effect of aviation NO_x emissions on local surface air quality around airports during the landing take–off cycle. As NO_x stringency assessments were undertaken it became apparent that the engine modifications necessary to reduce aviation NO_x emissions resulted in a fuel burn penalty and therefore, a CO_2 penalty. Hence, it was realised that a trade–off existed between the reduction of NO_x at the expense of CO_2 (Flemming and Ziegler, 2010; Ralph and Baker, 2010).

For the global mean surface temperature rise to remain below 2°C over pre–industrial

levels, atmospheric CO_2 (equivalent) concentrations must remain below at least 450 ppm. This cannot be achieved unless anthropogenic CO_2 emissions are mitigated. However, the aviation industry is expanding, ACARE (2011) predicts that by 2050, there will be 25 million commercial flights annually, compared with 9.4 million in 2011, which will result in a fuel burn increase from 228 Tg/year to as much as 1230 Tg/year for a BAU scenario. As outlined in Chapter 2, aviation emits both short– and long–lived climate forcers in the form of CO_2 and NO_x emissions respectively and therefore, can address greenhouse gas mitigation from two fronts, since both these emissions are regulated by ICAO.

As the aviation industry attempts to reduce its impact on the climate, it becomes clear that a trade–off exists between the emissions of NO_x and CO_2 (IPCC, 1999). The pressure on all industries to reduce CO_2 emissions suggests that any improvement in fuel burn efficiency, and therefore reduction in CO_2 emissions, would be beneficial, both to the climate and the industry (as reduced fuel burn = reduced costs). Regarding aviation, this can be achieved in terms of fuel burn per passenger kilometres in a number of ways including air traffic management (ATM), airframe design and weight improvements and increased engine efficiency. With current engine designs, to improve engine efficiency, temperature and pressure within the engine has tended to rise, therefore reducing fuel burn and the consequent CO_2 emissions. However, the increase in temperature and pressure results in the engine producing more NO_x emissions, which has to be combated through combustor design. Conversely, if the situation is viewed from an air pollution standpoint, a reduction in overall NO_x emissions is deemed more desirable. The technology required to reduce NO_x emissions is available for aircraft engines and generally requires re–designing the combustor, however it can add weight to the aircraft and reduced engine thermodynamic efficiency, resulting in higher fuel burn and thus, higher CO_2 emissions (Miake-Lye et al., 2000; Faber et al., 2008).

7.1.1 Mitigation within the aviation sector

As with all sectors emitting greenhouse gases, the topic of mitigation within aviation industry is of importance. With global emissions targets to meet, more and more emphasis is being put on 'cleaner' air travel with focus on reducing fuel use, better ATM and new technologies designed to increase efficiency, from taxiing for take–off through to landing at the destination. The general consensus is that aviation will be the last of the transport sectors still using fossil fuel, as it is more difficult to implement new fuel technology into

the global fleet of aircraft than it is to phase it into road or rail transport for example. This is due to an aircraft's long lifetime and the simultaneous world–wide change necessary in airports to accommodate a new fuel infrastructure, such as, for example liquid hydrogen.

As aviation is largely international by nature, the efforts for its mitigation need to be set over much larger areas and include all of the countries within the domain e.g. Europe. There are several targets designed to meet the needs of climate change mitigation, such as that set out by the Advisory Council for Aviation Research and Innovation in Europe (ACARE) who, by 2020, aim to reduce aviation CO_2 emissions by 50 percent and aviation NO_x emissions by 80 percent in new aircraft, compared to the aircraft they will be replacing (ACARE, 2001). By 2050, ACARE's aim is that aviation will be seen as an environmentally friendly means of transport, with CO_2 emissions reduced by 75 percent per passenger kilometre and NO_x emissions by 90 percent relative to new aircraft entering the fleet in 2000. They also envisage that the effect of aviation on the environment will be completely understood and the use of electric and hybrid–electric energy engines within the global fleet (ACARE, 2011). Airbus also outline a mitigation plan - the 'Smarter Skies' vision, consisting of five broad concepts each with a range of improvements to be implemented before 2050 (Airbus, 2015).

For Europe, the mitigation strategy of preference has been emissions trading in order to allow the continued growth of the industry. However, the EU ETS (emissions trading scheme) has limited success because of political difficulties and only applies for flights taking off and landing within Europe. It also encourages airlines to buy credits rather than spend the money on new, cleaner technologies or other ways of reducing their aircraft emissions (Gssling and Upham, 2009). Recently (2016) ICAO has finalised documentation on a global market based measures scheme – CORSIA which is a new carbon offsetting scheme for international aviation. The Carbon Offsetting and Reduction Scheme for International Aviation, or 'CORSIA', was developed to ensure that international aviation meets the goal of carbon neutral growth by 2020 which it cannot achieve through operations and technology improvement alone. CORSIA allows the CO_2 from international aviation to be offset by buying credits from the carbon market to ensure the extra CO_2 emitted is compensated for by a mitigation scheme somewhere else in the world, through projects such as planting trees or investing in renewable energy.

There is also the prospect of alternative fuels being introduced to the industry, such as hydrogen or biofuels. A different fuel would affect the outcomes of emissions trade–offs such as the NO_x – CO_2 trade–off being investigated here. While hydrogen fuel would

help to mitigate CO_2 emissions, it would result in high emissions of water vapour, which in the troposphere, is a potent GHG and therefore would hinder any attempt to limit the global warming contribution from the aviation industry.

It remains to be seen which of these mitigation measures go on to be implemented, and for many of them to be successful in meeting their targets, implementation would need to take place within the next few years to avoid delaying mitigation, as discussed in Section 7.3.

7.1.2 The trade-off between short and long lived climate forcer emissions

The mitigation of short–lived climate–forcers tends to be more appealing for policy makers than the mitigation of CO_2 . This is because it is generally cheaper to mitigate CH_4 , tropospheric O_3 and black carbon – all SLCFs, and the effects become apparent relatively quickly whereas CO_2 mitigation is expensive and the results not seen for decades in terms of global temperature change. Another consideration here is that many SLCFs are also air pollutants, which adds even more incentive to mitigate them first (Allen et al., 2016). In terms of the global climate however, the IPCC, and all the studies that contributed to the assessment reports, have shown that long-term global temperature change will be determined almost solely by anthropogenic CO_2 release over the entire industrial epoch. Overall, the consensus on the matter of short-term versus long-term pollutants is that both must be mitigated, each for different reasons.

7.2 Examining the Trade–offs Between Aviation NO_x and CO_2 Emissions using the New Net NO_x Parameterisation and Constant Emissions Experiments

7.2.1 Constant emissions experiments

As the new NO_x parameterisation was designed for two constant background atmospheric NO_x scenarios it was decided to keep all other variables constant in this initial parametric

study. Fuel was kept constant at 249.8 Tg per year – the observational fleet value at 2012, background CO_2 was kept at 404 ppm – the background value as of March 2016, therefore removing the transient nature of CO_2 modelling (see Chapter 6) and $EINO_x$ was kept constant at 13. As a result of this constant fuel, aviation CO_2 and NO_x emissions remained constant over the 100 year run at 786 Tg CO_2 and 3.24 Tg NO_x Yr^{-1} respectively (Figure 7.1 Note figure axis is in Tg N). This removes time varying elements from the study in order to gauge the response of the system to a simple input. This initial run is the base case and the constant aviation emissions were run in both the low NO_x and high NO_x backgrounds (Figures 7.2 and 7.3).

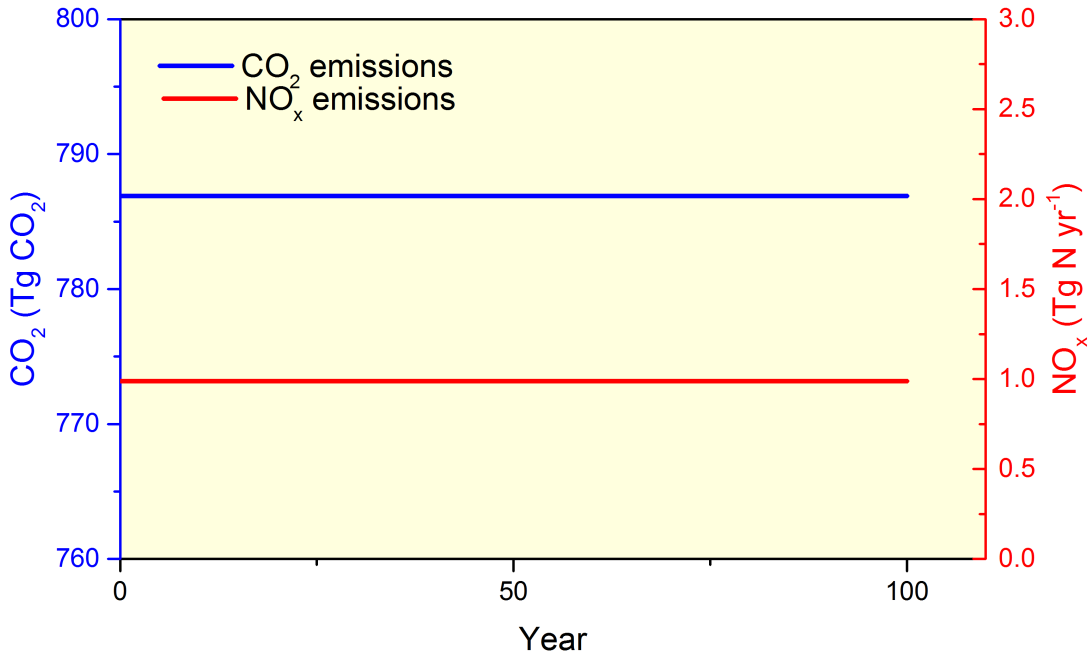

Figure 7.1: Aviation CO_2 and NO_x emissions resulting from constant fuel of 249 Tg. This is the base case scenario, where aviation emissions, $EINO_x$ and background concentrations of NO_x and CO_2 are kept constant, as described in the text.

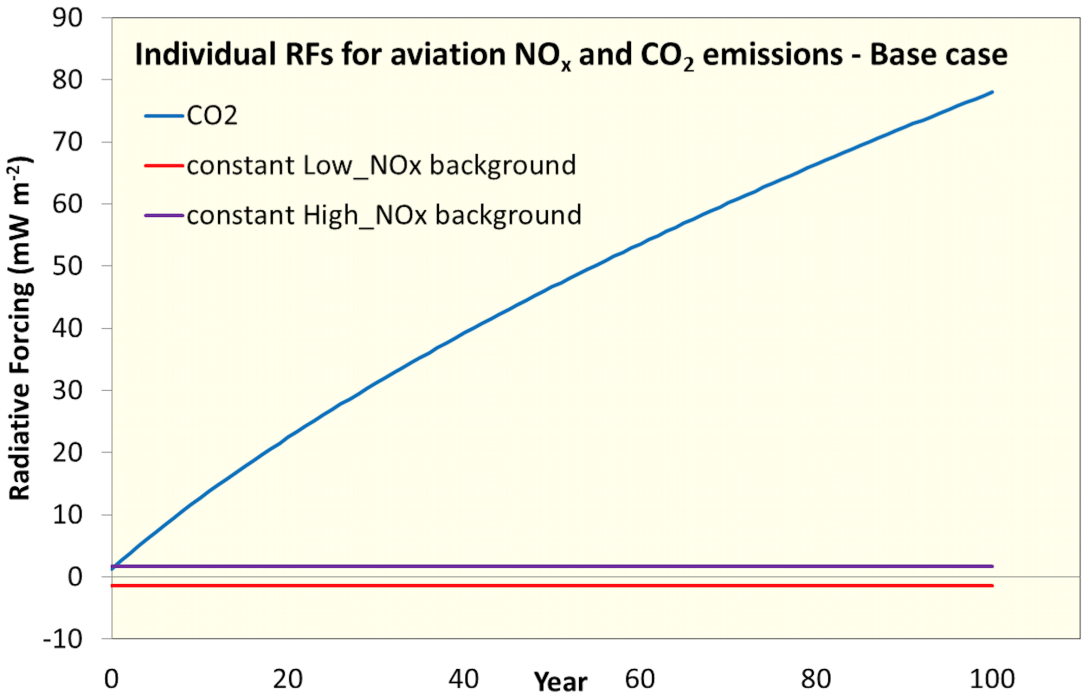

Figure 7.2: The RF (mW m^{-2}) of CO_2 in a constant background of 404 ppm CO_2 and NO_x , in the high NO_x and low NO_x backgrounds for the base case constant fuel as shown in Figure 7.1.

Figure 7.2 shows that when fuel and thus, emissions are kept constant, the RF from CO_2 emissions in a constant background is much stronger than that of the net NO_x forcing in both the low and high NO_x backgrounds. The forcing from CO_2 is positive, whereas the sign of the NO_x forcing is dependent on the background. This figure also demonstrates the cumulative nature of CO_2 , as forcing increases over the 100 year run, whereas the NO_x forcing remains constant as the emissions do over the entire run, due to its high reactivity and short lifetime in the atmosphere. Median temperature response is calculated as described in Chapter 6 and shown in Figure 7.3, again the temperature response from CO_2 is larger than that from NO_x . The temperature response from aviation NO_x emissions again depends on the background, with a low NO_x background producing a negative temperature response, and a high NO_x background, a positive response.

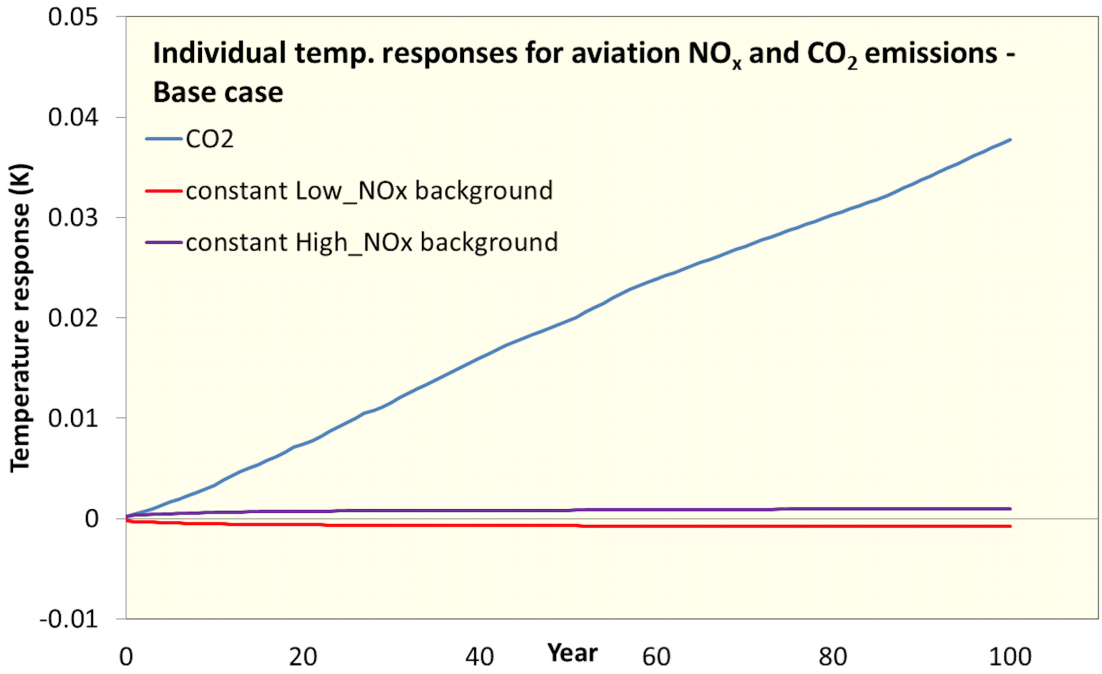

Figure 7.3: The temperature response (K) of CO_2 in a constant background of 404 ppm CO_2 and NO_x , in the high NO_x and low NO_x backgrounds for the base case constant fuel as shown in Figure 7.1.

The forcings of NO_x and CO_2 were then summed, for the low NO_x background and the high NO_x background to form a base case value of overall effect of aviation (neglecting the effects of BC, aerosols and contrails which were not within the scope of the study), with which to compare the trade–off experiments (Figure 7.4). Figure 7.4 shows that the sum of the forcing from aviation CO_2 and NO_x is an additional positive forcing which increases over time if aviation emissions and the background atmosphere remain constant. It is evident that CO_2 determines the majority of the overall forcing, the negative forcing of NO_x in the low NO_x background causes the overall sum of itself and the CO_2 forcing to be lower than the high NO_x background CO_2 and NO_x emissions combined, for both RF and the subsequent temperature response (Figure 7.4).

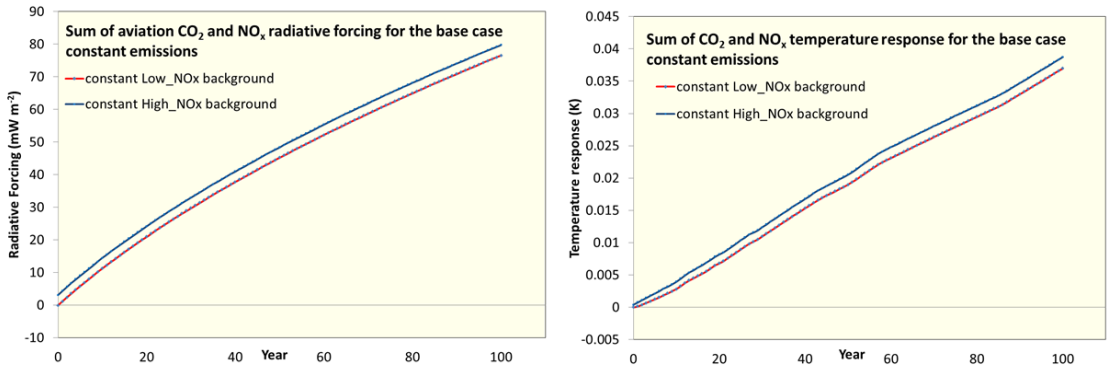

Figure 7.4: The sum of aviation CO_2 and NO_x RF (left) and temperature response (right) as a result of the constant base case emissions in the low NO_x and high NO_x background.

7.2.2 Perturbation experiment – NO_x is reduced by 20 percent below the base case incurring a 2 percent CO_2 penalty

To investigate the effects of trade–offs between aviation NO_x and CO_2 emissions, the base case is perturbed. A review of the current literature shows a lack of studies on the CO_2 - NO_x trade–off and that there are many variables involved with forming policies on the subject (aircraft and engine type, noise reduction, etc). The targets discussed in the ICAO CAEP forums include a few scenarios regarding reducing NO_x emissions and suggest a trade–off of a 2 percent CO_2 penalty for a 20 percent reduction in NO_x emissions. This particular percentage of trade–off appears in several studies on the subject (varying by a few percent) (Table 7.1). For this reason it was chosen for the first perturbation experiment in this study.

NO_x change	CO_2 change	Reference/scenario
-5%	+0.01%	ICAO env report 2010 (min)
-20%	+0.19%	ICAO env report 2010 (max)
-20%	+2%	DELFT report 2008 (Faber *et al.*, 2008)
-15% to -30%	+1% to +3%	DELFT report 2008 (Faber *et al.*, 2008)
-22%	+2%	LTTG CAEP7 (Newton, 2007)
+4%	-1% (a four to one trade-off)	Green, 2003

Table 7.1: Literature overview of trade-off studies and suggested CO_2 penalties for NO_x reduction.

The base case was perturbed to incur a 20 percent NO_x reduction with a 2 percent CO_2 penalty (Figures 7.5 and 7.6). This perturbation results in an overall additional positive RF and subsequently, temperature response, in both the low NO_x and high NO_x backgrounds, showing that an addition of a small amount of CO_2 has more of an impact than a large reduction in NO_x emissions.

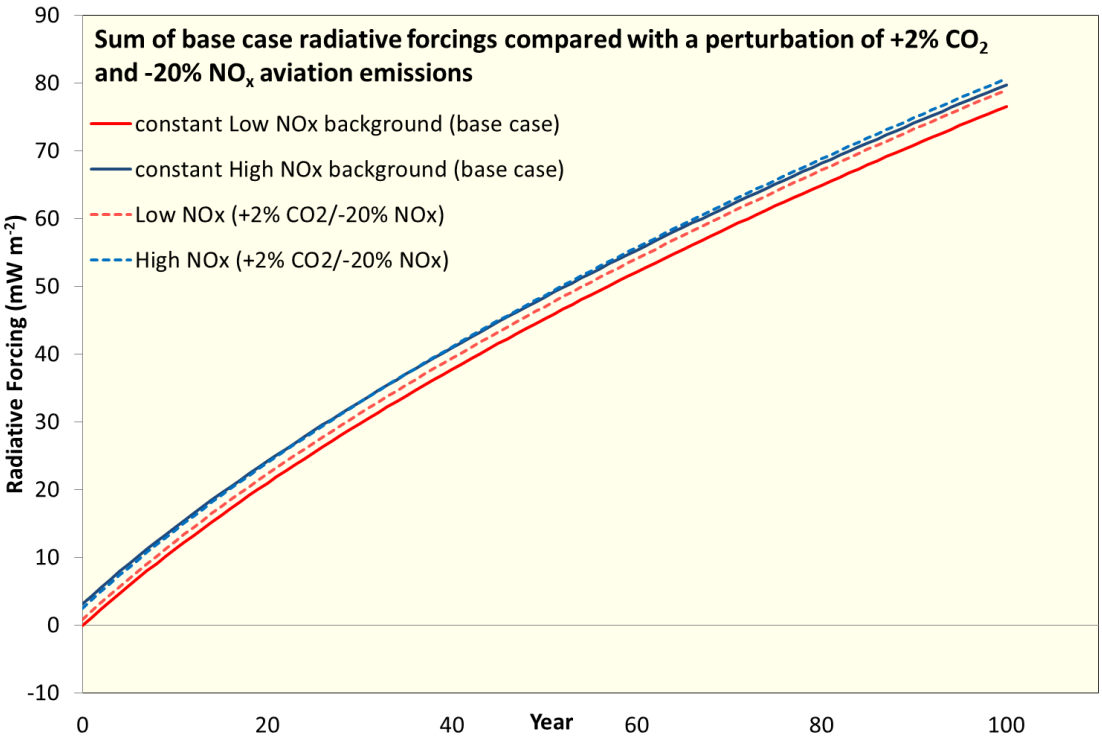

Figure 7.5: The sum of the radiative forcings of aviation NO_x and CO_2 when the base case is perturbed by adding 2 percent more CO_2 emissions and reducing NO_x emissions by 20 percent compared to the base case in the high NO_x background and low NO_x background, in comparison to the base case total RF.

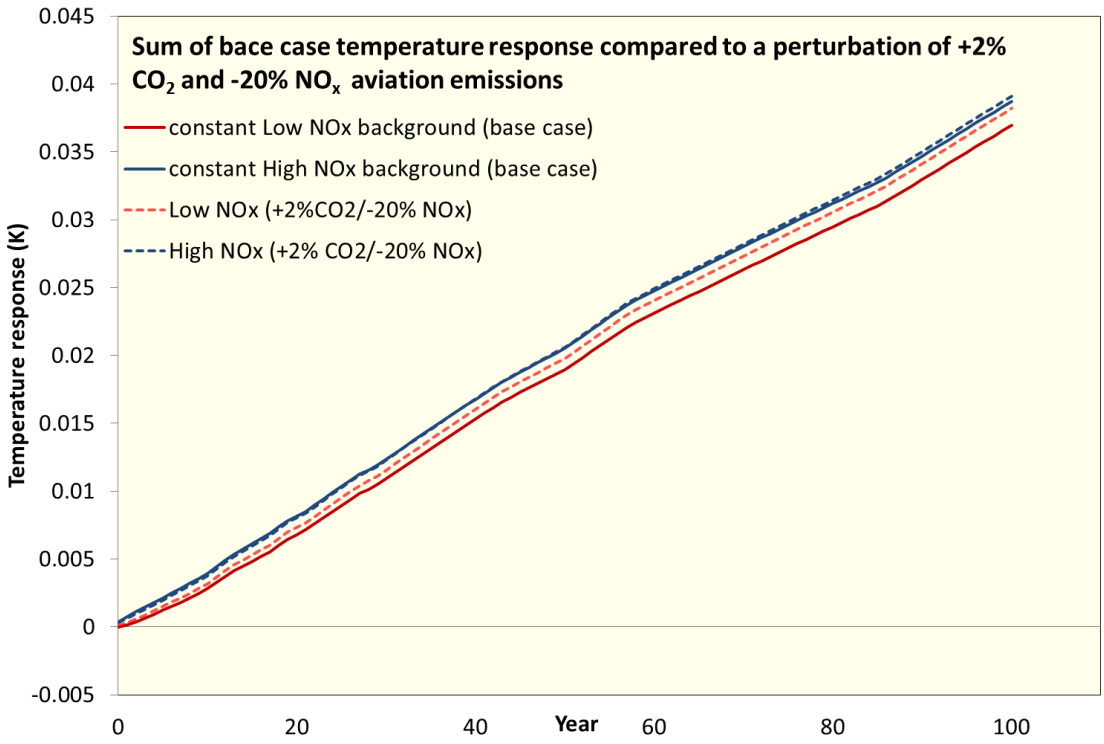

Figure 7.6: The sum of the temperature responses of aviation NO_x and CO_2 when the base case is perturbed by adding 2percent CO_2 emissions and reducing NO_x emissions by 20percent compared to the base case in the high NO_x background and low NO_x background, in comparison to the base case total temperature response.

7.2.3 NO_x reduction experiment – when CO_2 is increased by 2 percent, how much NO_x reduction is necessary to offset the associated increase in forcing?

Given that the first perturbation experiment clearly showed a net increase in RF for a strong NO_x reduction and a small CO_2 increase, further experiments were performed to determine the percentage of NO_x reduction required in order to maintain temperature response at the levels of the base case while incurring a CO_2 penalty of 2 percent. Reproducing the base case levels does not benefit climate, that would only be the case if temperature response goes below that of the base case, but reducing NO_x emissions would improve air pollution, which, while not considered in this study, is of consideration in present day policy.

Offsetting a 2°C increase in CO_2 emissions by reducing NO_x incrementally, in the constant high NO_x background

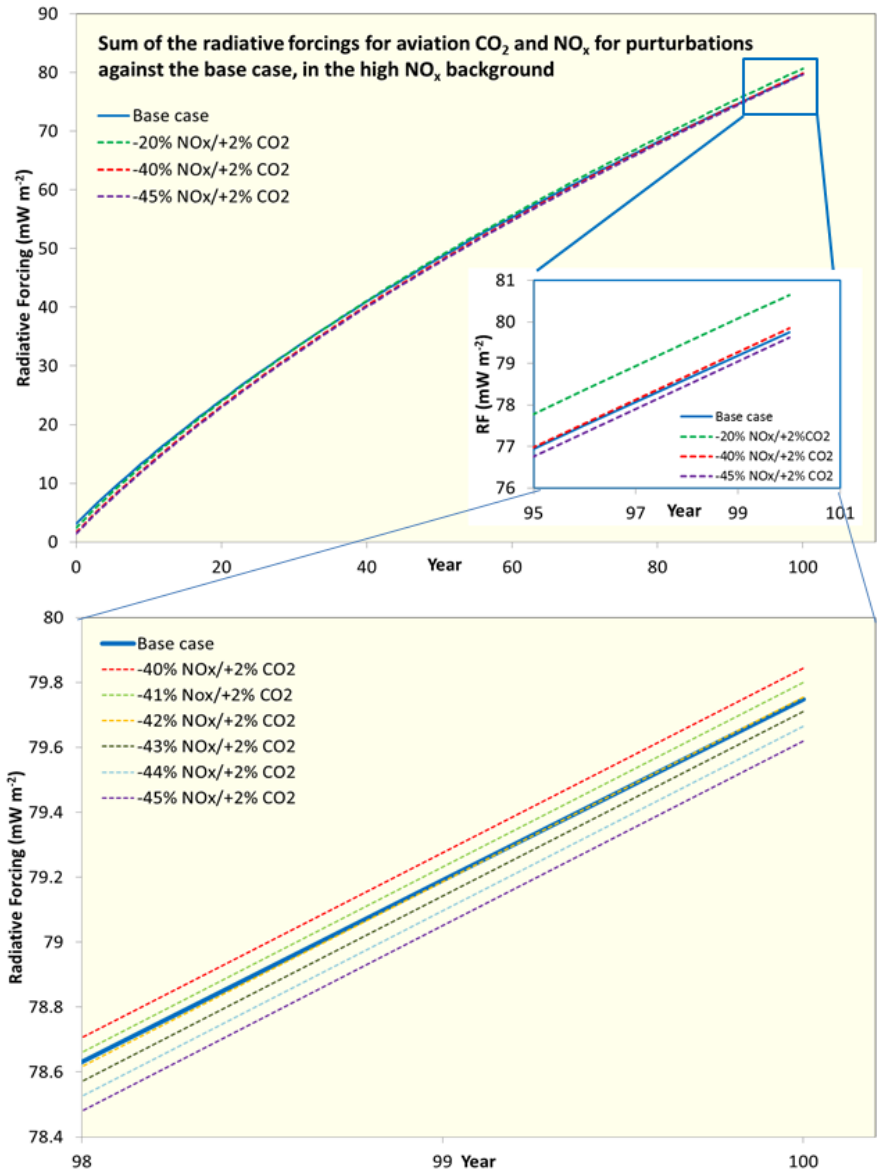

Figure 7.7: The sum of the radiative forcing from aviation NO_x and CO_2 where CO_2 has increase by 2 percent compared to the base case and NO_x has been reduced incrementally to determine how much NO_x reduction is needed to offset the additional RF that a 2 percent increase in CO_2 incurs compared to the base case value in the constant high NO_x background with constant emissions.

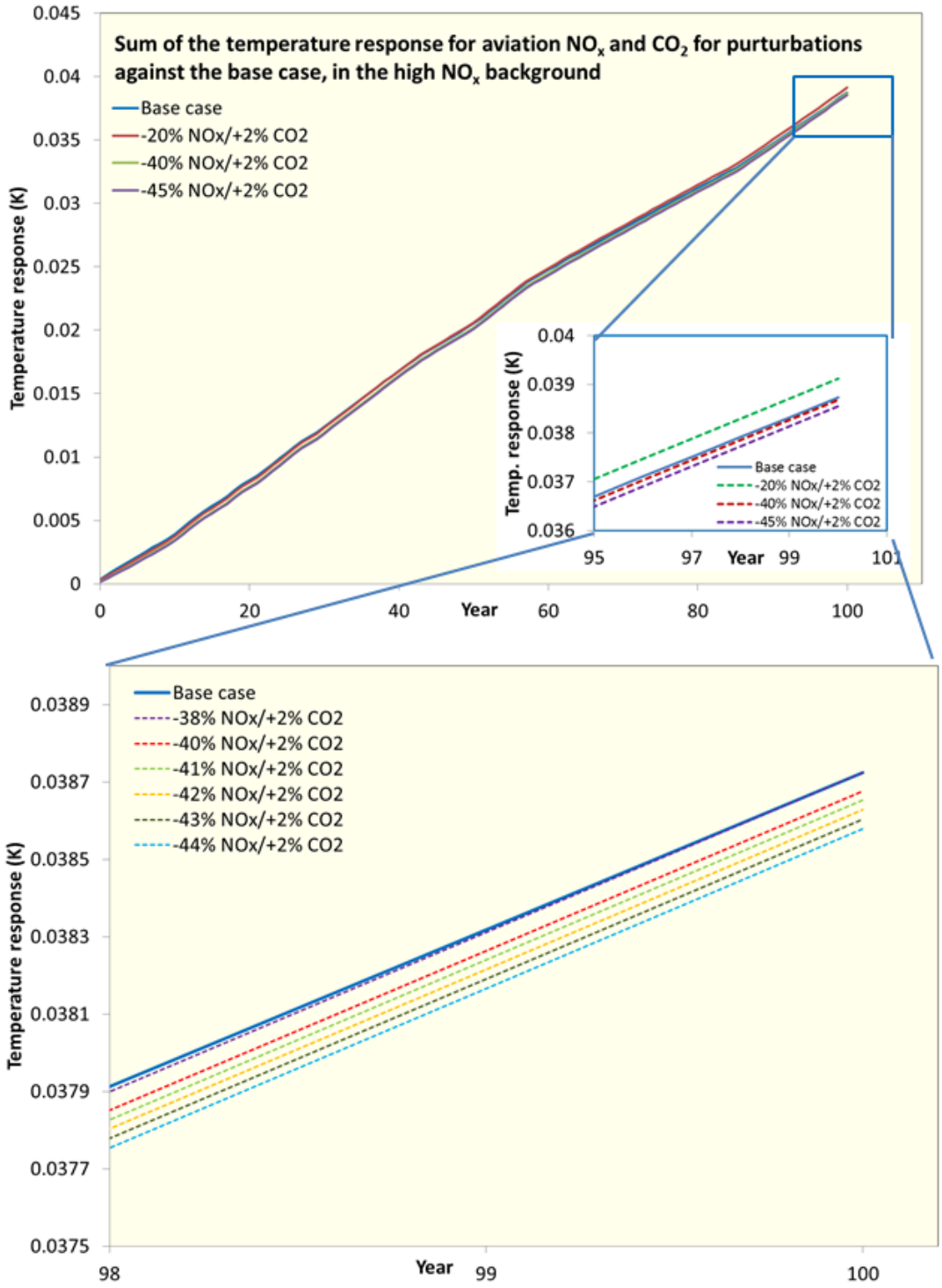

Figure 7.8: The sum of the radiaitve forcing from aviation NO_x and CO_2 where CO_2 has increase by 2 percent compared to the base case and NO_x has been reduced incrementally to determine how much NO_x reduction is needed to offset the additional radiative forcing occurring from the addition of 2 percent CO_2 compared to the base case value in the constant high NO_x background with constant emissions.

Results show that in the high NO_x background a reduction in NO_x does lead to an overall reduction in temperature response (Figures 7.7 and 7.8), hence it was then a matter of deducing, by how much. It was found that NO_x emissions must be reduced by 45 percent below the base case in order to reduce the radiative forcing to below that of the base case whilst incurring a 2 percent CO_2 penalty after 100 years. To offset the temperature response, only a 38 percent reduction in NO_x is necessary, as the system takes time to respond to additional forcing, whereas RF is an instantaneous response. Therefore, the time horizon is an important factor for temperature response calculations, due to the thermal inertia of the climate system.

Offsetting a 2°C increase in CO_2 emissions by reducing NO_x incrementally in the constant low NO_x background

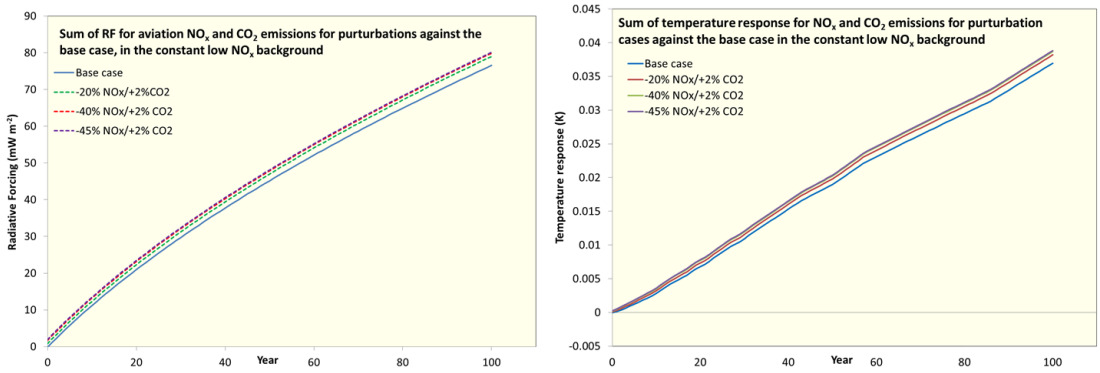

Figure 7.9: The sum of the radiative forcing (left) and temperature change (right) from aviation NO_x and CO_2 emissions for the base case and then a perturbation of plus 2 percent CO_2 emissions and incremental amounts of NO_x reduction in the constant low NO_x background and constant CO_2 background of 404 ppm.

In the low NO_x background, any reduction in NO_x causes temperatures to increase as the overall negative NO_x forcing is reduced - it becomes less negative. Therefore, in order to reduce temperature change below the value of the base case, aircraft NO_x emissions would need to increase, thereby increasing the negative forcing and reducing the overall forcing of NO_x and CO_2 combined. Thus, any additional NO_x is beneficial in terms of temperature response and subsequently, climate, while the background NO_x is low.

7.2.4 When CO_2 is increased by 2 percent, how much additional NO_x is necessary to counteract the change in forcing in the constant low NO_x background atmosphere?

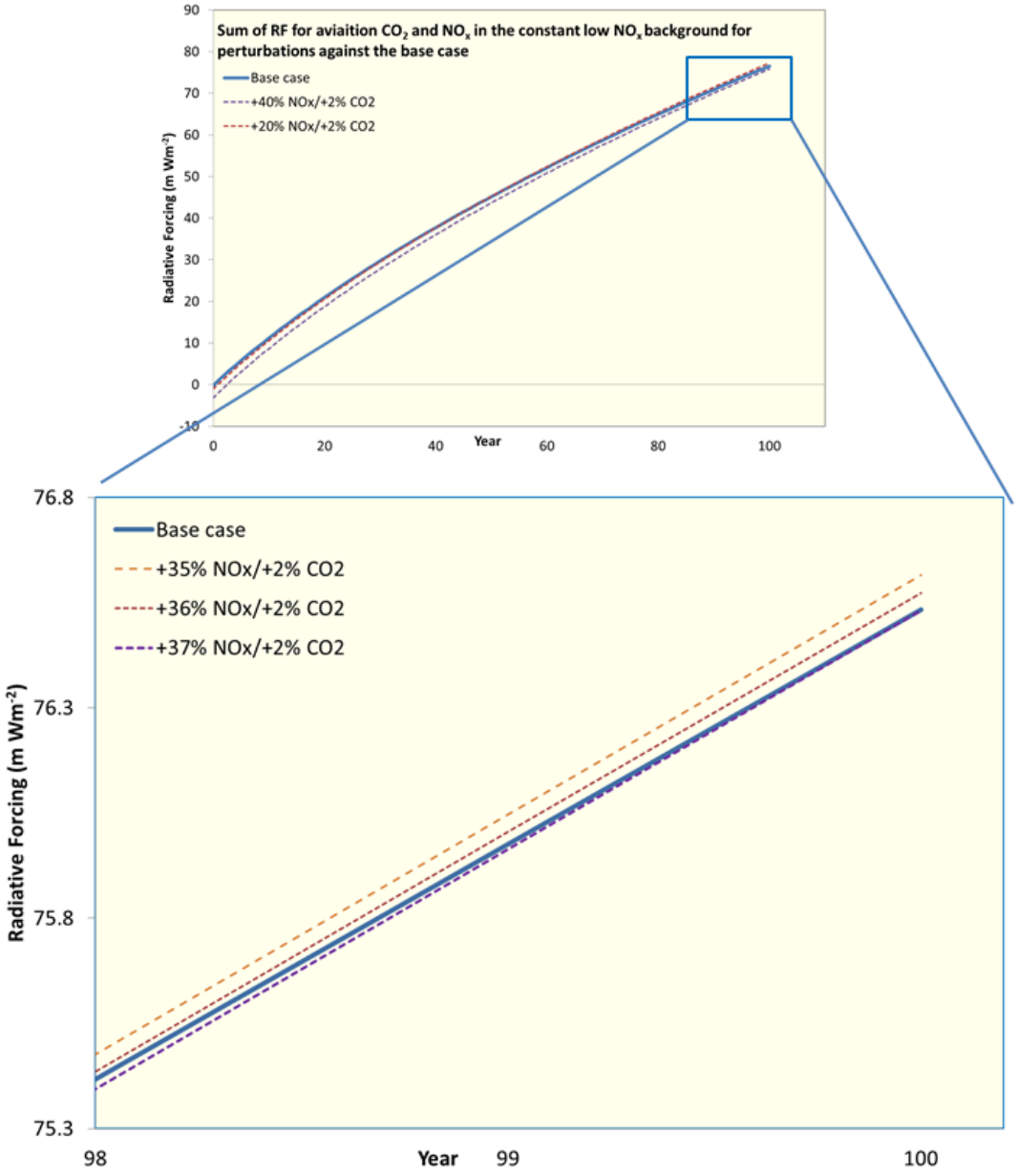

Figure 7.10: The sum of the radiative forcing (mW m^{-2}) for aviation CO_2 and NO_x emissions for the base case and then a perturbation of plus 2 percent CO_2 and increments of increasing NO_x emissions designed to offset the additional aviation CO_2 emissions in the constant low NO_x background.

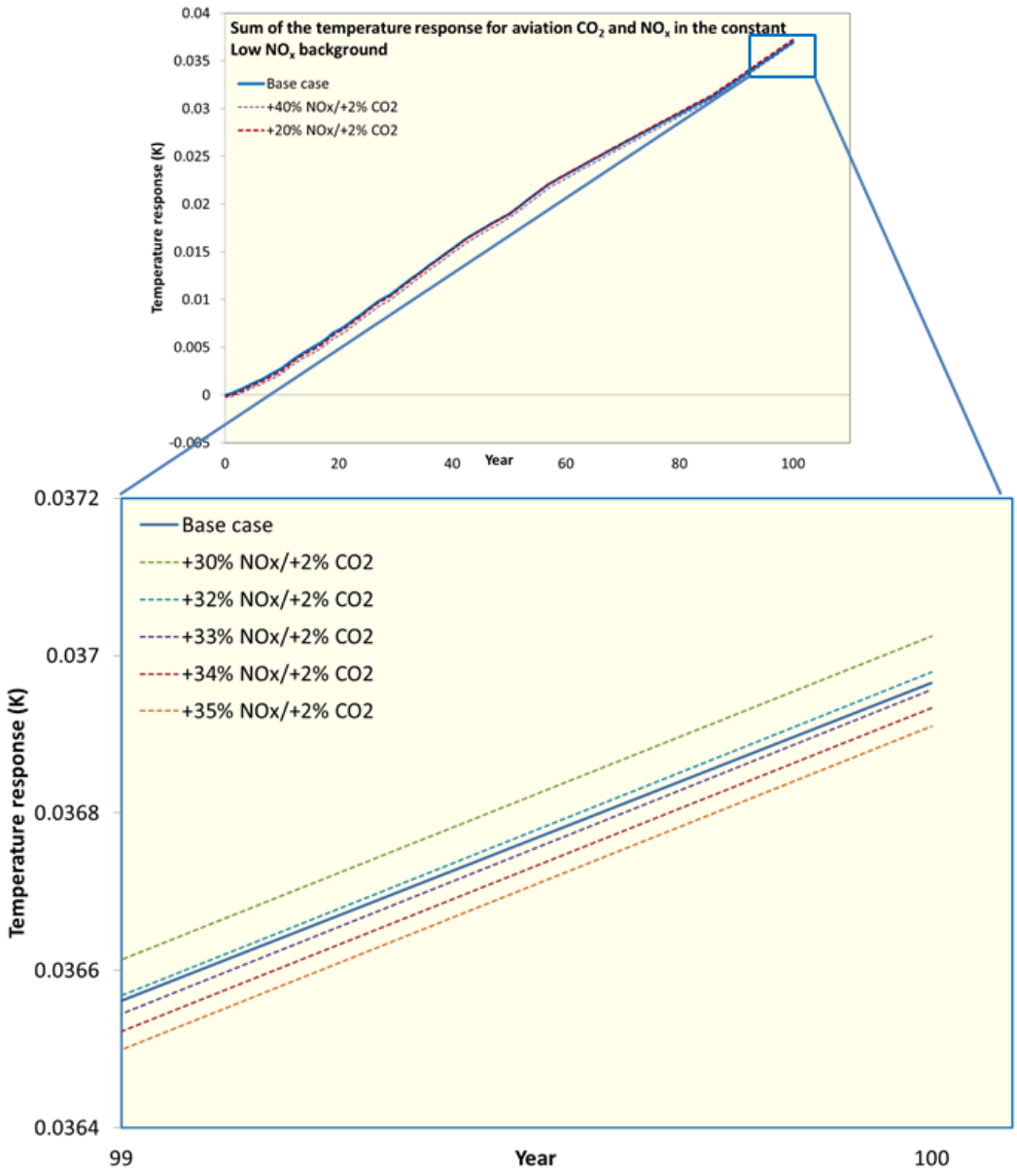

Figure 7.11: The sum of the temperature response (K) for aviation CO_2 and NO_x emissions for the base case and then a perturbation of plus 2 percent CO_2 and increments of increasing NO_x emissions designed to offset the additional aviation CO_2 emissions in the constant low NO_x background.

The preceding experiments show that in a low NO_x background, an addition of NO_x is needed to reduce the overall RF and temperature response, when CO_2 is increased by 2 percent. Experiments were performed to ascertain, in a low NO_x background, how much additional NO_x would be needed to counteract the rise of 2 percent CO_2 emissions and

the results are shown in Figures 7.10 and 7.11. It is shown that a NO_x increase of 37 percent is necessary to counteract the additional RF resulting from a 2 percent increase in CO_2 emissions over the base case and a NO_x increase of 33 percent brings the total temperature response, from aviation NO_x and CO_2 emissions, below that of the base case after 100 years of model run. Again, less additional NO_x is needed to counteract the change in temperature response than in RF as the temperature response includes the time taken for the system to respond to additional forcing, the thermal inertia, and so 'lags behind' the change in RF.

7.2.5 How much percentage CO_2 penalty is allowed when NO_x emissions are reduced by 20 percent in order not to incur any additional forcing above that of the base case?

The next set of experiments assumed that NO_x reduction is held at 20 percent - (due to some new technology perhaps). Model runs were undertaken in the aim of determining how much CO_2 penalty is allowed when NO_x emissions are held at –20 percent, in order to not incur a radiative forcing or temperature response penalty over that of the base case values.

Determining the maximum percentage CO_2 penalty, when NO_x emissions are reduced by 20 percent in order not to perturb overall forcing higher than that of the base case in the constant high NO_x background

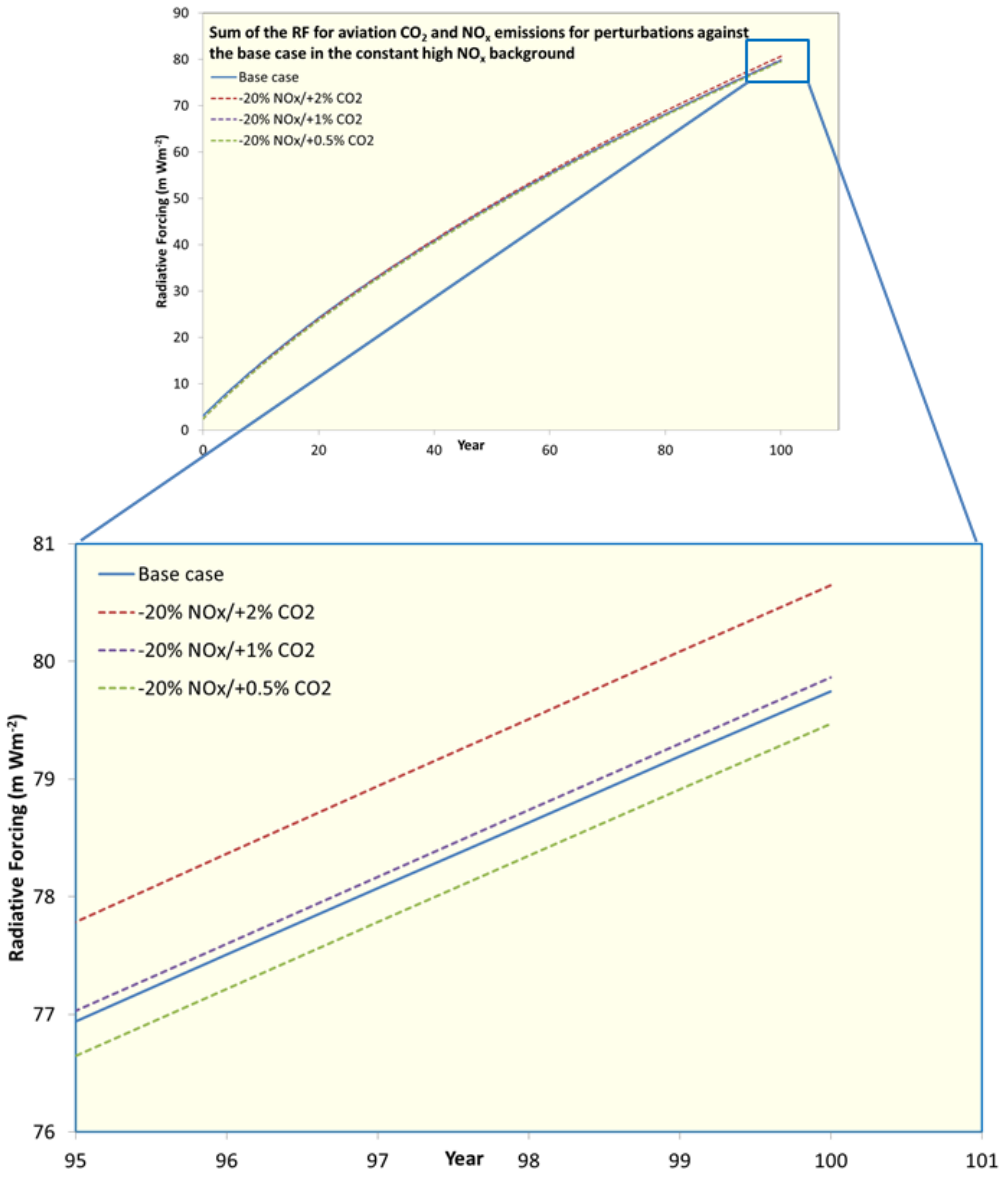

Figure 7.12: The sum of the radiative forcing (mW m^{-2}) for aviation CO_2 and NO_x emissions for the base case and then a perturbation of minus 20 percent NO_x and increments of increasing CO_2 emissions in the constant high NO_x background.

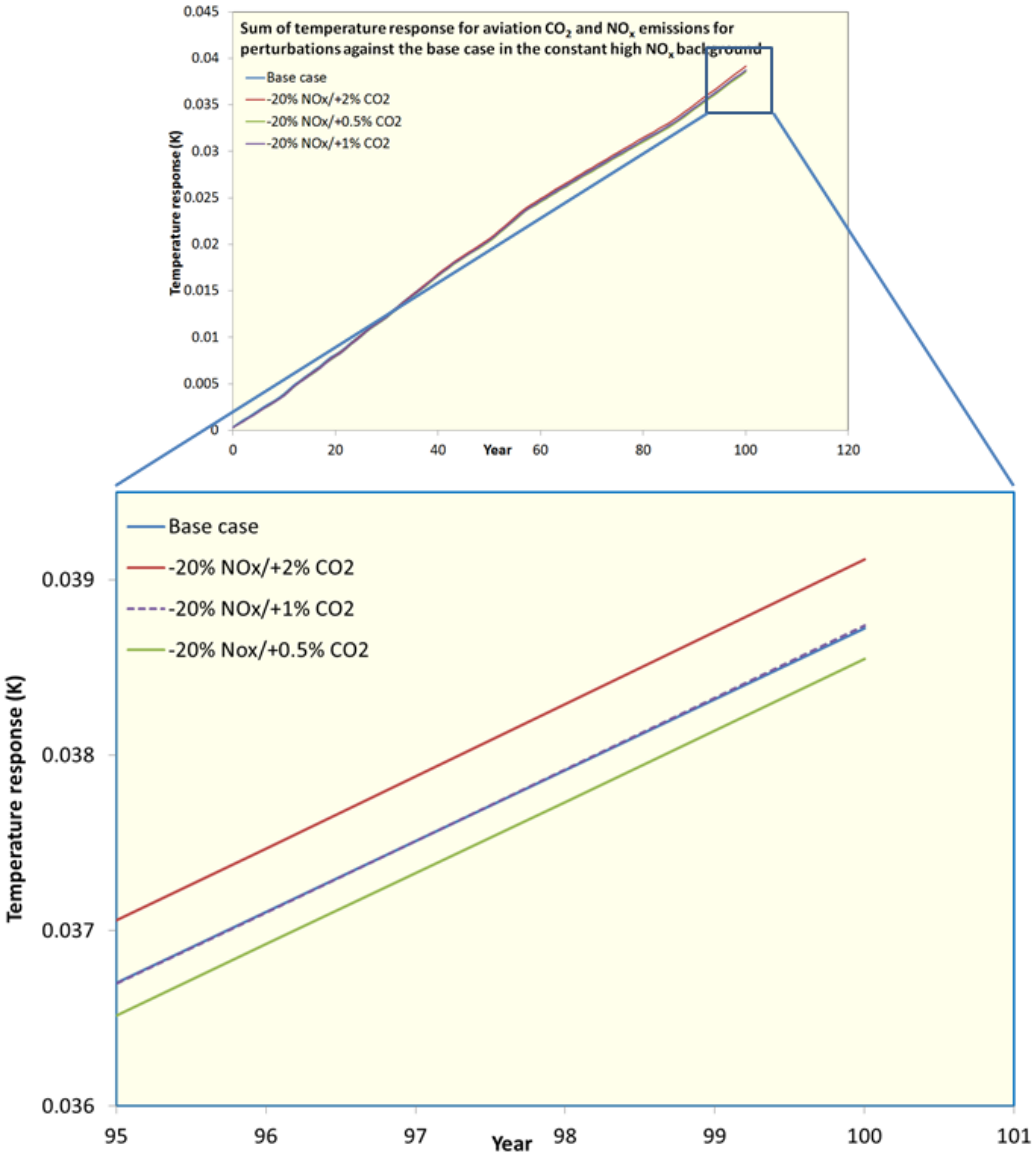

Figure 7.13: The sum of the temperature response (K) for aviation CO_2 and NO_x emissions for the base case and then a perturbation of minus 20 percent NO_x and increments of increasing CO_2 emissions in the constant high NO_x background.

In the high NO_x background, it was found that when NO_x emissions were reduced by 20 percent, the maximum CO_2 penalty can be only 0.5 percent greater than the base case. A penalty of 1 percent CO_2 caused both the radiative forcing and the temperature response to be higher than the base case value after a 100 year run (Figures 7.12 and 7.13).

Determining the maximum percentage CO_2 penalty, when NO_x emissions are reduced by 20 percent in order not to perturb overall forcing higher than that of the base case in the constant low NO_x background

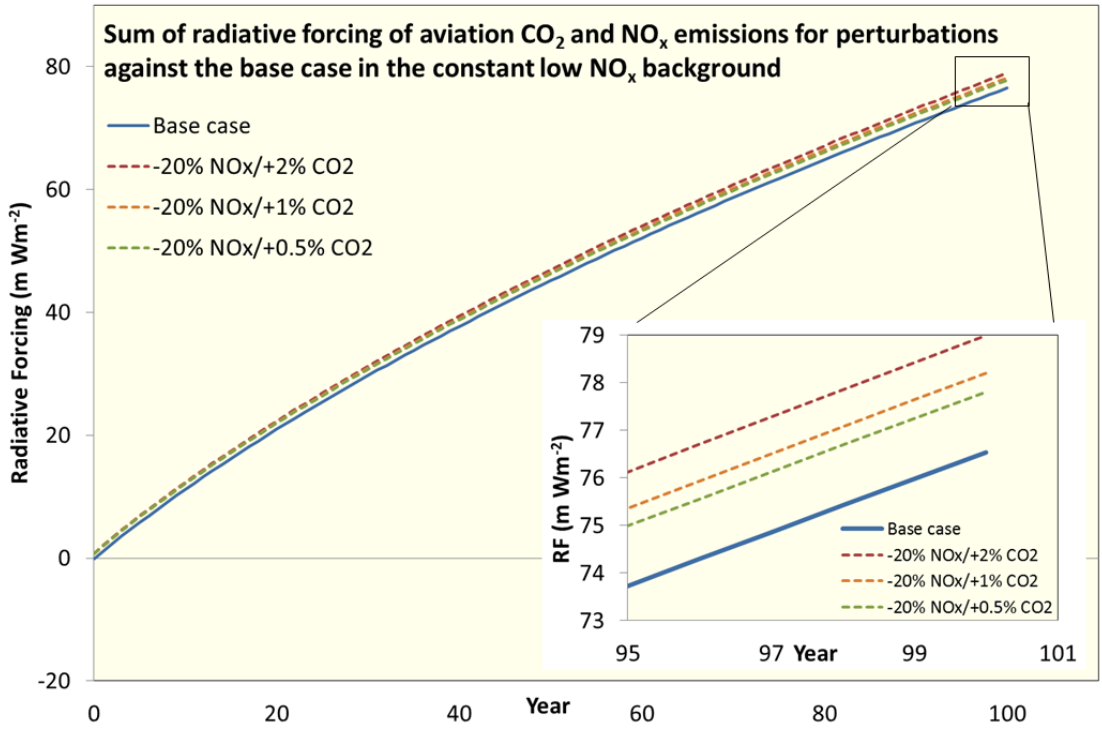

Figure 7.14: The sum of aviation NO_x and CO_2 radiative forcing (mW m^{-2}) for the base case and then three perturbation cases where NO_x was reduced by 20 percent and CO_2 was increased incrementally in the low NO_x background.

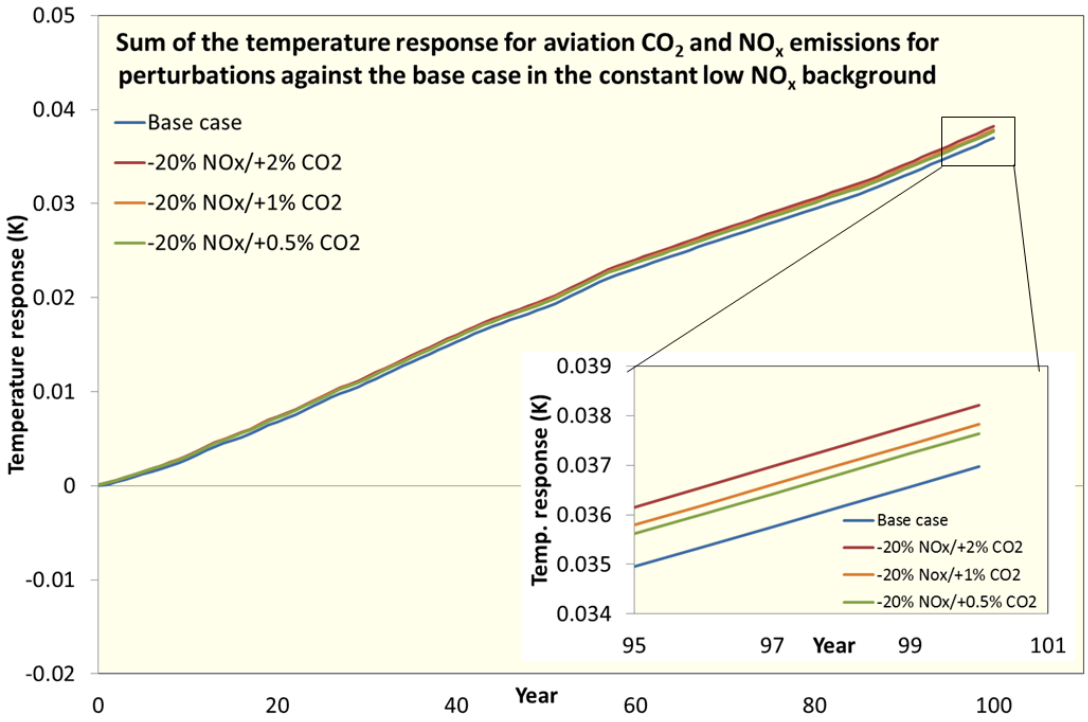

Figure 7.15: The sum of aviation NO_x and CO_2 temperature response (K) for the base case and then three perturbation cases where NO_x was reduced by 20 percent and CO_2 was increased incrementally in the low NO_x background.

Figures 7.14 and 7.15 show that as any reduction in NO_x in the low NO_x background causes an increase in RF and therefore temperature response, the reduction of 20 percent NO_x will cause the forcing to be higher than the base case before CO_2 is also increased. Therefore, any percentage of additional CO_2 will also increase the RF and temperature response further. In order to reduce the RF and temperature response below that of the base case, while NO_x emissions are held at –20 percent, the CO_2 emissions must be reduced below its base case value in order to counteract the rise in forcing due to NO_x reduction in the constant low NO_x background. Figures 7.16 and 7.17 Show that in this case, if NO_x is to be reduced by 20 percent below the base case value, then CO_2 must also be reduced by 1.5 percent below the base case to reduce overall radiative forcing and temperature response to below that of the base case, thus counteracting the additional forcing incurred by reducing NO_x in the constant low NO_x background.

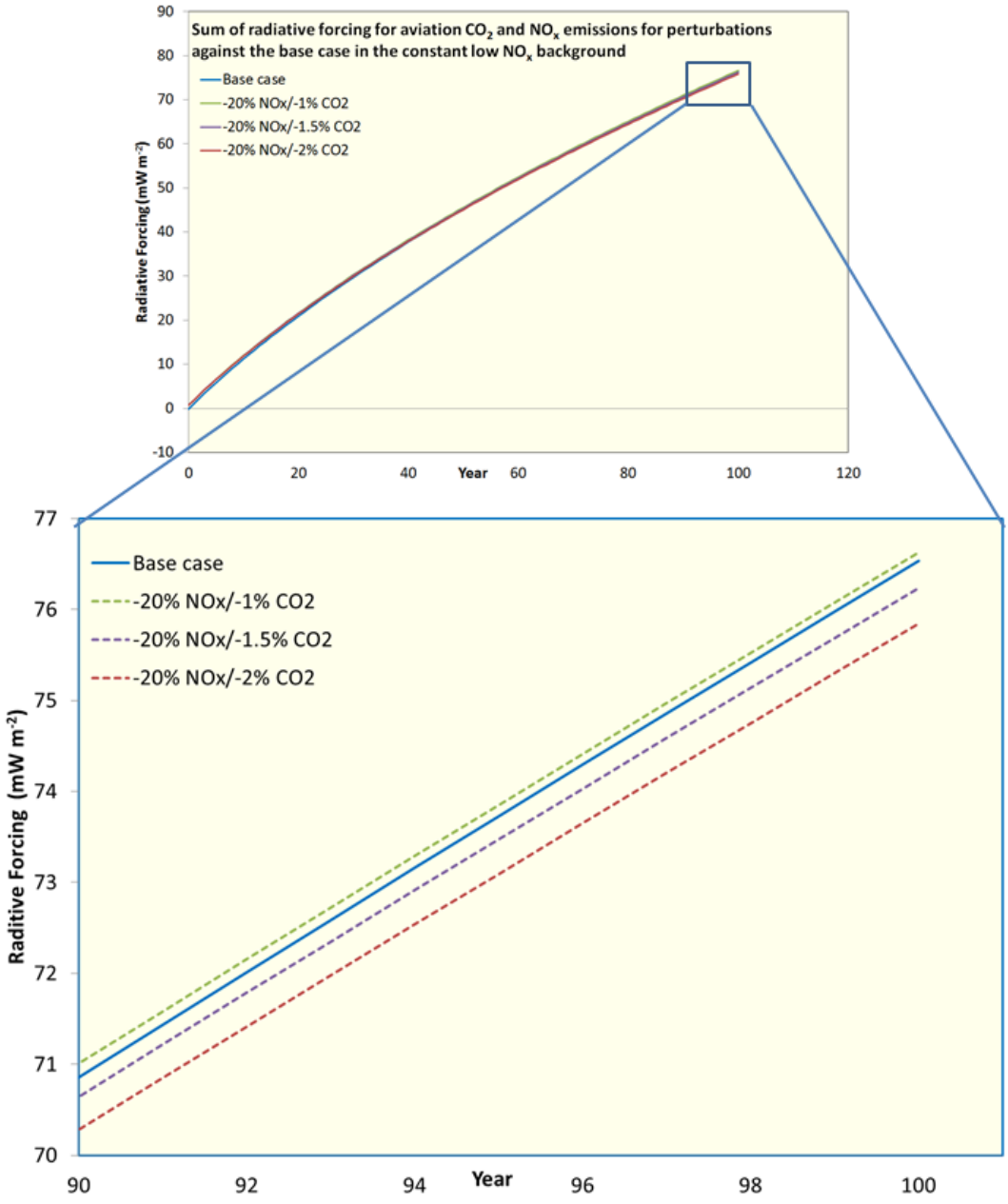

Figure 7.16: The sum of the radiative forcing (mW m^{-2}) for aviation CO_2 and NO_x emissions for the base case and then a perturbation of minus 20 percent NO_x and increments of decreasing CO_2 emissions in the constant low NO_x background.

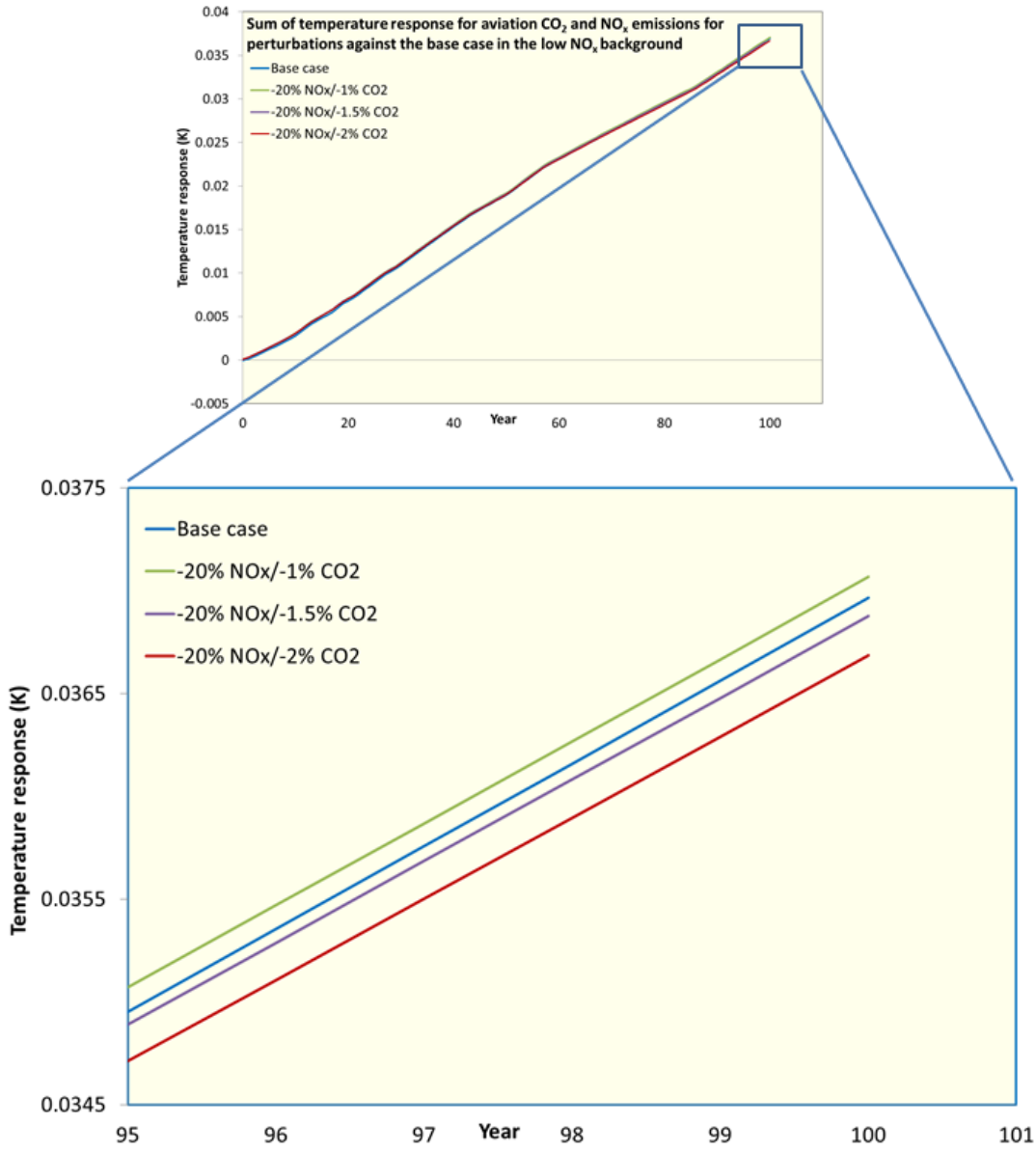

Figure 7.17: The sum of the temperature response (K) for aviation CO_2 and NO_x emissions for the base case and then a perturbation of minus 20 percent NO_x and increments of decreasing CO_2 emissions in the constant low NO_x background.

7.3 Effects of Delaying Mitigation Measures

The experiments performed here are part of a parametric study, where both background and aviation NO_x and CO_2 emissions are kept constant. The results establish that a trade–

off is present between aviation NO_x and CO_2 emissions, which is influenced by the state of the background atmosphere. These initial results show the measures which could be taken in the form of a percentage change of NO_x or CO_2 emissions for mitigation purposes, they also show the importance of CO_2 emissions in accounting for the majority of the forcing caused by aviation.

CO_2 is cumulative in the atmosphere, and thus continues to have an effect long after its initial emission. Therefore, even immediate cessation of all additional emissions will result in a peak warming many years into the future. An example of this is shown in Figure 7.18. An aviation scenario was run where emissions follow observations from 1940 2012, then increased by 1 percent per year until 2050 where they cease completely. This scenario was run in four different background atmospheres of the four RCPs (see Chapter 3). The results show that once emissions cease, the accumulation of those emissions over time continues to contribute an additional radiative forcing and positive temperature response for centuries to come. As RF is an instantaneous forcing it peaks with emissions and immediately begins to decline after emissions cease, peak warming however, takes place years after emissions have ceased due to the thermal inertia of the climate system – the time take for it to response to the additional forcing. Whereas NO_x emissions are short–lived and quickly react out of the atmosphere, CO_2 does not break down in the atmosphere or deposit on the earth's surface. Instead, after its initial release it undertakes a long residence time in the atmosphere before cycling throughout the earth's carbon reservoirs over centuries to thousands of years.

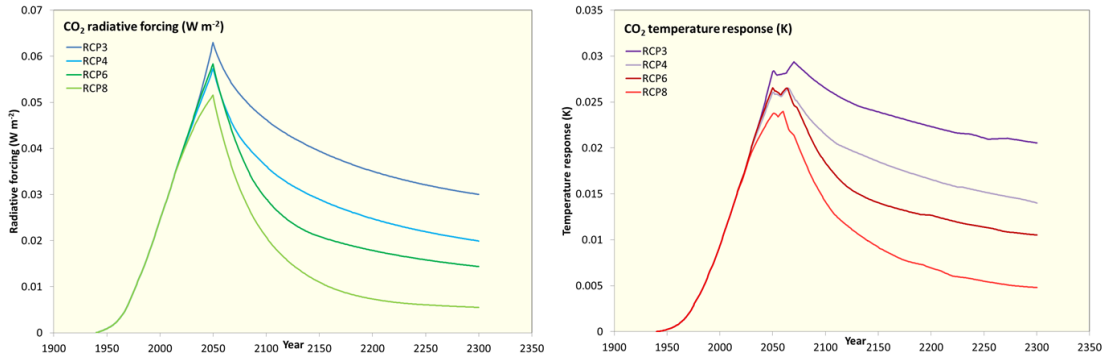

Figure 7.18: The radiative forcing (mW m^{-2})(left) and temperature response (K)(right) from aviation CO_2 emissions when an aviation emissions scenario is run in four different background atmospheric CO_2 states. The aviation emissions scenario was created where emissions follow observations from 1940 – 2012, and then were increased by 1 percent per year until 2050 where they cease completely. The four background atmospheric states are the four RCPs.

The long–lived nature of CO_2 after its release is an important consideration in its mitigation. While many sectors, such as aviation, have the opportunity to mitigate climate change from two fronts – by reducing short–lived or long–lived climate forcers, many will chose to mitigate short–term forcers as it is generally cheaper and easier than reducing CO_2 and the effects are immediate. Work by Allen (2015) shows the effect of delaying the mitigation of both short term and long-term forcers.

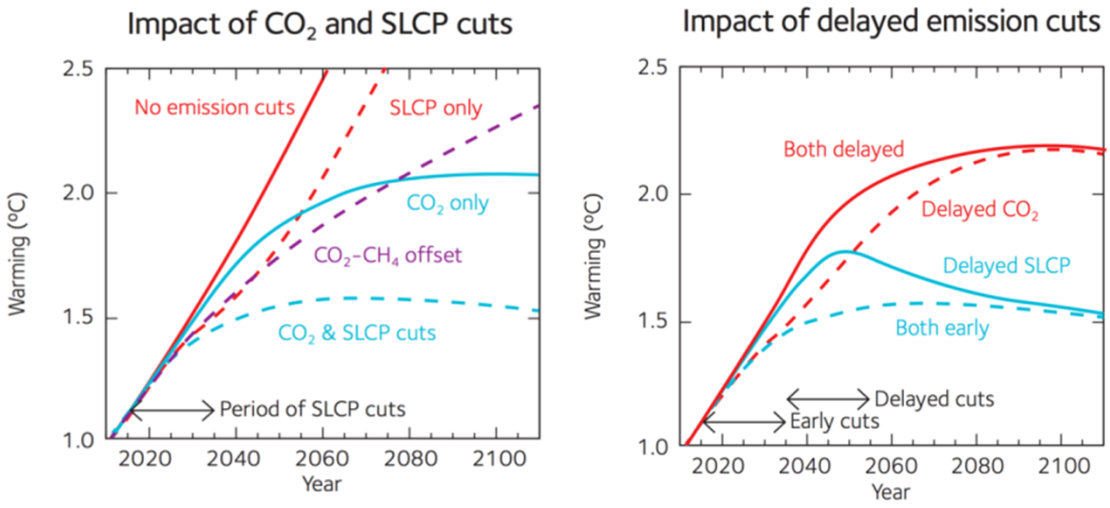

Figure 7.19: The left figure shows the temperature response (warming) resulting from idealized CO_2 emissions profiles and the effect of immediate cuts in CO_2 and/or short-lived climate forcers/pollutants (SLCF/SLCP). The red line shows the effect or business as usual, no emissions cuts, the light blue line shows the impact of immediately cutting CO_2 emissions in this particular idealized case, the dotted red shows the effect of immediately cutting SLCPs and the dotted light blue line shows the impact of immediately cutting both SLCPs and CO_2 . The right figure shows the impact on temperature response (warming) when cuts in CO_2 emissions are delayed (dotted red line), when cuts in SCLP emissions are delayed (light blue solid line), when both CO_2 and SLCP emission cuts are delayed (solid red line) and when both CO_2 and SLCP emissions are cut early or immediately (dotted light blue line). Taken from Allen (2015).

Figure 7.19 shows two important points; 1) that the mitigation of SLCFs has an immediate impact on reducing warming in the short term, but over the long term has little impact, whereas the immediate mitigation of CO_2 emissions will not show much impact on warming for several decades but when it does, the impact or reduction in warming will be greater. 2) that if both short–term and long–term climate–forcer mitigation are delayed, the short–term forcers may impact climate for a few years longer than they would have if cut earlier but the long–term forcer (CO_2), will impact on climate for decades to

centuries longer than they would have if cut earlier.

Even though a reduction in CO_2 emissions reduces warming by a greater amount in the long term, if actions on both CO_2 and STCF mitigation were taken immediately, the effect of the CO_2 mitigation remains less than that of the SLCF mitigation for several decades making them appear the more attractive mitigation pathway in the short term (Allen, 2015). This is where policy decisions may favour SLCF mitigation in terms of results and initial cost. As long as CO_2 emissions release keeps increasing, as it is at present, peak warming will also increase both in time and amount, as shown in Figure 7.18. The only way SLCF mitigation will have any impact on peak warming is if CO_2 mitigation is already under way and emissions are decreasing.

7.4 Conclusions

These experiments were designed to look at trade–offs between aviation CO_2 and NO_x emissions in the simplest way, using constant background values of CO_2 and NO_x , and constant emissions scenarios. The experiments used the parameterisation for NO_x described in Chapter 5 to model NO_x RF and the LinClim SCM to model CO_2 RF and temperature response and NO_x temperature response.

A base case was formulated where emissions, $EINO_x$ and background CO_2 and NO_x were kept at constant levels for a 100 year run. This was repeated in a low NO_x and a high NO_x background. It can be seen from the forcings resulting from these base cases that the majority of the overall aviation RF and temperature response (when aviation effect = CO_2 + NO_x) is a result of the CO_2 emissions. As shown in Chapter 6, the forcing from aviation NO_x emissions depends on the background NO_x levels, in a low NO_x background the overall NO_x RF and subsequent temperature response is negative, due to the higher levels of methane destruction, whereas in the high NO_x background the overall NO_x forcing is positive. When summed, the aviation NO_x emissions and CO_2 in the low NO_x environment give a slightly lower overall RF and temperature response than the sum of CO_2 and NO_x emissions in the high NO_x background.

A review of the literature revealed a common theoretical mitigation scenario, designed to reduce air pollution, of a 20 percent NO_x reduction for a 2 percent CO_2 penalty. These percentage changes were applied to the base case to form the initial perturbation case. The

results of the perturbation case showed that, in both the low and high NO_x backgrounds, the overall RF and temperature response were higher than the base case values, therefore a reduction of 20 percent NO_x was shown to be insufficient to counteract the effects of an addition of 2 percent CO_2 emissions.

The next experiments were designed to determine what percentage reduction of NO_x was in fact necessary in order to counteract the effects of the additional 2 percent CO_2 emissions. For the high NO_x background, experiments showed that for a 2 percent increase in CO_2 , NO_x emissions must be reduced by 43 percent to bring the RF back down to lower than the base case after 100 years but only reduced by 38 percent for the temperature response to equal that of the base case. The difference is due to the face that while RF is an instantaneous forcing, the temperature response shows the response of the whole climate system to a change in forcing – its thermal inertia, and so lags behind RF over time. The results for the low NO_x background show a more complex relationship, as the overall NO_x forcing is negative in the low NO_x background due to higher levels of methane reduction, a reduction in NO_x emissions, reduces the negative NO_x response, hence the sum of the NO_x and CO_2 forcings becomes more positive. Therefore, any reduction in NO_x emissions in the low NO_x background actually adds a positive forcing to the overall (CO_2 + NO_x) forcing, and thus creates a greater RF and temperature response than the base case after 100 years. In this case, to counteract the additional 2 percent of CO_2 , additional NO_x emissions are also required. It was found that for a 2 percent increase in CO_2 emissions, NO_x emission also had to increase by 37 percent to reduce the RF to equal with that of the base case after 100 years or by 33 percent to reduce temperature response to below that of the base case.

The next experiments assume NO_x reduction stays at 20 percent below the base case and determine how much CO_2 penalty is 'allowed' to ensure that overall RF and temperature response do not exceed that of the base case. In the high NO_x background, it was found that CO_2 could increase by 0.5 percent and both levels of RF and temperature response would remain below the base case but an increase of 1 percent would cause both to be higher than the base case. For the low NO_x background, again it becomes more complex. As any reduction in NO_x would push the RF and temperature response higher than that of the base case, any addition in CO_2 would cause an additional increase in RF and temperature response. Therefore, it was necessary to determine how much CO_2 reduction is needed in order to counteract the 20 percent reduction in NO_x emissions. It was found that a 1.5 percent reduction of CO_2 emissions reduced RF and temperature response suf-

ficiently, when NO_x emissions were 20 percent below that of the base case, so the values were below that of the base case after 100 years.

This chapter also looked at the effect of delaying the mitigation of both short–lived and long–lived climate–forcers. The cumulative nature of CO_2 in the atmosphere causes the impact of its initial release to extend over centuries. For this reason, any delay in its mitigation will cause peak warming to occur at a later and later date. If mitigation measures are put in place, the effect of reducing SLCFs will be seen almost immediately whereas the effects of CO_2 mitigation, while much greater, will only be seen over the longer term. It is this fact that may encourage the mitigation of short–term forcers over the mitigation of CO_2 .

Chapter 8

Conclusions and Further Work

8.1 Conclusions

As the effects of climate change become more apparent, industries are forced to mitigate their effect on the earth's climate. In the case of aviation, the main climate–changing effects are the emissions of CO_2 (a LLCF) and NO_x (a SLCF). It is known that a trade–off exists in in the mitigation of these two species, if aviation NO_x emissions are reduced a CO_2 penalty is incurred and vice–versa. The main aim of this study was to determine whether reduction of SLCFs such as aircraft NO_x , at the expense of CO_2 emissions is a potentially worse outcome or better outcome for global climate in the longer ($\sim$100 years) term, and therefore examine whether controlling aviation NO_x emissions would reduce or limit global temperature change.

Firstly, the impacts that aviation has on the atmosphere were assessed using the MOZART–3 chemistry transport model (CTM). When aircraft burn fuel, the main emissions are CO_2 , water vapour and NO_x . The CO_2 is produced as in any combustion engine and is cumulative in the atmosphere due to its relatively unreactive nature. After release it builds up in the atmosphere and eventually circulates throughout the earth's carbon reservoirs. All sources of anthropogenically emitted CO_2 mix in the atmosphere, hence it's origin is not important in its effects. The release of CO_2 emissions from aviation follows a linear relationship to fuel burnt, for every 1 kg of fuel burned, 3.16 kg CO_2 is emitted. Aviation NO_x emissions are more complex and the amount of NO_x emitted from an aircraft depends on engine specifications and external factors such as temperature and pressure.

Once emitted into the atmosphere, aviation NO_x emissions have two main effects, they cause an increase in ambient ozone concentrations which contributes a positive radiative forcing and therefore warming effect, and they also reduce methane lifetime. As methane is a greenhouse gas, its destruction contributes a negative radiative forcing or cooling effect. However, these effects do not simply cancel each other out as they occur at different locations and over different time–scales. The release of aviation NO_x emissions has two further effects which are taken into account in this study, the reduction of stratospheric water vapour and the destruction of ozone over the long–term, both of which contribute a small negative forcing.

To investigate the trade–offs between aviation NO_x and CO_2 emissions, a simple climate model was required, which allows long–term model runs to be performed quickly and inexpensively, while retaining the accuracy of 'parent' complex models. The LinClim SCM used in this study assumed a linear relationship between aviation NO_x emissions and the formation of ozone and destruction of methane, which is used to calculate RF. Therefore, an investigation in to the limits of this linear relationship was necessary. Another aspect which required study was the effect of the background atmospheric NO_x level on aviation NO_x emissions. Using the MOZART–3 CTM, aviation scenarios of increasing magnitude were run in two background atmospheric states, each with a different NO_x value, a low background NO_x value of 21.76 Tg N Yr^{-1} and a high background level of 44.75 Tg N Yr^{-1} The results showed that both the ozone burden and methane lifetime change show a linear relationship to aviation NO_x emissions up to approximately 3 Tg N yr^{-1}, after which the relationships become non–linear. It was also established that the background atmosphere is an important factor in the effect of aviation NO_x emissions, in the low NO_x background the average ozone production efficiency was 22.2, whereas in the high NO_x background it was only 17.2.

The results enabled the formation of a new parameterisation to calculate the radiative forcing resulting from aviation NO_x emissions, it takes both the non–linear nature of the NO_x -O_3 – CH_4 system and the effects of the background atmosphere into account. When the new parameterisation was used to calculate the RF from aviation NO_x emissions in a low NO_x and high NO_x background, it was shown that the overall net NO_x RF differs in sign between the two backgrounds. In the low NO_x background the net NO_x RF produced an overall negative forcing whereas in the high NO_x background the net NO_x RF was positive.

This new parameterisation was compared to the existing linear parameterisation used in

LinClim. The results showed that the existing paramterisation in LinClim overestimates the ozone burden resulting from aviation NO_x emissions as it assumes a linear relationship between the two. The methane RFs calculated by the two methods were closer, as at the values of aviation emissions used, the NO_x – CH_4 relationship is closer to linear than that of NO_x – O_3 . Due to the overestimation of ozone burden resulting from NO_x emissions, the RF calculated by LinClim is also overestimated compared to the values calculated using the new parameterisation.

The new parameterisation was then used to determine whether reduction of aircraft NO_x , at the expense of CO_2 emissions is a potentially worse outcome or better outcome for global climate in the longer term. For these experiments, a base case of constant aviation emissions was established and run in both the constant low NO_x and constant high NO_x backgrounds, with a constant background of 404 ppm CO_2 , for consistency, over a 100 year period. This established emissions and associated RF and temperature change of aviation CO_2 and NO_x emissions after 100 years, which were taken to constitute the overall effect of aviation in this experiment. Because net NO_x RF is negative in the low NO_x background, the combined effect of CO_2 and NO_x was slightly lower in the low NO_x background than in the high NO_x background.

The base case was then perturbed by decreasing NO_x emissions by 20 percent while incurring a 2 percent CO_2 penalty – a common scenario from literature on the subject. Although the perturbation reduced NO_x emissions by 10 times as much as CO_2 was increased, after 100 years the overall RF and associated temperature response from aviation (combined effect of NO_x and CO_2) increased. The next stage was to determine how much more NO_x emissions reduction was necessary in order to counteract that small increase of 2 percent CO_2 . In the high NO_x background, NO_x emissions had to be reduced by 43 percent to reduce the overall RF to the levels of the base case after 100 years. To reduce the temperature response to the value of the base case required only a 38 percent reduction in NO_x emissions, this is due to the thermal inertia of the climate system, which is taken into account when calculating temperature response, whereas RF is an instantaneous forcing. The results for the low NO_x background show a more complex relationship. Because the net NO_x forcing in this environment is negative, any reduction in NO_x emissions lessens the negative forcing, therefore the overall forcing from NO_x and CO_2 combined becomes more positive and is therefore higher than the perturbation case (minus 20 percent NO_x and plus 2 percent CO_2) after 100 years. Therefore, in the low NO_x background an addition of NO_x is needed, compared to the base case, to counteract the 2 percent increase in

CO_2 . It was determined that a 37 percent increase in NO_x emission sufficiently counteracted the 2 percent increase in CO_2 emissions for RF and 33 percent additional NO_x for temperature response.

The next trade–off experiments assumed that NO_x reduction remains at 20 percent below the base case and aimed to determine how much of a CO_2 penalty can be incurred before forcing rises above that of the base case. In the high NO_x background it was found that when NO_x was reduced by 20 percent below the base case a CO_2 penalty of 0.5 percent cold be incurred without RF and temperature change rising above that of the base case after 100 years, however a 1 percent increase saw both rise above the base case. Again, the results of the low NO_x background are more complex, the 20 percent reduction in NO_x emissions results in both the RF and temperature response rising above that of the base case after 100 years, meaning any CO_2 increase will only cause the RF and temperature response values even higher. The only solution in this situation is to reduce CO_2 emissions below that of the base case in order to reduce the RF and temperature response. Therefore, when NO_x emissions are reduced by 20 percent in the low NO_x background, a 1.5 percent reduction in CO_2 was necessary to reduce RF and temperature response to values below that of the base case after 100 years.

The experiment performed in this study show that controlling aviation NO_x emissions will not reduce or limit global warming, unless reduced substantially under specific background conditions, however, this will have a minimal effect on climate compared to the mitigation of CO_2 . From the perspective of air pollution, the reduction of NO_x at ground level could have significant benefit to human health, however if the background NO_x levels decline, reducing aviation NO_x emissions could cause an additional positive forcing.

”Technology exists to reduce aviation’s major emissions to varying degrees. Although reductions in emissions can compensate for some growth in air traffic, the actual growth expected over the next several decades may significantly exceed that which realizable reductions can counteract” Miake–Lye et al., (2000)

8.2 Further work

The next logical stage in the study of the trade–offs between aviation NO_x and CO_2 emissions would be to use the new parameterisation and method outlined in Chapter 7 to

investigate transient aviation fuel burn scenarios. ICAO creates scenarios based on low, medium and high technology growth amongst other factors. These scenarios run until 2050 and are created by experts in the industry, hence, they are a logical choice to use for further study, the beginnings of which are shown below.

Another step of the work would be to run additional NO_x backgrounds between the two values used for this study, both to narrow down the point at which net NO_x forcing becomes negative and allow this type of study to be applied to the 'real world' background values, to contribute to the understanding of what could happen in the near term and assess the possible future impacts of decisions made today.

The next logical step to continue the work of this study is to repeat the trade-off experiments with 'real' aviation scenarios. ICAO have produced a range of aviation scenarios which are dependent on various types of technological development and economic and industry growth. The scenarios extend from present day until 2050.

In this section one of the ICAO scenarios was run using the new parameterisation and LinClim to assess the effects of aviation NO_x and CO_2 emissions as described in Chapter 7. The fuel burn scenario was one of moderate technology development and CAEP 9 operational improvements and is shown in Figure 8.1.

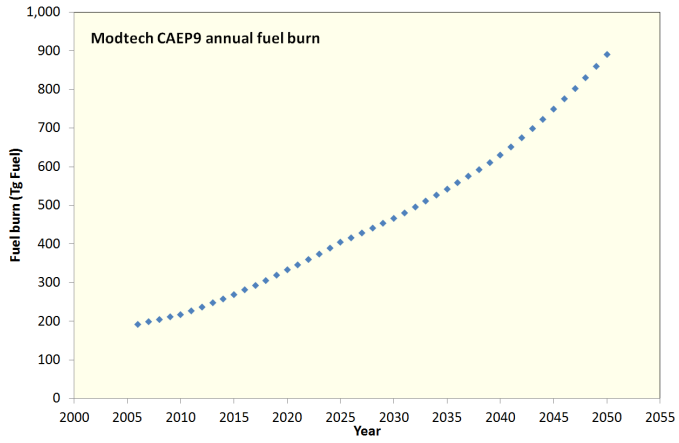

Figure 8.1: The moderate technology, CAEP9 operational improvements ICAO aviation.

From this a base case is established, which is then perturbed in the same way as the experiments shown in Chapter 7, by reducing the NO_x emissions by 20 percent incurring a 2 percent CO_2 penalty. The radiative forcing and the temperature responses for both the base case and the perturbation case are shown in Figures 8.2 and 8.3.

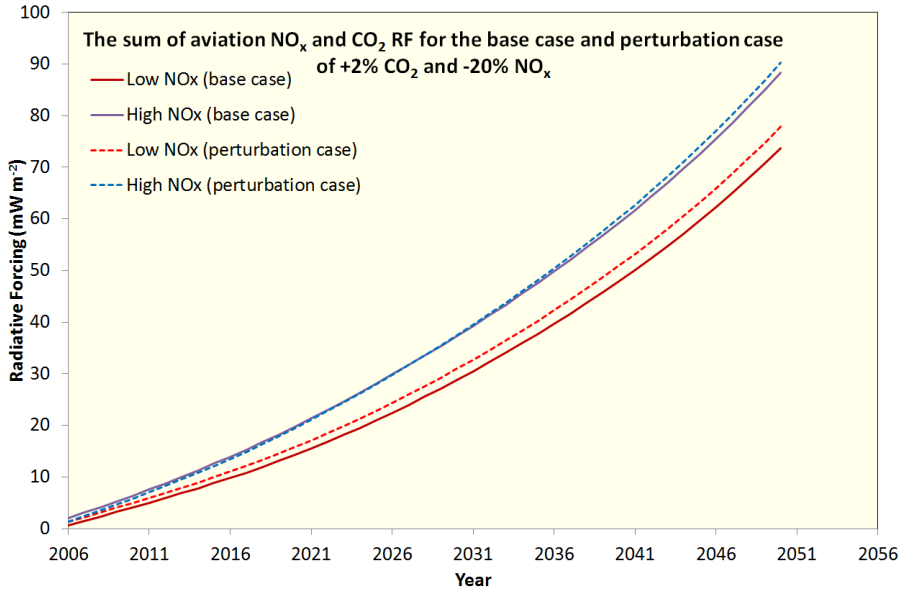

Figure 8.2: The radiative forcing (mW m^{-2}) of the base case and perturbation case for the moderate technology, CAEP 9 operational improvements ICAO aviation scenario.

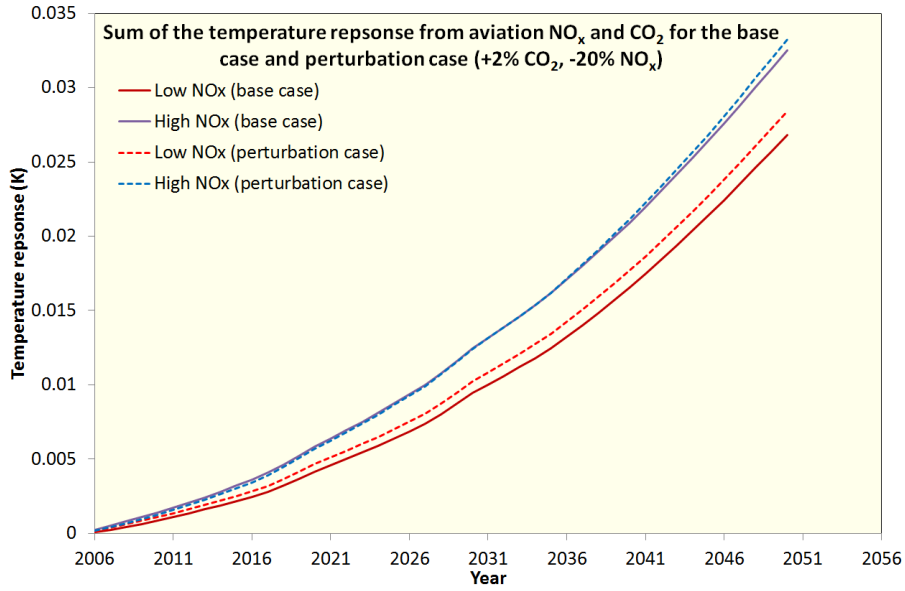

Figure 8.3: The temperature response (K) of the base case and perturbation case for the moderate technology, CAEP 9 operational improvements ICAO aviation scenario.

Figures 8.2 and 8.3 show that, as in the constant emissions experiment, the additional CO_2 emissions of the perturbation case, cause it to have a higher RF and temperature response than the base case at the end of the scenario, in this case 2050, despite the much

Low NOx bg		End point value (2050)	Perturbation cases				
Radiative forcing		Base Case	-20% NO_x, +2% CO_2	-40% NO_x, +2% CO_2	+20% NO_x, +2% CO_2	+15% NO_x, +2% CO_2	+16% NO_x, +2% CO_2
(mW m^{-2})	NO_x	-11.083	-8.689	-6.0951	-13.297	-12.759	-12.867
	CO_2	84.825	86.535	86.535	86.535	86.535	86.535
	Sum	73.742	77.845	80.4402	73.238	73.776	73.667

Table 8.1: The results of the base case and associated perturbation experiments for the ICAO moderate technology CAEP 9 operational improvements aviation scenario.

greater reduction in NO_x emissions. As in Chapter 7, the NO_x perturbation was then changed in increments in order to determine the NO_x perturbation necessary to counteract the additional CO_2 emissions.

In the low NO_x background atmosphere, it was established that a reduction in NO_x actually led to an increase in forcing, as the NO_x component had an overall negative forcing, therefore reducing NO_x, lessened the amount of negative forcing, thus increasing the overall forcing. In Chapter 7, it was discovered that additional NO_x emissions were required to reduce the overall forcing to below that of the base case. The same was found for the experiment here with the ICAO moderate technology scenario. Table 8.1 shows that NO_x needed to be increased by 16 percent more than the base case in order to counteract the increase in forcing due to additional CO_2 emissions in the perturbation case.

The next stage of further work would entail repeating this experiment in the high NO_x background.

Appendix A

Additional models needed for the study of aviation NO_x emissions

In order to generate the aviation emissions scenarios used in this study, additional data handling was necessary. Prior to the study beginning, the emissions scenarios used were formulated in the CATE department (MMU) using the FAST and PIANO models described below. Also, the results presented in Chapter 5 included ozone RF which was calculated by running the MOZART–3 CTM results through the Edwards-Sling radiative transfer model, which also took place in the CATE department at MMU.

FAST (Aircraft inventory model) and PIANO (aircraft performance model)

The emissions scenarios outlined in Chapter 3 are formulated using the FAST and PIANO aviation models. The Future Civil Aviation Scenario Software Tool (FAST) is a global model of aircraft emissions and movements. It is used to calculate aircraft emissions and fuel use over the long–term (up to $\sim$100 years) and works by combining databases of aircraft movement and fuel flow, which is provided by PIANO – a separate aircraft performance model. PIANO provides representative flight profiles to which actual aircraft movements and types are applied, FAST then calculates emissions and fuel consumption for each aircraft type and routes flown (Fichter, 2009). Owen et al., (2010) used FAST to calculate future emissions of CO_2 and NO_x resulting from aviation on a global scale, using 4 scenarios from the IPCC SRES. Simulations from FAST are represented on a 1 degree x

1 degree horizontal resolution and real flight level intervals (horizontal resolution) of 2000 feet (610 m). The calculation of CO_2 is relatively simple due to the relationship between fuel consumption and CO_2 emissions, the NO_x calculations however require an algorithm that corrects for altitude. Owen et al., (2010) calculated a total fuel consumption of 152 Tg from civil aviation for the year 2000 which agreed with other studies and therefore shows the reliability of the FAST model. The data output from FAST can be used as input for GCMs and CTMs and can also be input to simple climate models. In this study, the scenarios of global fleet movement and fuel usage came from FAST for use in the MOZART–3 CTM simulations carried out in Chapter 5.

Edward-Slingo Radiative Transfer Model (RTM)

The Edwards-Slingo offline radiative transfer model (Edwards and Slingo, 1996) is used in this study to calculate the radiative forcing (RF) from ozone formed due to aviation NO_x emissions in the troposphere, the results of which are presented in Chapter 5. It uses the δ Eddington form of the two-stream equations in the short-wave and long-wave spectral regions to calculate heating rates and radiative fluxes across the atmosphere (Edwards and Slingo, 1996). The long-wave defines HO, CO_2 , N_2O, O_3 and CH_4 and the short-wave also captures H_2O, CO_2 , O_3 and additionally O_2. Aerosols, halocarbons and chlorofluorocarbons however, are not included. Climatology, specifically humidity and temperature, are resolved from ERA-Interim data and averaged ISCCP (International Satellite Cloud Climatology Project) D2 data is used to determine the amount and position of water and ice clouds in the atmosphere and hence constitutes cloud treatment in the model. The model version used in this study was developed at the UK Meteorological Office

References

ACARE, 2001: *Strategic Research Agenda: Advisory Council for Aeronautics Research in Europe, Brussles*. ACARE.

— 2011: *Flightpath 2050 Europe's Vision for Aviation, Maintaining Global Leadership and Serving Societys Needs, Report of the High Level Group on Aviation Research*. European Commission.

Airbus, 2015: *Smarter Skies*. Airbus.

Allen, M., 2015: *Short Lived Promise: The Science and Policy of Cumulative and Short-Lived Climate Pollutants*. Oxford Martin Policy Paper, University of Oxford, UK.

Allen, M. R., J. S. Fuglestvedt, K. P. Shine, A. Reisinger, R. T. Pierrehumbert, and P. M. Forster, 2016: New use of global warming potentials to compare cumulative and short–lived climate pollutants. *Nature Climate Change*, **6**, 773 – 776, doi:10.1038/NCLIMATE2998.

Antoine, N. and I. Kroo, 2004: Aircraft optimization for minimal environmental impact. *Journal of Aircraft*, **41**, 790–797, doi:10.2514/1.71.

Archer, D., 2005: Fate of fossil fuel CO2 in geologic time. *Journal of Geophysical Research: Oceans*, **110**, doi:10.1029/2004JC002625.

Archer, D., M. Eby, V. Brovkin, A. Ridgwell, L. Cao, U. Mikolajewicz, K. Caldeira, K. Matsumoto, G. Munhoven, A. Montenegro, and K. Tokos, 2009: Atmospheric Lifetime of Fossil Fuel Carbon Dioxide. *Annual Review of Earth and Planetary Sciences*, **37**, 117–134, doi:10.1146/annurev.earth.031208.100206.

Azar, C. and D. J. A. Johansson, 2012: Valuing the non-CO2 climate impacts of aviation. *Climatic Change*, **111**, 559–579, doi:10.1007/s10584-011-0168-8.

Barrett, S. R. H., S. H. L. Yim, C. K. Gilmore, L. T. Murray, S. R. Kuhn, A. P. K. Tai, R. M. Yantosca, D. W. Byun, F. Ngan, X. Li, J. I. Levy, A. Ashok, J. Koo, H. M. Wong, O. Dessens, S. Balasubramanian, G. G. Fleming, M. N. Pearlson, C. Wollersheim, R. Malina, S. Arunachalam, F. S. Binkowski, E. M. Leibensperger, D. J. Jacob, J. I. Hileman, and I. A. Waitz, 2012: Public health, climate, and economic impacts of desulfurizing jet fuel. *Environmental Science and Technology*, **46**, 4275–4282, doi:10.1021/es203325a.

Bauer, S. E., D. Koch, N. Unger, S. M. Metzger, D. T. Shindell, and D. G. Streets, 2007: Nitrate aerosols today and in 2030: a global simulation including aerosols and tropospheric ozone. *Atmospheric Chemistry and Physics*, **7**, 5043–5059.

Berntsen, T. K. and I. S. A. Isaksen, 1999: Effects of lightning and convection on changes in tropospheric ozone due to NOx emissions from aircraft. *Tellus Series B-Chemical and Physical Meteorology*, **51**, 766–788, doi:10.1034/j.1600-0889.1999.t01-3-00003.x.

Booth, B. B. B., C. D. Jones, M. Collins, I. J. Totterdell, P. M. Cox, S. Sitch, C. Huntingford, R. A. Betts, G. R. Harris, and J. Lloyd, 2012: High sensitivity of future global warming to land carbon cycle processes. *Environmental Research Letters*, **7**, doi:10.1088/1748-9326/7/2/024002.

Boucher, O. and M. S. Reddy, 2008: Climate trade-off between black carbon and carbon dioxide emissions. *Energy Policy*, **36**, 193–200, doi:10.1016/j.enpol.2007.08.039.

Brasseur, G. P., D. A. Hauglustaine, S. Walters, P. J. Rasch, J. F. Muller, C. Granier, and X. X. Tie, 1998: MOZART, a global chemical transport model for ozone and related chemical tracers 1. Model description. *Journal of Geophysical Research-Atmospheres*, **103**, 28265–28289, doi:10.1029/98JD02397.

Christensen, J. H., T. R. Carter, M. Rummukainen, and G. Amanatidis, 2007: Evaluating the performance and utility of regional climate models: the PRUDENCE project. *Climatic Change*, **81**, 1–6, doi:10.1007/s10584-006-9211-6.

Ciais, P., C. Sabine, G. Bala, L. Bopp, V. Brovkin, J. Canadell, A. Chhabra, R. DeFries, J. Galloway, M. Heimann, C. Jones, C. Le Quere, R. B. Myneni, S. Piao, and P. Thornton, 2013: *Carbon and Other Biogeochemical Cycles. In Climate Change 2013: The Physical Science Basis. Contribution of Working Group I to the Fourth Assessment Report of the Intergovernmental Panel on Climate Change*. Cambridge University Press, Cambridge, United Kingdom and New York, NY, USA.

Daniel, J. S., S. Solomon, T. J. Sanford, M. McFarland, J. S. Fuglestvedt, and P. Friedlingstein, 2012: Limitations of single-basket trading: lessons from the Montreal Protocol for climate policy. *Climatic Change*, **111**, 241–248, doi:10.1007/s10584-011-0136-3.

Dee, D. P., S. M. Uppala, A. J. Simmons, P. Berrisford, P. Poli, S. Kobayashi, U. Andrae, M. A. Balmaseda, G. Balsamo, P. Bauer, P. Bechtold, A. C. M. Beljaars, L. van de Berg, J. Bidlot, N. Bormann, C. Delsol, R. Dragani, M. Fuentes, A. J. Geer, L. Haimberger, S. B. Healy, H. Hersbach, E. V. Holm, L. Isaksen, P. Kallberg, M. Koehler, M. Matricardi, A. P. McNally, B. M. Monge-Sanz, J. J. Morcrette, B. K. Park, C. Peubey, P. de Rosnay, C. Tavolato, J. N. Thepaut, and F. Vitart, 2011: The ERA-Interim reanalysis: configuration and performance of the data assimilation system. *Quarterly Journal of the Royal Meteorological Society*, **137**, 553–597, doi:10.1002/qj.828.

Dessens, O., M. O. Koehler, H. L. Rogers, R. L. Jones, and J. A. Pyle, 2014: Aviation and climate change. *Transport Policy*, **34**, 14–20, doi:10.1016/j.tranpol.2014.02.014.

Deuber, O., G. Luderer, and R. Sausen, 2014: CO2 equivalences for short–lived climate forcers. *Climatic Change*, **122**, 651–664, doi:10.1007/s10584-013-1014-y.

Edwards, J. M. and A. Slingo, 1996: Studies with a flexible new radiation code - Choosing a configuration for a large-scale model. *Quarterly Journal of the Royal Meteorological Society*, **122**, 689–719, doi:10.1002/qj.49712253107.

Emmons, L. K., E. C. Apel, J. F. Lamarque, P. G. Hess, M. Avery, D. Blake, W. Brune, T. Campos, J. Crawford, P. F. DeCarlo, S. Hall, B. Heikes, J. Holloway, J. L. Jimenez, D. J. Knapp, G. Kok, M. Mena-Carrasco, J. Olson, D. O'Sullivan, G. Sachse, J. Walega, P. Weibring, A. Weinheimer, and C. Wiedinmyer, 2010: Impact of Mexico City emissions on regional air quality from MOZART-4 simulations. *Atmospheric Chemistry and Physics*, **10**, 6195–6212, doi:10.5194/acp-10-6195-2010.

EuropeanCommission, 2008: *Communication from the Commission to the European Parliament, the Council, the European Economic and Social Committee and the Committee of the Regions - Single European Sky II: towards more sustainable and better performing aviation. COM 389 final.*. European Commission.

Faber, J., D. Greenwood, D. Lee, M. Mann, P. M. De Leon, D. Nelissen, B. Owen, M. Ralph, J. Tilston, A. van Velzen, et al., 2008: Lower nox at higher altitudes policies to reduce the climate impact of aviation nox emission. *CE Delft Solutions for Environment, Economy and Technology*.

Fichter, C., 2009: *Climate Impact of Air Traffic Emissions in Dependency of the Emission Location and Altitude. PhD Thesis.*. Manchester Metropolitan University.

Flemming, G. and U. Ziegler, 2010: *Environmental and Economic Assessment of NOx Stringency Scenarios, ICAO Environmental Report 2010, Chapter 2 - Aircraft Technology Improvements*. ICAO Montreal Canada.

— 2013: *Environmental Trends in Aviation to 2050, ICAO Environmental Report 2013*. ICAO Montreal Canada.

Forster, C., A. Stohl, P. James, and V. Thouret, 2003: The residence times of aircraft emissions in the stratosphere using a mean emission inventory and emissions along actual flight tracks. *Journal of Geophysical Research: Atmospheres*, **108**.

Forster, P., V. Ramaswamy, P. Artaxo, T. Berntsen, R. Betts, D. W. Fahey, J. Haywood, J. Lean, D. Lowe, G. Myhre, R. Nhanga, R. Prinn, G. Raga, M. Schulz, and R. Van Dorland, 2007: *Changes in Atmospheric Constituents and in Radiative Forcing. In: Climate Change 2007: The Physical Science Basis. Contribution of Working Group I to the Fourth Assessment Report of the Intergovernmental Panel on Climate Change (Technical Summary)*. Cambridge University Press, Cambridge, United Kingdom and New York, NY, USA, 130–234 pp.

Fry, M. M., V. Naik, J. J. West, M. D. Schwarzkopf, A. M. Fiore, W. J. Collins, F. J. Dentener, D. T. Shindell, C. Atherton, D. Bergmann, B. N. Duncan, P. Hess, I. A.

MacKenzie, E. Marmer, M. G. Schultz, S. Szopa, O. Wild, and G. Zeng, 2012: The influence of ozone precursor emissions from four world regions on tropospheric composition and radiative climate forcing. *Journal of Geophysical Research-Atmospheres*, **117**, doi:10.1029/2011JD017134.

Fuglestvedt, J. S., T. K. Berntsen, I. S. A. Isaksen, H. T. Mao, X. Z. Liang, and W. C. Wang, 1999: Climatic forcing of nitrogen oxides through changes in tropospheric ozone and methane; global 3D model studies. *Atmospheric Environment*, **33**, 961–977, doi:10.1016/S1352-2310(98)00217-9.

Fuglestvedt, J. S., K. P. Shine, T. Berntsen, J. Cook, D. S. Lee, A. Stenke, R. B. Skeie, G. J. M. Velders, and I. A. Waitz, 2010: Transport impacts on atmosphere and climate: Metrics. *Atmospheric Environment*, **44**, 4648–4677, doi:10.1016/j.atmosenv.2009.04.044.

Gauss, M., I. S. A. Isaksen, D. S. Lee, and O. A. Sovde, 2006: Impact of aircraft NOx emissions on the atmosphere - tradeoffs to reduce the impact. *Atmospheric Chemistry and Physics*, **6**, 1529–1548.

Gettelman, A. and R. B. Rood, 2016: *Demystifying Climate MOdels*. Springer.

Gille, J., J. Barnett, and Co-authors, 2008: High Resolution Dynamics Limb Sounder: Experiment overview, recovery, and validation of initial temperature data. *J. Geophys. Res.*, **113**, doi:10.1029/2007JD008824.

Gillett, N. P., V. K. Arora, D. Matthews, and M. R. Allen, 2013: Constraining the Ratio of Global Warming to Cumulative CO2 Emissions Using CMIP5 Simulations. *Journal of Climate*, **26**, 6844–6858, doi:10.1175/JCLI-D-12-00476.1.

Gilmore, C. K., S. R. H. Barrett, J. Koo, and Q. Wang, 2013: Temporal and spatial variability in the aviation nox–related o3 impact. *Environmental Research Letters*, **8**, 034027.

Gossling, S. and P. Upham, 2009: *Climate Change and Aviation - Issues, Challenges and Solutions*. Earthscan climate, Earthscan.

Grewe, V., M. Dameris, R. Hein, I. Kohler, and R. Sausen, 1999: Impact of future subsonic aircraft nox emissions on the atmospheric composition. *Geophysical Research Letters*, **26**, 47–50.

Hack, J. J., 1994: Parameterization of moist convection in the national center for atmospheric research community climate model (ccm2). *Journal of Geophysical Research: Atmospheres*, **99**, 5551–5568.

Hansen, J., I. Fung, A. Lacis, D. Rind, S. Lebedeff, R. Ruedy, G. Russell, and P. Stone, 1988: Global climate changes as forecast by goddard institute for space studies three-dimensional model. *Journal of Geophysical Research: Atmospheres*, **93**, 9341–9364.

Hansen, J., M. Sato, R. Ruedy, A. Lacis, and V. Oinas, 2000: Global warming in the twenty-first century - An alternative scenario. *Proceedings of the National Academy of Sciences of the United States of America*, **97**, 9875–9880.

Hasselmann, K., S. Hasselmann, R. Giering, V. Ocana, and H. VonStorch, 1997: Sensitivity study of optimal CO2 emission paths using a simplified structural integrated assessment model (SIAM). *Climatic Change*, **37**, 345–386, doi:10.1023/A:1005339625015.

Hidalgo, H. and P. J. Crutzen, 1977: The tropospheric and stratospheric composition perturbed by nox emissions of high-altitude aircraft. *Journal of Geophysical Research*, **82**, 5833–5866, doi:10.1029/JC082i037p05833.

Holmes, C. D., Q. Tang, and M. J. Prather, 2011: Uncertainties in climate assessment for the case of aviation NO. *Proceedings of the National Academy of Sciences of the United States of Ameica*, **108**, 10997–11002, doi:10.1073/pnas.1101458108.

Holstag, A. A. M. and B. A. Boville, 1993: Local versus nonlocal boundary-layer diffusion in a global climate model. *Journal of Climate*, **6**, 1825–1842, doi:10.1175/1520-0442(1993)006¡1825:LVNBLD¿2.0.CO;2.

Huntingford, C., J. A. Lowe, N. Howarth, N. H. A. Bowerman, L. K. Gohar, A. Otto, D. S. Lee, S. M. Smith, M. G. J. den Elzen, D. P. van Vuuren, R. J. Millar, and M. R. Allen, 2015: The implications of carbon dioxide and methane exchange for the heavy mitigation RCP2.6 scenario under two metrics. *Environmental Science and Policy*, **51**, 77–87, doi:10.1016/j.envsci.2015.03.013.

ICAO, 2009: *Global aviation CO2 emissions projections to 2050, Agenda item 2: Review of aviation emissions related activities within ICAO and internationally*. Group on INternational Aviation and Climate Change ICAO Montreal Canada, information paper GIACC 4 IP 1.

IPCC, 1999: Aviation and the global atmosphere. A special report of IPCC working groups I and III. Technical report.

Irvine, E. A., B. J. Hoskins, K. P. Shine, R. W. Lunnon, and C. Froemming, 2013: Characterizing North Atlantic weather patterns for climate-optimal aircraft routing. *Meteorological Applications*, **20**, 80–93, doi:10.1002/met.1291.

Isaksen, I. S. A., O. Hov, and E. Hesstvedt, 1978: Ozone generation over rural areas. *Environmental Science and Technology*, **12**, 1279–1284, doi:10.1021/es60147a011.

Jacobson, M. Z., 2002: Control of fossil-fuel particulate black carbon and organic matter, possibly the most effective method of slowing global warming. *Journal of Geophysical Research - Atmospheres*, **107**.

Johansson, D. J. A., U. M. Persson, and C. Azar, 2008: Uncertainty and learning: implications for the trade-off between short-lived and long-lived greenhouse gases. *Climatic Change*, **88**, 293–308, doi:10.1007/s10584-007-9381-x.

Jones, C., E. Robertson, V. Arora, P. Friedlingstein, E. Shevliakova, L. Bopp, V. Brovkin, T. Hajima, E. Kato, M. Kawamiya, S. Liddicoat, K. Lindsay, C. Reick, C. Roelandt, J. Segschneider, and J. Tjiputra, 2013: Twenty-first-century compatible co2 emissions and airborne fraction simulated by cmip5 earth system models under four representative concentration pathways. *Journal of Climate*, **26**, 4398–4413, doi:10.1175/JCLI-D-12-00554.1.

Joos, F., R. Roth, J. S. Fuglestvedt, G. P. Peters, I. G. Enting, W. von Bloh, V. Brovkin, E. J. Burke, M. Eby, N. R. Edwards, T. Friedrich, T. L. Froelicher, P. R. Halloran, P. B. Holden, C. Jones, T. Kleinen, F. T. Mackenzie, K. Matsumoto, M. Meinshausen, G. K. Plattner, A. Reisinger, J. Segschneider, G. Shaffer, M. Steinacher, K. Strassmann, K. Tanaka, A. Timmermann, and A. J. Weaver, 2013: Carbon dioxide and climate impulse response functions for the computation of greenhouse gas metrics: a multi-model analysis. *Atmospheric Chemistry and Physics*, **13**, 2793–2825, doi:10.5194/acp-13-2793-2013.

Khodayari, A., S. C. Olsen, and D. J. Wuebbles, 2014: Evaluation of aviation NOx-induced radiative forcings for 2005 and 2050. *ATMOSPHERIC ENVIRONMENT*, **91**, 95–103.

Khodayari, A., D. J. Wuebbles, S. C. Olsen, J. S. Fuglestvedt, T. Berntsen, M. T. Lund, I. Waitz, P. Wolfe, P. M. Forster, M. Meinshausen, D. S. Lee, and L. L. Lim, 2013: Intercomparison of the capabilities of simplified climate models to project the effects of aviation CO2 on climate. *Atmospheric Environment*, **75**, 321–328, doi:10.1016/j.atmosenv.2013.03.055.

Kinnison, D. E., G. P. Brasseur, S. Walters, R. R. Garcia, D. R. Marsh, F. Sassi, V. L. Harvey, C. E. Randall, L. Emmons, J. F. Lamarque, P. Hess, J. J. Orlando, X. X. Tie, W. Randel, L. L. Pan, A. Gettelman, C. Granier, T. Diehl, U. Niemeier, and A. J. Simmons, 2007: Sensitivity of chemical tracers to meteorological parameters in the MOZART-3 chemical transport model. *Journal of Geophysical Research - Atmospheres*, **112**, doi:10.1029/2006JD007879.

Kleinman, L. I., 1994: Low and high NOx tropospheric photochemistry. *Journal of Geophysical Research-Atmospheres*, **99**, 16831–16838, doi:10.1029/94JD01028.

Koehler, M. O., G. Radel, O. Dessens, K. P. Shine, H. L. Rogers, O. Wild, and J. A. Pyle, 2008: Impact of perturbations to nitrogen oxide emissions from global aviation. *Journal of Geophysical Research - Atmospheres*, **113**, doi:10.1029/2007JD009140.

Koehler, M. O., G. Raedel, K. P. Shine, H. L. Rogers, and J. A. Pyle, 2013: Latitudinal variation of the effect of aviation NOx emissions on atmospheric ozone and methane and related climate metrics. *Atmospheric Environment*, **64**, 1–9, doi:10.1016/j.atmosenv.2012.09.013.

Lacis, A. A., D. J. Wuebbles, and J. A. Logan, 1990: Radiative forcing of climate by chnages in the vertical distribution of ozone. *Journal of Geophysical Research - Atmospheres*, **95**, 9971–9981, doi:10.1029/JD095iD07p09971.

Lahsen, M., 2005: Seductive simulations? Uncertainty distribution around climate models. *Social Studies of Science*, **35**, 895–922, doi:10.1177/0306312705053049.

Lamarque, J. F., T. C. Bond, V. Eyring, C. Granier, A. Heil, Z. Klimont, D. Lee, C. Liousse, A. Mieville, B. Owen, M. G. Schultz, D. Shindell, S. J. Smith, E. Stehfest, J. Van Aardenne, O. R. Cooper, M. Kainuma, N. Mahowald, J. R. McConnell, V. Naik, K. Riahi, and D. P. van Vuuren, 2010: Historical (1850-2000) gridded anthropogenic and biomass burning emissions of reactive gases and aerosols: methodology and application. *Atmospheric Chemistry and Physics*, **10**, 7017–7039, doi:10.5194/acp-10-7017-2010.

Lee, D. S., D. W. Fahey, P. M. Forster, P. J. Newton, R. C. N. Wit, L. L. Lim, B. Owen, and R. Sausen, 2009: Aviation and global climate change in the 21st century. *Atmospheric Environment*, **43**, 3520–3537, doi:10.1016/j.atmosenv.2009.04.024.

Lee, D. S., L. L. Lim, and B. Owen, 2013a: Bridging the aviation co2 emissions gap: Why emissions trading is needed, manchester: Manchester metropolitan university.

— 2013b: Mitigating future aviation co2 emissions – timing is everything, manchester: Manchester metropolitan university.

Lee, D. S., L. L. Lim, and S. C. Raper: 2005, The role of aviation emissions in climate stabilization scenarios. *Poster at Avoiding Dangerous Climate Change Conference, Exeter, UK*, 1–3.

Lee, D. S., G. Pitari, V. Grewe, K. Gierens, J. E. Penner, A. Petzold, M. J. Prather, U. Schumann, A. Bais, T. Berntsen, D. Iachetti, L. L. Lim, and R. Sausen, 2010: Transport impacts on atmosphere and climate: Aviation. *Atmospheric Environment*, **44**, 4678–4734, doi:10.1016/j.atmosenv.2009.06.005.

Lim, L., D. S. Lee, R. Sausen, and M. Ponater: 2007, Quantifying the effects of aviation on radiative forcing and temperature with a climate response model. *Proceedings of an International Conference on Transport, Atmosphere and Climate (TAC)*, Office for Official Publications of the European Communities, Luxembourg, 202–208.

Lim, L., H. Preston, and D. S. Lee: 2009, Exploring the uncertainties involved in calculating temperature response from the transport sector. *Proceedings of an International Conference on Transport, Atmosphere and Climate (TAC2)*, Office for Official Publications of the European Communities, Luxembourg.

Lin, S. J. and R. B. Rood, 1996: Multidimensional flux-form semi-Lagrangian transport schemes. *Monthly Weather Review*, **124**, 2046–2070, doi:10.1175/1520-0493(1996)124¡2046:MFFSLT¿2.0.CO;2.

Lin, X., M. Trainer, and S. C. Liu, 1988: On the nonlinearity of the tropospheric ozone production. *Journal of Geophysical Research-Atmospheres*, **93**, 15879–15888, doi:10.1029/JD093iD12p15879.

Maier-Reimer, E. and K. Hasselmann, 1987: Transport and storage of CO2 in the ocean - an inorganic ocean-circulation carbon cycle model. *Climate Dynamics*, **2**, 63–90, doi:10.1007/BF01054491.

Mann, M., 2002: The value of multiple proxies. *Science*, **297**, 1481–1482, doi:10.1126/science.1074318.

Maslin, M. and P. Austin, 2012: Climate models at their limit. *Nature*, **486**, 183–184.

Masui, T., K. Matsumoto, Y. Hijioka, T. Kinoshita, T. Nozawa, S. Ishiwatari, E. Kato, P. R. Shukla, Y. Yamagata, and M. Kainuma, 2011: An emission pathway for stabilization at 6 Wm(-2) radiative forcing. *Climatic Change*, **109**, 59–76, doi:10.1007/s10584-011-0150-5.

McGuffie, K. and A. Henderson-Sellers, 2005: *A climate modelling primer*. John Wiley & Sons.

Mhyre, G., D. Shindell, F. M. Breon, W. Collins, J. Fuglestvedt, D. Koch, J. F. Lamarque, D. Lee, D. Mondozo, T. Nakajima, A. Robock, G. Stephens, T. Takomura, and H. Zhang, 2013: *Anthropogenic and Natural Radiative Forcing. In Climate Change 2013: The Physical Science Basis. Contribution of Working Group I to the Fourth Assessment Report of the Intergovernmental Panel on Climate Change*. Cambridge University Press, Cambridge, United Kingdom and New York, NY, USA.

Miake-Lye, R., I. Waitz, D. Fahey, H. Wesoky, and C. Wey, 2000: Aviation and the changing climate. *Aerospace America*, **38**, 35–39.

Montenegro, A., V. Brovkin, M. Eby, D. Archer, and A. J. Weaver, 2007: Long term fate of anthropogenic carbon. *Geophysical Research Letters*, **34**, doi:10.1029/2007GL030905.

Moss, R. H., J. A. Edmonds, K. A. Hibbard, M. R. Manning, S. K. Rose, D. P. van Vuuren, T. R. Carter, S. Emori, M. Kainuma, T. Kram, G. A. Meehl, J. F. B. Mitchell, N. Nakicenovic, K. Riahi, S. J. Smith, R. J. Stouffer, A. M. Thomson, J. P. Weyant, and T. J. Wilbanks, 2010: The next generation of scenarios for climate change research and assessment. *Nature*, **463**, 747–756, doi:10.1038/nature08823.

Muller, J. F., 1992: Geographical distribution and seasonal variation of surface emissions and deposition velocities of atmospheric trace gases. *Journal of Geophysical Research-Atmospheres*, **97**, 3787–3804.

Myhre, G., J. S. Nilsen, L. Gulstad, K. P. Shine, B. Rognerud, and I. S. A. Isaksen, 2007: Radiative forcing due to stratospheric water vapour from CH(4) oxidation. *Geophysical Research Letters*, **34**, doi:10.1029/2006GL027472.

Newton, P., 2007: Long-term Technology Goals for CAEP. *ICAO Colloquium on Aviation Emissions with Exhibition*.

Olivie, D. J. L. and G. P. Peters, 2013: Variation in emission metrics due to variation in CO2 and temperature impulse response functions. *EARTH SYSTEM DYNAMICS*, **4**, 267–286, doi:10.5194/esd-4-267-2013.

Owen, B., D. S. Lee, and L. Lim, 2010: Flying into the Future: Aviation Emissions Scenarios to 2050. *Environmental Science and Technology*, **44**, 2255–2260, doi:10.1021/es902530z.

Park, M., W. J. Randel, D. E. Kinnison, R. R. Garcia, and W. Choi, 2004: Seasonal variation of methane, water vapor, and nitrogen oxides near the tropopause: Satellite observations and model simulations. *Journal of Geophysical Research-Atmospheres*, **109**, doi:10.1029/2003JD003706.

Pickering, K. E., Y. S. Wang, W. K. Tao, C. Price, and J. F. Muller, 1998: Vertical distributions of lightning NOx for use in regional and global chemical transport models. *Journal of Geophysical Research-Atmospheres*, **103**, 31203–31216, doi:10.1029/98JD02651.

Pidwirny, M., 2006: *The Carbon Cycle – Fundamentals of Physical Geography, 2nd Ed.*. www.physicalgeography.net, accessed 10.11.2015.

Prather, M., D. Ehhalt, F. Dentener, R. Derwent, E. Dlugokencky, E. Holland, I. Isaksen, J. Katima, V. Kirchhoff, P. Matson, P. Midgly, and M. Wang, 2001: *Atmospheric Chemistry and Greenhouse Gases. In: Climate Change 2001: The Physical Science Basis. Contribution of Working Group I to the Third Assessment Report of the Intergovernmental Panel on Climate Change*. Cambridge University Press, Cambridge, United Kingdom and New York, NY, USA.

Prather, M. J., 1996: Time scales in atmospheric chemistry: Theory, GWPs for CH4 and CO, and runaway growth. *Geophysical Research Letters*, **23**, 2597–2600, doi:10.1029/96GL02371.

Prentice, I. C., G. D. Farquhar, M. J. R. Fasham, M. L. Goulden, M. Heimann, V. J. Jaramillo, H. S. Kheshgi, C. Le Quere, R. J. Scholes, and D. W. R. Wallace, 2001: *Climate Change 2001: The Physical Science Basis. Contribution of Working Group I to the Third Assessment Report of the Intergovernmental Panel on Climate Change*. Cambridge University Press, Cambridge, United Kingdom and New York, NY, USA.

Price, C., J. Penner, and M. Prather, 1997: Nox from lightning: 1. global distribution based on lightning physics. *Journal of Geophysical Research: Atmospheres*, **102**, 5929–5941.

Ralph, M., 2007: Report of the Independent Experts on the 2006 Reviews of NOx Technologies and the Setting of Medium and Long Term Goals. *7th Meeting of CAEP*.

Ralph, M. and S. Baker, 2010: *ICAO Technology Goals for NOx - Second Independent Expert Reviews, ICAO Environmental Report 2010, Chapter 2 - Aircraft Technology Improvements*. ICAO Montreal Canada.

Ramaswamy, V., O. Bouher, J. Haigh, D. Hauglustaine, J. Haywood, G. Myhre, T. Nakajima, G. Y. Shi, and S. Solomon, 2001: *Radiative Forcing of Climate Change. In: Climate Change 2001: The Physical Science Basis. Contribution of Working Group I to the Third Assessment Report of the Intergovernmental Panel on Climate Change*. Cambridge University Press, Cambridge, United Kingdom and New York, NY, USA.

Rao, S., K. Riahi, E. Stehfest, D. P. Van Vuuren, C. Cho, M. G. J. Den Elzen, M. Isaac, and J. van Vliet, 2008: IMAGE and MESSAGE scenarios limiting GHG concentration to low levels. *IIASA Interim Report IR-08-020*.

Rasch, P., N. Mahowald, and B. Eaton, 1997: Representations of transport, convection, and the hydrologic cycle in chemical transport models: Implications for the modeling of short-lived and soluble species. *Journal of Geophysical Research - Atmospheres*, **102**, 28127–28138.

Riahi, K., S. Rao, V. Krey, C. Cho, V. Chirkov, G. Fischer, G. Kindermann, N. Nakicenovic, and P. Rafaj, 2011: RCP 8.5-A scenario of comparatively high greenhouse gas emissions. *Climatic Change*, **109**, 33–57, doi:10.1007/s10584-011-0149-y.

Sausen, R., I. Isaksen, V. Grewe, D. Hauglustaine, D. Lee, G. Myhre, M. Kohler, G. Pitari, U. Schumann, F. Stordal, and C. Zerefos, 2005: Aviation radiative forcing in 2000: An update on IPCC (1999). *Meteorologische Zeitschrift*, **14**, 555–561, doi:10.1127/0941-2948/2005/0049.

Sausen, R. and U. Schumann, 2000: Estimates of the climate response to aircraft CO2 and NOx emissions scenarios. *Climatic Change*, **44**, 27–58, doi:10.1023/A:1005579306109.

Schleser, G., G. Helle, A. Lucke, and H. Vos, 1999: Isotope signals as climate proxies: the role of transfer functions in the study of terrestrial archives. *Quaternary Science Reviews*, **18**, 927–943, doi:10.1016/S0277-3791(99)00006-2.

Schmittner, A., A. Oschlies, H. D. Matthews, and E. D. Galbraith, 2008: Future changes in climate, ocean circulation, ecosystems, and biogeochemical cycling simulated for a business-as-usual CO2 emission scenario until year 4000 AD. *Global Biogeochemical Cycles*, **22**, doi:10.1029/2007GB002953.

Schulte, P., H. Schlager, H. Ziereis, U. Schumann, S. L. Baughcum, and F. Deidewig, 1997: NOx emission indices of subsonic long-range jet aircraft at cruise altitude: In situ measurements and predictions. *Journal of Geophysical Research-Atmospheres*, **102**, 21431–21442, doi:10.1029/97JD01526.

Shine, K. P., 2009: The global warming potential-the need for an interdisciplinary retrial. *CLIMATIC CHANGE*, **96**, 467–472, doi:10.1007/s10584-009-9647-6.

Shine, K. P., T. K. Berntsen, J. S. Fuglestvedt, and R. Sausen, 2005: Scientific issues in the design of metrics for inclusion of oxides of nitrogen in global climate agreements.

Proceedings of the National Academy of Sciences of the United States of America, **102**, 15768–15773, doi:10.1073/pnas.0506865102.

Shine, K. P., T. K. Berntsen, J. S. Fuglestvedt, R. B. Skeie, and N. Stuber, 2007: Comparing the climate effect of emissions of short- and long-lived climate agents. *Philosophical Transactions of the Royal Society A- Mathmatical Physical and Engneering Sciences*, **365**, 1903–1914, doi:10.1098/rsta.2007.2050.

Skowron, A., 2013: *The impact of emissions of nitrogen oxides from aviation on tropospheric chemistry - the counterbalancing roles of ozone and methane. PhD Thesis.*. Manchester Metropolitan University.

Skowron, A., D. S. Lee, and R. R. De Leon, 2013: The assessment of the impact of aviation NOx on ozone and other radiative forcing responses - The importance of representing cruise altitudes accurately. *Atmospheric Environment*, **74**, 159–168, doi:10.1016/j.atmosenv.2013.03.034.

— 2015: Variation of radiative forcings and global warming potentials from regional aviation NOx emissions. *Atmospheric Environment*, **104**, 69–78, doi:10.1016/j.atmosenv.2014.12.043.

Solomon, S., G. K. Plattner, R. Knutti, and P. Friedlingstein, 2009: Irreversible climate change due to carbon dioxide emissions. *Proceedings of the National Academy of Sciences of the United States of America*, **106**, 1704–1709, doi:10.1073/pnas.0812721106.

Solomon, S., D. Qin, M. Manning, R. B. Alley, T. Berntsen, L. Bindoff, Z. Chen, A. Chidthaisong, J. M. Gregory, G. C. Hegeri, M. Heimann, B. Hewitson, B. J. Hoskins, F. Joos, J. Jouzel, V. Kattsov, U. Lohmann, T. Matsuno, M. Molina, N. Nicholls, J. Overpeck, G. Raga, V. Ramaswamy, J. Ren, M. Rusticucci, R. Somerville, T. F. Stocker, P. Whetton, R. A. Wood, and D. Wratt, 2007: *Climate Change 2007: The Physical Science Basis. Contribution of Working Group I to the Fourth Assessment Report of the Intergovernmental Panel on Climate Change*. Cambridge University Press, Cambridge, United Kingdom and New York, NY, USA.

Sovde, O. A., S. Matthes, A. Skowron, D. Iachetti, L. Lim, B. Owen, O. Hodnebrog, G. Di Genova, G. Pitari, D. S. Lee, G. Myhre, and I. S. A. Isaksen, 2014: Aircraft emission mitigation by changing route altitude: A multi-model estimate of aircraft NOx emission impact on O-3 photochemistry. *Atmospheric Environment*, **95**, 468–479, doi:10.1016/j.atmosenv.2014.06.049.

Stevenson, D. S. and R. G. Derwent, 2009: Does the location of aircraft nitrogen oxide emissions affect their climate impact? *Geophysical Research Letters*, **36**, doi:10.1029/2009GL039422.

Stevenson, D. S., R. M. Doherty, M. G. Sanderson, W. J. Collins, C. E. Johnson, and R. G. Derwent, 2004: Radiative forcing from aircraft NOx emissions: Mechanisms and seasonal dependence. *Journal of Geophysical Research-Atmospheres*, **109**, doi:10.1029/2004JD004759.

Stevenson, D. S., C. E. Johnson, W. J. Collins, R. G. Derwent, K. P. Shine, and J. M. Edwards, 1998: Evolution of tropospheric ozone radiative forcing. *Geophysical Research Letters*, **25**, 3819–3822, doi:10.1029/1998GL900037.

Stocker, T., D. Qin, G.-K. Plattner, L. Alexander, S. Allen, N. Bindoff, F.-M. Breon, J. Church, U. Cubasch, S. Emori, P. Forster, P. Friedlingstein, N. Gillett, J. Gregory, D. Hartmann, E. Jansen, B. Kirtman, R. Knutti, K. Krishna Kumar, P. Lemke, J. Marotzke, V. Masson-Delmotte, G. Meehl, I. Mokhov, S. Piao, V. Ramaswamy, D. Randall, M. Rhein, M. Rojas, C. Sabine, D. Shindell, L. Talley, D. Vaughan, and S.-P. Xie, 2013: *Climate Change 2013: The Physical Science Basis. Contribution of Working Group I to the Fifth Assessment Report of the Intergovernmental Panel on Climate Change (Technical Summary)*. Cambridge University Press, Cambridge, United Kingdom and New York, NY, USA, 33–115 pp.

Stordal, F., M. Gauss, G. Myhre, E. Mancini, D. A. Hauglustaine, M. O. Koehler, T. Berntsen, E. J. G. Stordal, D. Iachetti, G. Pitari, and I. S. A. Isaksen, 2006: Trade-offs in climate effects through aircraft routing: forcing due to radiatively active gases. *Atmospheric Chemistry and Physics Discussions*, **6**, 10733–10771, doi:10.5194/acpd-6-10733-2006.

Thomson, A. M., K. V. Calvin, S. J. Smith, G. P. Kyle, A. Volke, P. Patel, S. Delgado-Arias, B. Bond-Lamberty, M. A. Wise, L. E. Clarke, and J. A. Edmonds, 2011: RCP4.5: a pathway for stabilization of radiative forcing by 2100. *Climatic Change*, **109**, 77–94, doi:10.1007/s10584-011-0151-4.

van Noije, T. P. C., H. J. Eskes, F. J. Dentener, D. S. Stevenson, K. Ellingsen, M. G. Schultz, O. Wild, M. Amann, C. S. Atherton, D. J. Bergmann, I. Bey, K. F. Boersma, T. Butler, J. Cofala, J. Drevet, A. M. Fiore, M. Gauss, D. A. Hauglustaine, L. W. Horowitz, I. S. A. Isaksen, M. C. Krol, J. F. Lamarque, M. G. Lawrence, R. V. Martin, V. Montanaro, J. F. Mueller, G. Pitari, M. J. Prather, J. A. Pyle, A. Richter, J. M. Rodriguez, N. H. Savage, S. E. Strahan, K. Sudo, S. Szopa, and M. van Roozendael, 2006: Multi-model ensemble simulations of tropospheric NO2 compared with GOME retrievals for the year 2000. *Atmospheric Chemistry and Physics*, **6**, 2943–2979.

van Vuuren, D. P., E. Stehfest, M. G. J. den Elzen, T. Kram, J. van Vliet, S. Deetman, M. Isaac, K. K. Goldewijk, A. Hof, A. M. Beltran, R. Oostenrijk, and B. van Ruijven, 2011: RCP2.6: exploring the possibility to keep global mean temperature increase below 2 degrees C. *Climatic Change*, **109**, 95–116, doi:10.1007/s10584-011-0152-3.

Warren, R., M. D. Mastrandrea, C. Hope, and A. F. Hof, 2010: Variation in the climatic response to SRES emissions scenarios in integrated assessment models. *Climatic Change*, **102**, 671–685, doi:10.1007/s10584-009-9769-x.

Wild, O., M. J. Prather, and H. Akimoto, 2001: Indirect long-term global radiative cooling from NOx emissions. *Geophysical Research Letters*, **28**, 1719–1722, doi:10.1029/2000GL012573.

Zhang, G. J. and N. A. Mcfarlane, 1995: Sensitivity of climate simulations to the parameterisation of cumulus convection in the Canadian climate centre general circulation model. *Atmosphere-Ocean*, **33**, 407–446.

Zickfeld, K. and T. Herrington, 2015: The time lag between a carbon dioxide emission and maximum warming increases with the size of the emission. *Environmental Research Letters*, **10**, doi:10.1088/1748-9326/10/3/031001.